Benefit and Cost Assessment of Integrating Arrival, Departure, and Surface Operations with ATD-2

NASA NRA Final Report

Contract Number: NNA16BD87C

March 30, 2018

Submitted To:

NASA Ames Research Center

Moffett Field, CA

Submitted By:

Aditya Saraf, Martin Popish, Marc Rose, Hamsa Balakrishnan, Jamie Cardillo, Sandeep Badrinath, Benjamin Levy, Valerie Sui, Kennis Chan, Peset Tan, Natasha Luch, Evan Lohn, and Brandon Huang

This Page Intentionally Left Blank

Table of Contents

The ATAC NASA Research Announcement (NRA) Team, consisting of ATAC Corporation (ATAC), MCR Federal Inc. and Massachusetts Institute of Technology (MIT), submits this **Final Report** in support of the NASA NRA project titled "Benefit and Cost Assessment of Integrating Arrival, Departure, and Surface Operations with ATD-2," (Contract Number: NNA16BD87C). This report describes the findings and conclusions from the research work performed for computing the benefits and costs of implementing the Airspace Technology Demonstration-2 (ATD-2) on a nationwide scale as well as provides descriptions of the simulation models and technical approaches developed in support of this work.

1. INTRODUCTION

The management of departure flights taking off from the airport surface, traveling through the terminal airspace, and merging into overhead en route traffic streams presents a complex scheduling and air traffic management (ATM) problem. This is especially true in metroplex regions where departures and arrivals to/from multiple, proximate airports compete for limited resources (e.g., mixed-use runways, shared departure-fixes, busy overhead traffic streams). Current-day metroplex traffic management practices lead to multiple operational shortfalls. These shortfalls include:

- Identical ticketed departure times, a pushback-when-ready operational paradigm, and reactive first-come-first-served (FCFS) management of clearances at ramp transition spots lead to inefficient departure sequences, causing taxi inefficiency (stop-and-go) and throughput loss;
- Lack of predictability in the departure process forces tower controllers to impose buffers (e.g., runway separation) to ensure safety and forces the receiving Terminal Radar Approach Control (TRACON) facility and Centers to impose inefficient departure restrictions (e.g., excess miles-in-trail (MIT) or approval requests (APREQs)) on airports, to make space for airborne merging; and
- Lack of predictability causes airlines to set excess scheduled block times, which limits fleet utilization and increases operating costs including personnel and fuel costs.

Under the ATD-2 subproject, NASA has started addressing these shortfalls by developing Integrated Arrival, Departure, Surface (IADS) technologies that comprise the ATD-2 system, and transitioning them to field implementation. These technologies aim to increase the predictability, efficiency, and throughput of metroplex operations while meeting future air traffic demand [NASA15]. It is expected that ATD-2 will bring improvements in predictability, efficiency, and throughput, leading to reduced environmental impact, greater predictability in airport surface resource allocation, and better, more coordinated scheduling across national, regional, and local traffic management initiatives. Quantification of these benefits needs the generation of reliable information regarding the operational shortfalls that ATD-2 can address, its benefit mechanisms, and relevant benefits metrics, and the use of this information to compute high-fidelity benefit-cost estimates of implementing the ATD-2 system at NAS-wide airports. The overarching objective of the research work described in this report is to fulfil this need by generating high-fidelity benefit and cost estimates of implementing NASA's ATD-2 system at major airports in the NAS.

First, we provide a brief overview of the ATD-2 concept and technologies.

1.1. The ATD-2 Concept and Technologies

NASA's ATD-2 system integrates arrival, departure, and surface scheduling concepts and technologies to demonstrate the benefits of an IADS traffic management system for metroplex environments. As shown in **Figure 1**, the operational environment for the ATD-2 system consists of a local metroplex airspace overlying one or more well-equipped airports (e.g., busy airports with surface surveillance radars installed) and multiple less-equipped airports (e.g., smaller, less busy airports without surface surveillance systems). Departures from these airports may share departure fixes on the TRACON boundary and merge into busy en route traffic streams in the Center airspace. Departures are subject to multiple restrictions including APREQs for specific destination-bound flights, MITs at en route merge points and departure fixes, Expected Departure Clearance Times (EDCTs) from Ground Delay Programs (GDPs), weather-related departure fix/gate closures, and takeoff time restrictions due to arrival metering constraints at a destination airport. The ATD- 2 system computes time- based departure schedules for all airports in the local metroplex while accounting for all national, regional and local departure restrictions listed above.

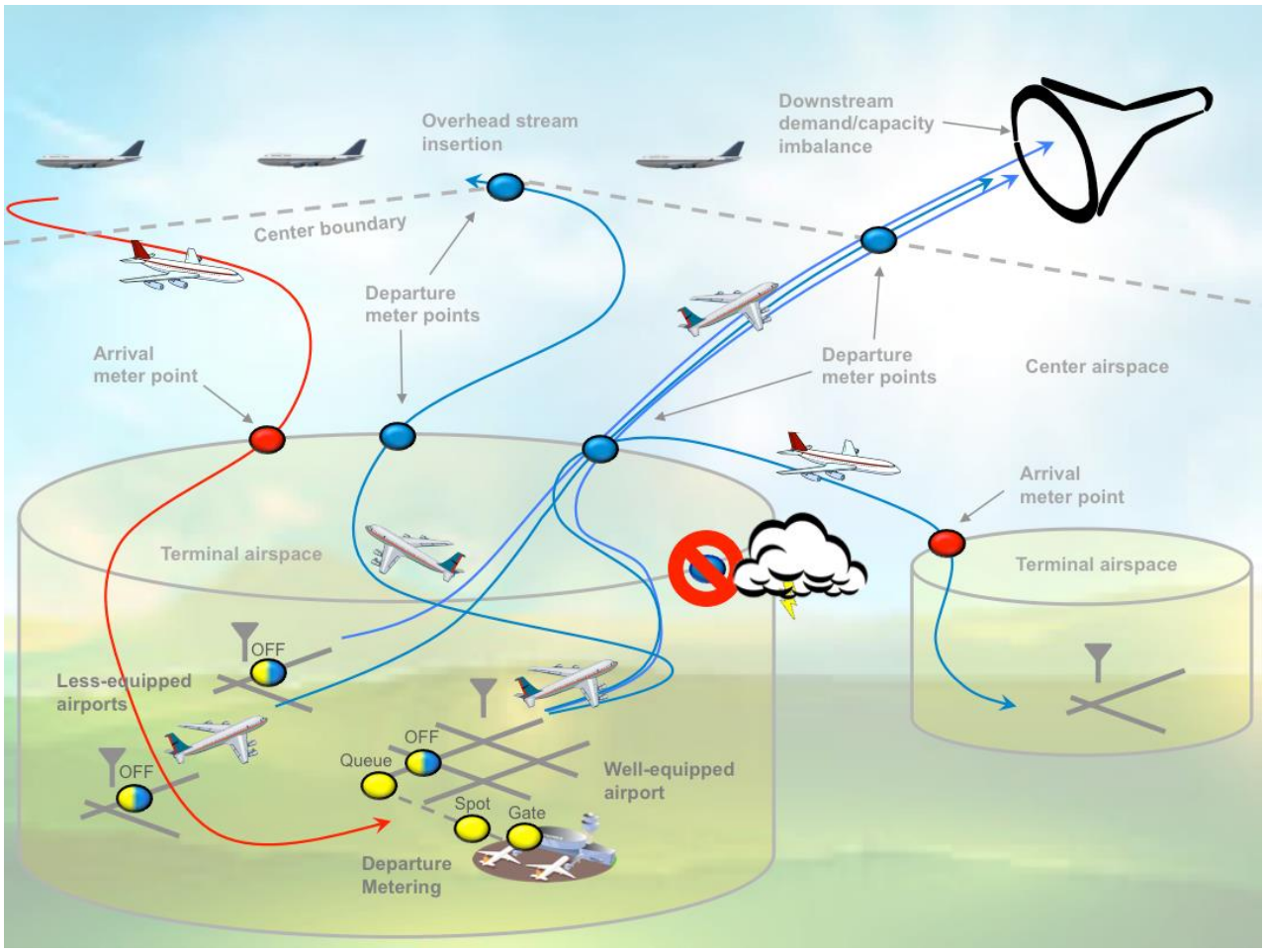

Figure 1. The operational environment for ATD-2 departure metering [NASA15]

The ATD-2 system consists of a single Airspace subsystem and multiple Surface subsystems (one for each airport in the metroplex). The Airspace subsystem applies local, regional and national departure restrictions to scheduled metroplex departure traffic demand and computes controlled

takeoff times that balance the demand with airspace capacity as well as equitably distribute any required delay and satisfy the departure restrictions. The controlled takeoff times are sent to the Surface Subsystems and act as constraints on their planning. The ATD-2 Surface Subsystems may be trajectory-based (in the case of well-equipped airports) or event-based (in the case of less-equipped airports). Trajectory-based ATD-2 Surface Subsystems provide detailed trajectory prediction and scheduling capabilities that minimize surface congestion and delay, whereas event-based ATD-2 Surface Subsystems provide simple takeoff time estimates based on aircraft status update-related events to support ATD-2 traffic scheduling. At the core of each Airspace and Surface Subsystem is a traffic scheduling algorithm that aims to balance traffic demand with capacity for key metroplex resources (e.g., runways, departure-fixes, overhead traffic stream merge points) while minimizing taxi and airborne delays by allocating hold times at the gates for departure flights (in the case of a Surface Subsystem) or controlled runway takeoff times (in the case of the Airspace Subsystem).

Further, ATD-2 involves a collaborative, strategic planning function that enables the airlines, airport traffic control towers (ATCTs) and TRACONs to collaboratively determine scheduling parameters and metering start/end times. The ATD-2 system also enables electronic two-way data-exchange between the airline operator and relevant FAA systems. This data exchange includes dissemination of flight operator information regarding aircraft pushback readiness and company priorities as well as early dissemination of departure restriction data and controlled gate/movement area entry/runway takeoff times to the flight operators.

ATD-2's state-of-the-art data-exchange, collaborative decision making and scheduling capabilities are expected to provide significant benefits in terms of taxi delay saving, fuel saving, passenger time saving and airline direct operating cost (ADOC) saving, as well as beneficial environmental impacts by reducing greenhouse gas emissions. Our research work aims to quantify these benefits.

Next, we discuss our overall project technical approach.

1.2. Overall Project Technical Approach

1.2.1. Benefits and Costs Estimation Methodology

We take a simulation-based approach for estimating ATD-2 benefits. To support this approach, we have developed a high-fidelity simulation environment for simulating aircraft trajectories in both the surface and airspace subsystems of the ATD-2 system, under current-day ATM procedures, as well as under ATD-2 procedures. Our approach compares performance metrics obtained by simulating airport and airspace operations under these two procedures on multiple, carefully chosen simulation days, and properly apportions the performance metrics differences to benefits provided by the ATD-2 system. High-fidelity fast-time simulations are conducted at a small number of airport sites and for carefully chosen simulation scenarios. Results from these simulations are extrapolated to annualized and nationwide scale using meticulous extrapolation approaches. To address the cost assessment part of the overall objective, we apply FAA-recommended cost assessment approaches to compute the cost associated with implementing the ATD-2 system at major U.S. airports. Finally, costs are compared against NAS-wide benefits, and a return on investment is calculated.

1.2.2. Project Technical Tasks

Our project technical approach consisted of six technical tasks. **Figure 2** shows the project technical tasks and how they interacted with each other. Our first task identified existing

operational shortfalls at busy airports and metroplexes that ATD-2 can address, and analyzed the mechanisms by which ATD-2 can alleviate these shortfalls. This task consisted of stakeholder interviews (including NASA researchers, FAA and airline operational personnel), a departure traffic management literature review and operational data analysis. Section 2 discusses this task in detail. Task 1 resulted in the identification of shortfalls, benefit mechanisms and benefit metrics that need to be modeled in a simulation platform for enabling a high-fidelity simulation-based benefits analysis. A parallel task (Task 2) performed extensive analysis on historical operational data at the FAA Core 30 airports with the objective to select three airport sites for detailed simulation-based benefits analysis of the ATD-2 system. Section 3 discusses this task in detail. For reasons explained in Section 3, this task resulted in the selection of the following three airports for detailed simulation-based analysis: (1) Charlotte Douglas International Airport (CLT), (2) Dallas Fort Worth International Airport (DFW) and (3) Newark Liberty International Airport (EWR). Furthermore, this task also identified a number of additional simulation modeling requirements specific to the three chosen airport sites.

After the modeling requirements were identified, Task 3 developed the simulation environment. We developed a hybrid, surface-airspace simulation environment to support our benefits assessments. For this purpose, we used NASA's Surface Operations Simulator and Scheduler (SOSS) platform as the model for simulating the transit of departure and arrival flights on the airport surface. In addition, we developed a supplementary platform called the Airspace Operations Simulator and Scheduler (AOSS), which simulated the transit of the departure flights after takeoff and until departure-fix crossing or (in the case of some flights) until the overhead en route traffic stream merge. AOSS also simulated the surface-airspace coordination process as well as surface traffic flow management actions for the implementation of traffic management initiatives such as APREQs, EDCTs, and MITs. Section 4 describes the combined surface-airspace simulation platform in detail.

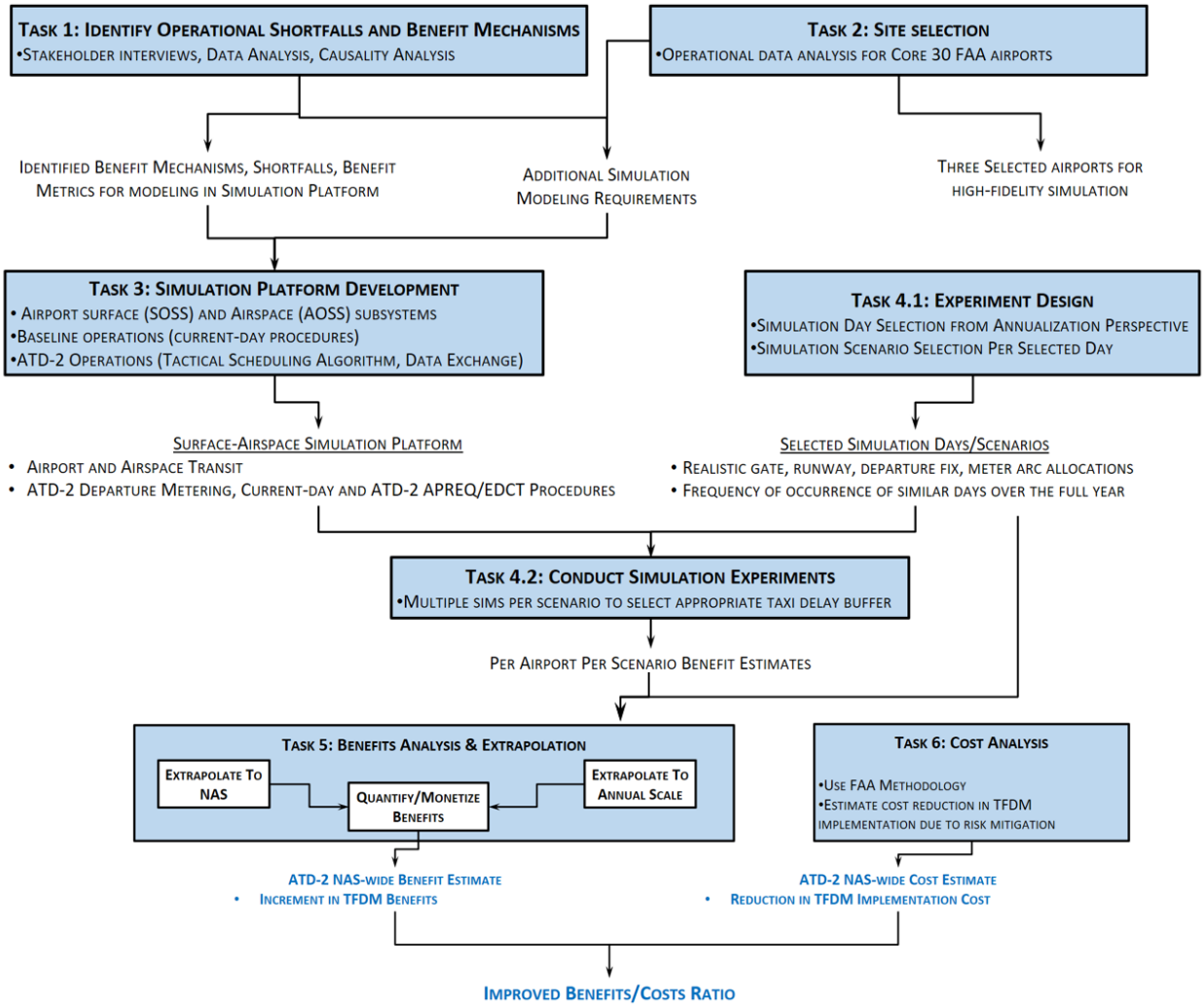

Figure 2. Project Technical Approach

In parallel with simulation platform development, Task 4.1 performed analysis of operational constraints (e.g., weather, Traffic Management Initiatives (TMIs)) and demand-capacity characteristics for the selected airports in order to carefully select a set of simulation scenarios, which will be representative of the conditions observed at the airports over the entire year. This resulted in the selection of a handful of simulation scenarios per airport along with multipliers for extrapolating the benefits results from simulations conducted for those scenarios to an annualized scale. Section 5 discusses this task.

Next, Task 4.2 conducted the simulation experiments for the selected scenarios using the developed simulation platform. Section 6 describes the results from these simulations.

After simulations at individual airports and the respective selected simulation scenarios were completed, we processed the simulation outputs to compute benefit metrics, monetize those metrics, and then extrapolate the computed benefits to a nationwide scale (i.e., estimate of the benefits of implementing ATD-2 at the FAA Core 30 airports) and to an annualized scale (i.e., estimate the total benefits that will accrue over the whole year). Task 5 (Benefits analysis & extrapolation), described in Sections 7 (nationalization) and 8 (annualization and monetization),

performed this benefits monetization and extrapolation. Task 6 (Cost Analysis), described in Section 9, followed the standard FAA prescribed methodology for estimating the ATD-2 implementation costs and what cost-impact ATD-2 will have on the implementation of the FAA's Terminal Flight Data Manager (TFDM) program. Finally, ATD-2 benefits were weighed against the ATD-2 costs and a return on investment analysis was performed. Section 10 describes the final results of the benefits costs analysis in addition to providing a self-contained summary of key outcomes from all the supporting tasks.

The rest of this document is divided into sections, each discussing the individual tasks shown in **Figure 2**, starting with Task 1 next. Each section is self-sufficient and if the reader wants to skip to a particular section of interest (e.g., Section 6 on the High-fidelity Simulation Results), he/she can do that without missing essential details. Moreover, Section 10 is a self-contained section, which summarizes the main results from each task and presents the final benefits and costs analysis. A reader, who is not interested in the details of the site selection, simulation development, and other tasks, can directly go to this section for obtaining the key outcomes of this research work.

2. TASK 1. IDENTIFY OPERATIONAL SHORTFALLS, ATD-2 BENEFIT MECHANISMS, AND ASSOCIATED BENEFIT METRICS

2.1. Overview

The overarching purpose of this NRA project was to assess benefits and costs of integrating arrival, departure and surface traffic management in metroplex regions. Our first step towards this goal was to perform comprehensive identification of (1) Operational shortfalls that ATD-2 can address, (2) Associated ATD-2 benefit mechanisms, and (3) Metrics that can be used to measure the associated benefits. We analyzed the operational shortfalls and benefit mechanisms related to the surface and airspace operations at all core 30 FAA airports, but special emphasis was placed on analyzing operations at key airport sites of importance including the three airports (CLT, DFW, and EWR) that we finally selected for detailed simulations.

2.2. Task Technical Approach

The following bullet points summarize our team's technical approach for identifying operational shortfalls and benefit mechanisms and mapping them to associated benefit metrics.

- Step 1: We leveraged past site visit reports, in-house SME know-how, and prior research experience to develop an initial characterization of operations at identified high-priority ATD-2 test sites: CLT, DFW, and EWR
- Step 2: After initial operations characterization, we conducted SME interviews to corroborate understanding of operations and to clarify any ambiguities.
- Step 3: Then, we performed formal derivation of shortfalls linking to ATD-2 benefit mechanisms and thereon to benefit metrics.
- Step 4: Finally, we conducted historical data analysis to quantify the identified benefit metrics for the core 30 FAA airports, with special emphasis on analyzing operations at CLT, EWR, and DFW.
- Step 5: We met with SMEs again to validate our identified benefit mechanisms and benefit metrics.

Next, we describe key findings from our analysis. We present the operational shortfalls that we identified for the three sites of interest first.

2.3. Identified CLT Operational Shortfalls Related to ATD-2

- CLT departures are frequently subject to controlled departure time restrictions due to APREQ or Call for Release TMIs imposed by the ZDC Center or other FAA facilities. Many departures are also subject to EDCT departure time restrictions due to active Ground Delay Programs at major destination airports. Many departures miss their APREQ or EDCT windows, which leads to congestion and delay problems downstream in the ZDC Center airspace, or at destination GDP airports.
- In addition, runway capacity is a limiting factor during heavy departure pushes. Coordinating runway departure time restrictions on multiple flights while maintaining sufficient departure demand pressure on the runway system and keeping the taxi-out times down becomes difficult for ground/local controllers during heavy departure pushes.

- There is no room for resequencing the departures after they have entered the movement area (because the movement area basically consists of a single taxiway). As a result, sequencing decisions have to be made well in advance, which does not always happen. This leads to inefficient sequencing of departures when they reach the departure runway.
- CLT has a large ramp area. Most of the taxi distance covered by departure flights is spent in the ramp area. After exiting the ramp areas, the departures line up along a single taxiway feeding the departure runway. Ramp transit introduces a large uncertainty in the total taxi-out time for departure flights. This taxi time uncertainty is introduced mainly because of the following constraints present in the ramp area: (1) There is a single-lane taxi-path near Terminals D and E, which is used in both directions. Frequent coordination is required to avoid head-on conflicts and gridlock situations in this region of the ramp, and excess time is spent in holding flights to let other flights cross the single-lane taxi-path. (2) Departures pushing back from certain Terminal areas (e.g., C and D) push back directly into the path of flights taxiing in the ramp area towards their departure runway or gate. Uncoordinated pushbacks from these terminal areas delay the ramp taxi process for other flights.
- Uncertainty in the Earliest Off Block Times (EOBTs) provided by the airlines to a departure metering tool is another shortfall, which prevents the departure metering tools from reliably estimating the runway system demand and computing efficient gate-hold delays.
- CLT has frequent overlapping departure and arrival banks. Gate conflicts occur when the previous arrival bank overlaps with a departure bank. In such cases, coordination is required to reroute arrival flights to hardstands until their gates are available, and/or expedite the pushback of the departure flight.

2.4. Identified DFW Operational Shortfalls Related to ATD-2

- A frequent problem faced by DFW TRACON controllers is that departure demand may quickly increase without warning. In such situations, terminal departure controllers have a very limited time window to react to the changes, since flights transition very quickly from the near-airport airspace into the TRACON airspace. There exists no TRACON decision support tool to plan for the upcoming demand and assist the terminal departure controllers in managing the unpredictable flow.
- DFW Tower determines departure runway-fix mapping (departure split) to balance runways; it does not consider traffic of DAL or satellite airports. DFW departures have free release, whereas departures from neighboring airports are usually required to call and request approval for departure. This leads to unfairly large delays for neighboring airport departures in times of departure-fix capacity constraints.
- DFW East runway departures do not use West side fixes and vice-versa; release coordination is required between towers if crossing (e.g., Southeast or Southwest fixes from west runways).
- DFW departures via 13L have been halted since they were deemed unsafe with DAL operations.
- NASA analysis of MIT operations at the DFW TRACON [CE11] showed that during July 2013 average departure delay due to miles-in-trail restrictions was much bigger than

average delay due to Outbound (overhead stream merge) and Inbound (TMA at IAH) departure scheduling. Figure 3 shows that under MIT operations, delays were more than five times bigger as compared to Inbound and Outbound scheduling operations.

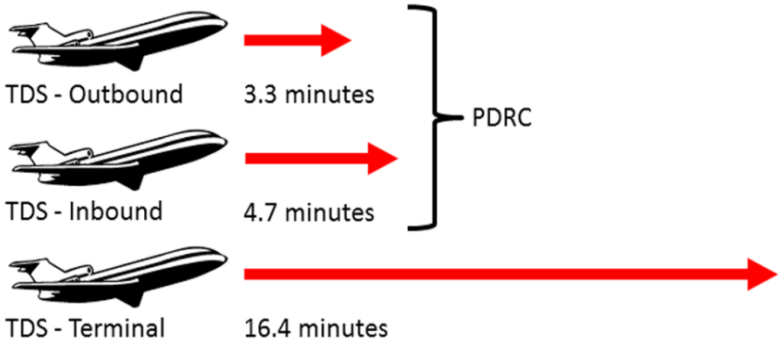

Figure 3. MIT operations led to much larger delays as compared to Inbound and Outbound scheduling operations at the DFW TRACON [CE11].

2.5. Identified EWR Operational Shortfalls Related to ATD-2

- Interactions between EWR Airport and the other airports in N90 result in a substantial number of departures held at sub-optimal altitudes because of surrounding traffic and airspace stratification (e.g., EWR departures held down due to overflying arrivals to LGA).
- Time-share constraints between TEB arrivals and EWR departures require coordination, increase workload, reduce through-put, and increase delays.
- Demand for use of departure fixes from departures from HPN and TEB reduces throughput and increases delays at EWR for departures filed for WAVEY and WHITE.
- In general, departure-fix sharing and merging constraints are the dominant constraints in the New York TRACON, more restrictive than any downstream en route merge constraints

Next, we outline the ATD-2 benefit mechanisms that we identified and discuss how they contribute to alleviating the operational shortfalls discussed above.

2.6. ATD-2 Benefit Mechanisms

The first step towards identifying ATD-2 benefit mechanisms was to identify what functional capabilities the ATD-2 system consisted of. The ATD-2 concept will be implemented and demonstrated in three phases, gradually adding more functions and attributes. We identified the following ATD-2 functions for each implementation phase based on review of the ATD-2 concept documents [N16]. While the ATD-2 concept is mature for the first phase, the second and third phases were under planning during the timeframe of Task 1 work, and are therefore described in less-precise terms.

ATD-2 Phase One functions and attributes

1. Update of the flight Estimated Off-Block Time (EOBT) by the Flight Operator (FO)
2. Estimate unimpeded travel using trajectory-based model

3. Generate runway schedule using First Come First Served (FCFS) policy, restriction time slots, and order of consideration
4. Specify critical flights by FO
5. Compute pushback times by applying delay margins per taxi segment
6. Automatic and semi-automatic call for release coordination between the tower and center
7. Dynamic closed loop control of pushback times

ATD-2 Phase Two functions and attributes

1. Meter flights at gate strategically
2. Connect to Time-Based Flow Management (TBFM) by scheduling departures from the major airports
3. Provide situational awareness to TRACON
4. Provide IADS information via Electronic Flight Strips (EFS)

ATD-2 Phase Three functions and attributes

1. Coordinate schedules between metroplex airports at departure fixes
2. Connect to TBFM by providing better information on internal departures from metroplex airports
3. Integrate tactical scheduling with EFS

Next, we outline the relevant benefit mechanisms for the three phases of the ATD-2 project.

Benefit Mechanisms for Phase One

1. The ATD-2 system receives updates of the flight Estimated Off-Block Time (EOBT) from the Flight Operators (FO) and uses them in its runway Estimated Time of Arrival (ETA) computations. More accurate EOBTs provide the ATD-2 system with more accurate start times for its runway ETA estimation. More accurate ETAs mean that the Target times computed by the ATD-2 Tactical Scheduler will be more reliable and more frequently achievable by the controlled flights. As a result, this benefit mechanism enables
    a. Increased runway and departure fix throughput
    b. Reduced taxi-out delay
    c. Reduced fuel burn
    d. Better conformance to controlled departure times
    e. Decreased controller workload (because more accurate ETAs lead to more achievable Target Takeoff Times (TTOTs) and hence lesser chance of missed slots, thus requiring less back and forth coordination between the tower and the Center

2. ATD-2 unimpeded taxi transit using trajectory-based model. Again, as in #1, this benefit mechanism manifests itself via more accurate runway ETAs. So, its benefits are the same as the ones listed under #1.
3. The ATD-2 Tactical Scheduler generates runway schedules using order of consideration and ration-by-schedule runway target time allocation. The order of consideration algorithm gives higher priority to flights impacted by APREQ or EDCT constraints, to flights that have more accurate EOBTs, as well as to flights that are closer to the runway takeoff in their taxi transit process.
    a. Better conformance to controlled departure times
    b. Reduced taxi-out delay and increased runway/departure-fix throughput, since the scheduler enables better runway departure sequences that can get the flights off of the airport surface faster.
    c. Reduced controller workload (no need for manual coordination of APREQ/EDCT times)
    d. Increased user satisfaction. Airlines are able to save delays on their most valuable flights by specifying a higher priority in the order of consideration for these flights.
4. The ATD-2 system computes Target pushback times for departures by back-computing from TTOTs while applying delay margins, per taxi segment. TOBTs or TMATs are computed, which, if closely adhered to, shifts the delays from the movement area to the ramp area, and many times right back to the gate.
    a. The TOBTs and TMATs effectively push the delay from the movement area to the ramp area and the gates. Reduced fuel-burn is the main manifestation of this benefit mechanism.
    b. Less movement area taxiway congestion and consequently lower workload for ground controllers
5. The ATD-2 system enables dynamic, closed loop control of pushback times via its Ramp Traffic Console tool. This enables the ramp controllers to closely monitor flights that are under different pre-pushback statuses including ready for pushback waiting for clearance, ready but holding because of ATD-2 delay, and not ready for pushback. The Ramp Traffic Console also enables the ramp controllers to closely adhere to the ATD-2 Tactical Scheduler-generated TOBTs when pushing back aircraft. As a result, the flow of departure traffic coming out of the ramp area is more predictable and metered to the correct flow rate for enabling sufficient pressure on the runway system while minimizing taxi-out times. The resultant benefits include
    a. Reduced taxi-out times
    b. More predictable taxi-out times
    c. Less movement area taxiway congestion and consequently lower workload for ground controllers
    d. Better adherence to controlled departure time windows

Benefit Mechanisms for Phase Two

1. In Phase Two, the ATD-2 system is expected to integrate strategic departure metering with the Phase One Tactical ATD-2 scheduler. Strategic departure metering will provide the airlines and the tower controllers, as well as receiving Center traffic managers, with a reliable estimate of expected future departure traffic flows. This will enable the decision-makers to wisely choose the settings for ground departure metering programs as well as airspace TMI restrictions such as APREQs and MITs. The expected benefits ensuing from this mechanism are
    a. Reduced ATD-2 gate hold-delays while maintaining smaller taxi-out times
    b. Reduced frequency and severity of APREQ and MIT restrictions
    c. Better predictability of runway departure flows
2. In Phase Two, the ATD-2 system is expected to integrate airport surface traffic scheduling with en route airspace scheduling components of the TBFM system under the Integrated Departure Airspace Concept (IDAC). With this capability in place, a two-way benefit will be achieved—airport surface traffic planning (e.g., ATD-2 Tactical Scheduler) will be able to consider a more accurate picture of airspace constraints when determining the runway schedules and sequences, and Center airspace planning (e.g., TBFM metering) will be able to consider a more accurate estimate of expected departure flows when determining Scheduler Times of Arrival (STAs) at key airspace fixes. This two-way coordination will enable smooth, un-delayed transit for departure flights from gate to en route traffic stream merge. The benefits resulting from this mechanism include
    a. Reduced airborne delays
    b. Increased conformance to the available merge-slots at the real constraint point (i.e., en route stream merge point), which is better from the perspective of delay management than increased conformance to controlled runway takeoff time windows
    c. Increased predictability of metroplex-wide operations
3. In Phase Two, the ATD-2 system is expected to start providing IADS scheduling information of electronic flight strips (EFS), which will lead to controller workload reduction and enhanced operational record-keeping benefits

Benefit Mechanisms for Phase Three

1. The ATD-2 system is expected to expand its scheduling capability to coordinate schedules between metroplex airports at departure fixes. This will provide the additional benefit of reduced taxi-out delays caused by departure-fix sharing constraints, especially in metroplexes such as New York TRACON.
2. In Phase Three, the ATD-2 system is expected to connect to the TBFM system by providing better information on internal departures from metroplex airports. The benefit accrued by this mechanism is reduced occurrence of double penalty delays, where a flight is first delayed at the origin airport because of a destination airport constraint and further delayed again at entry to the destination airport TRACON due to arrival congestion.

3. Phase Three is expected to fully integrate Tactical scheduling with EFS. This benefit mechanism is expected to provide reduced controller workload, as well as improved scheduling effectiveness because of new data-streams available to the scheduler (e.g., more up-to-date information about EOBTs, informed decisions based on quality of available data).

2.7. Mapping of Operational Shortfalls to Benefit Mechanisms and Benefit Metrics

After the operational shortfalls and benefit mechanisms were identified, our next step was to develop metrics for measuring the beneficial impacts of the ATD-2 system, specifically in relation to the identified shortfalls and benefit mechanisms. Based on our characterization of operational shortfalls and benefit mechanisms, and our understanding of the general simulation-based benefits assessment framework, we developed a list of metrics to measure the associated benefits of ATD-2. We list these metrics next, in the form of two tables: **Table 1** lists all the identified metrics and **Table 2** links shortfalls and benefit mechanisms to these metrics.

Table 1. Table of Metrics

Metric #	Metric
1	Taxi-Out Duration
2	Taxi-In Duration
3	Taxi-Out Delay
4	Taxi-In Delay
5	Taxi fuel consumption
6	On Time performance
7	Taxi Stops, Number, Location
8	Taxi Stops, Duration
9	Departure Queue Length
10	Taxi-Out Time Variance
11	Takeoff Time Prediction Accuracy
12	Departure Throughput
13	Scheduled Demand vs. Actual Throughput
14	Pushback time predictability
15	Arrival Throughput
16	Departure Fix Usage Efficiency
17	APREQ Compliance Rate
18	EDCT Compliance Rate
19	Target Time Compliance to ATD-2 Times
20	User Acceptability
21	Controller Workload

22	User Workload
23	Pass Back Delays
24	Level-flight sections
25	Blue-sky gridlock due to early arrivals
26	Sequence jumps between gate pushback, ramp exit, and runway entry
27	Degree to which departure sequence includes/does not include interleaving of departure-fix assignments
28	Airline direct operating cost
29	Airborne Transit Time Variance (runway takeoff to en route traffic stream merge)
30	Delay causality
31	On Time Performance (Pushback, Runway Takeoff)
32	On Time Performance (Landing, Gate In)
33	Airborne delays at destination airport for fitting into TBFM arrival flows
34	Arrival Throughput at ATD-2 airport
35	Gate availability at end of taxi-in
36	Excess in-trail separation at constraint point (departure-fix or en route merge fix)

Table 2. Mapping Shortfalls/Benefit Mechanisms to Metrics

Item #	Shortfall	Impact	Immediate Cause(s)	ATD-2 Benefit Mechanism(s)	Metric
1	Delay due to MIT or MINIT restriction over a departure fix	Excess taxi time, excess fuel burn, ADOC, excess passenger time, excess merging workload for TRACON controllers	Wrong sequence in departure queue (i.e., flights going to the MIT-impacted departure fix/flow in consecutive order	(1) Sequence control via TOBTs and TMATs (2) Improved ramp traffic management tools (3) Improved situational awareness about TMIs impacting individual flights (4) Improved Local/TRACON/Center controller situational awareness about expected demand	#9, #26, #27, #3, #16, #28, #21

2	Excess block time buffer	Lower aircraft utilization; Lower airline profitability	Unpredictable transit time from gate to takeoff and from takeoff to en route stream merge - motivates airlines to pad their schedules	(1) Improved accuracy of OFF time predictions (2) Metering of flights at gates and ramp holding areas reduces movement area congestion and keeps departure queues shorter - thereby making taxi-out times more predictable	#11, #10, #29, #3, #7, #30
3	Non-compliance to TMIs (EDCTs and APREQs)	Airborne delays at the downstream constraint point (departure fix, en route merge-point, TMA metering arc); Excess merging workload for en route controllers	Lack of awareness about TMIs impacting individual flights; impacted flights leaving gates/ramp area too early and merging into departure queue in wrong sequence	(1) APREQ/EDCT delay absorption at gate or in ramp via TOBTs and TMATs (2) Overall, shorter departure queues reduce Local controller's workload (3) Improved accuracy of OFF time prediction (enables TRACON and Center controllers to predict demand with more certainty)	#17, #18, #29, #32, #33, #21
4	Excess departure queue length (site-specific/configuration specific length or duration-through-queue)	Longer taxi times, difficulty in achieving departure-fix sequences and/or APREQ times and MIT spacing	Lack of control on the sequence of merge onto final taxiway where the departure queue builds	(1) Sequence control via TOBTs and TMATs (2) Management of queue sizes via gate holds and ramp area holds	#9, #12, #27
5	Delays due to re-filing for new departure fix (mitigated by data comm?)	Unnecessary taxi delays, disruption of departure-fix sequences due to late departure of a flight expected to takeoff earlier, under-utilization of runway and departure-fix capacity	Manual communication delays; lack of complete situational awareness at early stages in a flight's gate-to-runway transit	(1) Improved situational awareness about reassigned departure fix, early on in a flight's transit (alternative route known potentially while the flight is still at the gate) (2) Improved sequencing and scheduling which considers alternative allocated departure routes (3) Potential combined route assignment and scheduling	#3, #5, #7, #8, #13, #16, #21, #22

6	Excess taxi-out saltation (fuel burn) due to start/stop behavior	Excess airline fuel costs, increased uncertainty in gate-to-en route merge transit times causes airlines to set larger block time buffers	Long departure queues, congestion on the taxiway system	(1) Management of queue sizes via gate holds and ramp area holds	#3, #5, #7, #8
7	Excess arrival holding if airport is congested with mixed runway use configuration	Poor arrival on time performance for ATD-2 airport	Inefficient sequence of runway departures	(1) Sequence control via TOBTs and TMATs	#2, #34
8	Blue-sky grid-lock due to early arrivals	Poor arrival on time performance, congestion in the ramp area	Long gate holds for high utilization gates	(1) Sequence control via TOBTs and TMATs	#4, #35
9	Excess flight duration/distance to merge into main traffic flow	Excess fuel burned, increased airline costs	Lack of situational awareness about airspace constraints, lack of coordination for departure-fix or en route merge fix usage	(1) Sequence/timing control via TOBTs and TMATs	#29, #28
10	Underused departure capacity (# actual departures per unit time < typical service rate), both at runway and at downstream merge-points	Unnecessary surface delays	Larger than required gate delays starve the departure runway	(1) Scheduling algorithm with delay buffer	#12, #16, #13
11	Poor AIBT, ALDT punctuality at destination	On-time performance degradation	Non-compliance with required runway takeoff times	(1) Integration of APREQ times into scheduling algorithms	#32, #28

12	Loss of network capacity	Network disruption, increased airline costs	Lack of coordination for usage of shared airspace resources	(1) Integrated airspace and surface scheduling (2) Improved situational awareness about TMIs due to airspace constraints	#12, #13, #23, #16, #28
13	Inadvertent imposition of pass-back delays	Unnecessary surface delays, increased airline costs	Lack of flexibility in applying TMIs arising from en route or departure-fix constraints	(1) Time-based scheduling to control TOBTs and TMATs instead of rate based TMIs	#36, #13, #23, #16, #28

2.8. Identified Simulation Capability Requirements for Modeling ATD-2 Benefit Mechanisms and the Associated Shortfall Alleviation

The detailed analysis of operational shortfalls and benefit mechanisms discussed in this section allowed us to develop requirements for simulation capabilities required in the simulation platform for enabling a realistic benefits analysis of the ATD-2 system. We identified that in addition to realistic modeling of standard features of an airport surface simulation such as taxi routes, gate/runway/first fix allocations, airline schedules, runway minimum separations, etc., credible assessment of ATD-2 system benefits needs a simulation platform that contains the following features:

- Includes models of baseline, current-day procedures for implementing APREQ procedures, including the coordination between the airport tower and the receiving Center for fitting planned departures in a Time Based Flow Management (TBFM) meter arc
- Includes models of baseline, current-day procedures for implementing miles-in-trail restrictions at runway takeoff as well as modeling of the ground controller sequencing for avoiding consecutive departures going to the same constrained departure fix
- Includes models of current-day procedures for implementing Expect Departure Clearance Times (EDCTs) for ground delay program (GDP) impacted flights
- Includes a model of the ATD-2 Tactical Surface Scheduler with the full details of its internal scheduling, prioritization (order of consideration), earliest runway usage time prediction, delay back propagation, etc. steps
- Includes models of the transit of departure flights after they takeoff from the airport including merging into the overhead traffic streams at the departure-fix and at the TBFM meter arc

As we will discuss in Section 4 our simulation environment satisfies all the requirements identified here. Next, we discuss the task of selecting airport sites for detailed simulation-based benefit assessment.

3. TASK 2. SELECT SITES FOR DETAILED SIMULATIONS

As discussed above, our ATD-2 benefits estimation approach involved conducting detailed simulation based analyses at three carefully chosen airport sites. Results from detailed simulations at three sites were to be extrapolated to a nationwide scale (covering the FAA Core 30 airports) and an annualized scale. With this objective in mind, we sought to select three airport sites that possess the following desirable characteristics:

- They are distinct from each other in terms of the nature of their departure operations (nature of constraints, current-day departure management procedures, current-day delay impacts, etc.) and in terms of the impact that ATD-2 functions will have on their operations
- They together contain a wide variety of operational characteristics and ATD-2 related shortfalls to allow extrapolation of benefits from application of ATD-2 simulations at the three selected airports to the FAA Core 30 airports

Special consideration was given to the operational features that are relevant to current-day departure traffic management shortfalls, including:

- Observed high taxi-out delay levels
- Observed high taxi-out time variability
- Observed long departure queue lengths
- Mixed-use, intersecting, and closely-spaced parallel runways
- Varying ramp area types, some very constrained
- Significant departure airspace constraints such as departure-fix sharing, merging into busy overhead en route traffic streams, etc.
- Frequent imposition of external traffic management restrictions on departure flows such as miles-in-trail (MIT) restrictions or Approval Request (APREQ) restrictions

We first identified key site selection factors by which to evaluate and categorize a wide range of airports. Next, we determined metrics to evaluate the significance of each selection factor across various airports. We evaluated these metrics at the FAA Core 30 airports. For this evaluation we used recorded FAA Aviation System Performance Metrics (ASPM) data, Airport Surface Detection Equipment-Model X (ASDE-X) data (from NASA's Sherlock ATM data warehouse), analysis of airport maps and satellite photos, as well as our team's expertise and past work on airport operations analysis. Based on these metrics, we identified the degree to which each selection factor is prevalent at each of the Core 30 FAA airports. Finally, examining the factors, which are significant at each airport, we chose three airports that together cover a wide array of dissimilar operational features as well as stand to benefit significantly from the implementation of ATD-2 technologies.

Based on our analysis, we selected Newark Liberty International (EWR), Dallas Fort Worth International (DFW), and Charlotte/Douglas International (CLT) as the three airport sites of interest for detailed simulation-based analyses. The selected airports cover all the important features we have identified as outlined below:

- EWR has unique runway interaction geometry with one pair of closely spaced parallels as well as an intersecting runway, with arrivals required to cross an active departure runway to reach the terminal gates. EWR displays high variability in taxi-out times and gate pushback times as well as a high level of taxi-out delay and taxi-stop duration. Our analysis of airport runway capacity saturation shows that EWR operates under departure capacity saturation for around 80% of the time (based on normalized operation-time under departure saturation). Only two FAA Core 30 airports (LGA and PHL) spend a higher percentage of time under saturation than EWR. Also, EWR experiences higher local queuing delays relative to delay generated due to downstream restrictions or nominal sequencing activity. EWR is also the 2nd ranked airport in terms of the estimated potential to benefit from departure metering technologies as per our analysis (which looked at potential taxi-out delay savings as well as fuel savings that could result from departure metering). Moreover, EWR displays high levels of departure-fix sharing, departure flight altitude level-off inefficiencies, and local departure restrictions severity/frequency.
- DFW differs significantly from EWR in terms of its airport geometry and departure airspace configuration. Its runway system has relatively lower cross-runway interaction-impacts; the only dependencies are between arrivals and departures using closely-spaced parallel runways, and arrivals crossing an active departure runway to reach their gates. DFW displays medium levels of taxi-out delay, taxi stop duration, taxi-time variability, gate pushback time variability, and time spent under departure capacity saturation. DFW displayed a very low taxi-out time savings potential and medium fuel savings potential to benefit from departure metering. External departure restrictions and departure flight level-offs are significant constraining factors in the D10 TRACON airspace. D10 displays only a medium level of departure-fix sharing between DFW and other neighboring airports.
- CLT also displays an interesting but different runway interaction geometry—with independent parallel runways, an intersecting arrival-departure runway pair, mixed-use departure-heavy runway, and a large ramp area. CLT displays high taxi-out time variability, low gate pushback time variability, high taxi-out delay, high taxi stop duration, medium percentage of time spent under departure capacity saturation, and medium level of potential to benefit from departure metering in terms of taxi-out time savings and fuel savings. In terms of airspace constraints, CLT has almost non-existent departure-fix sharing and a small degree of TRACON departure altitude level-off inefficiencies, but a high level of external tactical departure scheduling constraints coming from neighboring Centers, as well as from Time Based Flow Management (TBFM) metering for the busy ATL arrival stream.

Next, we summarize the historical data analyses that we conducted for generating the selection factors discussed above. Details of the data analyses can be found in [ATAC17-2]. First, we describe our overall technical approach for site selection factors computation and then describe important selection factor metrics generation approaches and results.

3.1. Site Selection Factors Computation Approach

The following bullet points summarize our team's technical approach for computing the site selection factors.

- Step 1 collected a comprehensive set of historical operational metrics that are relevant to the selection of sites for detailed simulation-based evaluation of ATD-2 departure metering technologies. Our team identified these metrics using its deep expertise in analyzing airport operations.
- Step 2 leveraged our team's extensive data repository, as well as our past data analyses to compute the identified metrics using datasets that cover an extensive range of operations. For most of the metrics we looked at one month of historical operational data or more.

Next, we describe some of the important metrics from site-selection perspective. Note that we computed the metrics and characterized the selection factors for all Core 30 airports, but in the discussion we will present results for the three selected airports (CLT, EWR, and DFW) at a higher level of detail than the other Core 30 airports.

3.2. Characterization of Departure (Taxi-Out) Delays at FAA Core 30 Airports

Perhaps the most significant site selection factor—a must-have in an airport site selected for studying impacts of departure metering—is the presence of significant departure delay. Departure delay manifests in different forms – (i) taxi-out delay, (ii) number and duration of taxi stops, (iii) saturation of runway departure capacity, and (iv) excess queuing for constrained resources (such as departure runways). To evaluate the significance of departure delay at each candidate airport, we examine metrics related to all four of these manifestations.

3.2.1. Characterization of Taxi-Out Delay

Presence of significant taxi-out delays signifies inefficiencies or shortfalls in the management of taxiing traffic on the airport surface. In order to perform the analysis of taxi-out delays, we studied the nominal taxi patterns at the airports under study and identified the most-used ramp exit-to-departure runway combinations. For each combination, we calculated the distribution of movement area taxi-out times (runway entrance time minus spot crossing time). End-to-end stitched trajectory data from NASA's Sherlock ATM data warehouse were used to compute these times. The tenth percentile movement area taxi-out time was computed and assumed to represent the unimpeded taxi-out time for each ramp exit-point and departure runway pair. The difference between the actual and the tenth percentile taxi-out time thus represents the movement area taxi-out delay. Similar computations were performed to compute the gate to runway takeoff taxi time using OUT and OFF times available in the Aggregate Demand List (ADL) data. OUT and OFF times were available for only a small percentage of all departure flights.

Next, we present the metrics for the three selected airports and the remaining FAA Core 30 airports. **Figure 4** shows the mean OUT to OFF taxi-out delay and the mean Spot to Runway taxi-out delay (i.e., Active Movement Area, AMA taxi-out delay) for each of the Core 30 FAA airports, computed as per the definition above.

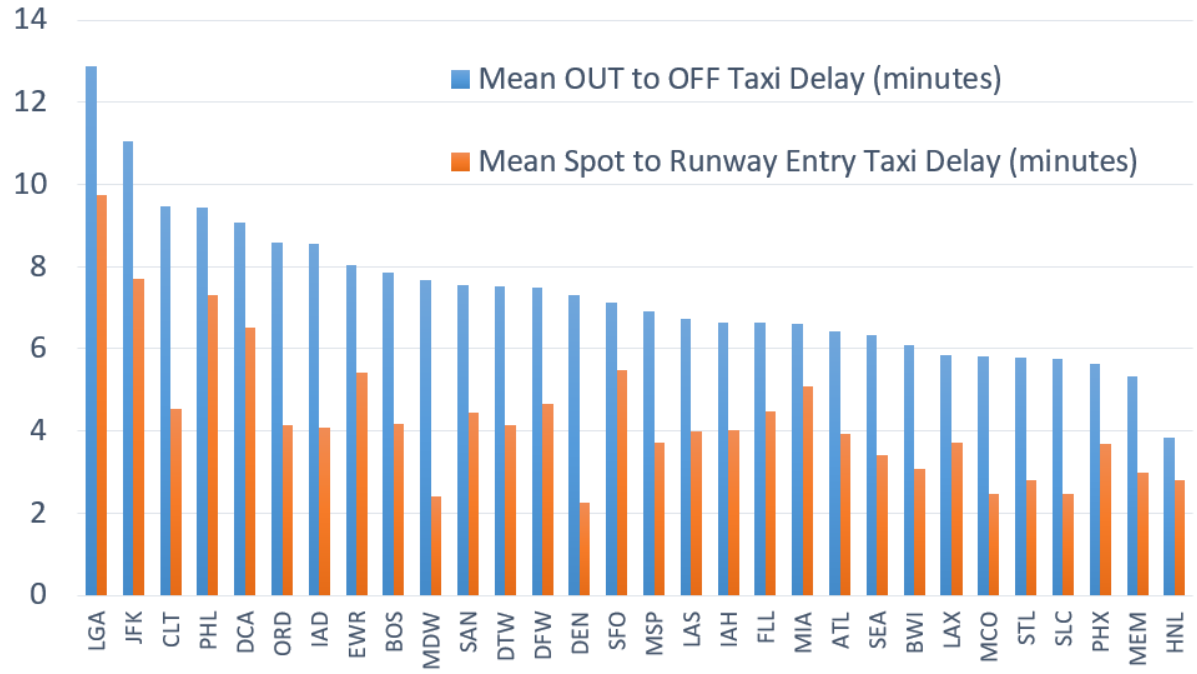

Figure 4. Taxi-Out Delay Characterization for Core 30 FAA Airports

Figure 5 shows the Standard deviation of total and AMA taxi-out time delays for the Core 30 FAA airports

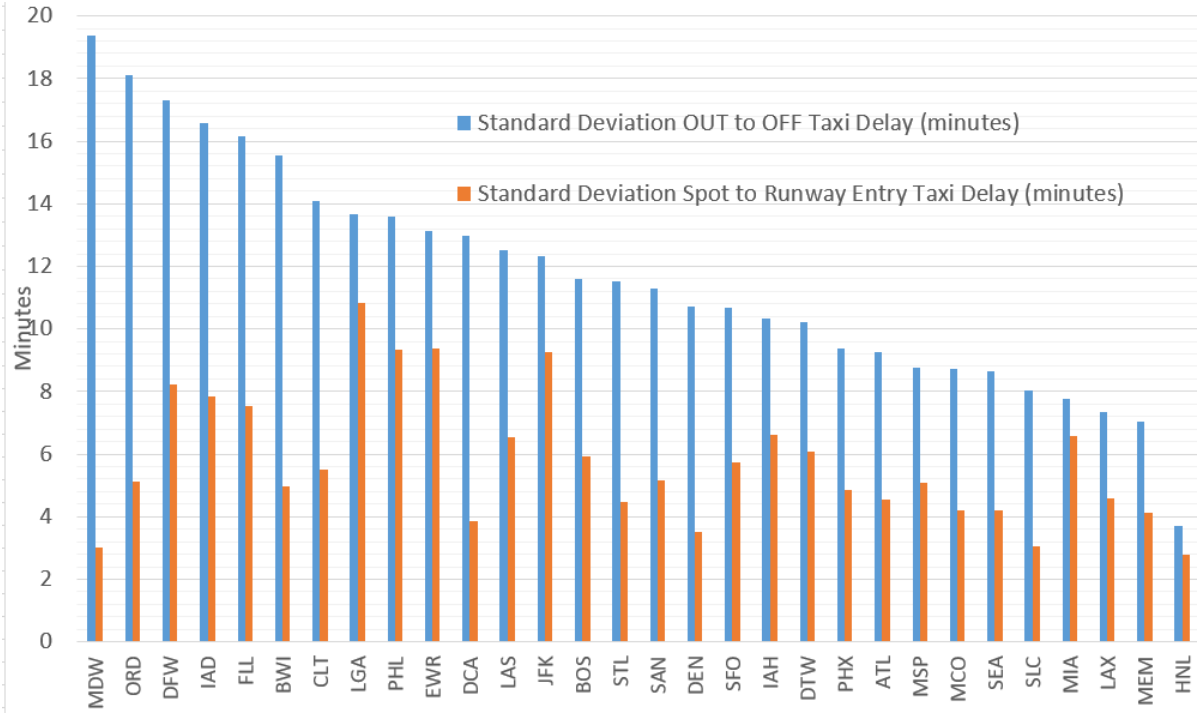

Figure 5. Characterization of the Predictability of Taxi-Out Times at the FAA Core 30 Airports

As seen from the Figure above, all three chosen airports display significant taxi-out delays and hence are good candidates for efficiency benefits evaluation of the ATD-2 system. Moreover, all three chosen airports display significant variance in their taxi times and thereby are also good candidates for evaluating the predictability benefits of ATD-2.

3.2.2. Characterization of Taxi-stops

Stopping on the airport surface is another indicator of shortfalls in current-day departure traffic management procedures. For analysis of taxi stops, we processed ASDE-X surface component of the end-to-end stitched trajectory data from NASA's Sherlock ATM data warehouse using surface track data filtering methods developed by ATAC. **Figure 6** shows the average count and duration of taxi-stops per flight at all the ASDE-X airports we analyzed.

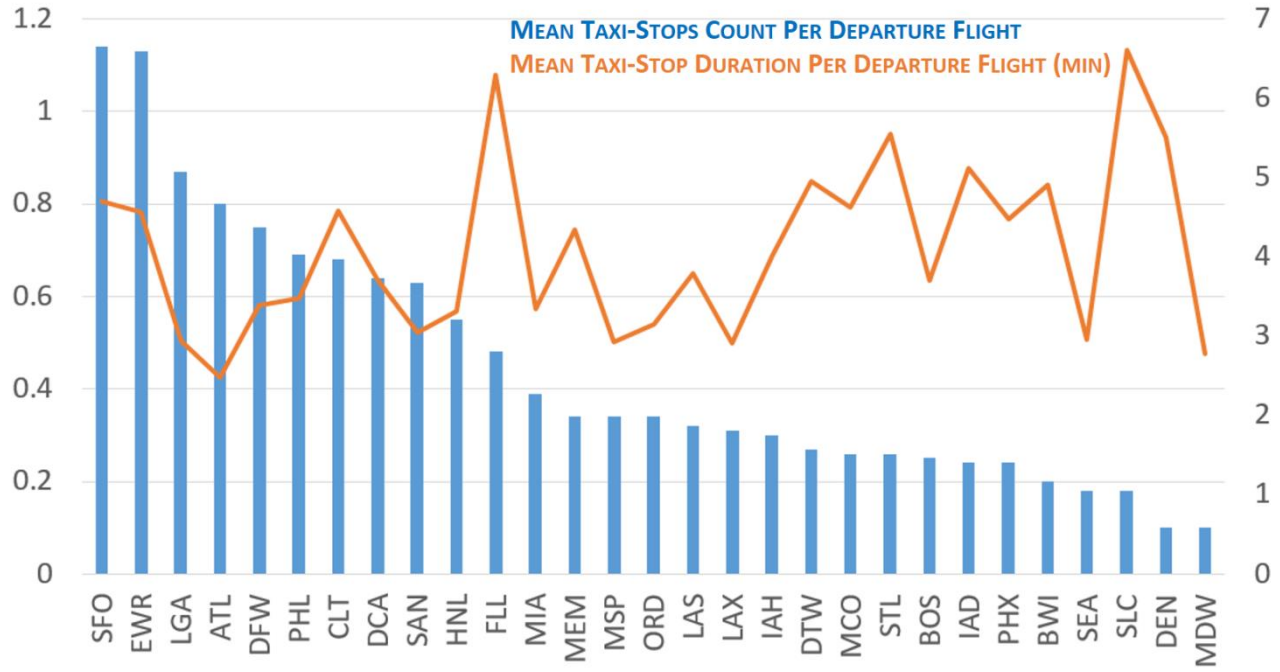

Figure 6. Mean Count and Duration of Taxi-Stops Per Departure Flight at ASDE-X Airports

As seen from the figure, the three chosen airports are in the top 10 of the airport list as sorted by the average count of taxi stops per departure. When sorted by the average taxi stop duration, EWR and CLT still fall within the top 10 airports. DFW falls back to rank 19 in this sorting order. So, it is clear that the representative airports capture a good level of variability in terms of taxi stops.

3.2.3. Characterization of Departure Throughput Saturation and Queuing & Sequencing Behavior at FAA Core 30 Airports

In this section, we compare the airports in terms of departure delay that is generated due to runway capacity limitation. We attempt to isolate this delay from departure delays that are caused by other factors such as downstream restrictions. This analysis is based on previous research that was conducted to identify the main choke points in the NAS [I15]. For each of the 77 airports reported in the ASPM database, a throughput saturation analysis was conducted to characterize and measure if and how often demand exceeded the capacity of the airport. First the modeling approach is described followed by the analysis results.

3.2.3.1. Modeling Approach

The historically reported throughput was plotted against the historically reported demand for each airport, as shown in Figure 7 for CLT. The throughput is plotted on the vertical axis and the demand is plotted on the horizontal axis. For this analysis, one plot was generated for each airport using the full 2012 fiscal year, without distinction between runway configuration and meteorological conditions.[1] The throughput plotted on the vertical axis was measured every minute as the number of departures in a time window which was set at twenty minutes. The demand plotted on the horizontal axis was measured every minute in two ways. In the left plot it was measured as the number of departures that pushback according to the reported OUT time in ASPM but did not take off yet according to the reported OFF time in ASPM. In the plot on the right side, it was measured as the number of departures that were due to take off but had not yet taken off at the time at which the demand was measured. To estimate when an aircraft was due to take off, the unimpeded travel time reported in ASPM was used. For departures, a flight was assumed to be due to take off at its reported pushback (OUT) time plus the unimpeded taxi-out time reported in ASPM. The throughput measurement was plotted at a time offset (the variable delta in the figures) from the demand measurement. The offset was selected for each airport as zero, five, or ten minutes. The offset that resulted in the highest correlation between the demand and the throughput was selected. In the examples, the offset (delta) is shown in the title of each plot.

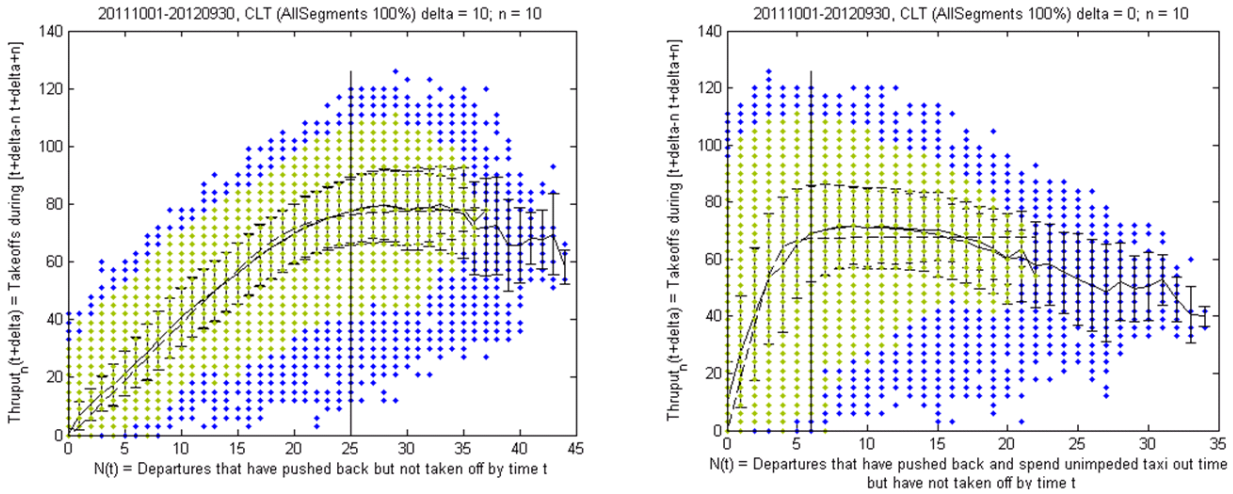

Figure 7. Throughput saturation analysis for CLT

The average throughput is computed at each demand value and connected with a solid line in each plot. Error bars show the variation in throughput at each demand value. As shown in Figure 7, the average throughput increases as demand increases, then saturates as the demand grows to values that exceed the throughput capacity. In order to identify and quantify the saturation of the throughput at high demand values, a hyperbolic curve was fitted to the average throughput versus demand data (dashed line in the Figure). The curve asymptotes toward a constant throughput value as demand tends to infinity. Before performing the curve fit, the least frequent throughput-demand pairs were eliminated as outliers representing rare and off-nominal conditions. (The removed pairs are the blue dots in the Figure and constitute 0.5 percent of all pairs.) The remaining pairs (green

[1] The analysis is designed to generate these plots per runway configuration and instrument/visual flight rules (IFR/VFR) conditions; however, due to the large number of airports analyzed this was not conducted in this analysis.

dots in the figures) were the only ones used in the curve fitting. The filtering excluded pairs of high demand and low throughput. These pairs represent off-nominal conditions, such as airport closure or bad weather events, where high demand accumulated due to lack of throughput. The filtering also excluded pairs of high throughput at all demand levels. These pairs represent rare reports of runway over-utilization.

The vertical lines in Figure 7 indicate where throughput saturation was assumed to occur in this analysis. The following criteria were used to identify the existence of throughput saturation and the saturation point along the fitted hyperbolic curve (the vertical line in the figures):

(1) The horizontal asymptote at high demand is below a threshold percentile throughput (which was set at the 95th percentile) and

(2) The slope of the curve flattens below a threshold (which was set at 0.05) which was taken as the location of throughput saturation.

These same criteria were applied consistently to all airports for comparison.[2] As shown by our analysis, EWR departure throughput saturated at thirteen departures on the surface and four departures in the runway queue (i.e., four departures have pushed back and traveled the nominal taxi-out time). DFW saturated with twenty-three on the airport surface and four departures in the runway queues, and CLT saturated with twenty-five departures on the surface and six departures in the runway queues.

3.2.3.2. Throughput Saturation Results

The airports were ranked based on three metrics: (1) the amount of time spent under saturation, (2) the amount of operations-time spent under saturation, and (3) the percentage of operations-time spent under saturation. Saturation meant that the demand was larger than the saturation point – the vertical line in Figure 7 indicating where saturation was observed – at each airport given the criteria used for the analysis. For this analysis, the threshold of the number of departures in the runway queue (the plots on the right side) was used. Figure 8 shows the airports that exhibited departure saturation, ranked based on the second metric (i.e., the percentage of operations-time spent under saturation).

Thirty-four of the seventy-seven airports exhibited departure throughput saturation. While LGA spent the largest amount of time under departure saturation, ATL led the airports in terms of the total operations-minutes under saturation. This indicates that there is higher probability to find LGA undergoing departure saturation at any time than ATL, which is expected since LGA runs departure queues almost all day. However, when the time spent under saturation is multiplied by the number of departures in the queue, ATL leads all the airports, followed by ORD. The other airports follow as shown in Figure 8. When the number of operations-time under saturation is normalized by the total amount of operations-time experienced at each airport, LGA takes the lead again, followed by PHL, EWR and IAH, ahead of ATL, ORD and JFK.

Comparing the three airports considered for the ATD-2 benefits assessment:

1. EWR spends a lot of time under saturation, followed by DFW and then CTL. Therefore, it is more likely for a flight to encounter a departure queue at EWR and DFW.

[2] The results are clearly sensitive to these criteria; however, the criteria were not varied in the analysis due to the large number of airports analyzed.

2. EWR exhibits significantly more departure-time under saturation than DFW and CLT. EWR can be classified as exhibiting high departure-time under saturation, while DFW and CLT are similar and exhibit moderate departure-time under saturation.

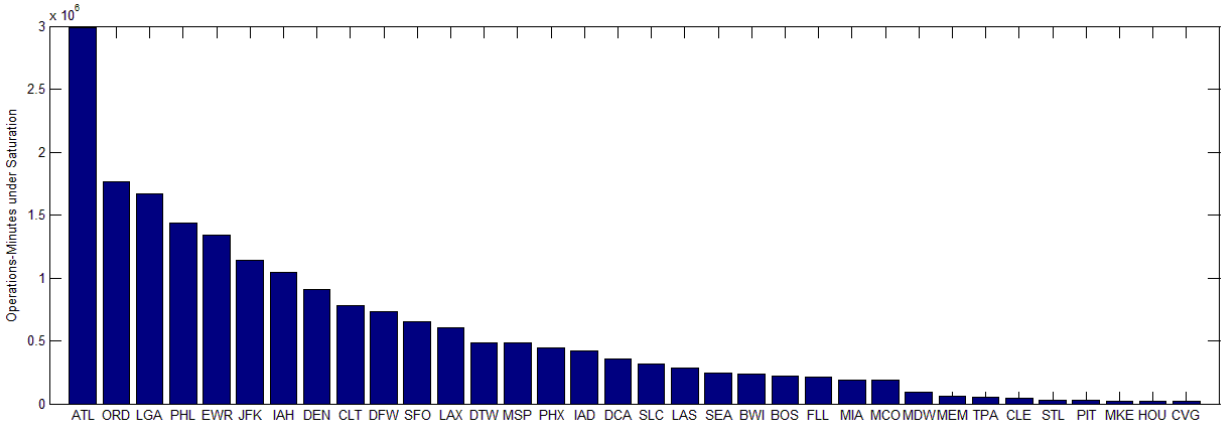

Figure 8. Airport ranking based on operation-time under departure saturation

3.2.4. Characterization of Departure Queuing & Sequencing Behavior

We conducted an analysis of queuing, sequencing and passing behavior at the Core 30 FAA airports. The ranking of the airports based on the total departure queuing delay is shown in Figure 9 for the top twenty-five airports. In order to gain insight on the causality of the delay, the total delay is decomposed into four components as shown in the four parts of the bar of each airport in the figure:

(1) The delay incurred by the subset of departures that experienced no queue at all and proceeded unimpeded to takeoff. These delays are due to flight-specific conditions, other constraints such as arrivals, or downstream restrictions.

(2) The delay incurred by the subset of departures that encountered only a FCFS queue. In other words, these are departures that took off in the same sequence as they were ready for takeoff (as indicated by their OUT time plus their nominal taxi-out time). These flights represent the queuing that is induced mainly by the capacity limitation of the local airport resources, mainly the runway capacity.

(3) The delay incurred by the subset of departures that were passed by at most five other departures, which were expected to takeoff later but took off earlier. These departures represent a moderate amount of passing that may be caused by nominal sequencing activities due, for example, to multiple runways, relative geographical location of entry points, and controller sequencing strategies. In addition, the passing may be due to conformance to downstream restrictions.

(4) The delay incurred by the subset of departures that were passed by more than five other departures which were expected to take off later but took off earlier. These departures represent large delays that are caused mainly by more than nominal sequencing activities, such as conformance to downstream restrictions.

The four subsets of departures constitute together the full sample, and their delays add up to the total. Along with the total delay information in Figure 9, Figure 10 provides the fraction of departures that belong to each of the four subsets for each of the airports. This figure gives insights into the

relative sample size for each of the subsets that contribute to the total delay and the chance that a departure may fall into one of the subsets. The selection of five departures as a threshold for nominal passing versus passing due to off nominal causes such as downstream restrictions was arbitrary and is used for adding insights into the decomposition of delays. The actual threshold that represents nominal passing may be different for different airports. Future extensions of this analysis may attempt to identify such a threshold that represents nominal passing, for example, based on the average number of other departures that a departure passes versus the number of other departures that pass a departure on average. The following observations are made on the information in Figure 9 and Figure 10:

1. The airport ranking based on the total departure queuing delay is consistent with the ranking by departure throughput saturation. ATL leads the airports in terms of total departure delay relative to unimpeded taxi-out followed by ORD, then LGA, LAX, PHL, and EWR. PHL drops a little in the rank, while LAX ranks higher.

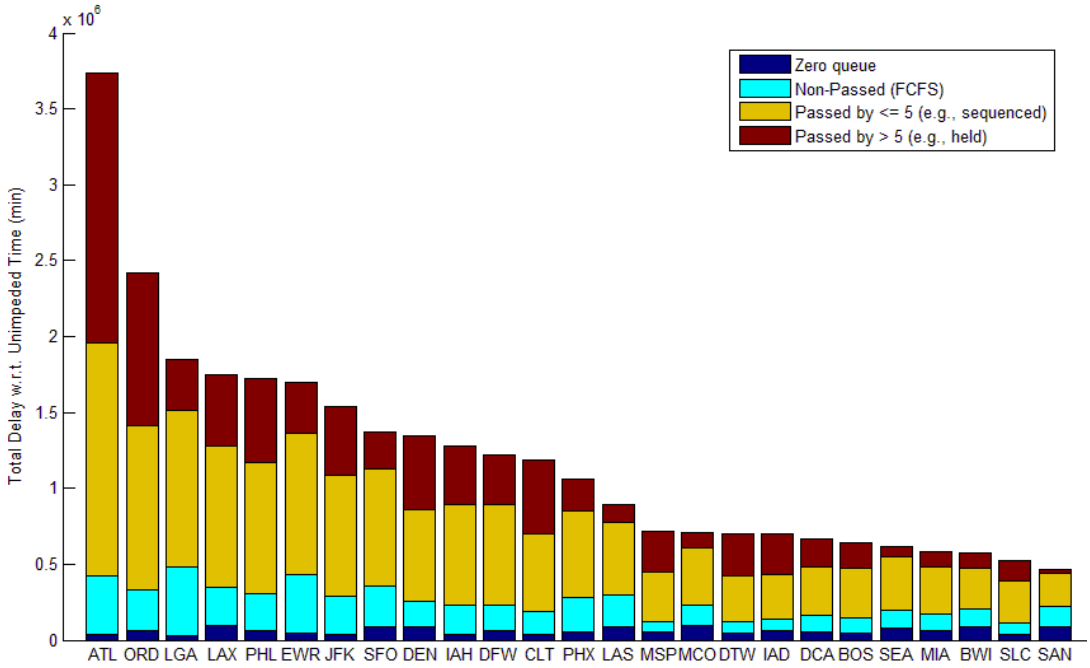

Figure 9. Airport ranking based on total departure delay relative to unimpeded taxi-out

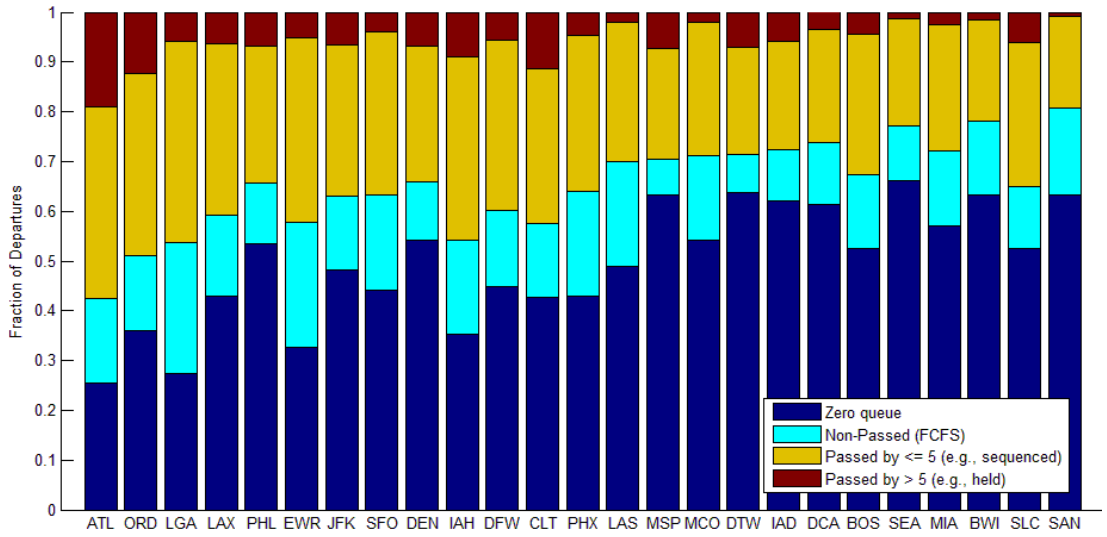

Figure 10. Distribution of departures based on queue composition

2. LGA, followed by EWR, leads the airports in total departure delay incurred by the non-passed flights and the fraction of departures that encountered FCFS queuing only, which reached twenty-five percent of departures. These observations indicate that LGA and EWR generate substantial local queuing delays relative to delay generated by downstream restrictions or nominal sequencing activity. This also indicates that LGA and EWR are more constrained airports where there is less opportunity to change the sequence of departures relative to their FCFS order, which is due in part to the number of departure runways available. Other airports that show significant delay due to FCFS queuing include: JFK, ORD, LAX, PHL, SFO, PHX, and LAS, indicating high ratios of local queuing delay relative to the total at these airports. Further analysis is needed in future extensions to identify the causality of these observed differences.

3. Generally, the fraction of departures that taxi out unimpeded with no queue increases as the ranking of the airport decreases. Some airports, such as PHL, JFK, and DEN, rank high in terms of total delay despite the relatively high fraction of departures that encounter no queue. Overall the amount of delay incurred by the unimpeded departures is small, as shown in Figure 9.

4. The fraction of departures that were passed by at most five other departures is comparable among the airports. However, the fraction of the departures that were passed by more than five other departures varies significantly. In addition to the largest airports, ATL and ORD, some lower-ranked airports exhibited significant fraction of departures that were passed by more than five – for example, CLT, MSP, DTW, and SLC. Correspondingly, these highly-passed departures incurred a relatively high proportion of the delay. One characteristic of these airports which may explain this observation is their location near other major airports – for example, CLT being close to ATL and DTW being close to ORD. These airports are known to struggle to depart flights into the overhead stream, which is typically busy with the traffic of the major airport. Hence these airports incur significant restrictions on the ground awaiting such opportunities.

3.3. Characterization of Airports' Delay-Saving Potential Due to Departure Metering

Besides the characterization of departure delays as discussed above, we also looked at a few other factors for airport site selection. One of those factors was an airport's potential to benefit from departure metering. Constraints on departing aircraft manifest in long departure queues in the absence of surface traffic flow control (e.g., departure gate-holding) and when there is excess demand compared to available airport departure capacity. The degree to which an airport can benefit from surface management primarily depends on the degree to which it experiences long departure queues. A departure metering tool is designed to manage a virtual queue, holding the length of the physical departure queue to some target number (e.g., 5 aircraft). If the physical departure queue rarely exceeds that number even without surface management, then a departure metering tool will have minimal impact. However, if the physical departure queue is much longer than this target, for long periods of time, departure metering and queue management will have a significant impact in terms of reducing queue length and taxi-out time.

Measurement of the length of the departure queue and estimation of the potential benefits realized by control to a target departure queue length allow comparison of this benefit pool estimate across many airports. This comparison, however, does not differentiate among causes at or between airports (e.g., TMI restrictions, airport surface choke-points, and uncoordinated departure push-back times).

We leveraged past work [SL11] performed by our team member for quantifying this benefit pool estimate for the ATD-2 system. Given the availability of ASDE-X surveillance data for multiple airports over the duration of a single month, [SL11] assessed the benefits of gate-holding afforded by controlling the departure queue length to different target queue lengths. Shown inFigure 11 are savings per airport as average daily savings (hrs) when the departure queue is constrained at target lengths of five and ten, respectively. For example, over 70 hrs per day of taxi-out duration could be saved at JFK Airport by maintaining a target departure queue length of five. The savings depicted in Figure 11 measured for 22 airports using an entire month ASDE-X data in March-April 2009.

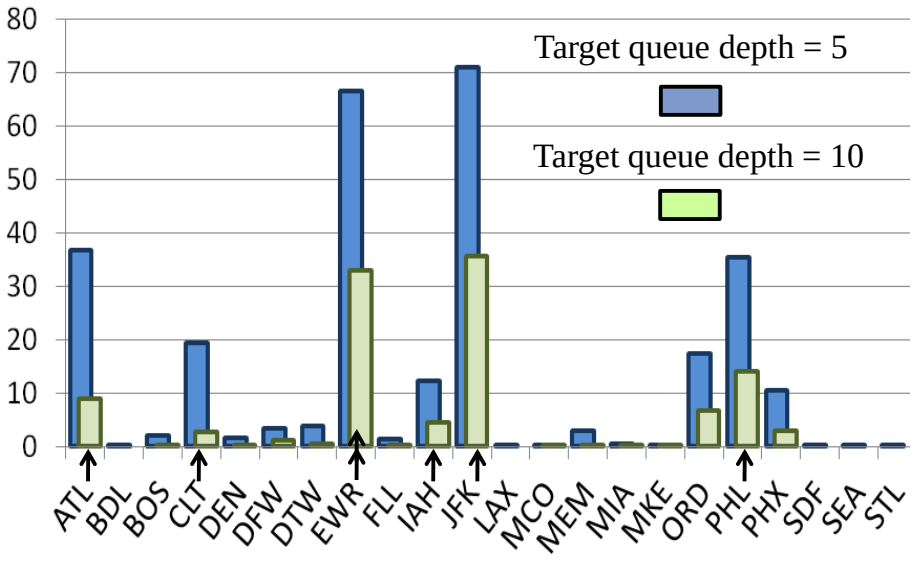

Figure 11. Taxi-out daily savings (hrs) for March-April 2009 (Stroiney and Levy, 2011)

The next question considered was the estimation of benefits at airports for which surveillance data were unavailable. Using the FAA's ASPM data source, [ASPM] determined the percent of time in March-April 2009 during which the departure call rate (i.e., ADR) exceeded the actual departure rate, as reported by each facility listed in Figure 11; this percentage represents the frequency for these airports under which demand exceeded capacity or for which demand could not be satisfied. The relationship between daily gate-holding savings at the target departure queue length of five and the percentage of demand-capacity imbalance is shown in Figure 12.

Referring to Figure 12, the airports for which data pairs were available are plotted as open blue diamond symbols. A zero-intercept quadratic best-fit line was determined for the airports given taxi-out savings (target departure queue length = 5) and % percentage of time that the ADR exceeded the departure rate; the best-fit line is depicted in Figure 12 as a solid, red line. The quadratic function was used to estimate the daily savings at other airports for which ASDE-X were unavailable in the time period of March-April 2009. Given the percentage of the time period of March-April 2009 in which the ADR exceeded the departure rate, the taxi-out duration benefits from gate-holding were estimated for airports such as LGA and DCA Airports (see Figure 12). Note that the extrapolations and estimates in Figure 12 do not account for delay synergies between airports within a metroplex, wherein airport interactions cause delays (e.g., JFK, LGA, and EWR Airports in the New York City area).

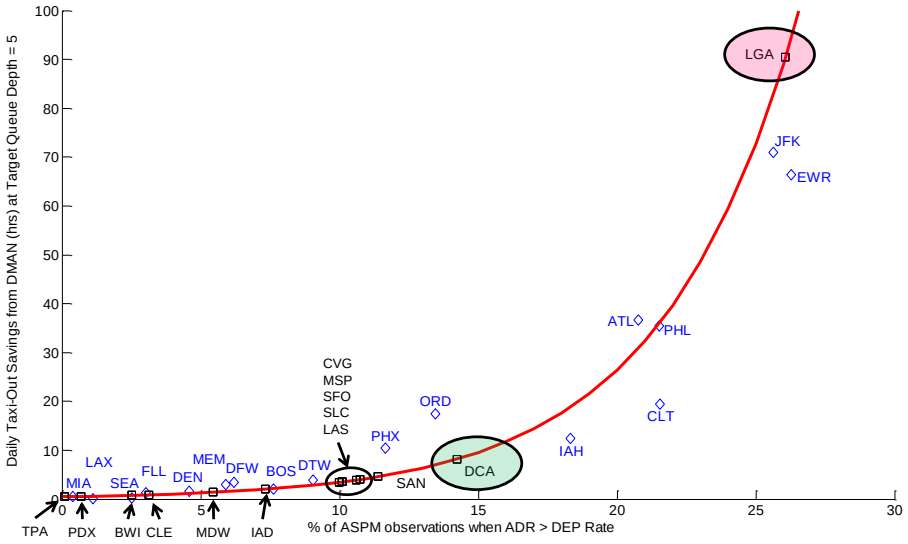

Figure 12. Daily taxi-out savings vs. demand-capacity imbalance (Stroiney and Levy, 2011)

In summary, among the chosen airports, EWR and CLT display a significant potential to benefit from departure metering technologies. DFW did not show significant benefit potential in our analysis. However, the analysis did not consider the effect of airspace restrictions and how much additional delay that adds to the departure transit. DFW displays a significant shortfall in terms of handling departure operations under externally imposed restrictions. In light of this shortfall DFW is also a good candidate for benefits evaluation of the ATD-2 system.

3.4. Characterization of Airports' Fuel Savings Potential

Further, to support airport site selection we leveraged our team members' past work for characterizing the fuel savings potential of departure metering tools like ATD-2 at the Core FAA 30 airports. In prior work [DB10], we evaluated the potential pool of fuel burn benefits that could

be obtained from surface traffic management. The pool of fuel burn benefits is obtained by comparing the baseline fuel burn (as corresponding to ASPM taxi-out times) to the fuel burn corresponding to an "unimpeded" taxi-out time. For each flight in 2007, we estimated the emissions contribution of the taxi-out portion of the flight. We then used the tail number to determine the type and number of engines used [JP Fleet Database 2008], and then the fuel burn and emissions indices from the ICAO engine databank [ICAO 2008]. We assume that aircraft are powered by their Auxiliary Power Units (APUs) during pushback and engine-start (for two minutes), and include the emissions from the APUs. Using the above information, the taxi-out fuel burn of flight i in kg, denoted FB_i, is given by

$$FB_i = T_i \times N_i \times FBI_i,$$

where T_i is the taxi-out time, N_i is the number of engines, and FBI_i is the fuel burn index per engine. In reality, the taxi-out emissions from an aircraft depend on factors for which data are not available, such as the throttle setting, ambient temperature, number of engines used to taxi, etc. We assume that in the baseline case, all engines are used to taxi out, and that the throttle setting is 7% of maximum thrust.

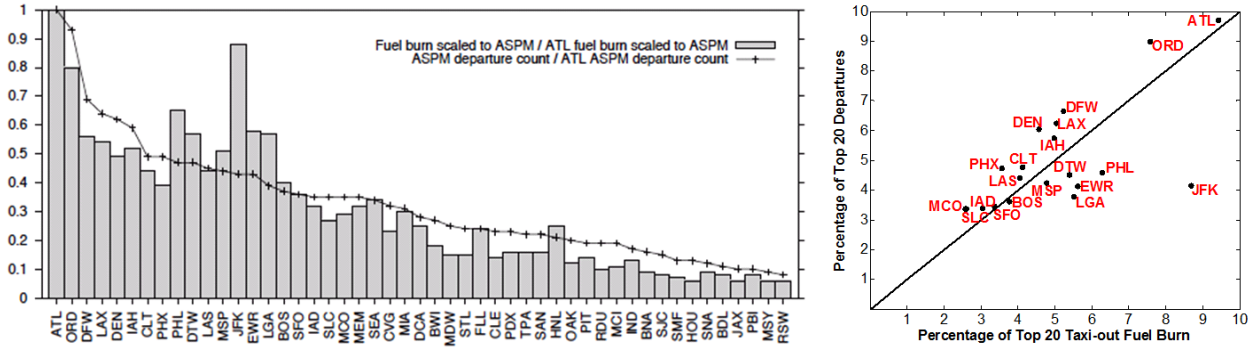

Figure 13. Baseline (2007) fuel burn for top 50 airports in terms of number of operations.

In the left Figure, the bars show the taxi-out fuel burn (normalized by the taxi-out fuel burn at ATL), while the line shows the number of departures (normalized by the number of departures at ATL). The airports are ordered by the number of operations. The scatter plot on the right shows the percentage of top 20 departure demand that each airport accounts for versus the associated fuel burn [DB10].

Figure 13 (left) shows the baseline fuel burn and number of departures for 2007, relative to the values at the nation's busiest airport, ATL. ATL served 490,735 departures that year, corresponding to an estimated 39.8 million gallons of taxi-out fuel burn. We also consider potential metrics to compare the relative fuel burn and emissions performance of different airports. One possible approach is to normalize the fuel burn at an airport by the maximum fuel burn among all airports (i.e., the fuel burn of ATL) and to compare this value with the departure count at the same airport, normalized using the departure count of ATL. This would allow us to draw conclusions of the form "Airport i consumes a fraction x of the fuel consumption at ATL, but faces (only) a fraction y of the ATL departure demand." These metrics are plotted in Figure 13 (right). Airports for which the departure metric (denoted by the lines with markers) is less than the fuel burn or emissions metric (denoted by the bars) can be considered to have weak emissions/fuel burn performance. It is important to note that this analysis was based on 2007 data, and that there have been demand shifts and capacity enhancements at several of the airports since then.

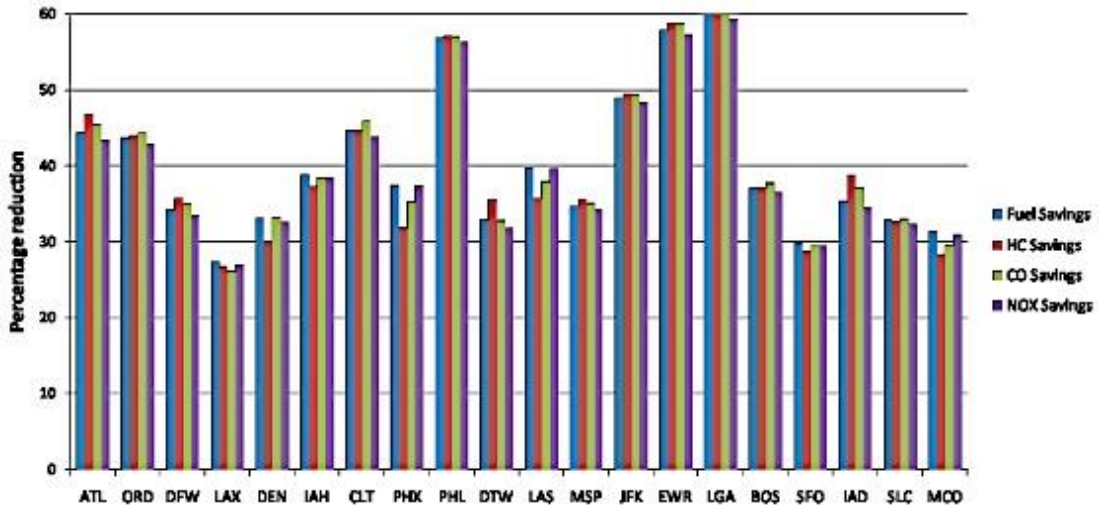

Figure 14. Potential for reductions in fuel burn and emissions through achieving unimpeded taxi times [DB10].

To estimate the total "pool of benefits" in fuel burn reduction that can be achieved by decreasing taxi times, we consider the ideal case, when every departing aircraft taxies for only the length of its unimpeded taxi-out time. This gives us the maximum possible benefit that can be achieved by surface management strategies. For example, at PHL, we have estimated that if every departure taxied out for the unimpeded taxi time (depending on its terminal, season, etc. – approximated by the tenth percentile of ASPM taxi-out times for the given terminal and season), we would achieve a theoretical reduction in taxi-out emissions and fuel burn of nearly 60%. Done naively, this would be equivalent to allowing only one (or very few) aircraft to taxi out at any given time. This would result in a decrease in airport throughput, and an increase in departure delays. We also approximated that at the top twenty busiest airports in the US, emissions and fuel reductions could range from 25% to 60%. Figure 14, which lists the airports in order of relative numbers of ASPM departures in 2007, illustrates anticipated reductions in fuel consumption and emissions. We recognize that unimpeded taxi times will be very difficult to achieve at airports; however, we believe that improved surface management approaches such as ATD-2, when implemented effectively, have the potential to decrease taxi-out delays in addition to emissions and fuel burn.

In summary, all three chosen airports demonstrated a significant benefit pool to save fuel and emissions through achieving more unimpeded taxi times, with EWR benefiting the most, CLT next, and DFW the least.

3.5. Site-Selection Summary

Section 3 described some of the site selection factors we computed and considered before selecting three airport sites (CLT, DFW, and EWR) for detailed simulation-based assessment. For a more comprehensive review of the site selection process we refer the readers to our NASA NRA Site Selection Report [ATAC16-2].

Next, we describe the task of developing the simulation environment for benefits analysis.

4. TASK 3. DEVELOP SIMULATION ENVIRONMENT

4.1. Simulation Environment Overview

Our technical approach for ATD-2 benefits estimation involved developing and utilizing a high-fidelity simulation environment for simulating aircraft trajectories in both the surface and airspace subsystems of the ATD-2 system, under current-day ATC procedures as well as under ATD-2 procedures. We took a mixed-fidelity modeling approach, where different domains within the ATD-2 subsystems are modeled at different levels of fidelity depending upon site-specific operational characteristics and the specific benefit mechanism being analyzed. Our modeling simulated all the key constraints faced by departure flights along their path from departure gate to overhead en route traffic stream merge. These constraints include traffic congestion in the ramp area and on movement area taxiways at the departure airport, capacity constraints on the departure airport runway system, capacity constraints at departure-fixes where flights from multiple TRACON airports merge, and miles-in-trail spacing constraints at entry points to overhead en route traffic streams. We generated a high-fidelity simulation environment for simulating operations at three airport sites: CLT, EWR, and DFW.

4.1.1. Airport Surface and Airspace Traffic Simulation

The core of our simulation environment is NASA's high-fidelity SOSS platform. SOSS simulates departure and arrival flight trajectories on the airport surface. We integrated SOSS with the ATAC Airspace Operations Simulator and Scheduler (AOSS). The AOSS has three components. The first component is a MATLAB-based queuing simulation that simulates aircraft trajectories along a network of frequently-flown airspace routes in the TRACON and en route airspaces. The second component simulates the Surface Traffic Flow Management control actions implemented by the ground and local controllers in order to ensure adherence to APREQ, EDCT and MIT TMIs. The third component simulates the coordination between the airport tower and receiving Center Traffic Flow Management, which involves fitting APREQ departure flights into time-slots on the Center meter arc timelines in accordance with the estimated runway takeoff times provided by the ATCT, and sending back runway release time constraints.

Figure 15 shows the interconnected SOSS-AOSS system. As shown in the Figure, SOSS transfers over the simulation-control of a departure flight to the airspace simulation component of AOSS when the departure flight takes off, i.e. , at the Actual Takeoff Time (ATOT). AOSS's airspace simulation component then simulates the movement of the departure flight along its airborne route from takeoff runway to departure fix and then on to an en route stream merge point. Along this route, we also simulate the transit through individual en route sectors in the flight's path. AOSS includes queuing-based airspace delay models for the departure-fix merge process, as well as the en route stream merge process. These models space the flights at the departure-fix or the meter arc based on the actual historical miles-in-trail restrictions that were active for those specific NAS elements. If no MIT restriction was imposed historically at a NAS element, then we imposed the standard spacing of 5 nmi between successive fix or arc crossings.

In addition to the focus ATD-2 airport departures, AOSS's airspace simulation also includes departures from satellite airports within the same TRACON (some of these merge with the focus airport departure flights at the departure-fixes), as well as departures from NAS-wide airports that merge with the focus ATD-2 airport's departures in the en route airspace (these flights merge with the focus airport departure flights at the TBFM-defined en route meter arcs). Runway takeoff

times, simulation entry times, airspace routes and departure-fix/meter arc crossing times for these "other" flights (non-focus airport departures) are derived from historical end-to-end merged radar track data obtained from NASA's Sherlock ATM data warehouse. As shown in the figure, at the end of the simulation we were able to extract the full simulated surface flight trajectories from SOSS and the full simulated airspace flight trajectories from AOSS.

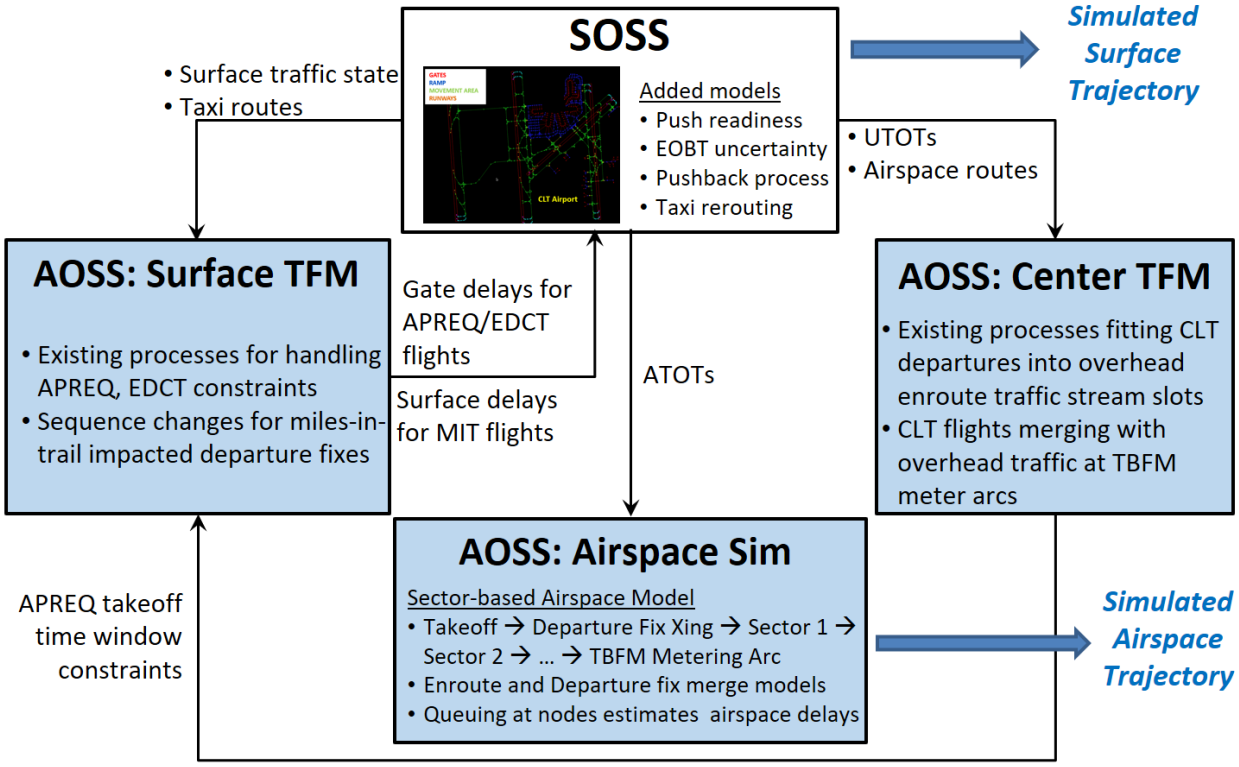

Figure 15. Integrated Surface Airspace Simulation Environment

4.1.2. Current-day (Baseline) Traffic Flow Management Control Actions Modeling

AOSS consists of two traffic flow management implementation components. The first component, Surface Traffic Flow Management (STFM), emulates current-day procedures for implementing TMIs such as APREQs, EDCTs and MITs. The second component, Center Traffic Flow Management (CTFM) emulates the runway release time coordination between the ATCT and the receiving Center.

4.1.2.1. STFM Actions

For APREQ-impacted flights, the STFM component simulates the following steps involved in today's APREQ implementation procedures: (1) When the APREQ-impacted departure flight is ready for pushback, the ATCT estimates its runway takeoff time using a rough estimate of taxi – out time derived from historical simulation data; (2) This ATCT runway takeoff time estimate is sent to the CTFM component; (3) When a controlled runway release time is received from the CTFM component, STFM computes another estimate of the flight's taxi-out time, which is different from the ATCT estimate computed in step 1 and uses this other taxi-out time estimate to compute an appropriate pushback time for the APREQ-impacted flight. A different taxi-out estimate is computed to emulate the current-day procedure of the runway release time being

communicated to the pilot and the pilot using his/her own taxi-out estimate to determine the appropriate pushback time. The pilot's taxi-out time estimate is different than the estimate used by the ATCT in step (1).

For EDCT-impacted flights, the STFM component adds a gate hold delay for the respective GDP being simulated to the flight's Scheduled Off Block Time to compute the actual pushback time. The gate hold delay is set equal to the average ground delay published in the historical GDP advisory, which is obtained from a Traffic Flow Management Initiatives database.

For MIT-impacted flights, STFM emulates the current-day ground controller sequencing decisions for avoiding consecutive flights going to the same departure-fix before they merge onto the final AMA taxiway that takes them to the departure runway. Different merge-locations are simulated for different airports and runway configurations.

4.1.2.2. CTFM Actions

The CTFM component simulates the coordination between the ATCT and the receiving Center for implementing surface delays on APREQ-impacted flights. As described above, for each APREQ-impacted flight, the CTFM component receives an estimate of the runway takeoff time from the ATCT (i.e., from the STFM component in the case of simulation). CTFM uses historical airspace transit time data to estimate the meter arc crossing times for APREQ-impacted flights. In addition to the focus airport departure flights, CTFM also has data on all other NAS flights that merge at the meter arcs. CTFM estimates the meter arc crossing times for these other departures also. Then, CTFM spaces these flights at the meter arc according to the published miles-in-trail restriction active for that meter arc and computes an acceptable time-slot in the meter arc timeline for the APREQ-impacted flight from the focus airport. Then, CTFM back-computes a controlled runway release time for that flight using the airspace transit time estimate and this controlled time is sent back to the ATCT (i.e., to STFM in the case of simulation).

4.1.3. ATD-2 Operations Simulation in AOSS

In the case of ATD-2 operations simulation, the APREQ-related modules of the STFM component are replaced with an emulation of the ATD-2 Tactical Surface Scheduler. The ATD-2 Tactical Scheduler computes more accurate taxi-out time estimates for APREQ-impacted flights and sends them to the CTFM component. The ATD-2 Tactical Surface Scheduler also back-computes the Target Off Block Time (TOBT) from the runway release time for APREQ flights. In addition, the scheduler also adds gate delays to other (non-APREQ) flights based on demand-capacity imbalances observed/estimated. The STFM modules that perform EDCT implementation and sequencing for departure-fix interleaving of flights are retained in the ATD-2 operations simulations.

In summary, the airspace simulation, STFM and CTFM components of the AOSS together enable high-fidelity modeling of the impact of APREQ, EDCT and MIT constraints on airport surface and airspace traffic, under both current-day (baseline) operations and ATD-2 operations.

4.1.4. Mixed-fidelity Models

As discussed above, we take a mixed-fidelity modeling approach. Figure 16 shows the different levels of modeling fidelity used in AOSS for simulating different operation types. As shown in the Figure, CLT departures to ATL are treated as special. Their trajectories are modeled by nodes and links starting at the CLT departure runway and ending at the landing runway at ATL. Trajectories

for CLT departures to Northeastern airports, which are most frequently impacted by traffic management initiatives (TMIs), are modeled starting at the departure runway and continuing on to their key en route merge point, usually falling within Washington D.C. Center (ZDC) airspace. For all other CLT departures the modeled routes end at the departure-fix merge. We also model routes for departures from CLT Satellite airports. For these departures, the routes are modeled from their departure runway until departure-fix merge. We also model all NAS-wide departures (non-CLT and non-CLT satellite departures) that interact with CLT departures going to the Northeast at some point in their transit. Modeling these "other" departures serves to create realistic en route slot fitting constraints for CLT departures and improves the simulation fidelity.

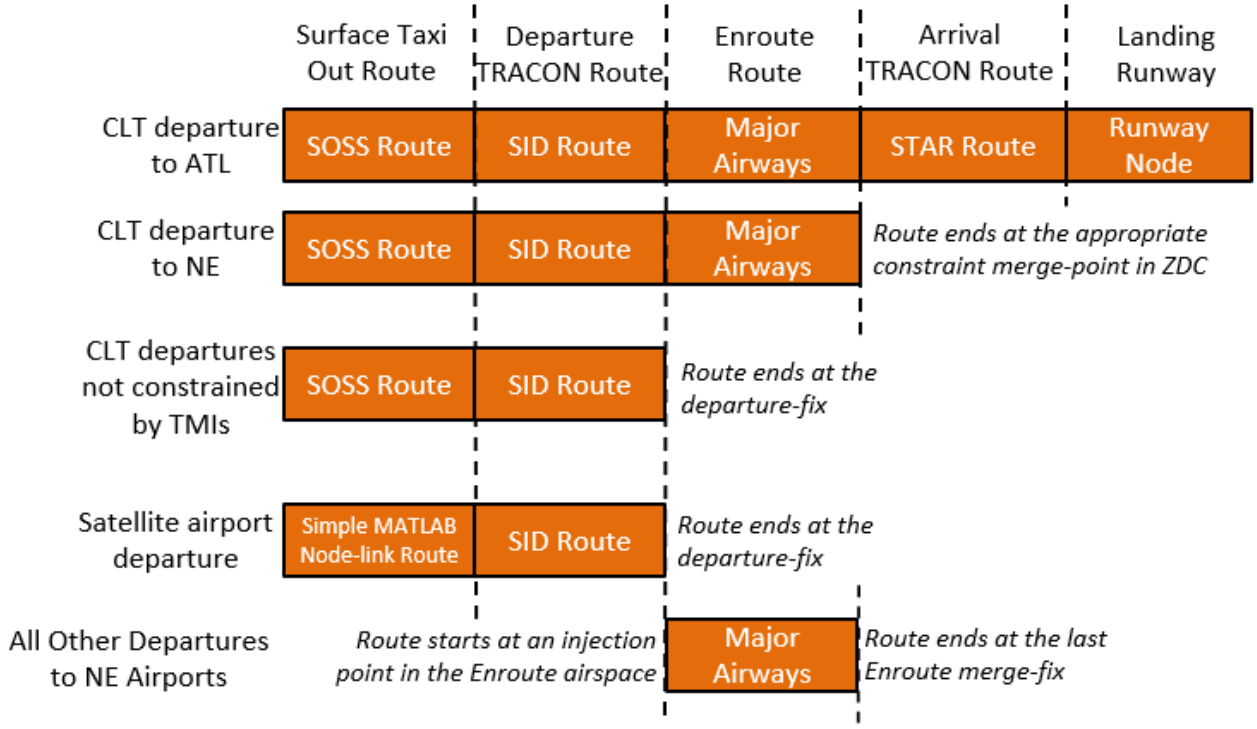

Figure 16. Different Scopes and Fidelities of Departure Airspace Trajectory Modeling

Next, we describe how the ATD-2 benefit mechanisms are modeled in our simulation platform.

4.2. How ATD-2 Benefit Mechanisms are Modeled in the Simulation Environment

Section 2 discussed our team's analysis of ATD-2 benefit mechanisms and the operational shortfalls that they alleviate. NASA also conducted a parallel analysis [C17] of ATD-2 benefit mechanisms and their results more or less agree with our findings. In this section, we leverage the key ATD-2 benefit mechanisms identified by NASA and describe how our simulation platform models these benefit mechanisms.

4.2.1. Benefit Mechanism # 1: Data Exchange

Data exchange is a foundational capability of the ATD-2 system. In addition to the sharing of data between ATD-2 software components, new data will be acquired and shared between Ramp and ATCT controllers to improve awareness of flight status and intent. Key data extracted and shared includes EOBT, runway usage intent, arrival ETAs, and TMI restrictions (APREQ, EDCT, and MIT). These data are further factored into flight-specific trajectory predictions by the ATD-2

Tactical Surface Scheduler, the outputs of which are shared between system users via timeline displays [C17].

Data exchange through ATD-2 provides more accurate traffic demand predictions, leading to better airline resource management (e.g., gate conflict resolutions) and better ATC capacity utilization and planning. This can lead to increases in capacity at the runway or airport level, which could further lead to reductions in time, delay, and fuel during peak traffic periods. In the longer term, such increases in capacity could allow airlines to operate more revenue flights.

Our combined surface-airspace simulation platform models this benefit mechanism as follows:

- Simulations model Push Ready Times and EOBTs different from Scheduled Off Block Times (SOBTs) on a per flight basis. We obtain the SOBTs from OAG and Flightaware data sources. Further, we leverage NASA's work on quantifying EOBT errors to develop uncertainty models for perturbing the SOBTs in order to obtain EOBTs (i.e., EOBT = SOBT + Perturbation 1) and further perturb the EOBTs to obtain the Push Ready Times (i.e., Push Ready Time = EOBT + Perturbation 2). EOBTs are communicated to the emulation of the ATD-2 Surface Tactical Scheduler in our simulation platform
- The ATD-2 Surface Tactical Scheduler model in our simulation platform utilizes EOBTs for computing more accurate traffic demand predictions (i.e., Earliest Runway Usage Times, ERUTs) and to plan runway system capacity utilization
- Further, we also model the full current-day and ATD-2 procedures for implementing APREQ and EDCT departure restrictions
    - For the current-day operations we simulate the full process, which includes the following steps: Pilot calls the ATCT at Push Ready Time, ATCT (i.e., STFM component in the simulation) estimates taxi-out time for that departure flight, ATCT (i.e., STFM) requests runway release time from the receiving Center, Center (i.e., CTFM) finds slot in overhead traffic stream, Sends back controlled runway release time, Pilot (i.e., STFM) estimates taxi-out and pushes back in order to make the APREQ window
    - In the case of ATD-2 operations simulation, the ATD-2 Tactical Surface Scheduler emulation uses accurate taxi-out time estimates to compute estimated takeoff times and sends the more accurate estimate to the Center in order to request runway release times for APREQ flights. Further, the scheduler allocates correct amount of gate delay to make APREQ window, with higher priority given to the APREQ flights. For non-APREQ flights also get appropriate gate delay allocation based on more accurate taxi-out time estimates (i.e., more accurate ERUTs)

4.2.2. Benefit Mechanism # 2: Demand Throttling Provided by Surface Metering

The ATD-2 system meters flights at the gate in order to throttle departure demand in keeping with capacity constraints, thus mitigating surface congestion and associated taxi delays. Through metering, a portion of the delay necessary to balance demand and capacity is taken at the gate prior to engine start, where delay absorption is most efficient. In addition to reducing taxi delays and saving fuel, reductions in surface congestion can also lead to fewer actions required by controllers to resolve surface traffic conflicts, thereby potentially reducing workload.

Our combined surface-airspace simulation platform models this benefit mechanism as follows:

- Our ATD-2 operations simulations include a full emulation of the ATD-2 Surface Tactical Scheduler. This emulation follows all the steps, order of consideration rules, and TOBT back-computation logic, in the actual ATD-2 scheduler. We also model the dynamics of the departure flights under scheduling transitioning from "UNCERTAIN" to "AT GATE PLANNED" to "AT GATE READY" and "TAXIING" phases
- Additional models for departure-fix miles-in-trail or minutes-in-trail restrictions are added to the schedulers for DFW and EWR
- The ATD-2 Tactical Scheduler model computes gate delays, which are simulated by imposing Scheduled Times of Release on appropriate departure flights in the SOSS platform.
- This simulates the demand throttling benefit mechanism

4.2.3. Benefit Mechanism # 3: Increased Predictability Provided by Surface Metering

Reduced surface congestion provided by Surface Metering, combined with better planning and resource management afforded through data exchange, can lead to more predictable aircraft movements. Together with EOBTs, reductions in taxi-out time variance could lead to substantial improvements in predicted takeoff times, which have considerable uncertainty in current operations.

Over the longer term, improved departure predictions can lead to better estimates of traffic demand on downstream airspace and airport resources, leading to fewer and less restrictive TMIs, with less buffers to compensate for uncertainty.

Over the longer term for airlines, more accurate predictions of gate-to-gate flight duration could lead to shorter scheduled block times, which today contain sizable buffers today to account for uncertainty. Reduction of scheduled block times can lead to substantial savings in direct-operating costs, allowing better utilization of airline equipage and personnel resources and reducing the occurrence of early arrivals competing with departures for limited gates.

Our combined surface-airspace simulation platform models this benefit mechanism as follows:

- As discussed above, our ATD-2 operations simulations include a full emulation of the ATD-2 Surface Tactical Scheduler. This enables us to reliably simulate the reduction in surface congestion afforded by ATD-2's demand throttling.
- SOSS simulations model realistic movement of all flights in the ramp and movement areas, while emulating the ramp, ground and local controller actions for maintaining safe separation between flights and creating safe and efficient merges at key taxiway intersection points. With lesser number of flights in the ramp and movement areas due to gate holds, SOSS naturally models a lesser need for delays on the airport surface for keeping flights safely separated, which leads to more predictable simulated taxi times and more predictable takeoff time estimates

4.2.4. Benefit Mechanism # 4: Integrated Airspace Scheduling

The ATD-2 system interfaces with the existing FAA Integrated Departure Arrival Capability (IDAC), which is a sub-component of TBFM, to allow the ATCT to electronically coordinate with the receiving Center for scheduling aircraft into overhead streams at constrained airspace meter points. With this capability, requests for APREQ times for overhead stream insertion can be made while aircraft are still at the gate, facilitated by timeline displays that allow ATCT to find feasible takeoff times based on improved trajectory predictions. This process can lead to more efficient and achievable APREQ times for controllers and pilots, making it potentially less likely that APREQs will need to be re-scheduled, thus reducing pilot/controller workload.

Furthermore, because ATCT can request well-informed APREQ times that work well for the local traffic situation, the overall APREQ-induced delay may be lower, thus potentially improving airline on-time performance and passenger connections.

Importantly, propagation of TMI information back to the gate with integration on ramp displays, allows for earlier awareness of TMI-restricted flights by airlines, improving airline predictions that can lead to better airline resource management decisions.

Our combined surface-airspace simulation platform models this benefit mechanism as follows:

- As discussed above, our simulations model the APREQ runway release time request process in full detail for both baseline and ATD-2 operations. Section 4.1 described how the STFM and CTFM components of the AOSS simulation platform enable high-fidelity modeling of the APREQ implementation process
- Due to the high-fidelity modeling in STFM and CTFM components, our simulations are able to simulate current-day less accurate taxi-out time estimates leading to inefficient runway release time requests, which may result in frequent need for re-scheduling and/or missed APREQ runway release time slots
- Furthermore, our ATD-2 operations simulations model more accurate, ATD-2 scheduler trajectory based taxi-out time estimates, which lead to efficient runway release time requests and therefore, less frequent need for re-scheduling and better adherence to the APREQ runway release time slots

4.2.5. Benefit Mechanism # 5: TMI Compliance

TMI-imposed controlled runway takeoff time restrictions in the form of APREQ times, EDCTs, and Miles-in-Trail (MIT) spacing requirements are factored directly into ATD-2 Tactical Surface scheduling of target takeoff times. These target takeoff times are propagated back into target off-block times resulting in push/hold advisories at the gate.

Managing TMIs in this manner allows for more efficient delay absorption, thereby reducing fuel and emissions. Staging aircraft to meet TMIs from the gate can also help further reduce congestion and the need for controllers to re-sequence flights on the highly-constrained airport surface at CLT, thus further improving flight efficiency and further reducing controller and pilot workload.

Early staging flights to meet TMIs through ATD-2 gate-hold advisories could contribute to better TMI compliance at takeoff, leading to fewer and less disruptive maneuvers once flights are airborne to adhere to downstream traffic-flow constraints.

Our combined surface-airspace simulation platform models this benefit mechanism as follows:

- Our model of the ATD-2 Tactical Surface Scheduler factors in TMI restrictions directly into its computation in the same way as the actual ATD-2 scheduler
    - APREQ and EDCT-impacted flights get a higher priority in the order of consideration as in the field-implementation of the scheduler
    - MIT and MINIT restrictions are handled in the spacing logic by requiring a departure going to a MIT or MINIT-restricted departure-fix to maintain the stipulated time spacing at runway takeoff with respect to the last departure to takeoff for the same departure-fix
- Appropriately spaced target runway takeoff times (including TMI time spacing) are back-propagated to compute required TOBTs. Thus, TMI impacted flights are held at their gates until the right time and released in order to reach the departure runway within the TMI-specified time window.
- Compliance with the APREQ and EDCT windows is measured post simulation

This concludes our discussion of how ATD-2 benefit mechanisms are modeled in our simulation platform. Next, we discuss technical details of our simulation platform components starting with the airport simulator, SOSS.

4.3. SOSS Airport Surface Simulation Models

As discussed above, we use NASA's SOSS simulation platform for simulating the movement of flights on the surface of the focus airport. NASA's SOSS is a fast-time simulation platform used to simulate airport surface operations and support rapid prototyping of surface scheduling algorithms. SOSS includes a high-fidelity node-link model of airport gates, taxi paths, and runways on the airport's surface. It also includes trajectory-based models for simulating aircraft moving on the airport surface, with aircraft type-specific surface transit speed modeling and special runway speed transit modeling. SOSS also includes models of pilot self-separation which prevents flights from getting too close to each other. SOSS is not designed to be a standalone modeling tool. It is designed to be used in conjunction with external scheduling components. When integrated with external schedulers it is SOSS's job to move aircraft on the surface according to the recommended schedule and monitor separation violations and scheduling conformance.

In this section we describe pertinent characteristics of the SOSS airport surface models that we developed in support of our benefits assessment work. Before developing these models for the three selected detailed simulation airport sites, we studied the most-used runway configurations at these three airports and selected the top two most-used configurations for modeling at each airport for model development. Our analysis of runway configuration data over the time-range 01-01-2016 to 12-31-2016 indicated the runway configuration usage shown in Table 3. We developed (or updated existing models for) SOSS airport models for each of these six runway configurations.

Table 3. Most-Used Runway Configurations at the Focus Study Airports in 2016

Airport	Configuration Name	Departure Runways	Arrival Runways	Percent of Time Used (Computed over regular operation hours only*)
CLT	South-flow	18C, 18L	18R, 23, 18C	21.15%
CLT	North-flow	36C, 36R	36L, 36C, 36R	48.12%
EWR	South-flow	22R	22L	44.26%
EWR	North-flow	4L	4R	33.19%
DFW	East-flow	17R, 18L	13R, 17C, 17L, 18R	40.36%
DFW	West-flow	31L, 35L, 36R	31R, 35C, 35R, 36L	20.39%
* Regular operation hours are from 5 am to 10 pm local time.				

Our base year project report [ATAC17-2] outlined key features of these models and described the modeling and analysis tools that we created to support their development. Here, we only provide a brief summary of the model features and upgrades we added to the SOSS airport models to enhance their fidelity and ensure better matching with real historical operations data. We present this brief summary in tabular format in **Table 4**. The brief summary will be followed by a discussion of validation results we obtained after making all the upgrades to the SOSS models.

Table 4. Summary of SOSS model enhancements implemented to improve validation against real, historical operations data

SOSS Model Feature Added or Validation Exercise Conducted	Description
SOSS airport node-link model generation	ATAC developed a semi-automated process for generating new SOSS airport node-link models as well as for modifying existing SOSS models. This process leveraged tools developed by NASA's SOSS Simulation Team, mainly Dr. Robert Windhorst's Airport Modeler, as well as ATAC's SIMMOD PRO simulation platform. SIMMOD PRO includes a click-and-drag functionality for creating new nodes representing airport gates, taxiway intersections, and important locations on the runways. We leveraged this functionality to first create initial node-link airport models. We then developed a SIMMOD-to-SOSS convertor for converting SIMMOD PRO model files to SOSS input file format. After developing initial node-link models in SIMMOD PRO, we applied this SIMMOD-to-SOSS convertor to obtain SOSS nodes and links input files. Any modification needs that were identified after simulating airport

	surface operations using these files in SOSS were first implemented in SIMMOD and then re-converted to SOSS format. Model generation leveraged high-fidelity historical data on gate allocations, scheduled gate departure times, actual landing times, runway allocations, departure fix allocations, en route sectors crossed, etc. derived from a combination multiple data sources including OAG, Flightaware, ASDE-X, and end-to-end merged flight track data from NASA's Sherlock data warehouse.
Automated SOSS airport taxi route generation	ATAC developed an in-house tool to create realistic SOSS taxi routes by first analyzing ASDE-X data and then converting the observed most commonly-used taxi routes into appropriate sequences of SOSS nodes in SOSS route format. Since the number of taxi routes grows to be unmanageable to specify manually, even for modestly sized airports, this tool aimed to expedite the route building process with automatic pathfinding. For those familiar with it, this tool sought to emulate NASA's RouteBuilder.jar, while providing some enhancements. The enhancements included (1) separate development of gate-to-spot and spot-to-runway portions of the taxi route, and (2) the ability to use airport sectors/polygons to specify routes. The second enhancement enabled a SOSS model developer to easily translate most commonly observed routes in real operational data into an input specification for the SOSS taxi route generation tool.
SOSS airport taxi speed validation	ATAC performed validation of nominal taxi speeds per aircraft type as included in the SOSS simulation platform aircraft types database, by comparing the taxi-speeds with actual observed speeds in ASDE-X data. Where necessary, modifications were made to the SOSS aircraft types database to match the modeled taxi speeds closely with the observed speeds.
SOSS runway separations validation	SOSS specifies a temporal or spatial distance between two consecutive runway accesses/operations. Fidelity of the SOSS simulations depends to a high degree on the accuracy of these minimum runway separation specifications. ATAC performed rigorous validation of all permutations of SOSS runway separation values by comparing the modeled separations against respective minimum separations found in ASDE-X data. The SOSS separation values were found to be correct in all the cases.
SOSS enhancements for better validation against real operational data	ATAC made a number of modifications to the initial SOSS airport models to enable better agreement between the simulated and actual historical operations. These modifications include:

	• Modifying modeled taxi routes and runway exit/entry-points where they do not match with the real operations • Adding models for enabling more realistic emulation of local controller departure runway clearances, which included adding buffer separations to account for the human delays in clearing departures for takeoff • Adding models for ground controller sequencing actions

After making all the SOSS model enhancements summarized in **Table 4**, we compared the simulation outputs before the enhancements and after the enhancements with counterpart real, operational data from the same historical day that was modeled in SOSS. As an example, we present the before and after validation comparison data from a simulation of the 7/21/2016 test simulation day. We simulated the airport operations from 0900-1700 UTC on 7/21/2016 and compared the simulation results against the actual operations on the same day for flight-to-flight comparison. The base year report [ATAC17-2] described the validation results in detail. Here, we present the summary results from the comparison of simulation VS reality ***before*** our SOSS enhancements (we call this Round 1 simulation) and the comparison of simulation VS reality ***after*** our SOSS enhancements (we call this Round 2 simulation).

Taxi-Out Times Validation. Figure 17 demonstrates the improvement brought about by our SOSS model enhancements in matching the simulated taxi-out times with the real historical taxi-out times. In this figure, we plot the simulated taxi-out times (ramp times in the top-half, movement area times in the bottom-half) per 15-minute time-bin as a percentage of the actual taxi times for flights pushing back in the same time-bin. The ideal match would be equivalent to the green line in both the plots (i.e., simulated times are always equal to or 100% of the actual times). We see from this figure that Round 2 simulations achieved a big improvement in matching the ramp area taxi-out times. However, there was no improvement in movement area taxi-out times.

We defined an "area under the error curve" metric as a measure of how the taxi-out times matched with reality in Round 2 versus Round 1. To compute this metric we looked at the individual time-bin taxi-out time differences (Real – Round 1 or Real – Round 2) and computed the "area under the error curve," i.e., summed up the differences across all the time-bins. Note negative differences also count as area under the curve. Computing the "area under the curve" metric, we see that Round 2 provided a 70% improvement in the ramp area taxi times whereas for movement area taxi-out times there was no improvement.

After obtaining these validation results, we have added further enhancements to SOSS using an external scheduler for simulating more realistic emulation of local controller departure runway clearances, which have improved the match between simulated and real movement area taxi-out times further. Sections 6.2, 6.3, and 6.4 discuss more recent validation results for the three detailed simulation airport sites, respectively.

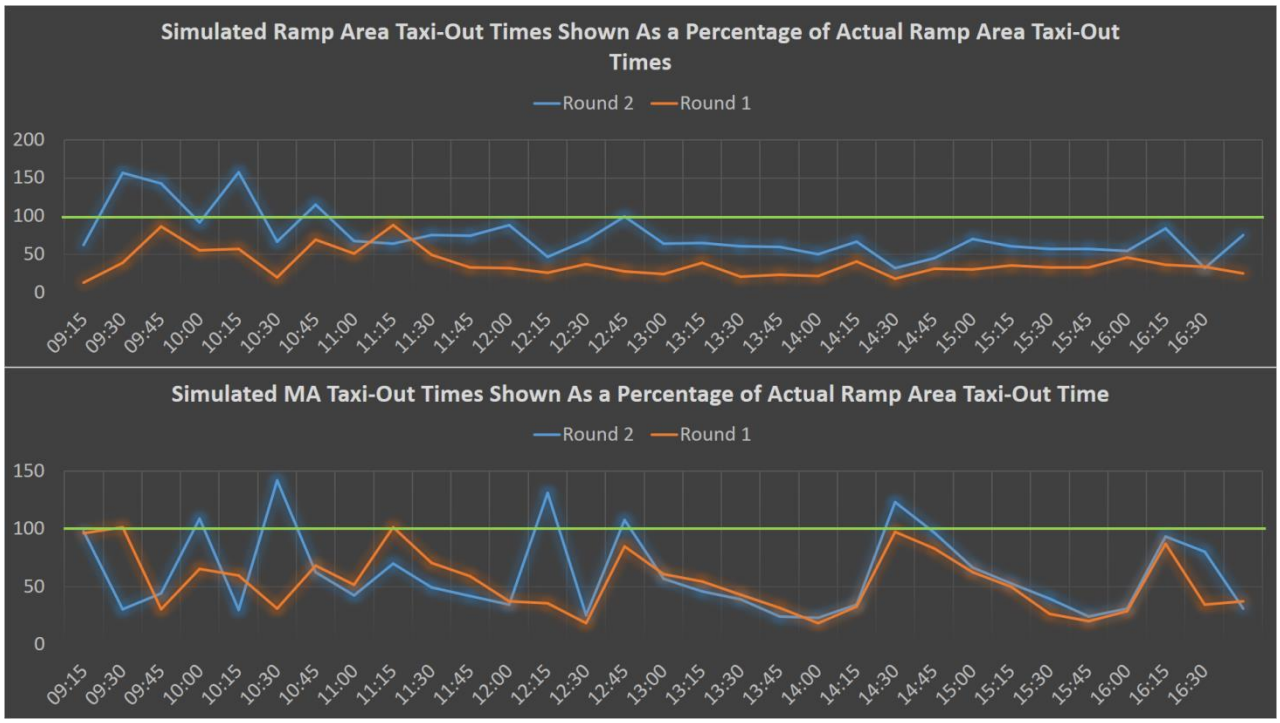

Figure 17. Simulated Taxi-Out Times Plotted as the Percentage of Actual Taxi-Out Times, Green Line Shows Ideal 100% Match

Taxi-In Times Validation. Figure 18 demonstrates the taxi-in time improvement in Round 2 simulations as compared to Round 1. As we did for the taxi-out times before, here we plot the simulated taxi-in times (ramp times in the top-half, movement area times in the bottom-half) per 15-minute time-bin as a percentage of the actual taxi-in times for flights landing in the same time-bin. The ideal match would be equivalent to the green line in both the plots (i.e., simulated times are always equal to or 100% of the actual times). We see Figure 18 that Round 2 simulations achieved big improvement in matching the ramp area taxi-in times. There was very little improvement in movement area taxi-in times, but they were already very close to the actual movement area taxi-in times. Further, computing the "area under the curve" metric used above, we see that Round 2 provided a 89% improvement in the ramp area taxi-in times and 6% improvement for movement area taxi-in times over Round 1.

In conclusion, after Round 2 validation the taxi-in times match very well with their actual counterpart taxi-in times. We believe we are at a good enough validation level for taxi-in times, in general.

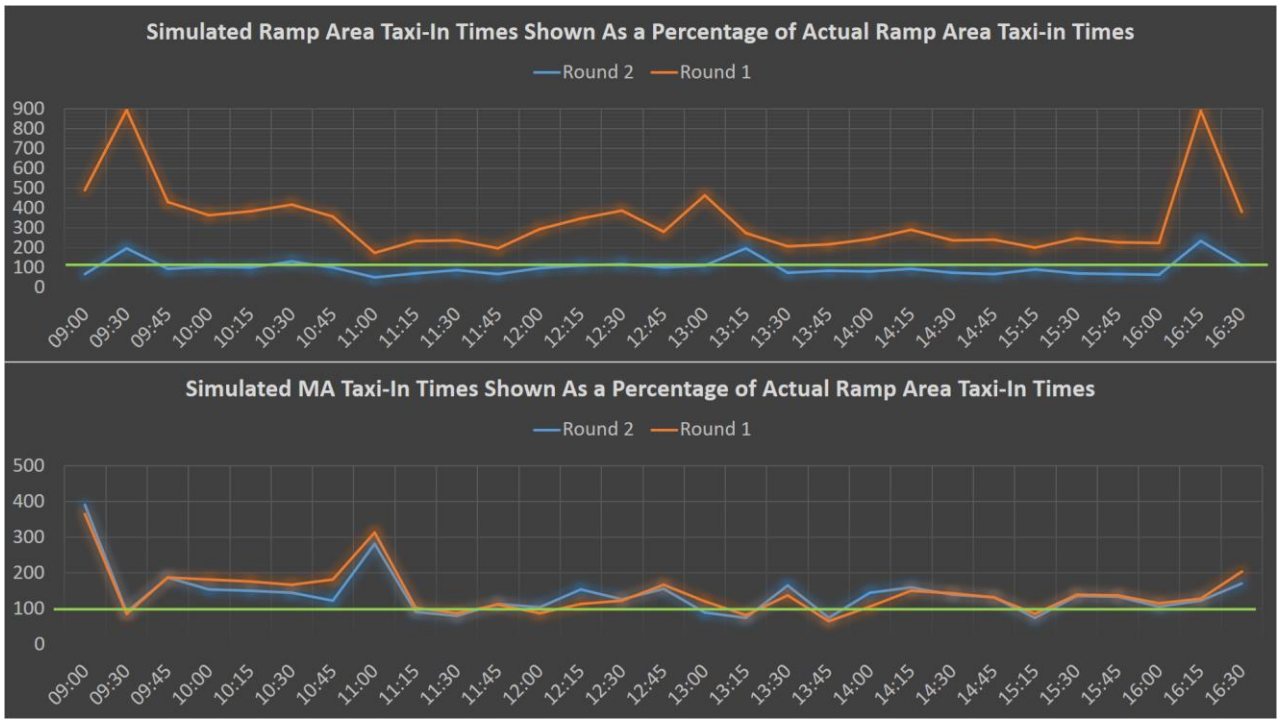

Figure 18. Simulated Taxi-in Times Plotted as the Percentage of Actual Taxi-in Times, Green Line Shows Ideal 100% Match

This section summarized the work done in generating and validating the SOSS airport surface simulation models. Next, we discuss the airspace simulation component of the AOSS model.

4.4. AOSS Airspace Simulation Component

As discussed in Section 4.1, AOSS consists of three major components. The STFM and CTFM components were discussed in good detail in that section. Here, we present more details of the third AOSS component – airspace simulation model.

The AOSS airspace simulation component is a MATLAB-based queuing simulation, which simulates aircraft trajectories along a network of frequently-flown airspace routes. SOSS transfers over the simulation-control of a departure flight to AOSS at the departure takeoff point. AOSS then simulates the movement of the departure flight along its airborne route from takeoff runway to the departure fix and then on through a series of en route sectors to an en route TBFM meter arc, where the departure flight merges with the overhead en route traffic streams. In addition to focus airport departures, the AOSS airspace simulation component also models transit of other interacting flights from their respective simulation injection points to appropriate en route meter arcs. Interacting flights consist of departures originating from satellite airports within the same TRACON as the focus ATD-2 airport, as well as departures originating from other NAS-wide airports and merging with the ATD-2 airport departures in the en route airspace. AOSS includes queuing simulation based models of the departure-fix merge process as well as the en route meter arc merge process. The key AOSS airspace simulation components are (i) flight airspace route models that represent most commonly flown airspace routes (in both TRACON and en route airspace), (ii) transit time models for individual sectors within the airspace routes network, and (iii) queue control methodology for simulating the merging of aircraft at key metering points in the

airspace route network. The next three sub-sections (4.4.1, 4.4.2, and 4.4.3) describe these three simulation components.

4.4.1. AOSS Airspace Routes Network

The AOSS airspace routes network consists of the airspace routes most commonly used by departures from the focus ATD-2 airport and its satellite airports with which the focus airport departures share TRACON boundary departure fixes, as well as all other NAS-wide traffic that interacts with the focus ATD-2 airport departures in en route airspace. We describe the airspace node-link network development approach and results using CLT as the example focus ATD-2 airport. After that, we present the airspace route networks for DFW and EWR.

4.4.1.1. CLT AOSS Airspace Routes Model

The first step in the development of the airspace routes network was to analyze historical CLT, CLT-satellite, and other interacting departure tracks to determine the major departure flows and the major constraint points where the CLT departures merge with other traffic during their transit from runway takeoff to en route stream merge. In our simulation modeling work, we have focused on modeling en route merge problems for CLT departures going to destination airports in the Northeast U.S. only. We used end-to-end merged surveillance track data from NASA's Sherlock ATM data warehouse for the departure flow analysis task. Sherlock data processing modules fuse air traffic control automation and radar data from nationwide ARTCCs, regional TRACONs, and ASDE-X feeds from all major airports in the U.S. with other flight and environmental data into multi-dimensional flight tracks that cover NAS-wide IFR traffic in the U.S. from end-to-end. To obtain a working dataset, we first analyzed CLT airport runway configuration data from the ASPM metrics database to identify eight days when the South-flow runway configuration was active. Then, we obtained the end-to-end merged Sherlock ATM data warehouse track data for these eight days. We applied multiple ATAC track data bundling, processing, and visualization tools in conjunction with multiple manual processes for identifying and classifying tracks into appropriate bundles that form the route network, as well as reducing the complexity of the network by removing unnecessary nodes and links. The following is a description of the major steps involved in this process.

- Visualize track data for all flights with internal ATAC tool to manually identify 5-15 common merge points (i.e., en route meter arcs); give each point a name, latitude, and longitude in an input file.
- Correlate the merge-points observed in the historical track data with the TBFM meter arc locations obtained from NASA [CCC17] and allocate the appropriate merge-points to the respective TBFM meter arc
- Use the same visualization to pick 3-5 simulation injection nodes (see Section 4.4.2 for definition of injection node) and manually enter these into another input file
- Run a C# application with the following automated processing pipeline:
    - Assign each CLT and CLT satellite flight (collectively "CLT-origin flights") to a departure fix by picking the departure fix that the flight track data comes closest to.
    - Determine which en route sector(s) each CLT-origin flight passes through by performing geo-spatial comparisons between track points and sector boundaries.

  - Remove all en route sectors not passed through by CLT-origin flights from consideration for the remainder of analysis
  - Compute and assign the closest injection node to each non-CLT-origin flight
  - Determine en route sector(s) for non-CLT-origin flights with same procedure used for CLT-origin flights. Flights found to not pass through any en route sectors identified above are excluded from the remainder of analysis. Allocate non-CLT-origin flights to the appropriate meter arcs where they merge with CLT traffic
  - The above steps result in a summary file containing all sector/meter arc crossing and flight information for all remaining (approximately 5700) flights.
  - The summary file further parsed into separate file defining airspace route (i.e., sequence of departure-fix and sectors) per flight.
- Run a Matlab program designed to pull all information out of the airspace route file to convert them to Matlab objects usable for AOSS simulation.

We followed the process described in the steps above to obtain progressively simplified airspace route networks until we had reduced the network to an acceptable level of complexity without sacrificing modeling accuracy. Figure 19 shows the final CLT airspace route network that we used in our combined surface-airspace simulations.

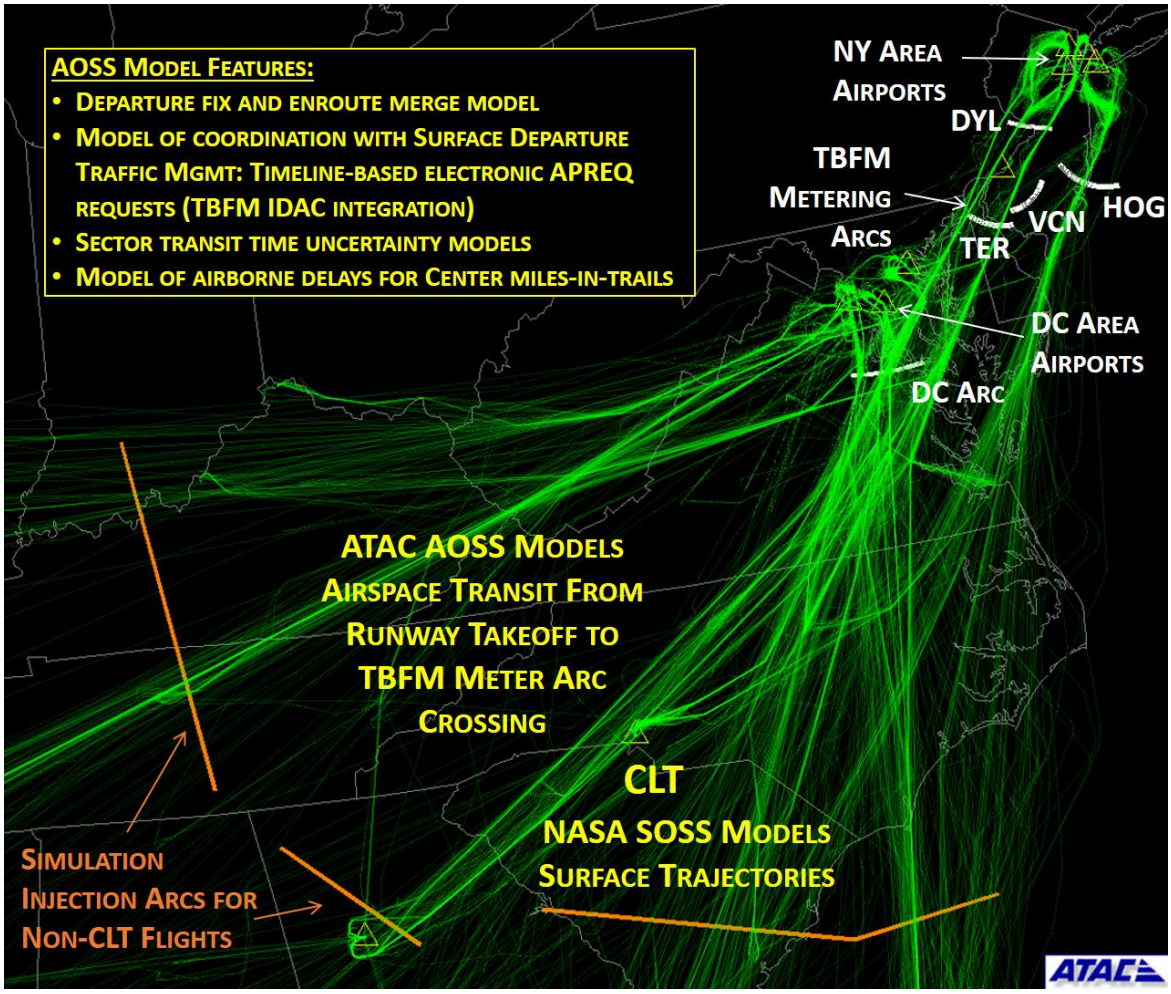

Figure 19. CLT airspace route network showing the simulation injection points and TBFM meter arcs components

4.4.1.2. DFW AOSS Airspace Routes Model

The airspace route network generation process for the DFW airspace model followed the same procedure as the CLT airspace network model. For DFW, we modeled the following meter arcs in the en route airspace:

- ZME meter arcs ZME-FSM, ZME-RZC, and ZME-UJMTXK and ZKC meter arcs ZKC-LCT, ZKC-SGF, ZKC-TUL, where DFW and DAL departures going to ORD and MDW are frequently metered to
- ZHU meter arcs ZHU-CWK, ZHU-DAS, ZHU-LLO, ZHU-TNV where DFW and DAL departures going to IAH and HOU are frequently metered to
- ZKC meter arcs ZKC-LCT, ZKC-LBL and ZAB meter arc ZAB-CLM, where DFW and DAL departures going to DEN are frequently metered to

Figure 20 shows these modeled meter arcs superimposed on DFW departures to the specific destination airports, which experience the most departure restrictions. These destination airports

are ORD, MDW, DEN, HOU, and IAH. All DFW TRACON internal departures as well as all NAS-wide departures going to the above mentioned destination airports and passing through the modeled en route meter arcs are included in the airspace simulation. Each of these departure flights is allocated an appropriate departure fix, simulation injection point, an airspace route consisting of a series of en route sectors and ending in a meter arc.

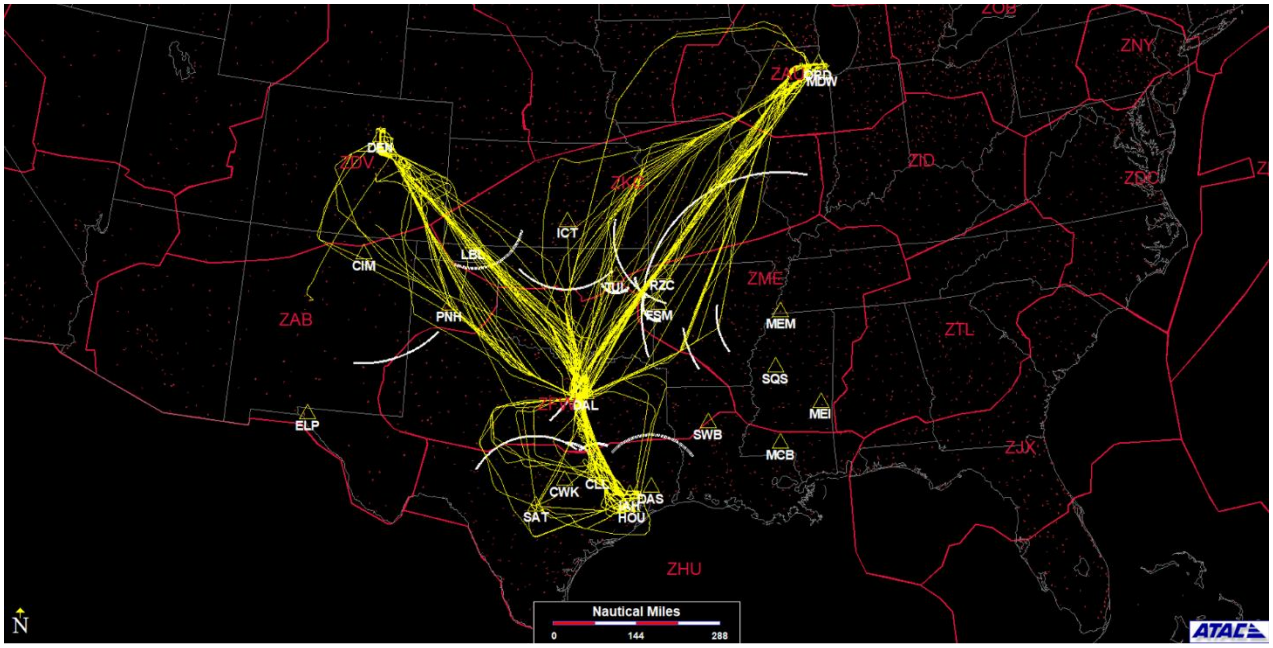

Figure 20. Modeled en route meter arcs at which DFW and DAL departures are frequently metered, shown here along with DFW departure tracks going to ORD, MDW, DEN, HOU, and IAH

4.4.1.3. EWR AOSS Airspace Routes Model

The airspace route network generation process for the EWR airspace model followed the same procedure as the CLT airspace network model, with one difference. The difference was that we did not extend the EWR airspace model into the en route airspace but ended all the departure airspace routes at the respective departure fixes. Departure fix merging represents the most restraining constraint on New York TRACON departures. Once the flights cross the departure-fixes they do not face significant en route merging constraints. Rather other airports that lie underneath the major New York area exit en route routes face constraints for fitting into the New York exit traffic streams. As a result, for ATD-2 benefits assessment we deemed it appropriate to end the extent of airspace routes to the boundary of the New York TRACON. **Figure 21** shows the modeled departure fixes along with departure traffic on an average day from EWR, JFK, LGA, and TEB.

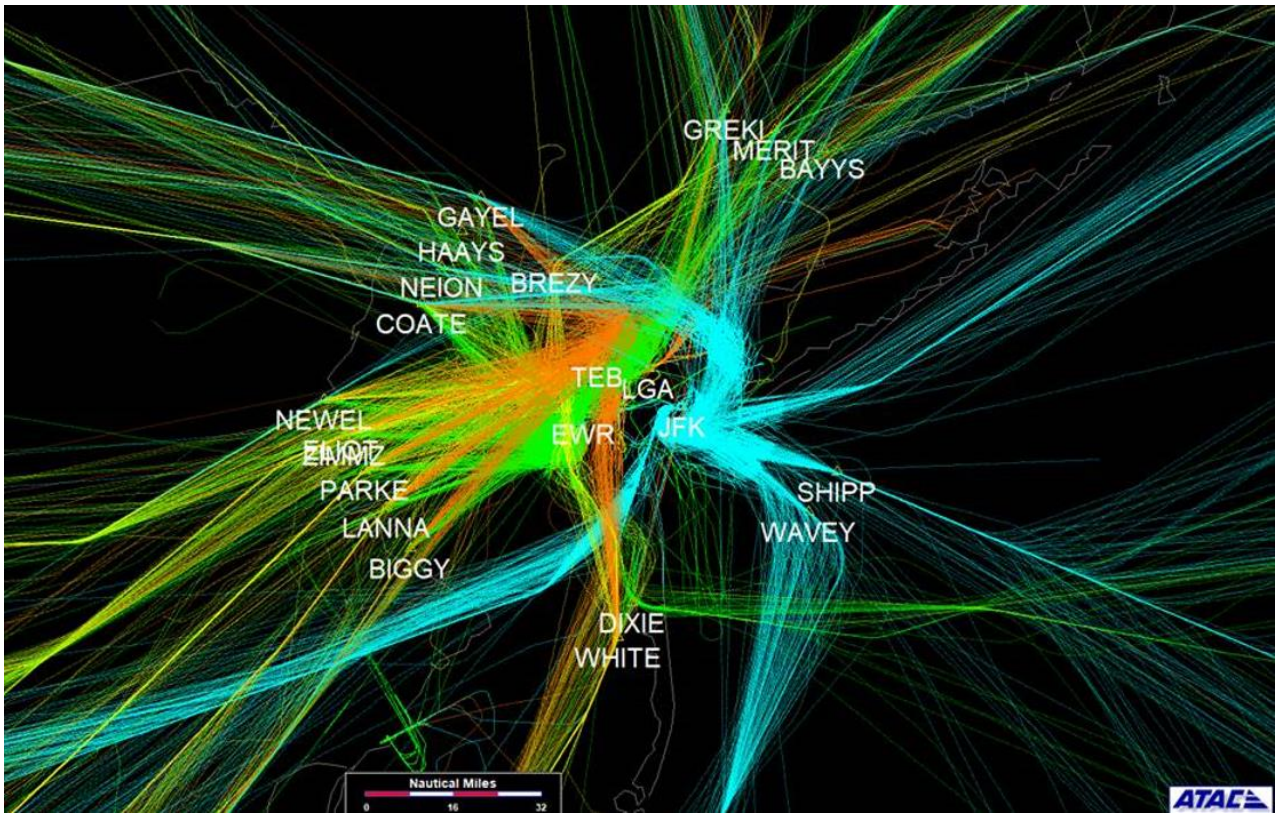

Figure 21. Modeled departure fixes shown here with EWR (green), JFK (blue), LGA (orange), and TEB (yellow) departure traffic

4.4.2. Transit Time Models for Airspace Network Links

The sections of a departure flight's airspace route are each associated with characteristic transit times. These transit times are derived from analysis of historical operational data (end-to-end merged Sherlock trajectory data). The typical airspace route for a focus airport departure flight (e.g., CLT departure flight) starts at the runway takeoff node, continues on to the departure-fix node, then passes through a series of en route sectors and ends at the en route meter arc where it merges with other traffic flows going to the same destination. The transit time models TRACON airspace transit time from the runway takeoff node to a departure fix as well as individual sector transit times for the sectors in the flight's path. For focus ATD-2 airport satellite departures (e.g., departures from smaller airports within the CLT TRACON), the airspace route consists of a simple node representing the departure runway, a departure-fix node, and (if the departure merges with overhead en route traffic) a series of en route sectors followed by the final meter arc. The transit time model for CLT-satellite airport departures includes departure runway node to the departure-fix transit time model and individual sector transit time models for its en route sectors. For all other non-focus airport, non- satellite departure flights, the route starts at a simulation injection node, which is defined somewhere in the en route airspace, mostly on the boundary between two Centers. The route then continues on through one or more en route sectors and ends at a final en route meter arc. Transit time models for these flights include sector transit time models for the individual en route sectors within the flight's path.

The TRACON airspace and en route airspace transit times are derived by applying ATAC in-house tools for detecting and computing fix-crossing times and sector boundary crossing times. The airborne transit time model utilizes a distribution of transit times to identify the 10th percentile transit time as the simulated unimpeded transit time. Simulated transit times are computed separately for each aircraft type that was found in the Sherlock track data.

Note that unimpeded transit times are used to simulate the movement of flights over links. The delays due to airspace congestion are added by simulating queues at key merge nodes in the airspace route network. The purpose of this queuing simulation is not to accurately simulate the 4-dimensional (4D) trajectory of flights but to provide a good approximation of the congestion related delay that the flights will incur in their combined surface and airspace transit from gate to en route stream merge. The next section describes the queue control methodology used to simulate delays at the queues.

4.4.3. Queue Control at Key Airspace Merge Points

The algorithm for queue control at key nodes is the main driver for the AOSS fast-time simulation platform. Figure 22 shows the main steps involved in the AOSS simulation. The surface simulation part is only applicable to satellite airports in the vicinity of the main focus ATD-2 airport. Each of the major control points in the node-link network (the satellite airport gate-groups, the departure runways, the departure-fixes, and the enroute stream merge-fixes) is associated with a queue. The rest of this section describes how the simulation manages the entry and exit times for individual flights to/from these queues. The fast-time simulation works in discrete time-steps equal to the SOSS scheduler call interval. At each time-step, the simulation processes through the seven steps shown in Figure 22.

Step 1: Departure Pushback Management at Satellite Airports. In this step, the simulation first determines how many departure flights will be ready for pushing back at the current time-step. When simulating current-day departure operations, the Pushback Readiness Time for a flight is computed by adding a random perturbation to the flight's Scheduled Gate Departure Time. This models pre-pushback delays. In current-day operations simulation, flights push back when they are ready (i.e., at their Pushback Readiness Time).

While simulating ATD-2 operations, the flight is assumed to be ready for pushback at its Pushback Readiness Time, but holds at the gate until the Target Off Block Time (TOBT). TOBT is the required gate pushback time computed by ATD-2 scheduling algorithm. Note that the scheduling algorithm performs all computations based on the knowledge of Scheduled Gate Departure Times and/or Estimated Off Block Times (EOBTs) where they are available; it does not know the exact time when the flight would be ready to push back (i.e., Pushback Readiness Times).

After identifying the flights that are ready for pushback at the current time-step, the simulation pushes them back by updating their actual gate pushback time.

Step 2: Taxi-out Time Calculation. In this step, the simulation identifies aircraft that have pushed back at the current time-step and updates the actual runway queue entry times for these flights using a taxi-out time model. Different taxi-out time (transit time) models used by the simulation platform were discussed in the previous section. It is assumed that the flights will enter the runway departure queue in the first-come first-served (FCFS) order. The FCFS runway queue entry order may be modified if there is an instance of two successive new runway queue entrants with the same allocated departure-fix. In such cases, we simulate the sequencing decisions made by Ground

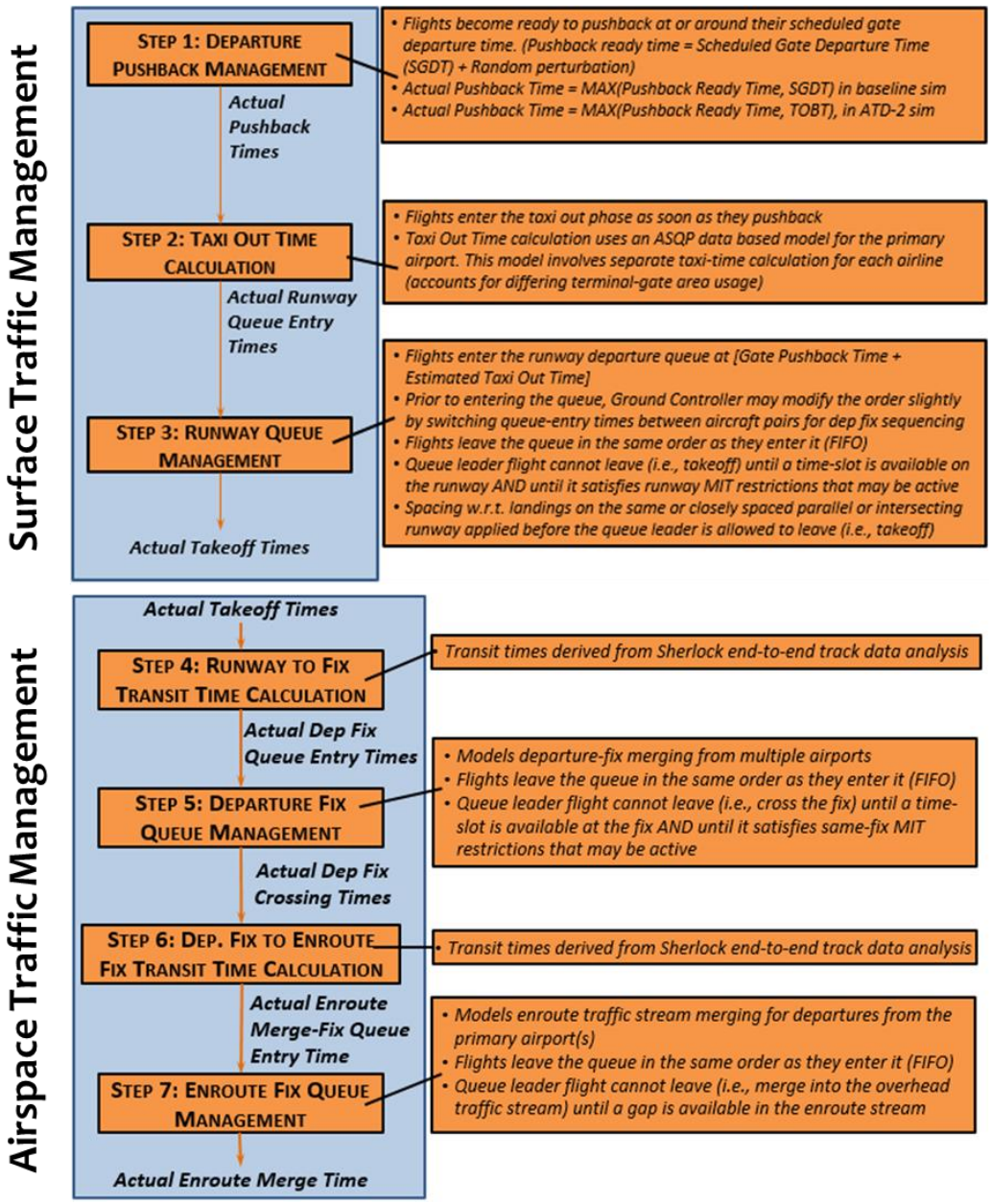

Figure 22. AOSS Queuing Simulation Steps. Note: Surface Traffic Management steps are only applicable to satellite airports in the vicinity of the focus ATD-2 airport. For the focus airport, AOSS only simulates the post-takeoff part of its trajectory

Controllers by allowing sequence switches to avoid two successive flights going to the same departure-fix. A sequence switch is allowed only if the runway queue entry times of the flights switching sequence with each other fall within an allowed range of time (we used a 2-minute allowed time range for our simulation platform). This 2-minute restriction models limited re-sequencing leeway available to the ground controllers in reality.

Step 3: Runway Queue Management. In this step, the simulation determines whether the leader of each runway queue can leave the queue (i.e., take off from the runway) at this time-step. Two criteria are used to determine if the flight can take off or not—(i) runway minimum separation

requirement for safety is satisfied: This constraint is not applied by enforcing an exact required time separation. Instead, we divide the runway time-line into time-slots, each time-slot being of sufficient length based on a called runway departure rate (obtained from ASPM data). Then we allow only one departure to take off per runway time-slot; (ii) MIT separation requirement for consecutive flights going to the same departure fix is satisfied: To enforce this separation requirement (if a MIT restriction is active for the runway under consideration), the simulation keeps track of the last flight to depart from each runway to each departure-fix. The current leader of the runway queue is not allowed to depart until it satisfies the prescribed MIT separation with the last departure flight to the same fix to takeoff from that runway. MIT restrictions may be specific to certain departure flows, e.g., some restrictions are only applicable to departures going to certain destination airport(s). Our simulation platform enforces such special MIT restrictions also.

If the current leader of the runway queue is eligible for taking off during this time-step (i.e., if it satisfies the above two conditions), then the simulation updates its actual runway takeoff time. Then the simulation evaluates whether the next flight in the runway queue (the new leader of the queue) is eligible for takeoff during this time-step. This process continues until a leader is found that cannot take off during this time-step.

Note, steps 1-3 are only applicable to satellite airport departures.

Step 4: Runway to Departure Fix Transit Time Computation. At each time-step, the simulation identifies the flights that have taken off during this time-step. These flights include satellite airport departures that are processed through the surface part of the AOSS simulation (i.e., Steps 1-3) and the main focus ATD-2 airport departures whose surface transit is simulated by SOSS. For our CLT-focused example, AOSS obtains data on the current and predicted positions of CLT departure flights from SOSS using the SOSS Common Algorithm Interface. In other words, AOSS acts as an external scheduler for SOSS. For the CLT and CLT-satellite flights that are identified to be taking off in the current time-step, Step 4 computes and updates their actual departure-fix queue entry time by adding the estimated runway-to-fix transit time to the flight's runway takeoff time.

Step 5: Departure Fix Queue Management. In this step, the simulation evaluates whether the leader of the departure-fix queue can leave the queue (i.e., cross the departure-fix) during this time-step. The criterion used to determine if the flight can cross the departure-fix is the minimum separation requirement with respect to the previous flight that crossed the departure-fix. Rather than implementing this as a straight time-difference computation, the simulation (similar to its handling of runway minimum separations) divides the departure-fix timeline into time-slots. The length of each time-slot is computed by assuming that the controllers will try to maintain an on-average seven miles in-trail separation between consecutive departure-fix crossings (this is a number we found out from discussions with former controllers) and the flights will cross the departure-fix at 250 knots. If a MIT restriction is active at that departure-fix, then time-slots are calculated assuming the bigger MIT restriction. The flight can cross the departure-fix if the departure-fix time-slot associated with the current time-step is available. In this case, the simulation updates the flight's actual departure fix crossing time.

Step 6: Departure Fix to Enroute Merge Point Transit Time Calculation/Enroute Merge Point to Enroute Merge Point Transit Time Calculation. In this step, the simulation computes and updates the actual enroute merge-point queue entry time for each new departure-fix crossing, by adding the estimated departure-fix to merge-fix transit time to the flight's departure-fix crossing

time. In general, Step 6 computes enroute merge-point queue entry times for all airborne departures once they exit from the previous enroute fix queue or enter the simulation at their simulation injection point.

Step 7: Enroute Stream Merge Point Queue Management. In this step, the simulation determines whether the leader of a merge-fix queue can leave the queue (i.e., merge with the enroute traffic stream). The leader can merge into the enroute traffic stream only if a traffic gap concurrent with the current time-step is available. Merge-fix crossing is modeled as fitting flights into 8 nm-wide merge-slots, some of which are already occupied by overflights or departures from different airports.

In Step 7, if an enroute traffic gap is available at the current time-step and a flight is waiting in the enroute merge-fix queue, then the simulation updates the flight's actual enroute stream merge time. The flight leaves the current enroute merge-node at this time-step. At the next time-step the simulation will compute its entry time to the queue for the next node in its route. Finally, the flight exits the simulation at the time of its release from the last airspace node in its route.

4.5. ATD-2 Tactical Surface Scheduler Emulation

In order to support high-fidelity assessment of ATD-2 benefits, ATAC has developed an emulation of NASA's ATD-2 Tactical Surface Scheduler. This section provides an overview of the component processing steps of this emulation algorithm and presents a step-by-step walkthrough of the processing steps to aid the validation of the emulation algorithm against the real-time ATD-2 Tactical Surface Scheduler. The ATAC ATD-2 scheduler emulation followed all the prediction, sorting, prioritization, and spacing steps outlined in NASA's ATD-2 scheduler specification documentation [B17]

Next, we describe a step-by-step walkthrough of an example scheduling scenario consisting of set of arrival, departure and crossing flights operating on the CLT surface during an actual SOSS-AOSS simulation step, and provide a tabular depiction of the relevant scheduling data at each step of the ATD-2 Tactical Surface Scheduler algorithm.

Step 1: To start with, at each scheduling time-step, the scheduler obtains the latest information from the simulation platform about flights on the CLT surface as well as flights predicted to land and pushback within a user-defined Planning Time Horizon. Planning Horizon was set to 45 minutes in all simulations. The scheduling time-step was set to 30 seconds. The scheduler parses this information into access-friendly programming structures. Table 1 shows the scheduling information obtained by the ATAC scheduler during one step of the SOSS-AOSS simulation. Table 1 shows 18C operations in green background, 18L operations in orange background and 18R operations in bkue background. As seen from the Table, there are 13 departures and one arrival scheduled for operation on runway 18C, 12 departures scheduled to operate from runway 18L and 5 arrivals scheduled to land on runway 18R. The 18R arrivals also cross runway 18C at its intersection with Taxiway S. As shown in Table 1, the scheduler predicts the Earliest Times of Arrival (ETAs) for all arrivals, departures and crossers. The rightmost column of the table outlines potential scheduling problems in terms of consecutive operations being too close to each other or being impacted by TMIs. Please note that two departures (AWI3819 and AAL2091) scheduled to depart from runway 18C are impacted by APREQ runway release time constraints.

Callsign	opType	WtClass	Runway	Runway Xing Node	Gate	Runway ETA	APREQ Rwy Release Time	Runway Xing ETA	SOBT	EOBT	Flight Status	Runway SEP (seconds)	PROBLEMS
AAL2062	ARR	D	18C		Gate_C_08	11:06					RAMP_TAXI_IN		
DAL671	DEP	D	18C		Gate_A_03	11:08			11:02	11:02	RAMP_TAXI_OUT	120	
JIA5093	DEP	E	18C		Gate_E_29	11:26			11:13	11:13	AT_GATE	1080	
JIA5268	DEP	E	18C		Gate_E_11	11:28			11:16	11:16	AT_GATE	120	
JIA5061	DEP	E	18C		Gate_E_15	11:30			11:19	11:19	AT_GATE	120	
FFT200	DEP	D	18C		Gate_A_08	11:30			11:23	11:23	AT_GATE	0	SEP SMALL
AWI3819	DEP	E	18C		Gate_E_01	11:35	11:40		11:23	11:23	AT_GATE	300	APREQ
JIA5042	DEP	E	18C		Gate_E_07	11:35			11:23	11:23	AT_GATE	0	SEP SMALL
AAL2091	DEP	D	18C		Gate_B_10	11:36	11:42		11:28	11:28	AT_GATE	60	SEP SMALL, APREQ
AAL662	DEP	D	18C		Gate_B_13	11:37			11:29	11:29	AT_GATE	60	SEP SMALL
AAL1909	DEP	D	18C		Gate_C_03	11:38			11:29	11:29	AT_GATE	60	SEP SMALL
JIA5277	DEP	E	18C		Gate_E_23	11:39			11:27	11:27	AT_GATE	60	SEP SMALL
AAL1993	DEP	D	18C		Gate_B_03	11:41			11:35	11:35	AT_GATE	120	
JIA5073	DEP	E	18C		Gate_E_13	11:45			11:33	11:33	AT_GATE	240	
AAL1877	DEP	D	18L		Gate_B_11	11:09			10:57	10:57	RAMP_TAXI_OUT		
GJS6245	DEP	E	18L		Gate_A_01	11:10			11:00	11:00	RAMP_TAXI_OUT	60	SEP SMALL
SWA766	DEP	D	18L		Gate_A_06	11:20			11:10	11:10	AT_GATE	600	
JIA5039	DEP	E	18L		Gate_E_16a	11:26			11:23	11:23	AT_GATE	360	
AAL1654	DEP	D	18L		Gate_C_18	11:30			11:23	11:23	AT_GATE	240	
AAL2042	DEP	D	18L		Gate_B_15	11:31			11:22	11:22	AT_GATE	60	SEP SMALL
JIA5432	DEP	E	18L		Gate_E_25	11:32			11:28	11:28	AT_GATE	60	SEP SMALL
AAL1956	DEP	D	18L		Gate_C_04	11:34			11:28	11:28	AT_GATE	120	
JIA5252	DEP	E	18L		Gate_E_17	11:34			11:30	11:30	AT_GATE	0	SEP SMALL
AAL1732	DEP	D	18L		Gate_B_16	11:35			11:27	11:27	AT_GATE	60	SEP SMALL
PDT4973	DEP	E	18L		Gate_E_34	11:37			11:33	11:33	AT_GATE	120	
AAL1903	DEP	D	18L		Gate_C_06	11:38			11:32	11:32	AT_GATE	60	SEP SMALL
PDT4935	ARR	E	18R	S_12	Gate_E_29	11:12		11:15			IN_AIR		
JIA5295	ARR	E	18R	S_12	Gate_E_28	11:14		11:18			IN_AIR	120	
JIA5355	ARR	E	18R	S_12	Gate_E_06	11:19		11:23			IN_AIR	300	
JIA5160	ARR	E	18R	S_12	Gate_E_15	11:25		11:30			IN_AIR	360	
AAL1944	ARR	D	18R	S_12	Gate_C_13	11:32		11:37			IN_AIR	420	

Table 5. Example scheduling scenario used for stepping through scheduling algorithm steps

Step 2: In Step 2, the scheduler applies an Order of Consideration algorithm to allocate priorities to individual flights based on their current positions and estimated active times. First, the scheduler analyzes the current position of flights already active on the airport surface to determine if they are in ramp taxi or movement area taxi. For flights still at their gates, the scheduler compares their predicted gate pushback times (including flights for which the airlines have provided their estimates – Estimated Off Block Times, EOBTs), against the current time to determine if the flights are "ready" (i.e., already called in ready to pushback), or "planned" (i.e., have provided EOBTs and their EOBT is within the next 10 minutes), or "uncertain" (i.e., have either not provided an EOBT or are not estimated to pushback within the next 10 minutes). In addition, the scheduler also assesses the predicted landing times for arrival flights still in the air. Table 2 shows the assigned priorities for the scheduling scenario under study. Table 3 explains the numerical priorities that the scheduler has assigned to the flights.

Note that Table 2 only shows departures taking off from and arrivals landing on runways 18C and 18L. Arrivals landing on runways 23 and 18R are not considered for scheduling, but they are considered while determining Scheduled operation times for 18C and 18L departures. Arrivals landing on 18R also cross the active runway 18C. But, crossings are not considered during the first pass. First, all the arrival landings are scheduled (without delay), then all departures and finally, after all departures are scheduled, we perform a second scheduling pass to fit crossers in between arrival landing and departure takeoff operations on 18C.

Callsign	opType	WtClass	Runway	Gate	Runway ETA	APREQ Rwy Release Time	SOBT	EOBT	Flight Status	Priority
AAL2062	ARR	D	18C	Gate_C_08	11:06				RAMP_TAXI_IN	5
DAL671	DEP	D	18C	Gate_A_03	11:08		11:02	11:02	RAMP_TAXI_OUT	8
JIA5093	DEP	E	18C	Gate_E_29	11:26		11:13	11:13	AT_GATE	11
JIA5268	DEP	E	18C	Gate_E_11	11:28		11:16	11:16	AT_GATE	11
JIA5061	DEP	E	18C	Gate_E_15	11:30		11:19	11:19	AT_GATE	12
FFT200	DEP	D	18C	Gate_A_08	11:30		11:23	11:23	AT_GATE	12
AWI3819	DEP	E	18C	Gate_E_01	11:35	11:40	11:23	11:23	AT_GATE	6
JIA5042	DEP	E	18C	Gate_E_07	11:35		11:23	11:23	AT_GATE	12
AAL2091	DEP	D	18C	Gate_B_10	11:36	11:42	11:28	11:28	AT_GATE	6
AAL662	DEP	D	18C	Gate_B_13	11:37		11:29	11:29	AT_GATE	12
AAL1909	DEP	D	18C	Gate_C_03	11:38		11:29	11:29	AT_GATE	12
JIA5277	DEP	E	18C	Gate_E_23	11:39		11:27	11:27	AT_GATE	12
AAL1993	DEP	D	18C	Gate_B_03	11:41		11:35	11:35	AT_GATE	12
JIA5073	DEP	E	18C	Gate_E_13	11:45		11:33	11:33	AT_GATE	12
AAL1877	DEP	D	18L	Gate_B_11	11:09		10:57	10:57	RAMP_TAXI_OUT	8
GJS6245	DEP	E	18L	Gate_A_01	11:10		11:00	11:00	RAMP_TAXI_OUT	8
SWA766	DEP	D	18L	Gate_A_06	11:20		11:10	11:10	AT_GATE	11
JIA5039	DEP	E	18L	Gate_E_16a	11:26		11:23	11:23	AT_GATE	12
AAL1654	DEP	D	18L	Gate_C_18	11:30		11:23	11:23	AT_GATE	12
AAL2042	DEP	D	18L	Gate_B_15	11:31		11:22	11:22	AT_GATE	12
JIA5432	DEP	E	18L	Gate_E_25	11:32		11:28	11:28	AT_GATE	12
AAL1956	DEP	D	18L	Gate_C_04	11:34		11:28	11:28	AT_GATE	12
JIA5252	DEP	E	18L	Gate_E_17	11:34		11:30	11:30	AT_GATE	12
AAL1732	DEP	D	18L	Gate_B_16	11:35		11:27	11:27	AT_GATE	12
PDT4973	DEP	E	18L	Gate_E_34	11:37		11:33	11:33	AT_GATE	12
AAL1903	DEP	D	18L	Gate_C_06	11:38		11:32	11:32	AT_GATE	12

Table 6. Scheduling information after Step 2, which allocates priorities to the flights

(1) EMERGENCY_ARRIVAL (gate, airborne, taxi): Never used
(2) EMERGENCY_DEPARTURE (gate, airborne, taxi): Never used
(3) NO_PRIORITY_ARRIVAL (airborne): All airborne arrivals
(4) EXEMPT_ARRIVAL_TAXI (taxi): Never used
(5) NO_PRIORITY_ARRIVAL_TAXI (taxi): All taxiing arrivals
(6) APREQ_DEPARTURE (gate & taxi): All APREQ-impacted departures at gate and in taxi
(7) EDCT_DEPARTURE (gate & taxi): All EDCT-impacted departures at gate and in taxi
(8) NO_PRIORITY_DEPARTURE_TAXI (taxi): All other departures in taxi
(9) EXEMPT_DEPARTURE (gate): Never used
(10) GATE_DEPARTURE_READY (gate): All departures at gate whose ready time is already in the past
(11) GATE_DEPARTURE_PLANNED (gate): All AAL at gate departures whose ready time is in the next 10 minutes
(12) GATE_DEPARTURE_UNCERTAIN (gate): All other at gate departures
(13) UNKNOWN_PRIORITY: All others

Table 7. Numerical priority level indicators used by the scheduling algorithm

As seen from Table 2, the one arrival, which landed on 18C prior to the start of this scheduling cycle, got assigned priority 5 (NO_PRIORITY_ARRIVAL_TAXI) because it is in the taxi phase of its transit. Note that the scheduling cycle being analyzed started at 11:06 UTC. AWI2091 and AAL2091 were assigned priority 6, because they have APREQ runway release time constraints. DAL671, AAL1877 and GJS6245 were the only departures in taxi phase, so they were assigned priority 8 (NO_PRIORITY_DEPARTURE_TAXI). All other departures were at their gates at the beginning of the scheduling cycle. None of the departures were ready for pushback at the start of

the scheduling cycle. Departures with their EOBTs within the next 10 minutes were assigned to priority 11 (GATE_DEPARTURE_PLANNED). All other departures were assigned to priority 12 (GATE_DEPARTURE_UNCERTAIN).

Step 3: All subsequent steps after step 2 process individual flights according to the Order of Consideration, which means that the flight with higher priority (i.e., lower priority category number) are processed first. Within the same priority category, flights are processed in the order of their Runway ETAs. Arrivals in air are the highest priority (emergency arrivals and emergency departures are the top priority category as per Table 3, but we do not consider emergency flights in our scheduler evaluation process). The arrivals are scheduled first. They are allocated Scheduled Times of Arrival (STAs) on the runway equal to their ETAs.

Step 4: Next in the order of consideration are APREQ and EDCT departures. In our example scheduling scenario there are two departures with APREQ runway release time constraints. The scheduler next schedules these two departures. They are allocated a runway STA equal to the start of the APREQ release time window (= APREQ Runway Release Time – 1 minute). No spacing rules are applied when computing the Runway STAs for these flights. From Runway STAs, the scheduler back-computes the required Target Off Block Time (TOBT) for releasing the flights from their gates. The resultant Runway STAs and TOBTs for the scheduled APREQ departures in Step 3 as well as resultant Runway STAs for landing arrivals scheduled in Step 2, are shown in Table 4.

Callsign	opType	WtClass	Runway	Gate	APREQ Rwy Release Time	SOBT	EOBT	Flight Status	Priority	Scheduler Prediction: Runway ETA	Scheduler Computation: Runway STA	Scheduler Computation: TOBT
AAL2062	ARR	D	18C	Gate_C_08				RAMP_TAXI_IN	5	11:02	11:02	
DAL671	DEP	D	18C	Gate_A_03		11:02	11:02	RAMP_TAXI_OUT	8	11:08		
JIA5093	DEP	E	18C	Gate_E_29		11:13	11:13	AT_GATE	11	11:26		
JIA5268	DEP	E	18C	Gate_E_11		11:16	11:16	AT_GATE	11	11:28		
JIA5061	DEP	E	18C	Gate_E_15		11:19	11:19	AT_GATE	12	11:30		
FFT200	DEP	D	18C	Gate_A_08		11:23	11:23	AT_GATE	12	11:30		
AWI3819	DEP	E	18C	Gate_E_01	11:40	11:23	11:23	AT_GATE	6	11:35	11:39	11:27
JIA5042	DEP	E	18C	Gate_E_07		11:23	11:23	AT_GATE	12	11:35		
AAL2091	DEP	D	18C	Gate_B_10	11:42	11:28	11:28	AT_GATE	6	11:36	11:41	11:33
AAL662	DEP	D	18C	Gate_B_13		11:29	11:29	AT_GATE	12	11:37		
AAL1909	DEP	D	18C	Gate_C_03		11:29	11:29	AT_GATE	12	11:38		
JIA5277	DEP	E	18C	Gate_E_23		11:27	11:27	AT_GATE	12	11:39		
AAL1993	DEP	D	18C	Gate_B_03		11:35	11:35	AT_GATE	12	11:41		
JIA5073	DEP	E	18C	Gate_E_13		11:33	11:33	AT_GATE	12	11:45		
AAL1877	DEP	D	18L	Gate_B_11		10:57	10:57	RAMP_TAXI_OUT	8	11:09		
GJS6245	DEP	E	18L	Gate_A_01		11:00	11:00	RAMP_TAXI_OUT	8	11:10		
SWA766	DEP	D	18L	Gate_A_06		11:10	11:10	AT_GATE	11	11:20		
JIA5039	DEP	E	18L	Gate_E_16a		11:23	11:23	AT_GATE	12	11:26		
AAL1654	DEP	D	18L	Gate_C_18		11:23	11:23	AT_GATE	12	11:30		
AAL2042	DEP	D	18L	Gate_B_15		11:22	11:22	AT_GATE	12	11:31		
JIA5432	DEP	E	18L	Gate_E_25		11:28	11:28	AT_GATE	12	11:32		
AAL1956	DEP	D	18L	Gate_C_04		11:28	11:28	AT_GATE	12	11:34		
JIA5252	DEP	E	18L	Gate_E_17		11:30	11:30	AT_GATE	12	11:34		
AAL1732	DEP	D	18L	Gate_B_16		11:27	11:27	AT_GATE	12	11:35		
PDT4973	DEP	E	18L	Gate_E_34		11:33	11:33	AT_GATE	12	11:37		
AAL1903	DEP	D	18L	Gate_C_06		11:32	11:32	AT_GATE	12	11:38		

Table 8. Step 4 schedules APREQ and EDCT-impacted departure flights

As seen from Table 4, the one arrival landing on runway 18C got scheduled right at its runway landing time, whereas the two APREQ-impacted flights got scheduled 1 minute prior to their APREQ Runway Release Times, with associated delays at the gate.

Step 5: Next in the order of consideration are taxiing departures (NO_PRIORITY_DEPARTURE_TAXI). The departures are selected for scheduling in the order of their Runway ETAs. For each next departure selected for scheduling, the scheduler checks safe separation against the following types of operations:

Weight classes and weight-class dependent separation values for this spacing evaluation is obtained based on the latest models provided by NASA [Z17]. We believe the same weight classes and separation rules are used in the real-time NASA ATD-2 Tactical Surface Scheduler.

Table 5 below shows the Runway STAs computed for the three taxiing departure flights present in the scheduling scenario. None of the flights required any delays because their Runway ETAs were sufficiently separated with respect to prior and next operations on their same runways as well as runway 23 arrivals.

Callsign	opType	WtClass	Runway	Gate	Runway ETA	APREQ Rwy Release Time	SOBT	EOBT	Flight Status	Priority	Scheduler Prediction: Runway ETA	Scheduler Computation: Runway STA	Scheduler Computation: TOBT
AAL2062	ARR	D	18C	Gate_C_08	11:06				RAMP_TAXI_IN	5	11:02	11:02	
DAL671	DEP	D	18C	Gate_A_03	11:08		11:02	11:02	RAMP_TAXI_OUT	8	11:08	11:08	11:02
JIA5093	DEP	E	18C	Gate_E_29	11:26		11:13	11:13	AT_GATE	11	11:26		
JIA5268	DEP	E	18C	Gate_E_11	11:28		11:16	11:16	AT_GATE	11	11:28		
JIA5061	DEP	E	18C	Gate_E_15	11:30		11:19	11:19	AT_GATE	12	11:30		
FFT200	DEP	D	18C	Gate_A_08	11:30		11:23	11:23	AT_GATE	12	11:30		
AWI3819	DEP	E	18C	Gate_E_01	11:35	11:39	11:23	11:23	AT_GATE	6	11:35	11:39	11:27
JIA5042	DEP	E	18C	Gate_E_07	11:35		11:23	11:23	AT_GATE	12	11:35		
AAL2091	DEP	D	18C	Gate_B_10	11:36	11:41	11:28	11:28	AT_GATE	6	11:36	11:41	11:33
AAL662	DEP	D	18C	Gate_B_13	11:37		11:29	11:29	AT_GATE	12	11:37		
AAL1909	DEP	D	18C	Gate_C_03	11:38		11:29	11:29	AT_GATE	12	11:38		
JIA5277	DEP	E	18C	Gate_E_23	11:39		11:27	11:27	AT_GATE	12	11:39		
AAL1993	DEP	D	18C	Gate_B_03	11:41		11:35	11:35	AT_GATE	12	11:41		
JIA5073	DEP	E	18C	Gate_E_13	11:45		11:33	11:33	AT_GATE	12	11:45		
AAL1877	DEP	D	18L	Gate_B_11	11:09		10:57	10:57	RAMP_TAXI_OUT	8	11:09	11:09	10:57
GJS6245	DEP	E	18L	Gate_A_01	11:10		11:00	11:00	RAMP_TAXI_OUT	8	11:10	11:10	11:00
SWA766	DEP	D	18L	Gate_A_06	11:20		11:10	11:10	AT_GATE	11	11:20		
JIA5039	DEP	E	18L	Gate_E_16a	11:26		11:23	11:23	AT_GATE	12	11:26		
AAL1654	DEP	D	18L	Gate_C_18	11:30		11:23	11:23	AT_GATE	12	11:30		
AAL2042	DEP	D	18L	Gate_B_15	11:31		11:22	11:22	AT_GATE	12	11:31		
JIA5432	DEP	E	18L	Gate_E_25	11:32		11:28	11:28	AT_GATE	12	11:32		
AAL1956	DEP	D	18L	Gate_C_04	11:34		11:28	11:28	AT_GATE	12	11:34		
JIA5252	DEP	E	18L	Gate_E_17	11:34		11:30	11:30	AT_GATE	12	11:34		
AAL1732	DEP	D	18L	Gate_B_16	11:35		11:27	11:27	AT_GATE	12	11:35		
PDT4973	DEP	E	18L	Gate_E_34	11:37		11:33	11:33	AT_GATE	12	11:37		
AAL1903	DEP	D	18L	Gate_C_06	11:38		11:32	11:32	AT_GATE	12	11:38		

Table 9. Step 5 schedules all taxiing departures by applying runway system separations

Step 6: Next in the order of consideration, are departure flights that are waiting at their gates and are ready for pushback. In the scheduling scenario we studied there were no at gate ready flights. As a result, Step 6 did not schedule any flights.

Step 7: Next in the order of consideration, are departure flights, which are waiting at their gates and which have airline-reported EOBTs within the next 10 minutes. For our scheduling scenario, this represents the set of at gate flights, which have EOBTs between 11:06 and 11:16. There are three such flights in the scheduling scenario. Table 6 shows the result of scheduling actions performed by Step 7, which schedules these three flights. The runway ETAs of these flights are sufficiently separated with respect to leading and following flights on the same runway as well as with respect to other interacting flights. Hence, all the three flights get assigned Runway STAs equal to their Runway ETAs and zero gate delays (i.e., TOBT = EOBT) as a result.

Callsign	opType	WtClass	Runway	Gate	Runway ETA	APREQ Rwy Release Time	SOBT	EOBT	Flight Status	Priority	Scheduler Prediction: Runway ETA	Scheduler Computation: Runway STA	Scheduler Computation: TOBT
AAL2062	ARR	D	18C	Gate_C_08	11:06				RAMP_TAXI_IN	5	11:02	11:02	
DAL671	DEP	D	18C	Gate_A_03	11:08		11:02	11:02	RAMP_TAXI_OUT	8	11:08	11:08	11:02
JIA5093	DEP	E	18C	Gate_E_29	11:26		11:13	11:13	AT_GATE	11	11:26	11:26	11:13
JIA5268	DEP	E	18C	Gate_E_11	11:28		11:16	11:16	AT_GATE	11	11:28	11:28	11:16
JIA5061	DEP	E	18C	Gate_E_15	11:30		11:19	11:19	AT_GATE	12	11:30		
FFT200	DEP	D	18C	Gate_A_08	11:30		11:23	11:23	AT_GATE	12	11:30		
AWI3819	DEP	E	18C	Gate_E_01	11:35	11:39	11:23	11:23	AT_GATE	6	11:35	11:39	11:27
JIA5042	DEP	E	18C	Gate_E_07	11:35		11:23	11:23	AT_GATE	12	11:35		
AAL2091	DEP	D	18C	Gate_B_10	11:36	11:41	11:28	11:28	AT_GATE	6	11:36	11:41	11:33
AAL662	DEP	D	18C	Gate_B_13	11:37		11:29	11:29	AT_GATE	12	11:37		
AAL1909	DEP	D	18C	Gate_C_03	11:38		11:29	11:29	AT_GATE	12	11:38		
JIA5277	DEP	E	18C	Gate_E_23	11:39		11:27	11:27	AT_GATE	12	11:39		
AAL1993	DEP	D	18C	Gate_B_03	11:41		11:35	11:35	AT_GATE	12	11:41		
JIA5073	DEP	E	18C	Gate_E_13	11:45		11:33	11:33	AT_GATE	12	11:45		
AAL1877	DEP	D	18L	Gate_B_11	11:09		10:57	10:57	RAMP_TAXI_OUT	8	11:09	11:09	10:57
GJS6245	DEP	E	18L	Gate_A_01	11:10		11:00	11:00	RAMP_TAXI_OUT	8	11:10	11:10	11:00
SWA766	DEP	D	18L	Gate_A_06	11:20		11:10	11:10	AT_GATE	11	11:20	11:20	11:10
JIA5039	DEP	E	18L	Gate_E_16a	11:26		11:23	11:23	AT_GATE	12	11:26		
AAL1654	DEP	D	18L	Gate_C_18	11:30		11:23	11:23	AT_GATE	12	11:30		
AAL2042	DEP	D	18L	Gate_B_15	11:31		11:22	11:22	AT_GATE	12	11:31		
JIA5432	DEP	E	18L	Gate_E_25	11:32		11:28	11:28	AT_GATE	12	11:32		
AAL1956	DEP	D	18L	Gate_C_04	11:34		11:28	11:28	AT_GATE	12	11:34		
JIA5252	DEP	E	18L	Gate_E_17	11:34		11:30	11:30	AT_GATE	12	11:34		
AAL1732	DEP	D	18L	Gate_B_16	11:35		11:27	11:27	AT_GATE	12	11:35		
PDT4973	DEP	E	18L	Gate_E_34	11:37		11:33	11:33	AT_GATE	12	11:37		
AAL1903	DEP	D	18L	Gate_C_06	11:38		11:32	11:32	AT_GATE	12	11:38		

Table 10. Step 7 schedules all at gate "planned" departure flights

Step 8: Next and last in the order of consideration, are the at gate departure flights which have their EOBTs more than 10 minutes in the future. These belong to the at gate uncertain priority class of flights. Step 8 schedules these flights, selecting each flight in the ascending order of Runway ETAs. Table 7 shows the result of the scheduling Step 8. As seen from the Table, all the arrival landings and departure takeoffs are scheduled at this point. Some departure flights receive scheduling delays as seen from the last column of this table. For example, flights AWI3819 and AAL2091, both receive 4 and 5 minutes of delay respectively because they had delayed runway release times due to APREQ constraints. In addition to the APREQ-impacted flights, few other flights also receive delays due to runway separation constraints. As seen from Table 7, flights AAL1909, JIA5277, and AAL1993, scheduled to depart from runway 18C, have their Runway ETAs too close to each other and also too close to the Runway ETA of the previous departure on 18C (AAL662). As a result, they receive 2, 3 and 2 minutes of delays, respectively. Similarly, AAL1732 on runway 18L receives a 1 minute delay to keep it sufficiently separated from a prior same runway departure, JIA5252. All separations are weight-class dependent and use the same weight class definitions and separation matrices as the NASA ATD-2 Tactical Surface Scheduler.

Callsign	opType	WtClass	Runway	Gate	Runway ETA	APREQ Rwy Release Time	SOBT	EOBT	Flight Status	Priority	Scheduler Prediction: Runway ETA	Scheduler Computation: Runway STA	Scheduler Computation: TOBT	Delay
AAL2062	ARR	D	18C	Gate_C_08	11:06				RAMP_TAXI_IN	5	11:02	11:02		0
DAL671	DEP	D	18C	Gate_A_03	11:08		11:02	11:02	RAMP_TAXI_OUT	8	11:08	11:08	11:02	0:00
JIA5093	DEP	E	18C	Gate_E_29	11:26		11:13	11:13	AT_GATE	11	11:26	11:26	11:13	0:00
JIA5268	DEP	E	18C	Gate_E_11	11:28		11:16	11:16	AT_GATE	11	11:28	11:28	11:16	0:00
JIA5061	DEP	E	18C	Gate_E_15	11:30		11:19	11:19	AT_GATE	12	11:30	11:31	11:19	0:00
FFT200	DEP	D	18C	Gate_A_08	11:30		11:23	11:23	AT_GATE	12	11:30	11:30	11:23	0:00
AWI3819	DEP	E	18C	Gate_E_01	11:35	11:39	11:23	11:23	AT_GATE	6	11:35	11:39	11:27	0:04
JIA5042	DEP	E	18C	Gate_E_07	11:35		11:23	11:23	AT_GATE	12	11:35	11:35	11:23	0:00
AAL2091	DEP	D	18C	Gate_B_10	11:36	11:41	11:28	11:28	AT_GATE	6	11:36	11:41	11:33	0:05
AAL662	DEP	D	18C	Gate_B_13	11:37		11:29	11:29	AT_GATE	12	11:37	11:37	11:29	0:00
AAL1909	DEP	D	18C	Gate_C_03	11:38		11:29	11:29	AT_GATE	12	11:38	11:40	11:31	0:02
JIA5277	DEP	E	18C	Gate_E_23	11:39		11:27	11:27	AT_GATE	12	11:39	11:42	11:30	0:03
AAL1993	DEP	D	18C	Gate_B_03	11:41		11:35	11:35	AT_GATE	12	11:41	11:43	11:37	0:02
JIA5073	DEP	E	18C	Gate_E_13	11:45		11:33	11:33	AT_GATE	12	11:45	11:45	11:33	0:00
AAL1877	DEP	D	18L	Gate_B_11	11:09		10:57	10:57	RAMP_TAXI_OUT	8	11:09	11:09	10:57	0:00
GJS6245	DEP	E	18L	Gate_A_01	11:10		11:00	11:00	RAMP_TAXI_OUT	8	11:10	11:10	11:00	0:00
SWA766	DEP	D	18L	Gate_A_06	11:20		11:10	11:10	AT_GATE	11	11:20	11:20	11:10	0:00
JIA5039	DEP	E	18L	Gate_E_16a	11:26		11:23	11:23	AT_GATE	12	11:26	11:26	11:23	0:00
AAL1654	DEP	D	18L	Gate_C_18	11:30		11:23	11:23	AT_GATE	12	11:30	11:30	11:23	0:00
AAL2042	DEP	D	18L	Gate_B_15	11:31		11:22	11:22	AT_GATE	12	11:31	11:31	11:22	0:00
JIA5432	DEP	E	18L	Gate_E_25	11:32		11:28	11:28	AT_GATE	12	11:32	11:32	11:28	0:00
AAL1956	DEP	D	18L	Gate_C_04	11:34		11:28	11:28	AT_GATE	12	11:34	11:35	11:28	0:00
JIA5252	DEP	E	18L	Gate_E_17	11:34		11:30	11:30	AT_GATE	12	11:34	11:34	11:30	0:00
AAL1732	DEP	D	18L	Gate_B_16	11:35		11:27	11:27	AT_GATE	12	11:35	11:36	11:28	0:01
PDT4973	DEP	E	18L	Gate_E_34	11:37		11:33	11:33	AT_GATE	12	11:37	11:37	11:33	0:00
AAL1903	DEP	D	18L	Gate_C_06	11:38		11:32	11:32	AT_GATE	12	11:38	11:39	11:32	0:00

Table 11. Step 8 schedules the remaining at gate "uncertain" departure flights

Step 9: At this point, all the landings and takeoffs have been scheduled on both the departure /mixed-use runways. Now, as per NASA scheduler design, the scheduler makes a second pass through the scheduling cycle. This time, the scheduler specifically schedules runway crossings of active runway 18C for 18R arrival landings, which cross 18C during their taxi process. Table 8 shows the taxiing arrivals estimated to cross runway 18C in the future, in blue background, interspersed with the scheduled departures and arrivals on 18C (scheduled arrivals and departures means the flights that have already been assigned Runway STAs by the scheduler). As seen from the Table, the crossing flights have their Runway Crossing ETAs interspersed in between the Runway STAs of already scheduled arrival and departure flights.

Callsign	opType	WtClass	Runway	Runway Xing Node	Gate	Flight Status	Priority	Runway ETA	Scheduler Computation: Runway STA
DAL671	DEP	D	18C		Gate_A_03	RAMP_TAXI_OUT	8	11:08	11:08
PDT4935	XING	E	18C	S_12	Gate_E_29	IN_AIR	3	11:15	
JIA5295	XING	E	18C	S_12	Gate_E_28	IN_AIR	3	11:18	
JIA5355	XING	E	18C	S_12	Gate_E_06	IN_AIR	3	11:23	
JIA5093	DEP	E	18C		Gate_E_29	AT_GATE	11	11:26	11:26
JIA5268	DEP	E	18C		Gate_E_11	AT_GATE	11	11:28	11:28
FFT200	DEP	D	18C		Gate_A_08	AT_GATE	12	11:30	11:30
JIA5061	DEP	E	18C		Gate_E_15	AT_GATE	12	11:30	11:31
JIA5160	XING	E	18C	S_12	Gate_E_15	IN_AIR	3	11:30	
AWI3819	DEP	E	18C		Gate_E_01	AT_GATE	6	11:35	11:39
JIA5042	DEP	E	18C		Gate_E_07	AT_GATE	12	11:35	11:35
AAL2091	DEP	D	18C		Gate_B_10	AT_GATE	6	11:36	11:41
AAL662	DEP	D	18C		Gate_B_13	AT_GATE	12	11:37	11:37
AAL1944	XING	D	18C	S_12	Gate_C_13	IN_AIR	3	11:37	
AAL1909	DEP	D	18C		Gate_C_03	AT_GATE	12	11:38	11:40
JIA5277	DEP	E	18C		Gate_E_23	AT_GATE	12	11:39	11:42
AAL1993	DEP	D	18C		Gate_B_03	AT_GATE	12	11:41	11:43
JIA5073	DEP	E	18C		Gate_E_13	AT_GATE	12	11:45	11:45
AAL2062	ARR	D	18C		Gate_C_08	RAMP_TAXI_IN	5		11:02

Table 12. Step 9 addresses the arrival taxi flights scheduled to cross active departure runways

Step 9 processes the crossing flights in the ascending order of their Runway Crossing ETAs. For each flight in this order, the scheduler algorithm finds the leading and trailing operation on the same runway based on the flight's Runway Crossing ETA. It tries to schedule the crossing in between these two operations, if possible. If there is not enough spacing in between the immediate follower and immediate leader operations, then the scheduler tries to schedule the crossing in between the next two operations on the runway, and so on, until a safely spaced crossing time is obtained.

Safe separations for crossing flights are defined by checking against the following conditions:

- Crossing after Crossing: Each next crosser must be spaced by at least 5 seconds after the prior crosser
- Crossing before Arrival: To be able to cross, the next arrival landing scheduled on the runway must be at least 1000 ft away from the runway threshold
- Crossing after Arrival: To be able to cross, the previous arrival landing scheduled on the runway must have already crossed the taxiway intersection of the crossing and be at least 1800 ft away from the runway threshold
- Crossing after Departure: To be able to cross, the previous departure taking off from the runway must have already crossed the taxiway intersection of the crossing and be at least 1800 ft away from the runway threshold
- Departure after Crossing: To be able to cross, the next departure's scheduled takeoff roll start should be at least 5 seconds in the future (enough for the crossing to cross the runway)

- Each of the distance based spacing requirements (Crossing before Arrival, Crossing after Arrival, and Crossing after Departure) were roughly converted into a 10 second spacing between the start of the crossing taxi and the prior or next arrival/departure operation for computation simplicity.

Step 9 applies an algorithm similar to the one used for scheduling departure takeoffs in between already scheduled departures and landings on the same runway for Steps 5-8. Table 9 shows the results of the runway crossing scheduling step 9. As seen from the Table most of the crossings were scheduled without any major delays. (There were small 10-second delays in some cases to space with respect to the prior departure, but those are not visible in the Table because it rounds the times to the closest minute.)

Callsign	opType	WtClass	Runway	Runway Xing Node	Gate	Flight Status	Priority	Runway ETA	Scheduler Computation: Runway STA
DAL671	DEP	D	18C		Gate_A_03	RAMP_TAXI_OUT	8	11:08	11:08
PDT4935	XING	E	18C	S_12	Gate_E_29	IN_AIR	3	11:15	11:15
JIA5295	XING	E	18C	S_12	Gate_E_28	IN_AIR	3	11:18	11:18
JIA5355	XING	E	18C	S_12	Gate_E_06	IN_AIR	3	11:23	11:23
JIA5093	DEP	E	18C		Gate_E_29	AT_GATE	11	11:26	11:26
JIA5268	DEP	E	18C		Gate_E_11	AT_GATE	11	11:28	11:28
JIA5061	DEP	E	18C		Gate_E_15	AT_GATE	12	11:30	11:31
FFT200	DEP	D	18C		Gate_A_08	AT_GATE	12	11:30	11:30
JIA5160	XING	E	18C	S_12	Gate_E_15	IN_AIR	3	11:30	11:30
AWI3819	DEP	E	18C		Gate_E_01	AT_GATE	6	11:35	11:39
JIA5042	DEP	E	18C		Gate_E_07	AT_GATE	12	11:35	11:35
AAL2091	DEP	D	18C		Gate_B_10	AT_GATE	6	11:36	11:41
AAL662	DEP	D	18C		Gate_B_13	AT_GATE	12	11:37	11:37
AAL1944	XING	D	18C	S_12	Gate_C_13	IN_AIR	3	11:37	11:37
AAL1909	DEP	D	18C		Gate_C_03	AT_GATE	12	11:38	11:40
JIA5277	DEP	E	18C		Gate_E_23	AT_GATE	12	11:39	11:42
AAL1993	DEP	D	18C		Gate_B_03	AT_GATE	12	11:41	11:43
JIA5073	DEP	E	18C		Gate_E_13	AT_GATE	12	11:45	11:45

Table 13. Step 9 schedules the runway18C crossings by finding time spaces between consecutive departure operations on runway 18C

This concludes our discussion of the different components of the combined surface-airspace simulation environment that we developed to support high-fidelity benefits analysis simulation experiments. Next, we discuss our approach for designing the simulation experiment matrix.

5. TASK 4 SIMULATION EXPERIMENT DESIGN AND EXECUTION

Our technical approach for benefits estimation was to conduct high-fidelity baseline and ATD-2 operations simulations at a small number of simulation scenarios and then extrapolate the simulated benefits of the ATD-2 system to an annualized and nationalized scale. Obtaining reliable benefits estimates requires careful selection of the simulation dates and simulation scenarios. This section describes our meticulous process for selecting appropriate simulation days and other scenario settings for conducting a set of experiments that formed the basis for extrapolation. First, we describe our approach for selecting simulation days from historical dates.

5.1. Simulation Days Selection

5.1.1. Overall Approach for Simulation Date Selection

Simulation date selection provides the conditions by which simulation estimates the potential benefits obtainable from the ATD-2 program. The simulation date selection informs the scaling of the ATD-2 simulation results to an NAS-wide benefit estimation based on magnitude of benefits and the frequency of occurrence. Weather and demand are the principal factors which govern date selection. As such, we propose a methodology to select simulation dates to bound the benefits estimate and serve to test the SOSS model validity. Table 14 shows the conditions and expected outcome of benefits estimation from the model.

Simulation date	Departure demand at KCLT	Daily delay at KCLT		Weather impact		TMI constraints		Expected ATD-2 Benefit
		Departure	Taxi-out	CONUS	KCLT	APREQ index	MIT index	
1/9/16	low	Mod	low	low	low	low	N/A	low
5/6/16	high	Mod	high	mod	mod	mod	mod	highest
6/17/2016	high	High	mod	high	high	mod	mod	moderate
8/30/2016	low	Low	mod	high	high	high	N/A	low
6/28/2016	low	Mod	high	mod	mod	low	high	moderate
8/1/2016	mod	High	high	high	mod	high	high	moderate

Table 14. Simulation Date Selection Conditions

Conditions on 5/6/16, as described in Table 14, provide the upper bound of benefits achievable from the ATD-2 model. Demand is high and ATM constraints are imposed to manage demand-capacity imbalance, but weather conditions are moderate near KCLT airport and across the CONUS. As such, these conditions provide an upper bound on the benefits, scaled by frequency of occurrence and other modeling efforts.

On 6/17/16, demand is high, and constraints are imposed to manage demand-capacity imbalance, where capacity is reduced by poor weather conditions. For these conditions, we expect the benefits of the ATD-2 model to be moderate, since the implementation of the ATD-2 technology under these conditions can only mitigate so much delay; in other words, the conditions are poor, but some delay is recoverable.

Low benefits on 1/9/2016 should be expected, given ‘blue-sky’ conditions, low demand, and few constraints. Similarly, with low demand under poor weather conditions (i.e., 8/30/16), low model

benefits should result; this condition serves as an additional check on the model validation, as the model should make no unnecessary recommendations or changes.

Finally, we propose two simulation dates on which the APREQ and MIT impact indices were high, respectively, as 6/28/16 and 8/1/16.

Two independent date selection methodologies have been developed and are integrated to provide the simulation dates, for the conditions described in Table 14. Under the first approach, we present the methodology for assessing the combined impact of weather and demand on as-flown flights for 20 canonical dates for fiscal year 2016 (10/12/2015 to 9/23/2016), as developed by the US Federal Aviation Administration, and the two additional dates of high APREQ and MIT impact indices. The second approach is based on analysis of constraints in NTML data.

5.1.2. Weather Impact Traffic Index Approach

Based on the Weather-Impact Traffic Index (WITI) construct developed by S. Klein, we extended and applied the original methodology to estimate the WITI score for the 22 dates in Table 15. We adapted the original WITI methodology from a CONUS-wide assessment to allow application of smaller-scale regions (e.g., ARTCCs, regions about the simulation airports of KCLT, KDFW, and KEWR). The use of smaller regions to estimation region-specific WITI scores for KCLT Airport shows the impact of traffic demand and poor weather on the local WITI conditions near KCLT Airport, thereby offering a mechanism for CONUS-wide benefits scaling. We present the approach to our region-based WITI methodology for KCLT Airport, using convective weather data and as-flown IFR flight data.

Quarter	Date	Day of Week	Federal Holiday
1	10/12/2015	Monday	Columbus Day
	10/13/2015	Tuesday	None
	11/11/2015	Wednesday	Veterans' Day
	12/04/2015	Friday	None
	12/27/2015	Sunday	None
2	01/09/2016	Saturday	None
	01/24/2016	Sunday	None
	03/03/2016	Thursday	None
	03/06/2016	Sunday	None
	03/17/2016	Thursday	None
3	04/07/2016	Thursday	None
	05/06/2016	Friday	None
	05/21/2016	Saturday	None
	06/17/2016	Friday	None
	06/27/2016	Monday	None

4	07/18/2016	Monday	None
	08/04/2016	Thursday	None
	08/30/2016	Tuesday	None
	09/10/2016	Saturday	None
	09/23/2016	Friday	None
High APREQ	06/28/2016	Tuesday	None
High MIT	09/23/2016	Friday	None

Table 15. FAA Canonical Analysis Dates and Dates of High TMI Impact, FY2015

5.1.2.1. Adapted WITI Estimation Methodology

As described by Dr. Klein [AK01], the weather impact traffic index (WITI) is a score that is comprised of the superposition of traffic position data and convective weather data position. More formally [AK01], the enroute WITI score is the sum of all national convective weather data (NCWD) times the number of flights per day per flow between any two OEP-35 airports; this analysis did not include flights to and from KHON.

The procedure for implementing our version of en-route WITI score at ARTCC, CONUS, and airport regions is described below. Data were acquired for the map of the CONUS (lower-48) as a latitude/longitude map on a WGS-84 ellipsoid (GADM01). Convective weather data were retrieved from a historical archive maintained at the Iowa State University (ISU01). Delay data as daily total departure delay (minutes) and daily total taxi-out delay (minutes) were obtained from the FAA's ASPM database for FY2015 for KCLT Airport. Flight data were obtained from the FAA's TFMSC database.

Preparation of the CONUS map and its sub-regions was first accomplished by projecting the latitude/longitude of the map coordinates to a cylindrical Mercator projection (zone 14, km units). A bounding box was used to remove CA and HI to create the lower CONUS projection map. The high-altitude boundaries for ARTCCs in the lower-CONUS region were superimposed on the Mercator map, using the same cartographic transformation. Regions of 100 nm radius were subtended around the locations of KCLT, KDFW, and KEWR to emulate the concept of a super-TRACON or metroplex (i.e., 'airport circle'). Finally, the lower-CONUS map was tessellated into hexagonal cells, as the most efficient means of tessellating a map with irregular boundaries (S-M01). The hexagonal cells each have a unique index in which the presence of a flight trajectory position or weather cell position may be recorded. All hexagonal cells in any ARTCC are disjoint from hexagonal cells in adjoining ARTCC regions; hexagonal cells in the three 'airport circles' are subsets of the CONUS-wide set of cells, but overlap with cells in surrounding and adjacent ARTCC regions. The location of the ARTCC regions and 'airport circles' on the projected CONUS map with the hexagonal cells is shown on Figure 23). Each hexagonal cell has a radius of approximately 40 nm, to emulate the typical dimensions of an airport TRACON.

Inspection of Figure 23 and its regions shows that WITI scores per unit time can be computed for these sets of regions:

- all flights in CONUS

- all flights in each ARTCC
- all flights in over each target airport circle
- departures (arrivals) to/from target airport in CONUS
- departures (arrivals) to/from target airport in each ARTCC
- departures (arrivals) to/from over each target airport circle

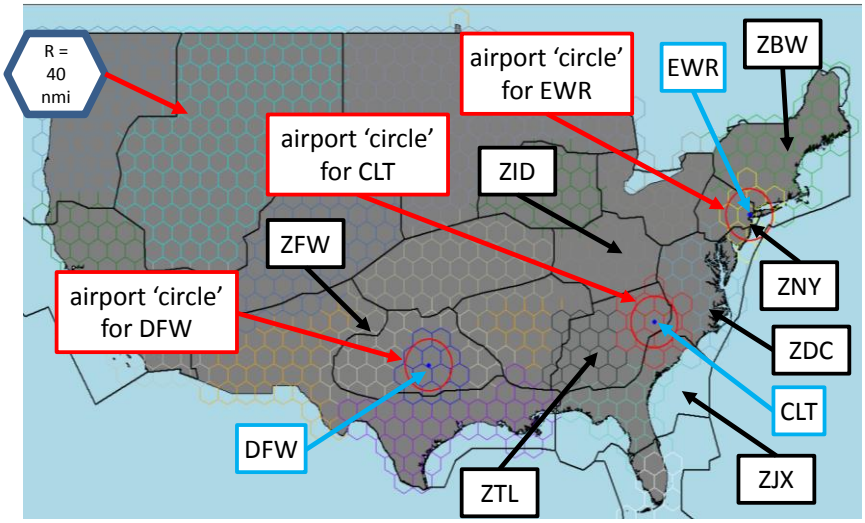

Figure 23. WITI "Inspection" Regions

The second step in the WITI data preparation was the acquisition and manipulation of convective weather data (ISU01) for 8-bit reflectivity. These data, as depicted in Figure 24, show the Doppler weather reflectivity on 8/4/2016, from 22:00 to 23:00 UTC, as measured in dBZ units. For the purposes of this work, we considered convective weather to be severe for WITI calculation at dBZ values of at least 35 dBZ. Convective weather data from the Iowa State University archive were retrieved for time intervals of 48 hrs at time interval values of 1 hr (UTC) around each date in Table 15. The data were converted from pixel locations and magnitude to latitude, longitude, and dBZ value (ISU02). The latitude and longitude values of each convective weather datum location were registered to the CONUS map with the same cartographic transformation as used to convert the map and its regions (i.e., cylindrical Mercator projection).

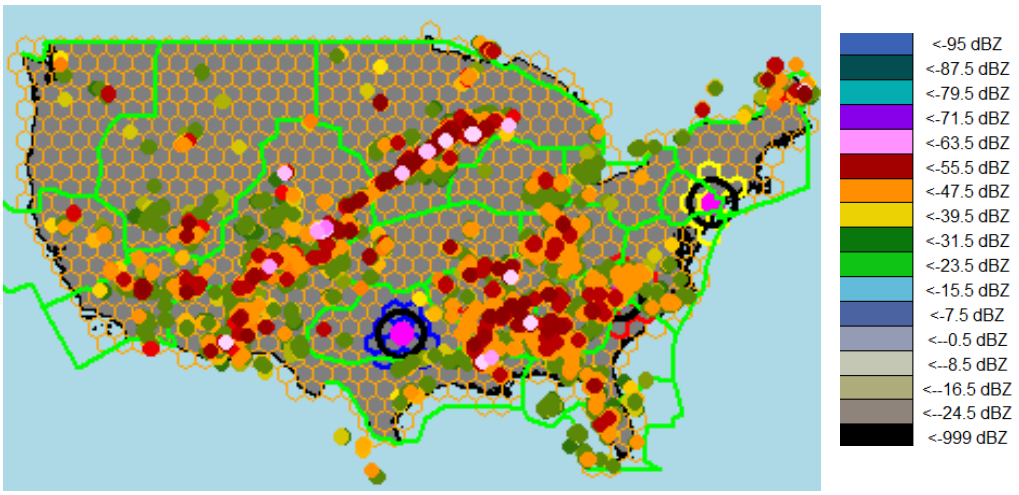

Figure 24. Doppler Radar Weather Data, 8/4/1016, 22:00 UTC

The last step in the data preparation process was the creation of the aircraft trajectories from the TFMSC data. From the FAA description, the TFMSC data, "…are created when pilots file flight plans and/or when flights are detected by the National Airspace System (NAS), usually via RADAR" [FAA01]. The TFMSC data contained the origin-destination airports for 34 of the OEP-35 airports, the departure date and hour as local time, the flight length (nm), and the flight duration (minutes). Flight duration is determined from 'wheels-up' (i.e., AZ message from TFMS) to 'wheels-down' (i.e., DZ message from TFMS). Great-circle trajectories as latitude and longitude positions were created for each pairwise origin-destination airport using the airport location data (latitude, longitude) and a WGS-84 ellipsoid. Track points along each trajectory were transformed to the map projection in units of km with sufficient granularity to ensure that no map hexagonal cell would not contain a flight track position whose great-circle path crossed that cell. Examples of flights on 8/4/2016 from 22:00 to 23:00 UTC are shown in Figure 25.

Local departure times as date and nearest hour were converted to UTC based on time zone, time of year, and location. For this analysis, all flights departing between 2015-11-01 02:00:00 and 2016-03-13 02:00:00 EST were cast to UTC using standard time. Flights with dates during daylight savings time were adjusted accordingly, except for departures from KPHX Airport (Arizona does not observe the daylight savings time change). Ground speed for each track was computed given the total flight track distance and flight duration from the TFMSC data, and was assumed to be constant with time.

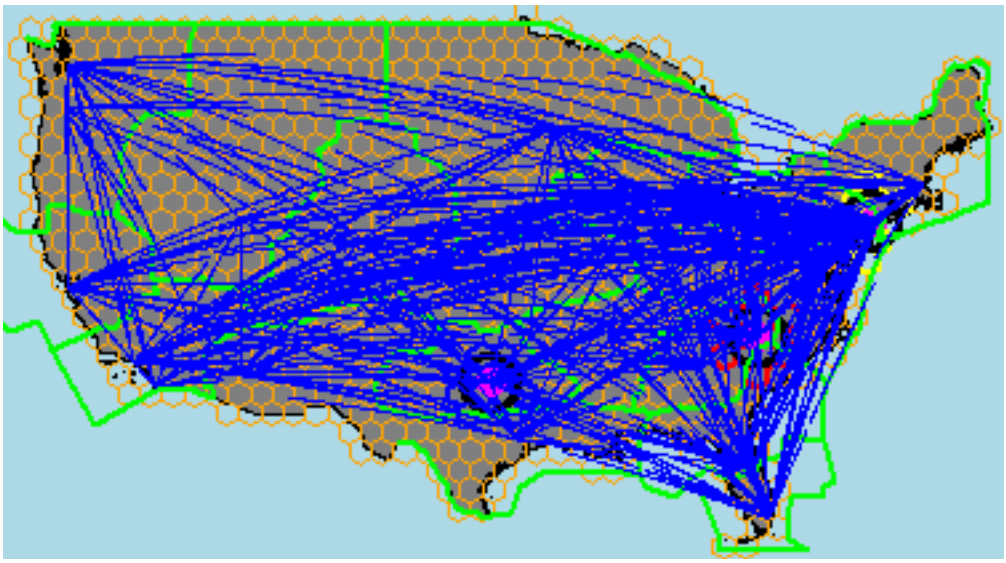

Figure 25. Flight Paths on 08/04/2016, 22:00 UTC

Given the superposition of convective weather location and flight track locations for each UTC hour, the WITI score for any geographic region was computed as the sum of the number of hexagonal cells containing a convective weather reflectivity of at least 35 dBZ and the number of flight track positions within that cell.

Shown on Table 16 are the canonical dates and two dates with high APREQ and MIT indices. Other columns provide data on daily total WITI scores per region. Three ARTCCs (i.e., ZDC, ZID, and ZJX) nearest to KCLT Airport were chosen for ARTCC-specific WITI computation. For the section of columns in Table 16, with the 'all in' subtitle, these columns reflect the WITI score for any flight in that ARTCC, regardless of origin airport. Next, WITI scores in the three ARTCCs are provided for departures from KCLT only, in the columns with the subtitle 'departures from KCLT in.' Finally, WITI scores for flights crossing the 'airport circle' around KCLT Airport are provided in the last two columns of Table 16. Dates in Table 16 which were holidays are denoted in yellow highlight.

		Daily WITI Scores										
	departures from KCLT	all flights in					departures from KCLT in				over KCLT	
date		CONUS	ZDC	ZID	ZJX	ZTL	ZDC	ZID	ZJX	ZTL	KCLT dep	all flts
10/12/2015	740	155500	12895	8434	5462	6492	936	309	266	822	1328	3703
10/13/2015	730	157082	13693	9149	5631	6743	1046	337	284	856	1372	3847
11/11/2015	747	155318	14286	9145	6111	6940	1021	427	300	930	1403	4007
12/4/2015	734	152845	14028	8694	6303	6785	991	289	273	776	1227	3936
12/27/2015	735	146178	12845	7592	6927	6672	895	360	241	740	1197	3720
01/09/2016	656	129464	11700	7005	6214	5962	895	229	242	738	1077	3406
1/24/2016	570	85965	2060	3986	4894	4785	267	269	185	543	708	1757
3/3/2016	744	152479	13636	8687	6550	6906	894	364	277	814	1230	3891
3/6/2016	712	138473	12337	7549	6755	6496	832	320	283	766	1256	3599
3/17/2016	754	158937	14319	9154	7019	7191	955	386	299	870	1279	4105
4/7/2016	761	153144	13336	8813	6552	6912	888	410	290	821	1291	3875
5/6/2016	763	158000	13488	8826	5945	6854	941	312	265	826	1317	3922
5/21/2016	685	148508	12596	7619	6236	6334	852	247	269	725	1142	3585
6/17/2016	756	170407	14385	9464	6090	6793	1009	333	274	827	1375	3969
6/27/2016	736	170023	14153	8969	6195	6961	944	300	257	783	1322	3931
7/18/2016	757	164351	12663	8601	5934	6896	857	397	256	822	1304	3799
8/4/2016	751	173238	14234	9544	6143	7026	973	364	265	827	1359	3907
8/30/2016	649	162828	13491	9088	5642	6712	994	324	272	823	1333	3805
9/10/2016	590	139696	11376	7229	5456	5761	855	317	248	748	1209	3262
6/28/2016	733	168978	12782	8891	5639	5336	780	364	261	859	1270	3423
8/1/2016	745	166941	13809	9140	5902	6841	949	372	261	834	1272	3852
9/23/2016	736	166941	14101	9456	5781	6871	976	339	261	847	1358	3973

Table 16. Departure Counts at KCLT and Regional WITI Scores

5.1.3. APREQ and Miles-in-Trail Impact Methodology

An analysis of historical departure restrictions was conducted with two purposes in mind. One purpose was to support the simulation date selection analysis described in the previous section, by providing data on the extent and severity of departure restrictions occurring each day during FAA fiscal year 2015. The second purpose was to support accurate and realistic modeling of these restrictions in our team's surface-airspace simulation platform for the selected simulation days.

Our analysis looked at two types of departure restrictions—miles-in-trail restrictions (MITs) and Approval Requests (APREQs)—imposed on departures taking off from the focus model airports (CLT, EWR and DFW). We analyzed one year's worth of National Traffic Management Log (NTML) data for the FAA fiscal year 2015 to support this analysis. The NTML data provide a

single system for automated coordination, logging, and communication of traffic management initiatives (TMIs) throughout the NAS. NTML is a part of the Traffic Flow Management System (TFMS). Center Traffic Management Units (TMUs) as well as ATC System Command Center (ATCSCC) traffic managers enter new TMIs and update existing TMIs via a graphical TFMS tool. These entries are converted into database entries which are stored to aid TFM decision making and post operations analysis. More pertinent to the topic at hand, the NTML data contains a record of historically implemented MIT and APREQ departure restrictions (along with many other types of TMIs) including the times during which the restriction was active, the requesting and providing FAA facility, size of the restriction, and other relevant information such as which departure flows are impacted by the restriction. The data are stored as a series of TMI restriction records. Each record includes information about a new restriction imposed by a FAA facility or it could be an update to an existing restriction. Since one of our aims was to select days with different levels of extent of MIT and APREQ occurrence (e.g., number, duration, and size of restrictions), as well as different levels of the severity of their impact (e.g., departure delay impact) on the focus airport departure flows, we developed two measures or indices to help us with our analysis—an MIT Restriction Impact Index and an APREQ Restriction Impact Index. Both these indices are computed for each focus airport per day as explained below.

Daily MIT Restriction Impact Index. This is a measure of how severely an airport was impacted by MIT restrictions on a particular day. The computation of this score starts by accessing NTML data records for one day at a time. The per-day records are first filtered using multiple criteria to a smaller set of records containing features more relevant to the problem at hand. For our purpose, the filtering criteria consisted of the following: (i) restriction is provided by the airport under consideration (e.g., CLT), (ii) the constrained NAS element causing the restriction is relevant to the problem we are focusing on (e.g., for the CLT case, NAS elements of interest are constrained to Northeast destination airports or enroute waypoints/sectors through which departure flows travel from CLT to the Northeast airports), and (iii) the restriction type is MIT.

After the relevant NTML records are filtered, we next apply complex processing to assess whether each subsequent record represents a new restriction or if it represents an extension or update to an existing (already active) restriction. Identification of new or existing restriction is not straightforward because the restriction records originate from human controllers' input into a graphical tool, and this human input process creates multiple discrepancies and peculiar features within the data records.

After this processing, records belonging to each individual restriction are merged, and the real start and end times for each restriction are computed. For MIT records the impact index is formed by identifying two sets of flights that depart during the restriction active duration: Set 1 consists of flights that are directly impacted by the MIT, (i.e., are flying out to the impacted destination airport(s) or flying through the impacted departure-fix or enroute-fix); Set 2 consists of flights that are indirectly impacted by the MIT restriction – these are flights that depart within +/- 2 minutes of a departure flight that is directly impacted by a MIT restriction. The MIT impact index is then computed as follows:

> **Daily MIT Impact Index = [Number of flights in Set 1 + 0.5 X Number of flights in Set 2] X MIT size, summed over all the MIT restrictions active during the day.**

Daily APREQ Restriction Impact Index.

For APREQ records the severity score is formed in a similar way except instead of the MIT size the number is multiplied by a constant (e.g., 10):

> **Daily APREQ Impact Index = [Number of flights in Set 1 + 0.5 X Number of flights in Set 2] X 10**, summed over all the APREQ restrictions active during the day, where

Set 1 = Flights directly impacted by an APREQ restriction (i.e., departure flights flying out to the impacted destination airport(s) or flying through the impacted departure-fix or enroute-fix)

Set 2 = Flights that depart within +/- 2 minutes of a departure flight that is directly impacted by an APREQ restriction.

Table 17 presents the APREQ and MIT index scores for the analysis dates considered in this study.

date	departures from KCLT	APREQ Impact Index	MIT Impact Index
10/12/2015	740	2090	40
10/13/2015	730	705	165
11/11/2015	747	808	N/A
12/4/2015	734	N/A	N/A
12/27/2015	735	200	0
01/09/2016	656	28	N/A
1/24/2016	570	23	0
3/3/2016	744	N/A	790
3/6/2016	712	483	165
3/17/2016	754	325	N/A
4/7/2016	761	545	344
5/6/2016	763	478	N/A
5/21/2016	685	553	234
6/17/2016	756	185	775
6/27/2016	736	473	270
7/18/2016	757	448	1748
8/4/2016	751	2055	N/A
8/30/2016	649	5215	N/A
9/10/2016	590	1723	N/A
6/28/2016	733	468	3507
8/1/2016	745	6053	2495
9/23/2016	736	3150	N/A

Table 17. APREQ and MIT Index Scores for KCLT Airport

5.1.4. Methodology Integration and Simulation Date Selection

Separately, two methods of assessing constraints on departures from KCLT Airport exist, as described in Section 5.1.2 and Section 5.1.3. The integration methodology presented below

provides the selection of simulation dates according to the format and criteria listed in Table 14. As such, we create a cumulative mass distribution and its rank for relevant criteria per day at KCLT Airport:

- Number of ASPM departures (see Section 5.1.3)
- APREQ Index (see Section 5.1.3)
- MIT Index (see Section 5.1.3)
- Total daily departure delay (minutes)
- Total daily taxi-out delay (minutes)
- Daily WITI scores for all geographic regions (see Section 5.1.2)

The use of the rank statistics for the above-listed metrics allows us to choose the dates which satisfy the differing conditions of demand, constraint (e.g., APREQ, MIT), and weather. In particular, the geographical WITI scores allow the identification of dates with low weather impacts and high demand, both at the CONUS-scale and in the locality of KCLT Airport. The WITI scores per region also allow the separation of local traffic impact on departures from KCLT and the extrapolation of the impact of CONUS-wide weather and demand on the departure and taxi-out delays at KCLT Airport. The results of this analysis are presented in Table 18.

	departures from KCLT		TMI Impact Indices				Daily Total KCLT Delays (min)				daily witi sums																					
							KCLT Delays		Taxi-Out		all flights in										departures from KCLT in								over KCLT			
date	count	rank	APREQ	rank	MIT	rank	value	rank	value	rank	CONUS	rank	ZDC	rank	ZID	rank	ZJX	rank	ZTL	rank	ZDC	rank	ZID	rank	ZJX	rank	ZTL	rank	KCLT dep	rank	all flts	rank
10/12/15	740	10	2090	4	40	12	3564	21	3805	19	155500	12	12895	14	8434	16	5462	20	6492	17	936	12	309	17	266	11	822	11	1328	7	3703	16
10/13/15	730	16	705	8	165	10	4657	17	4042	16	157082	11	13693	9	9149	5	5631	19	6743	13	1046	1	337	11	284	4	856	4	1372	3	3847	12
11/11/15	747	7	808	7			5803	15	4186	13	155318	13	14286	3	9145	6	6111	11	6940	4	1021	2	427	1	300	1	930	1	1403	1	4007	2
12/04/15	734	14					5490	16	4513	9	152845	15	14028	7	8694	13	6303	6	6785	12	991	5	289	19	273	8	776	16	1227	17	3936	5
12/27/15	735	13	200	18	0	14	17688	3	3513	21	146178	18	12845	15	7592	18	6927	2	6672	15	895	13	360	9	241	21	740	19	1197	19	3720	15
01/09/16	656	19	28	20			6226	13	4064	15	129464	21	11700	20	7005	21	6214	8	5962	19	895	13	229	22	242	20	738	20	1077	21	3406	20
01/24/16	570	22	0	21	790	5	18852	2	2831	22	85965	22	2060	22	3986	22	4894	22	4785	22	267	22	269	20	185	22	543	22	708	22	1757	22
03/03/16	744	9	483	12	165	10	8456	10	3908	18	152479	16	13636	10	8687	14	6550	5	6906	6	894	15	364	6	277	6	814	14	1230	16	3891	9
03/06/16	712	17	325	17			4315	19	3956	17	138473	20	12337	19	7549	19	6755	3	6496	16	832	20	320	14	283	5	766	17	1256	15	3599	17
03/17/16	754	5	545	11	344	7	5862	14	4393	10	158937	9	14319	2	9154	4	7019	1	7191	1	955	8	386	4	299	2	870	2	1279	12	4105	1
04/07/16	761	2	478	13			8049	11	4812	7	153144	14	13336	13	8813	12	6552	4	6912	5	888	16	410	2	290	3	821	13	1291	11	3875	10
05/06/16	763	1	553	10	234	9	8850	9	5492	4	158000	10	13488	12	8826	11	5945	13	6854	9	941	11	312	16	265	12	826	9	1317	9	3922	7
05/21/16	685	18	185	19	775	6	16010	4	4197	12	148508	17	12596	18	7619	17	6236	7	6334	18	852	19	247	21	269	10	725	21	1142	20	3585	18
06/17/16	756	4	473	14	270	8	11149	7	4713	8	170407	2	14385	1	9464	2	6090	12	6793	11	1009	3	333	12	274	7	827	7	1375	2	3969	4
06/27/16	736	11	448	16	1748	3	24358	1	7071	1	170023	3	14153	5	8969	9	6195	9	6961	3	944	10	300	18	257	17	783	15	1322	8	3931	6
07/18/16	757	3	630	9	1015	4	12295	6	5279	5	164351	6	12663	17	8601	15	5934	14	6896	7	857	17	397	3	256	18	822	11	1304	10	3799	14
08/04/16	751	6	2055	5	0	13	7784	12	5742	2	173238	1	14234	4	9544	1	6143	10	7026	2	973	7	364	6	265	12	827	7	1359	4	3907	8
08/30/16	649	20	5215	2			3399	22	4177	14	162828	7	13491	11	9088	8	5642	17	6712	14	994	4	324	13	272	9	823	10	1333	6	3805	13
09/10/16	590	21	1723	6			4060	20	3523	20	139696	19	11376	21	7229	20	5456	21	5761	20	855	18	317	15	248	19	748	18	1209	18	3262	21
06/28/16	733	15	468	15	3507	1	9365	8	5616	3	159008	8	12782	16	8891	10	5639	18	5336	21	780	21	364	6	261	14	859	3	1270	14	3423	19
08/01/16	745	8	6053	1	2495	2	13592	5	5258	6	168978	4	13809	8	9140	7	5902	15	6841	10	949	9	372	5	261	14	834	6	1272	13	3852	11
09/23/16	736	11	3150	3			4333	18	4301	11	166941	5	14101	6	9456	3	5781	16	6871	8	976	6	339	10	261	14	847	5	1358	5	3973	3

Table 18. Integrated Date Selection Methodology Result

For each row entry in Table 18, we created a cumulative mass likelihood (i.e., sample probability of exceedance). The cumulative mass likelihood for each metric-date combination was ranked, with rank 1 for the highest cumulative mass likelihood value per metric and rank 22 (number of rows in Table 18). Finally, we devised categorical variables for each metric based on rank ranges, where $1 \leq \text{rank} \leq 7$ demarked 'high', $8 \leq \text{rank} \leq 14$, denoted 'moderate,' and $15 \leq \text{rank} \leq 22$ indicated 'low.' On 5/6/2016, the conditions were high departure demand at KCLT, moderate to high daily delay at KCLT (departure delays and taxi-out delays), moderate weather impact across the CONUS and over KCLT, and moderate TMI constraints (APREQ and MIT impact indices). The results of the ranking and categorical classifications are presented in Table 19.

	TMI impact index		weather impact		departure	daily total delays	
date	APREQ	MIT	CONUS	KCLT	demand	departure	taxi-out
10/12/2015	high	mod	mod	high	mod	low	low
10/13/2015	mod	mod	mod	high	low	low	low
11/11/2015	high		mod	high	high	low	mod
12/4/2015			low	low	mod	low	mod
12/27/2015	low	mod	low	low	mod	high	low
1/9/16	low		low	low	low	mod	low
1/24/2016	low	high	low	low	low	high	low
3/3/2016	mod	mod	low	low	mod	mod	low
3/6/2016	low		low	low	low	low	low
3/17/2016	mod	high	mod	mod	high	mod	mod
4/7/2016	mod		mod	mod	high	mod	high
5/6/16	mod	mod	mod	mod	high	mod	high
5/21/2016	low	high	low	low	low	high	mod
6/17/2016	mod	mod	high	high	high	high	mod
6/27/2016	low	high	high	mod	mod	high	high
7/18/2016	mod	high	high	mod	high	high	high
8/4/2016	high	mod	high	high	high	mod	high
8/30/2016	high		high	high	low	low	mod
9/10/2016	high		low	low	low	low	low
6/28/2016	low	high	mod	mod	low	mod	high
8/1/2016	high	high	high	mod	mod	high	high
9/23/2016	high		high	high	mod	low	mod

ranking ranges and categories		
category	lower	upper
low	22	15
mod	14	8
high	7	1

color key
Base Selected Dates
Alternate Dates with High APREQ/MIT

Table 19. Ranking and Categorical Variable Results for Simulation Dates

This concludes our discussion of simulation dates selection. Next, we outline our simulation test plan for conducting a series of simulation experiments leading up to the benefits analysis and sensitivity studies.

5.2. Simulation Experiment Matrix

As discussed above, we identified a set of simulation days for each airport based on a comparative analysis of historical weather, traffic demand-vs-capacity and TMI impact data, at the local and national levels. After this step, we further analyzed the actual airport surface traffic on the selected days and carefully down-selected timeframes for simulation on each of the selected days. We considered the following factors when selecting the simulation timeframes: (1) We wanted to keep a balanced mix of runway configurations (two configurations simulated per airport) in the selected simulation timeframes as much as possible; (2) The start of a simulation timeframe had to match with a time-period in actual operations when there were only a small number of departure flights on the airport surface just before the simulation start time. This factor enabled us to provide each of our simulations with a realistic "initial condition," rather than starting the simulation in the middle of a busy operational period on the actual historical day; (3) We wanted to keep the total number of simulation days to a manageable level (maximum 6 days per airport).

With these factors in mind, we down-selected to the following simulation matrix consisting of six simulation days for each of CLT and DFW, and four simulation days for EWR. This simulation matrix required us to design and conduct a total of 32 simulation experiments using the SOSS-AOSS simulation platform.

Table 20. Simulation experiment matrix showing the total 32 high-fidelity, SOSS-AOSS simulations conducted in support of the ATD-2 benefits assessments

Airport	Date	MCR Day Rank	Runway Config	Sim Timeframe	Baseline Sim #	ATD-2 Sim #
CLT	6/15/2016	1	South Flow	1000-1600 UTC	1	2
CLT	5/17/2016	2	South Flow	0900-1700 UTC	3	4
CLT	6/1/2016	3	North Flow	1000-1500 UTC	5	6
CLT	6/2/2016	4	South Flow	1200-1500 UTC	7	8
CLT	5/6/2016	5	North Flow	1600-2100 UTC	9	10
CLT	5/31/2016	7	North Flow	1600-2100 UTC	11	12
DFW	5/12/2016	1	East Flow	1000-1700 UTC	13	14
DFW	6/3/2016	2	West Flow	1500-2100 UTC	15	16
DFW	7/5/2016	3	West Flow	1500-2100 UTC	17	18
DFW	7/17/2016	4	West Flow	1000-1600 UTC	19	20
DFW	7/28/2016	5	West Flow	1000-1600 UTC	21	22
DFW	6/4/2016	6	East Flow	1700-2300 UTC	23	24

EWR	7/21/2016	1	South Flow	0800-1800 UTC	25	26
EWR	7/29/2016	2	North Flow	0900-1800 UTC	27	28
EWR	5/6/2016	3	North Flow	1400-2000 UTC	29	30
EWR	7/3/2016	5	South Flow	0900-1600 UTC	31	32

In addition to these 32 simulations, we also conducted three sensitivity studies. These studies were the following:

1. Simulation study to assess the effects of each departure flight pushing back at exactly its Scheduled Off Block Time, focused on the CLT North Flow configuration
2. Simulation study to assess the benefits of adding Phase II functionality: Strategic Scheduler for optimum queue delay buffer parameter setting, focused on the relatively more challenging CLT South Flow configuration, and
3. Leverage a past simulation study to assess the benefits of adding Phase III Integrated Airspace Scheduling capability, focused on the New York airspace

5.3. Simulation Execution

Simulations were conducted using a networked combination of two computers: one, a Linux laptop running NASA's SOSS simulation platform, and the second a Windows laptop running the MATLAB-based AOSS platform. AOSS acted as an external "scheduler" for SOSS, with SOSS periodically (every 30 seconds of simulation time) calling AOSS and waiting for AOSS to send back airport surface delay advisories. The following steps were followed for executing each individual simulation:

1. First, the SOSS surface traffic demand set was generated using a combination of OAG and Flightaware data (for gate allocation and scheduled gate departure time data) and ASDE-X data (for runway allocation, taxi route allocation, etc.), from the historical day that was selected for simulation
2. Corresponding airspace traffic demand set was generated by using the end-to-end merged Sherlock track data and applying a number of ATAC track processing scripts, for the same day
3. The set of APREQ, GDP and MIT advisories that were active during the same historical day were obtained by parsing the NTML database as well as from the FAA system command center website (http://www.fly.faa.gov/adv/advAdvisoryForm.jsp). The restriction start and end times, restriction sizes, and impacted NAS elements were entered into the AOSS simulation platform for reliable simulation of these departure restrictions. **Figure 26** shows the different TMI restrictions modeled from historical TMI databases and input as restrictions for each simulation scenario, using CLT as an example (the same inputs apply to DFW and EWR simulations).
4. Simulation was started by running SOSS and AOSS in tandem
5. After the simulation finished, surface trajectory data was saved from the SOSS platform and airspace trajectory data was saved from the AOSS platform

6. Post-processing scripts were then applied to compute performance metrics from the simulation output data
7. The same procedure was repeated for two settings per day – one a baseline (current-day) operations simulation and one an ATD-2 operations simulation

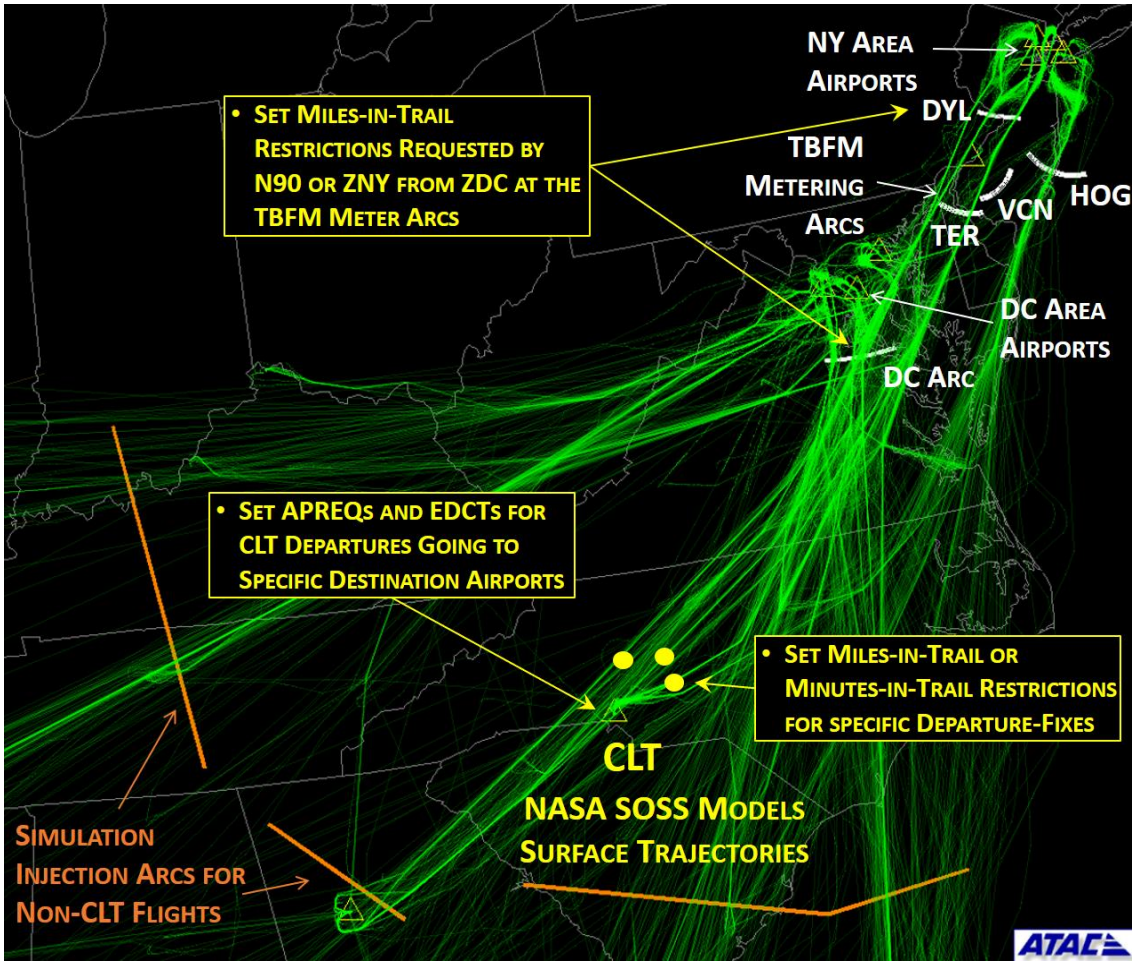

Figure 26. Different TMI restrictions modeled from historical data, and input for each simulation scenario

This concludes our description of the high-fidelity simulation experiment design and simulation execution task. Next, we describe the results from high-fidelity simulations.

6. RESULTS FROM HIGH-FIDELITY SIMULATIONS

This section outlines the results from high-fidelity SOSS-AOSS simulations. We present results showing comparison of departure operation performance between the baseline (current-day procedures) simulation and the ATD-2 (departure metering procedures) simulation, as well as the comparison of simulated operations against real, historical operational data for validation purposes. We begin by summarizing the high-level benefits estimated for each of the simulation scenarios we simulated, in Section 6.1. Following the summary, we present details of two simulation scenarios per airport site, including detailed benefits and validation results, in Sections 6.2 (for CLT), 6.3 (for DFW), and 6.4 (for EWR), respectively. For the remaining simulation scenarios per airport site, we refer the readers to Appendix A (Section 12) for the benefits and validation results.

6.1. Summary of ATD-2 Benefits Results (CLT, DFW, EWR)

The key performance metric from the benefits computation perspective was the amount of taxi out time savings provided by ATD-2 for each simulation scenario. **Table 21** shows the summary taxi out time savings per scenario in terms of the percentage saving over the average taxi out time in the baseline simulation, observed over the duration of the simulation timeframe. Since we simulated only a part of each selected simulation day, we applied a full day multiplier to go from part-day benefits to full-day benefits. We developed this full day multiplier by analyzing the real, historical observed taxi out delays during the simulation timeframe in comparison to the delays over the entire duration of the day. The last column of the table shows the full day benefits. These benefits were used in the annualization computations, which we discuss in Section 8.

Table 21. Summary Taxi Out Time Savings Results from Individual Simulation Scenarios

Airport	Simulation Day	Annualization Day Rank	Runway Config	Simulation Timeframe (UTC)	Taxi-Out Time Savings During Sim Time (%, min)	Full Day Multiplier	Full Day Benefits (min)
CLT	6/15/2016	1	South	1000-1600	9.82, 422	3.19	1346
CLT	5/17/2016	2	South	0900-1700	5.71, 325	2.16	702
CLT	6/1/2016	3	North	1000-1500	8.97, 368	5.02	1847
CLT	6/2/2016	4	South	1200-1500	5.85, 324	9.18	1217
CLT	5/6/2016	5	North	1600-2100	15.13, 708	2.23	1579
CLT	5/31/2016	7	North	1600-2100	3.8, 155	3.49	541
		CLT AVERAGE DAILY SAVING (~699 DEPARTURES PER DAY)=					**1.72 MIN**
DFW	5/12/2016	1	East	1000-1700	8.16, 551	2.4	1322
DFW	6/4/2016	6	East	1700-2300	14, 869	2.54	2207
DFW	6/3/2016	2	West	1500-2100	8.38, 626	3.34	2091
DFW	7/5/2016	3	West	1500-2100	10.6, 728	2.57	1871
DFW	7/17/2016	4	West	1000-1600	10.7, 511	3.05	1559
DFW	7/28/2016	5	West	1000-1600	6.39, 289	4.16	1202

		DFW AVERAGE DAILY SAVING (~905 DEPARTURES PER DAY)=					**1.89 MIN**
EWR	5/6/2016	3	North	1400-2000	9.7, 249	5.25	1307
EWR	7/21/2016	1	South	0800-1800	6.55, 319	2.78	887
EWR	7/29/2016	2	North	0900-1800	7.24, 295	3.11	917
EWR	7/3/2016	5	South	0900-1600	21.69, 761	2.93	2230
		EWR AVERAGE DAILY SAVING (~905 DEPARTURES PER DAY)=					**2.34 MIN**

As seen from the table and also summarized in **Figure 27**, on an average, the ATD-2 system provided around 2 minutes of taxi-out time savings per departure at CLT and DFW. For EWR, the benefit was slightly above two minutes per departure flight.

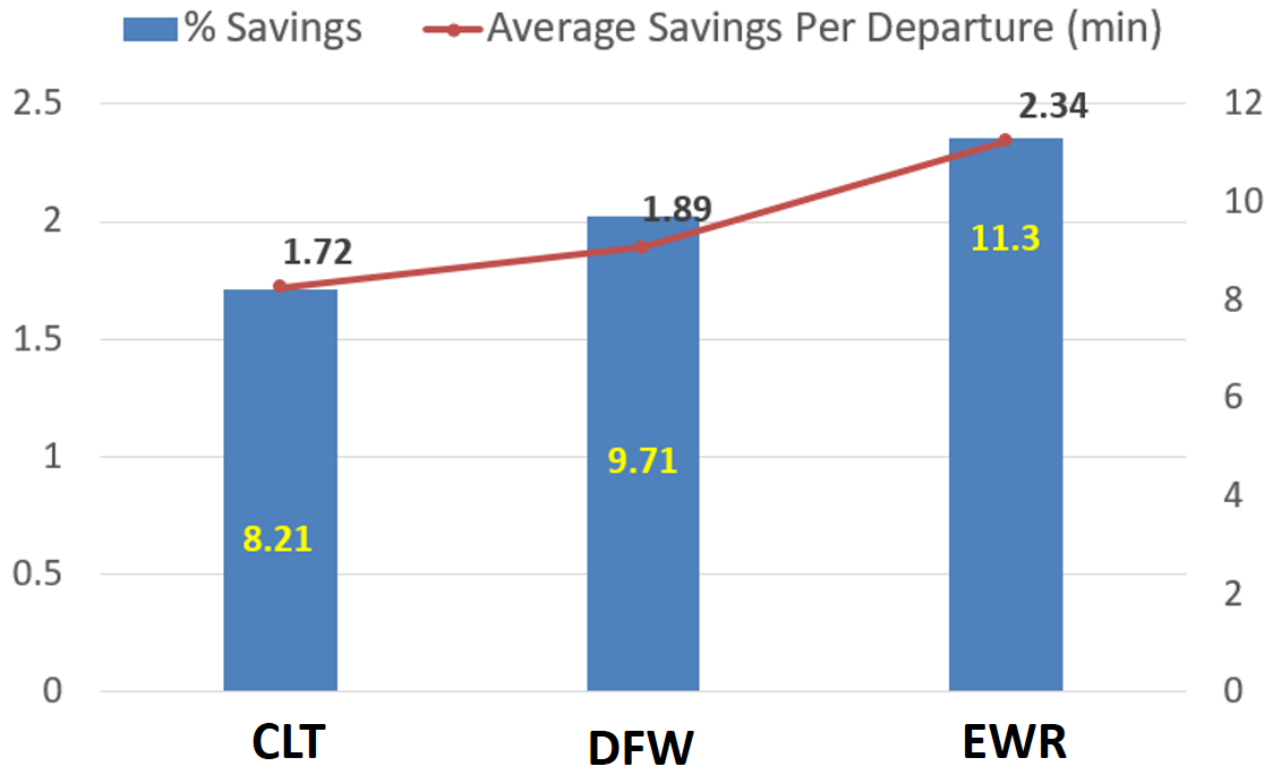

Figure 27. Percent and average per departure flight taxi-out time savings at the three airports, averaged over all the simulations per airport

Furthermore, taking a deeper look into the benefits results at CLT, we see that ATD-2 system shows on an average higher benefits during the North-flow configuration as compared to the South-flow configuration (see **Figure 28**).

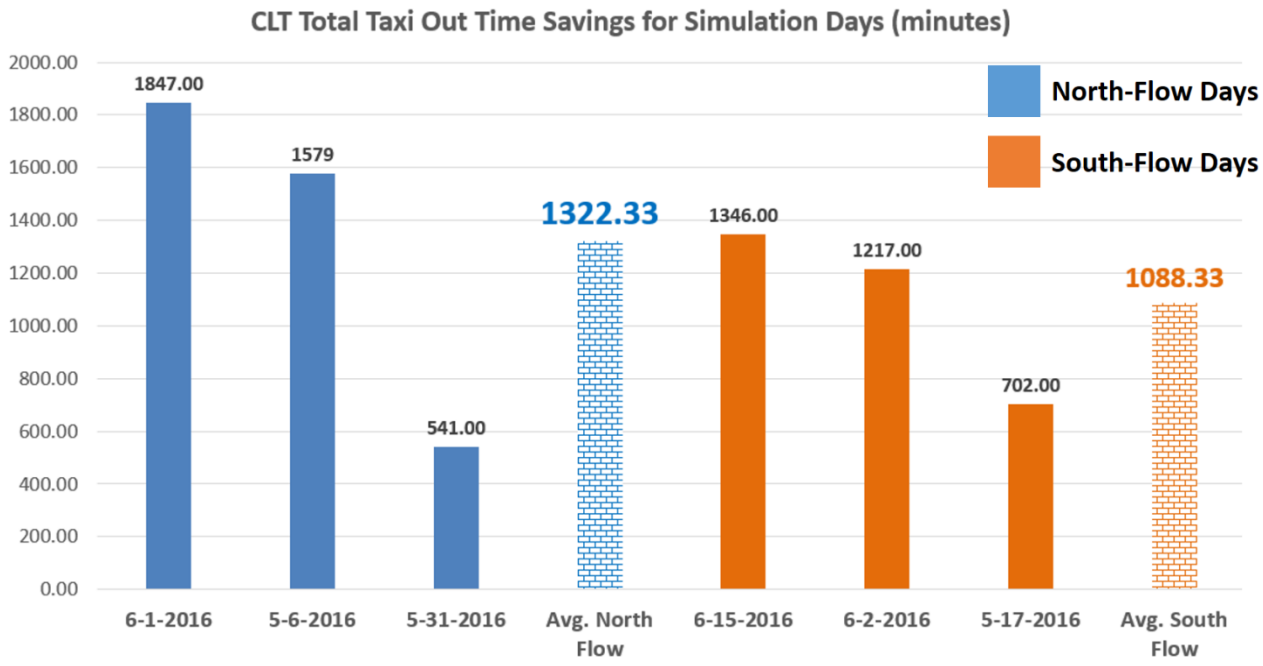

Figure 28. At CLT, ATD-2 provides higher benefits during North-flow configuration as compared to South-flow.

Next, we discuss the results from each simulation scenario for the three airports, in detail.

6.2. CLT Simulations Details

This section presents detailed analysis of two simulated baseline VS ATD-2 operations scenarios for CLT. First, we provide some background on the nature of CLT departure operations, by discussing the banked structure of departure operations at CLT. **Figure 29** shows nine individual departure banks that occur daily at CLT. These departure banks were identified by applying curve fitting to per minute wheels-off counts over a 3-month period (May-July 2016), and then identifying the local minima and maxima of the fitted curve. The table inset into **Figure 29** shows the start and end times of individual departure banks in CLT local time. Our finding of the nine departure banks and their start/end times matches closely with a parallel analysis conducted by NASA and American Airlines. As we will see in the individual simulation scenario sections next, each simulation scenario covered at least three of the departure banks identified in **Figure 29** and between the different scenarios that we simulated, we were able to cover almost all the departure banks.

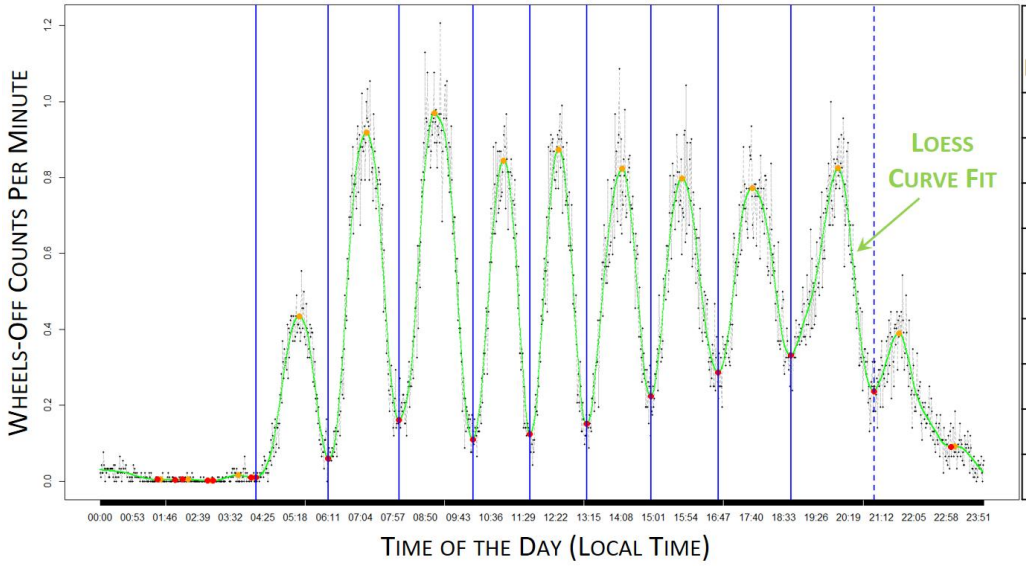

Bank Number	Start Time	End time
1	5:00	8:30
2	8:45	10:30
3	10:45	12:00
4	12:30	13:30
5	13:45	15:15
6	15:30	17:15
7	17:20	18:45
8	19:00	21:20
9	21:45	23:00

Figure 29. Nine distinct departure banks were identified to occur each day at CLT.

Next, we describe the results from simulating individual scenarios in separate sections. For each simulated scenario, its respective section (coming next) will include the following descriptive components: (1) A description of the simulation scenario including the active runway configuration, the number of departure and arrival operations by runway used, and the active traffic management initiatives simulated; (2) The baseline versus ATD-2 benefits in terms of taxi time savings; (3) Analysis of ATD-2's impact on the airport's on time performance; (4) Analysis of the impact of ATD-2 on airport departure throughput, (5) Validation metrics for comparing simulated operations against actual operations on the same historical day as well as against historical distributions on similar days (i.e., days with the same active runway configuration during the simulated timeframe), (6) In-depth analysis of the observed simulation output data to justify the observed benefits and apportion observed benefits to the correct ATD-2 benefit mechanisms.

6.2.1. CLT Simulation Day 1 Results (6/15/2016, South Flow)

The first scenario we describe involved the simulation of CLT airport arrival and departure traffic on 06/15/2016 during the 1000-1600 UTC timeframe. This simulation timeframe covers CLT departure banks # 2, 3 and 4.

6.2.1.1. Simulation Scenario Description

CLT was under the South-flow runway configuration during the selected simulation time-period, with departures operating on runways 18C and 18L, and arrivals operating on runways 23, 18C and 18R, as shown in **Figure 30**. Runway 18C was operating in a mixed-use mode.

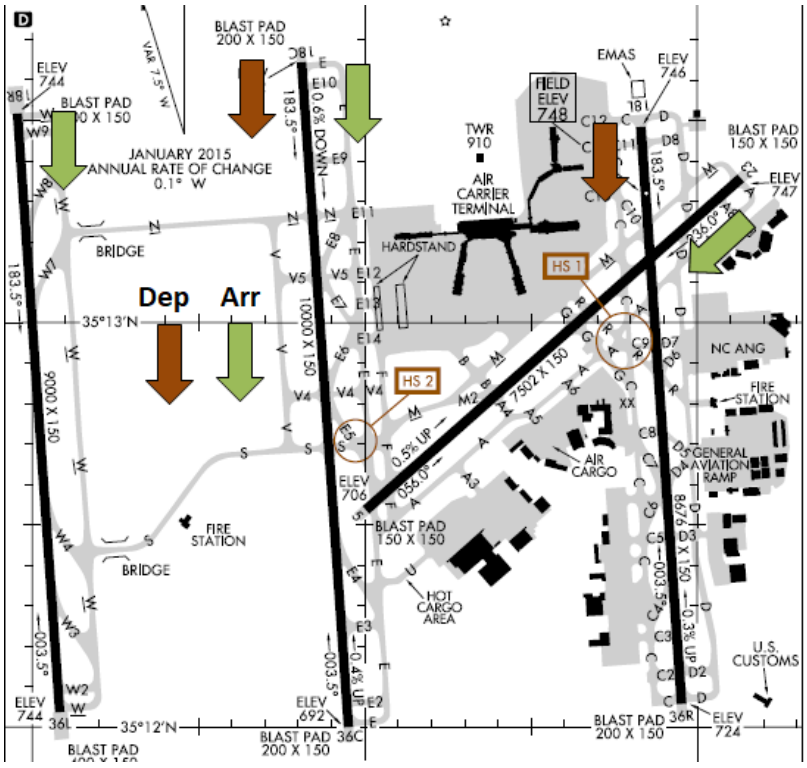

Figure 30. CLT South Flow Runway Configuration Runway Usage

The table below outlines the number of total departures and arrivals using the individual active runways during the simulated timeframe.

	18L	18C	18R	23	Operation Counts by Type
Departures	112	128	0	0	240
Arrivals	0	63	125	55	243
Total Ops Per Runway	112	191	125	55	483

The simulations also emulated the implementation of surface traffic flow management initiatives such as APREQs, miles-in-trail restrictions and Ground Delay Programs as described in Section 4.2. In this particular scenario, we simulated the following traffic management initiatives that were active during the 1000-1600 UTC timeframe on the actual 06/15/2016 day.

TMI Type	TMI Requesting Facility	Providing Facility	TMI Start	TMI End	Departures to
APREQ	ZTL	CLT	10:30	16:00	ORD
APREQ	ZDC	CLT	12:00	23:59	DCA
APREQ	ZDC	CLT	10:30	23:59	LGA
APREQ	ZDC	CLT	12:30	23:59	EWR

APREQ	ZTL	CLT	12:40	14:20	DTW

6.2.1.2. Benefits Results: Taxi-time Savings

Our simulation results for this scenario showed that the ATD-2 system saved around 10% of the total taxi-out time over all the departures, as shown in **Figure 31**. Similar levels of taxi-out time savings (percentage-wise) were seen in the active movement area (AMA) taxi-out times as well as the ramp taxi times.

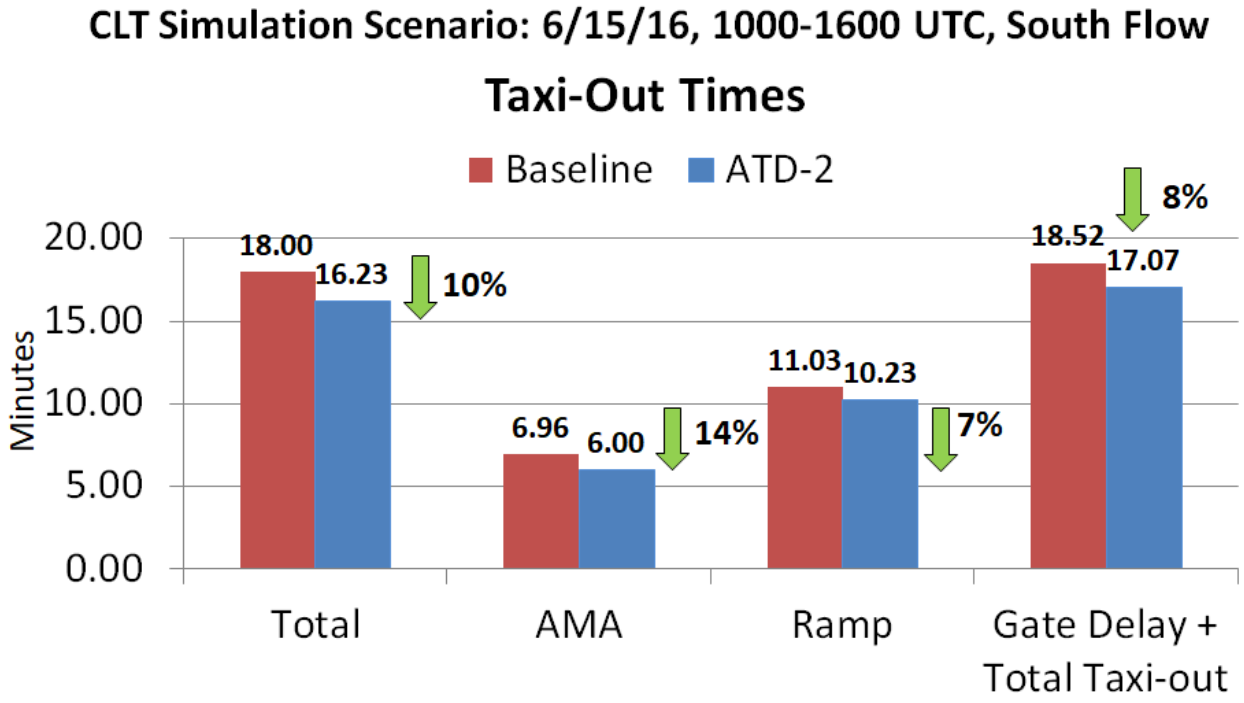

Figure 31. Taxi-Out Time Savings Benefits Estimated by Baseline VS ATD-2 Simulations for the 06/15/2016 1000-1600 UTC simulation scenario

Further, we also computed the total transit time for each departure consisting of the excess time spent at the gate in the ATD-2 simulation (i.e., ATD-2 system imposed gate delay) and the taxi transit from gate pushback to runway takeoff. This total transit time metric is the fourth pair of bars shown in **Figure 31**. As seen from the figure, with the ATD-2 system there is a 8% drop in the total transit time metric on an average.

We also analyzed the impact of ATD-2 departure metering on arrival taxi-in times. **Figure 32** shows that with the ATD-2 system operating there was a slight increase in the taxi-in times. Based on post-simulation SME analysis, we are not very confident about the validity of the beneficial or detrimental impact on arrival taxi-in times seen in the simulations. As a result, we have decided to account for arrival taxi-in savings benefit as a separate component in our overall, ATD-2 benefits computation. This component can be taken out of the final benefits numbers if that is deemed appropriate. As the reader will see in Sections 8 and 10, we present two versions of the overall ATD-2 system benefits, one including the arrival taxi-in savings benefits and one excluding them.

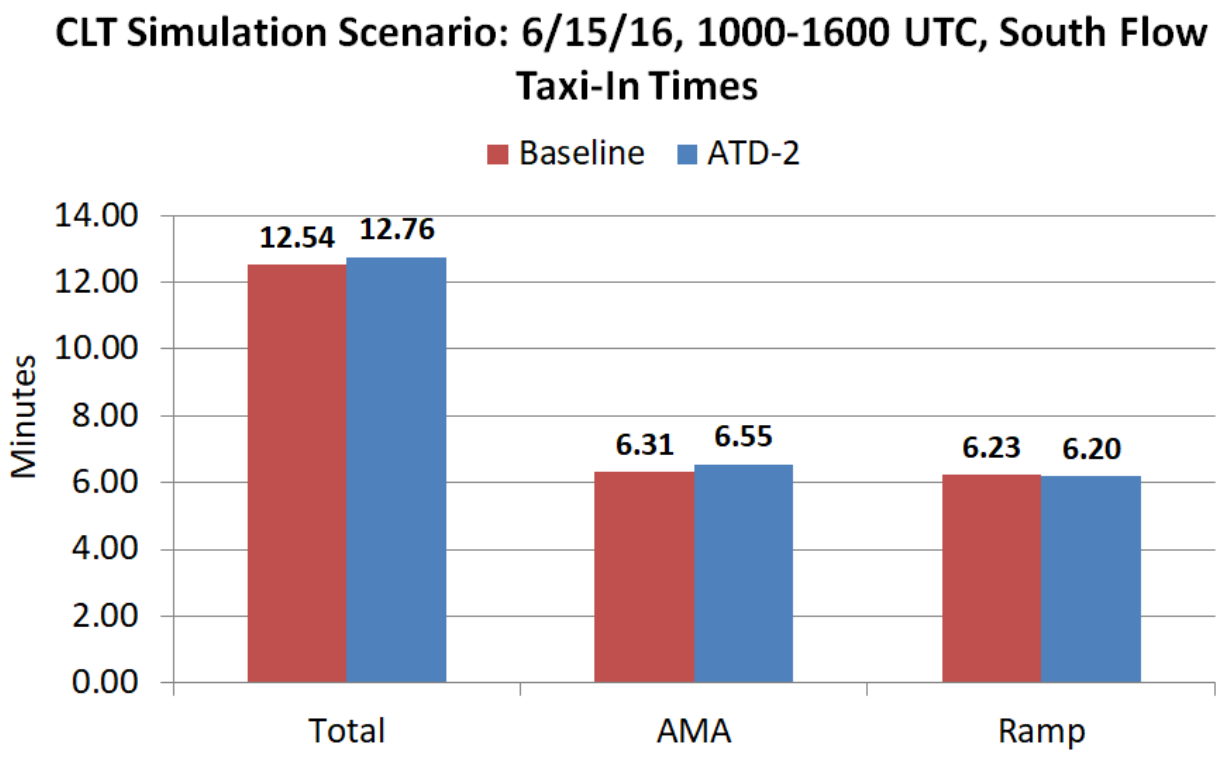

Figure 32. Taxi-In Time Savings Benefits Estimated by Baseline VS ATD-2 Simulations for the 06/15/2016 1000-1600 UTC simulation scenario

6.2.1.3. Analysis of On-Time Performance for Departure Flights

An important consideration for user-acceptance of the ATD-2 system is the question of what impact do the ATD-2 gate delays have on the overall On time performance of the airport in terms of late or early runway takeoff times. In relation to this aspect, we analyzed the runway takeoff time difference for each departure flight between the baseline simulation (current-day procedures) and the ATD-2 simulation (departure metering procedures). **Figure 33** shows the results of this analysis. The right half of this figure shows a histogram of runway takeoff time differences per flight (ATD-2 simulation takeoff time – Baseline simulation takeoff time). Left-half of the figure shows the runway takeoff time differences as a function of the actual takeoff time. As seen from the figure, a big majority of the flights (~76%) took off either at the same time or earlier in the ATD-2 operations, whereas 24% of the flights took off later as compared to the baseline simulation. Moreover, out of the 24% flights departing late in the ATD-2 simulation, around three quarters of them departed less than 2 minutes late than their counterpart departure in the ATD-2 simulation.

This demonstrates that the ATD-2 system had a positive impact on the On time performance of the airport, in general, but there were some flights that took off later than their baseline runway takeoff time. In general, if bringing the number of flights that takeoff later than baseline down (closer to zero) is of high importance to the airlines, then there are tools/settings available in the ATD-2 system, which can be modified to reduce the negative impact on certain flights. These tools/ settings include the optimal selection of the ATD-2 Tactical Surface Scheduler's taxi delay buffer parameter as well as modifications to how the ATD-2 Scheduler estimates earliest runway usage

times for departure flights for scheduling purposes as well as how it back-computes gate delays from the target runway takeoff times. But, before making these changes in the operational ATD-2 system, more simulation-based sensitivity tests are required to assess multiple alternatives and select the best.

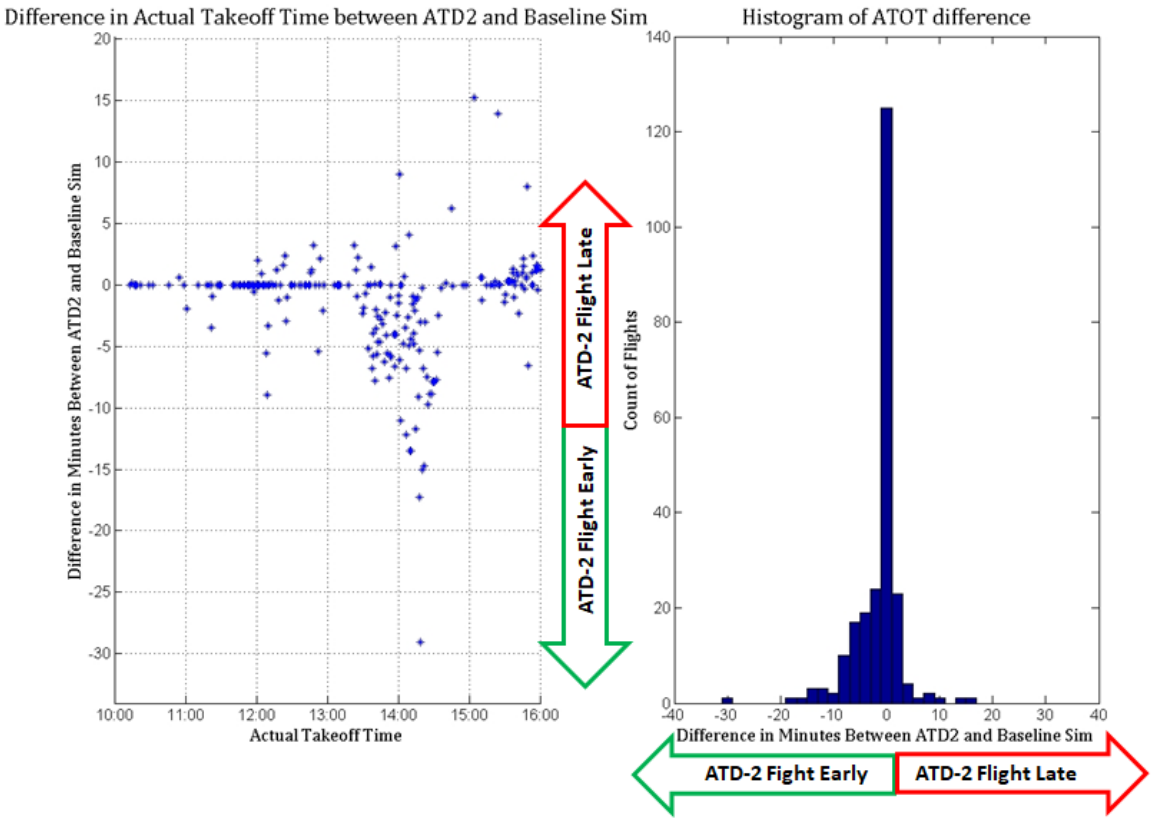

Figure 33. Analysis of On-Time Runway Takeoff Performance – Baseline VS ATD-2

Further, we also computed the percentage of departure flights in the baseline and ATD-2 simulations that had taxi out times within the taxi-out budget times provided by American Airlines to NASA. **Figure 34** shows the histograms of total taxi-out time plus gate hold per flight minus the corresponding AAL taxi-out budget, with the data for baseline simulation shown in the top-half (red bars) and the data for the ATD-2 simulation shown in the bottom half (blue bars). Our computations show that in the baseline simulation around 83% of the mainline and 80% of the regional flights took off with a delay of less than 15 minutes with respect to the SOBT plus the airline budgeted taxi out time, whereas in the case of ATD-2 operations these numbers were higher 87% and 87%, respectively. Moreover, the percentage of mainline and regional flights, which had shorter taxi-out times than the budgeted taxi-out times, was also higher in the ATD-2 simulations as compared to baseline (see figure for the percentages). This data demonstrates that the ATD-2 system had a beneficial impact on the airport's on time performance.

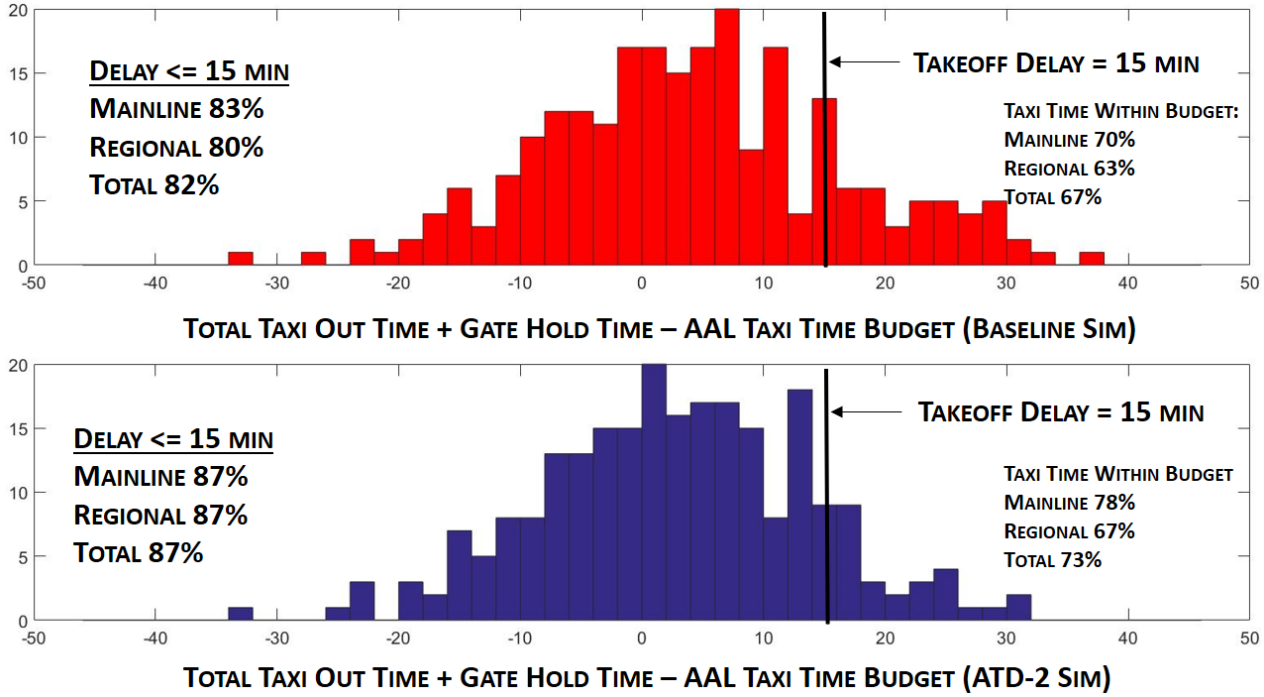

Figure 34. ATD-2 system had a beneficial impact on the airport's on time performance as per an analysis of Total Taxi-out Times as compared to AAL Taxi Out Time budget

6.2.1.4. Analysis of ATD-2's Impact on Airport Departure Throughput

Our simulation results show that the ATD-2 system did not have a major negative or positive impact on the overall airport throughput. **Figure 35** shows the cumulative airport throughput (i.e., the number of departures that have already taken off at time 't') throughout the simulation timeframe. As seen from the figure, the baseline cumulative airport throughput line (red dashed line) falls either on or below the ATD-2 cumulative airport throughput line (blue solid line) for most of the simulation timeframe, with only a few places where it goes above the blue line by 1-2 departure aircraft. This demonstrates that the ATD-2 system does not have a negative impact on the airport's throughput despite prescribing gate holds.

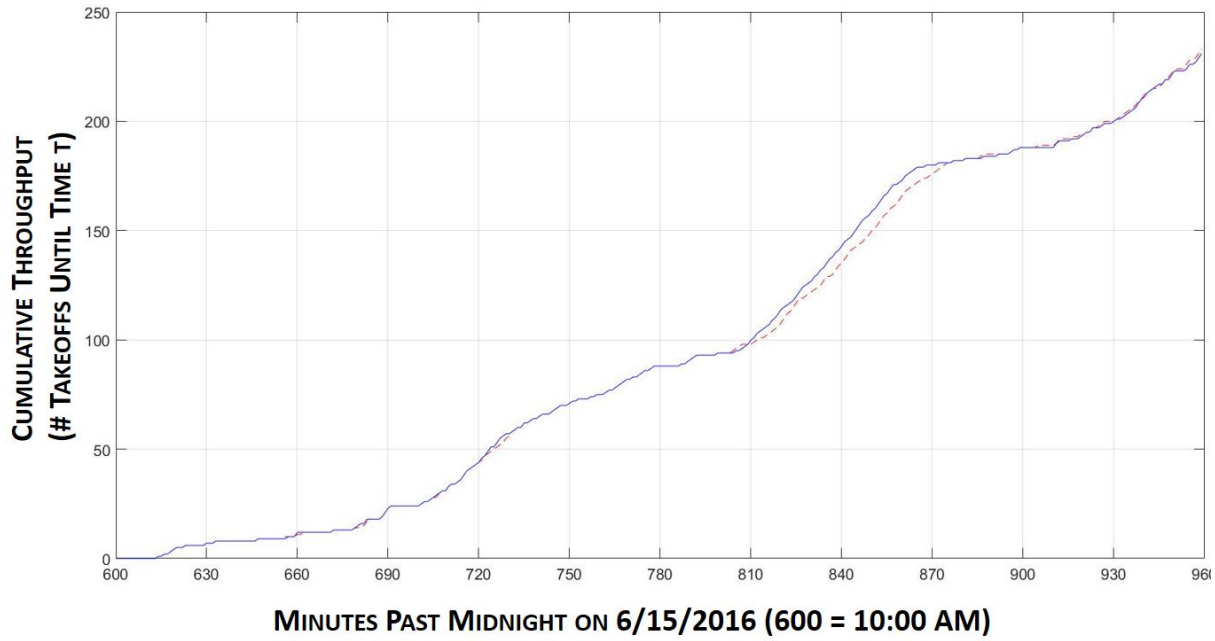

Figure 35. Cumulative airport throughput (baseline sim: red dashed line; ATD-2 sim: blue solid line) shows very little impact of ATD-2 gate holds on departure throughput

Figure 36 shows the cumulative departure throughputs separately for the two active departure runways (18C and 18L), again demonstrating that the ATD-2 system had very little impact on the individual runway throughputs.

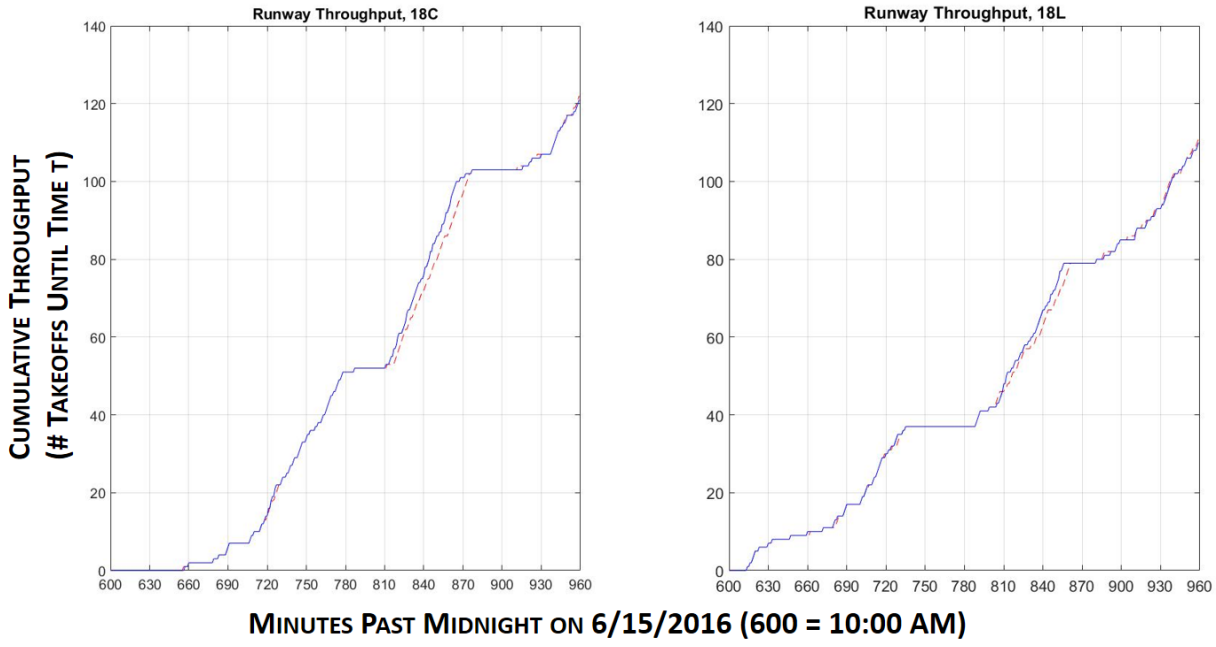

Figure 36. Cumulative airport throughput in the baseline simulation (red dashed line) and the ATD-2 simulation (blue solid line) shown for two departure runways separately

6.2.1.5. Simulation Validation

This section presents results from comparing simulation outputs with operational metrics from real operational data on the same historical day, as well as with a distribution of the same operational metrics computed over a set of similar days over a period of three months. The left-hand side of **Figure 37** shows the comparison of takeoff counts per 15-minute bin over the duration of the simulation, with the simulated counts shown by the red line, the actual counts on the day of operations shown by the blue line, and a region covering the 10-th to 90-th percentile takeoff counts per 15-minute bin over similar historical time-bins shown by the green region. For computing the green region, similar historical time-bins for comparison against the simulation day metrics were chosen based on the detection of the same active runway configuration as the simulated configuration in those time-bins. For example, for the 16:30-16:45 UTC bin, we identified all 16:30-16:45 UTC bins over a period of three months (May-July 2016). Out of these bins, we identified those bins during which CLT had a South-flow runway configuration active. These identified same-configuration bins were used to compute the 10-th and 90-th percentile runway takeoff counts.

As seen from the left-hand side of **Figure 37**, the simulated takeoff counts follow the general trend of the actual runway takeoff counts, with three departure banks clearly visible. The discrepancies between simulated versus actual counts at the beginning and end of the simulation time-period can be attributed to the fact that we only included flights that pushed back after 10:00 UTC and before 16:00 UTC in the simulation. By doing so, we missed some of the departure flights at either end of the simulation time-period.

The right-hand side of **Figure 37** shows similar plot for the simulated versus actual gate out counts. Again, we see that the simulation followed the general trend of the actual counts with discrepancies at the beginning and end of the simulation timeframe attributed to flights that were by design not included in the simulation set.

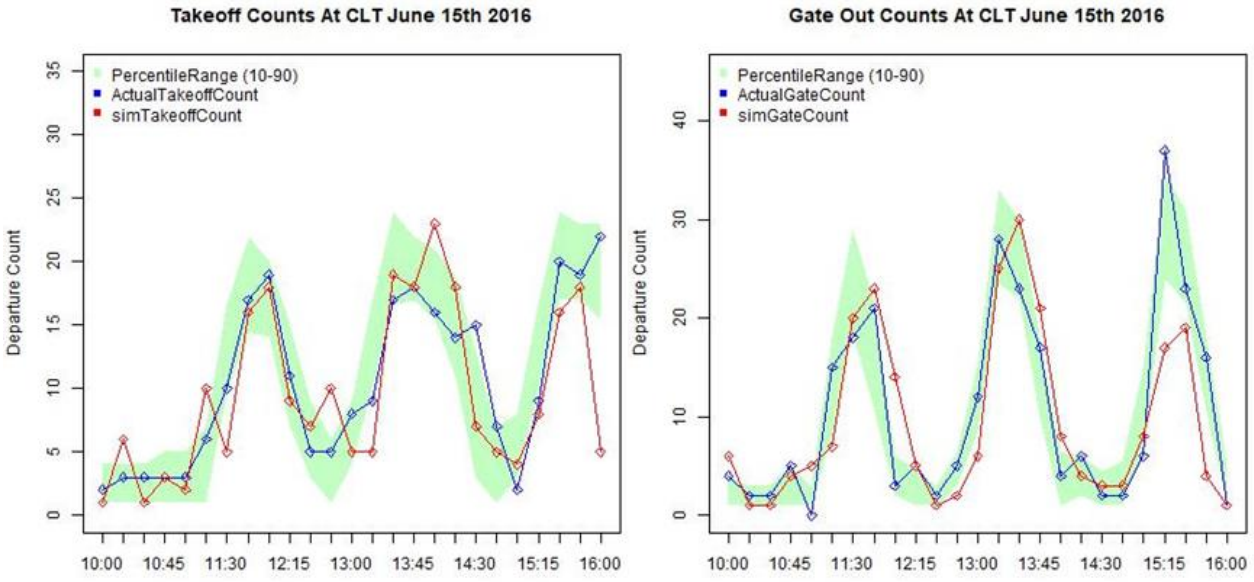

Figure 37. Runway Off and Gate Out Counts Validation – Simulation Versus Real Operations

Further, we also validated the taxi-out times by comparing simulated times against real historical operational taxi-out times from the same day as well as with a distribution of taxi-out times over similar days. **Figure 38** shows the comparison of simulated and actual taxi-out times, with AMA taxi-out time comparison showed in the left half of the figure and the total (AMA + Ramp) taxi-out time comparison shown in the right half of the figure. As seen from the figures, the taxi-out times do not match very closely, but simulated taxi-out times follow the general trend of the actual observed simulated taxi-times with a couple of peaks visible in both simulated and actual data. The discrepancies at the beginning and end of the simulation timeframe can again be attributed to the fact that we had excluded flights outside the 10:00-16:00 UTC timeframe from the simulation by design, whereas in the actual operations they appear in the taxi-out time plots. The discrepancies between actual and simulated taxi-out times outside the beginning and ending time-bins can be attributed to multiple factors including, erroneous actual Gate OUT time data, differences in the handling of departure takeoff clearances between actual operations and simulation (human local controller clearances may contain additional delays due to the fact that the local controller is handling multiple arrival and departure clearances at the same time), and differences in simulated versus actual ramp and spot merge handling.

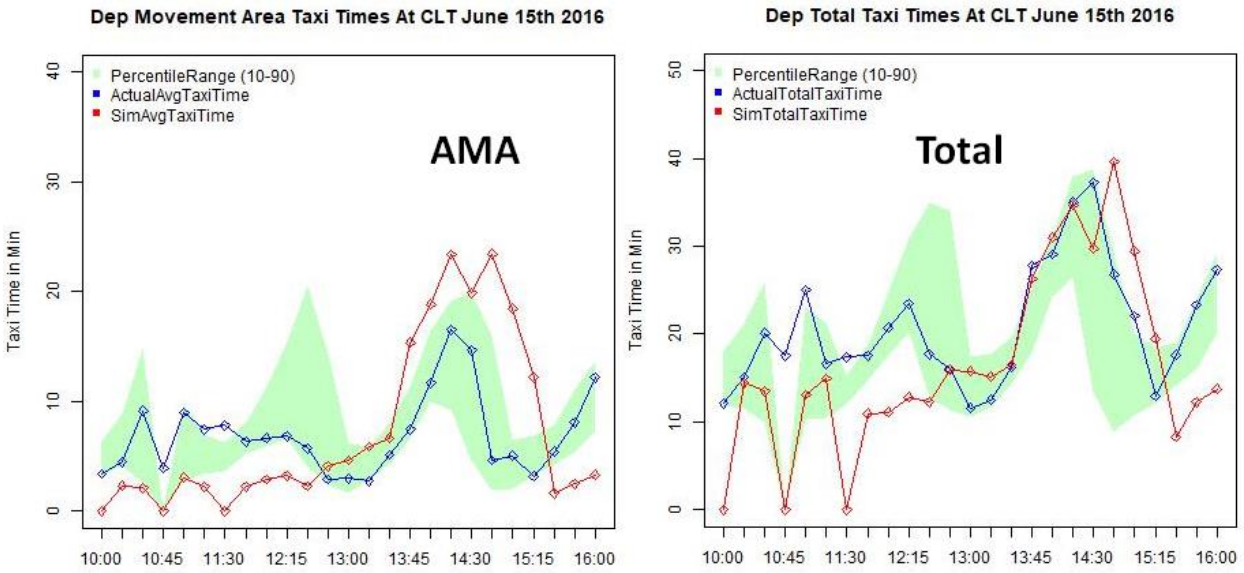

Figure 38. Taxi-Out Time Validation – Simulation Versus Real Operations

6.2.1.6. Analysis of Benefit Mechanism Contributions to ATD-2 Benefits

Analysis of simulation output data showed that three benefit mechanisms played a major role in providing taxi-out time savings. These were: (1) Demand throttling provided by Surface Departure Metering advisories (i.e., gate-holds); (2) Data exchange, especially more efficient electronic coordination of APREQ restrictions; and (3) More predictable surface movements leading to better TMI compliance. We discuss each of these benefit mechanisms with supporting data analyses next.

Benefit Mechanism #1: Demand throttling provided by Surface Departure Metering advisories (i.e., gate-holds). As discussed above, our ATD-2 simulations included a full emulation of NASA's ATD-2 Tactical Surface Scheduler, which computed gate delays for departure flights in

order to reduce taxi-out times but at the same time keeping sufficient pressure on the departure runways. **Figure 39** shows the gate delay difference (i.e., ATD-2 simulation Gate OUT Time – Baseline simulation Gate OUT time) for each simulated departure flight. The right half of the figure shows a histogram of the gate delay differences, whereas the left half of the figure shows the gate delay difference plotted along the simulation timeline. We can see that the ATD-2 scheduler added a significant amount of gate delays over and above the baseline simulation. Moreover, the left-half plot shows that the ATD-2 scheduler allocated majority of the gate delays during the time-periods when the departure demand on the CLT runways was at its peak, i.e., at or near the peaks of the major departure banks included in the simulation. There are some gate delay difference points below the zero line in the plot on the left.

These were flights that received higher gate delays in the baseline simulation because of active APREQs to their destination airports. Here also, we see that the ATD-2 scheduler handled these flights with smaller gate delays than in the baseline simulation. This was an effect of more efficient coordination with the receiving Center, which included sending more accurate runway takeoff time estimates to the Center, and after the Center sends back the controlled runway release time computing the required gate release time using a more accurate taxi-out time estimate. This benefit mechanism is discussed later. For the demand throttling benefit mechanism that we are discussing here, it would suffice to observe that the ATD-2 scheduler correctly allocated gate delays during the especially busy peak time-periods.

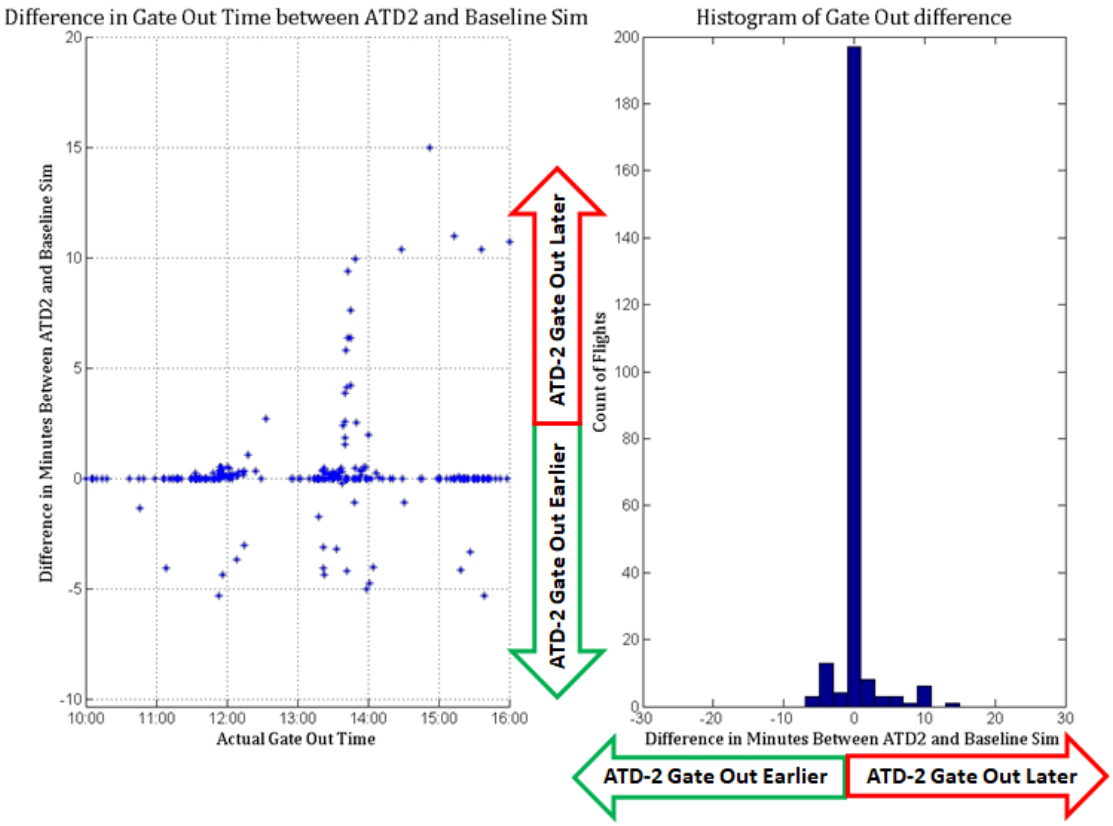

Figure 39. Gate Delay Difference, ATD-2 Operations – Baseline Operations

The beneficial effect that these tactical gate delays had on surface congestion can be seen in **Figure 40**. This figure plots the difference in Taxi-out Times (ATD-2 – Baseline) as a function of the difference in departure queue lengths experienced by the respective flights in the ATD-2 and Baseline simulations. Departure queue length experienced by a flight is defined as the number of flights taking off between the time the subject flight reaches the spot and the time it takes off. The expectation is that with ATD-2 prescribed gate-holds, departure flights will in general experience shorter departure queues leading to shorter taxi times.

As seen from the figure, ~68% of the flights experienced smaller departure queue lengths, a result of the demand throttling provided by the tactical scheduler allocated gate delays and as a result experienced shorter taxi-out times. Moreover, an additional ~8% flights experienced slightly longer queues in the ATD-2 operations, but still managed to have smaller taxi-out times. In the case of these flights, although there were more flights ahead of them in the departure queue when they reached the spot, the runway takeoff times for those flights were sufficiently spaced out as a result of the gate delays and hence the flight was able to take off after spending a smaller time in taxi. Around 2.5% of the flights experienced longer queues than the baseline simulation and as a result experienced longer taxi-out times. Moreover, around 21% of the flights experienced shorter queues, yet had longer taxi-out times. These longer taxi-out times are an indication that the ATD-2 scheduler settings may need fine tuning, both in simulations as well as in the field. It is our opinion that future efforts to assess different settings and algorithmic alternatives (e.g., taxi-out time prediction methods) in a fast-time simulation environment will be highly beneficial for optimizing the performance of the ATD-2 system in the field.

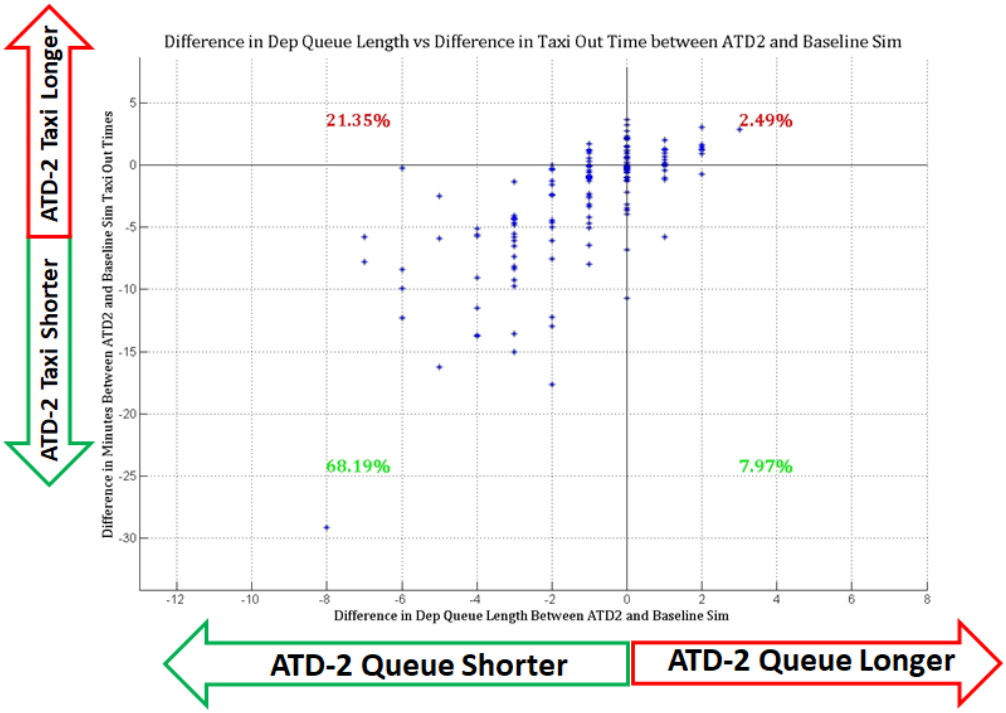

Figure 40. Taxi Out Time Difference (ATD-2 – Baseline) plotted as a function of Difference in Departure Queue Lengths Experienced by Flights at the Spot (ATD-2 – Baseline)

In summary, the demand throttling provided by ATD-2 Tactical Surface Scheduler-imposed gate delays contributed towards reducing the taxi-out times for departure flights in general. Next, we

discuss another benefit mechanism, which we found especially beneficial for APREQ-impacted departure flights.

Benefit Mechanism # 2: Data exchange for APREQ Coordination. As discussed above, our simulation platform models the full data exchange process for APREQ flights including both, the current-day procedures as modeled in the baseline simulations and the ATD-2 electronic negotiation, accurate takeoff time estimate communication to the Center, and preferential scheduling modeled in the ATD-2 simulations. The effect of differences in handling the APREQ flights can be clearly seen in **Figure 41**. As seen from the figure, APREQ-impacted flights benefited same amount as other flights from the ATD-2 system on this day. We see a drop of around 1.5 minutes on an average in their taxi-out times and around 10% drop in their taxi-out time standard deviation, as compared to the baseline simulation. These same statistics for all departure flights are a drop of 1.7 minutes on an average in the taxi-out times and a 20% drop in the standard deviation. Whereas, for non-APREQ flights the respective statistics are a 1.8-minute taxi-out time drop on an average and a 20% drop in the taxi-out time standard deviation. This shows that the ATD-2 system handled the APREQ flights more efficiently than the current-day procedures. Next, we will discuss an additional related benefit mechanism – higher TMI compliance.

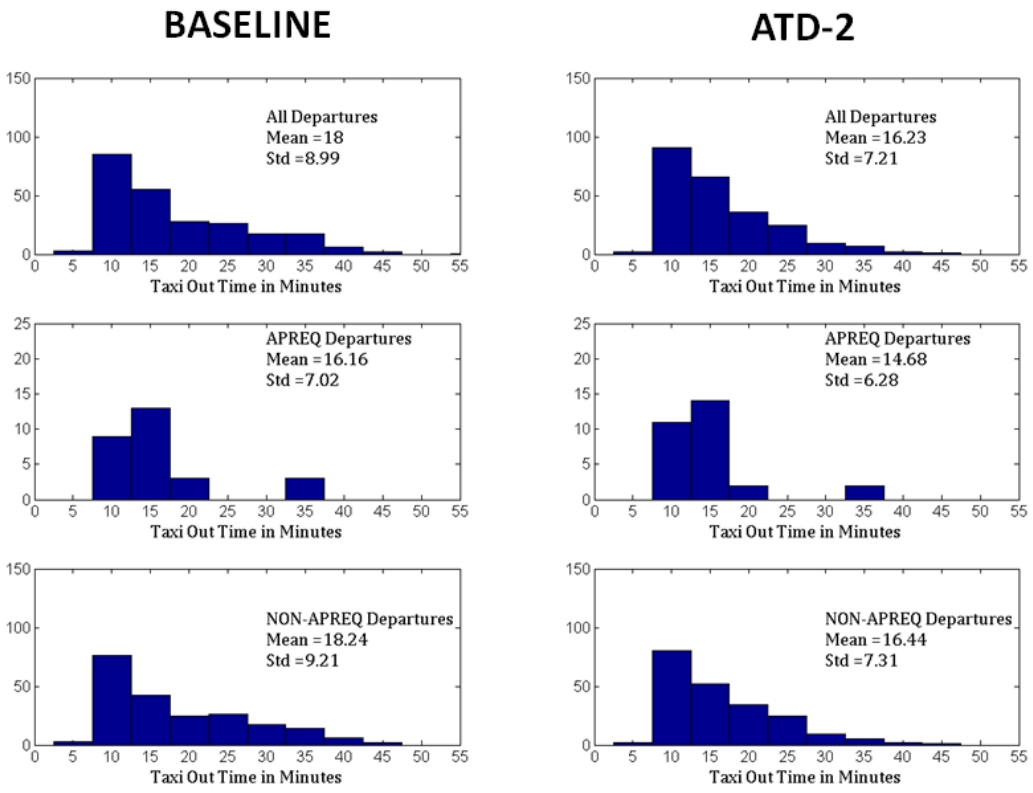

Figure 41. Taxi-Out Times (Mean and Variance) for All, APREQ and Non-APREQ flights for Baseline and ATD-2 Operations

Benefit Mechanism #3: Higher TMI Compliance. As a result of the modeled ATD-2 process for handling APREQ flights we saw tighter compliance with APREQ runway release times for departure flights in our ATD-2 simulations as compared to the baseline simulations. **Figure 42** shows the counts of APREQ-impacted departure flights taking off within different timeframes as compared to their respective APREQ runway release time. In general, six out of the 29 APREQ-impacted flights took off within the prescribed +2/-1 minute window in the ATD-2 simulation, with none departing in that window in the baseline simulation. Also, 25 out of the 29 APREQ-impacted flights departed within +5/-5 minutes of the APREQ runway release time in the ATD-2 simulation as compared to only two in the baseline simulation.

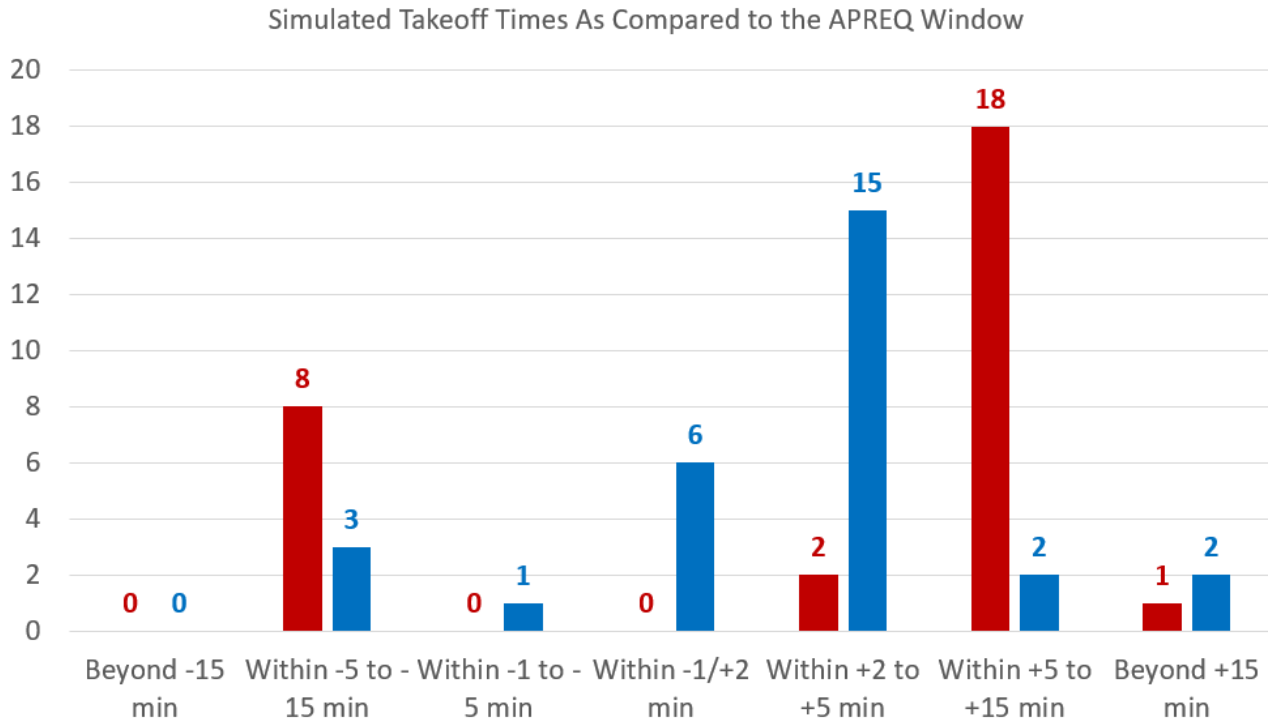

Figure 42. APREQ compliance for simulated baseline (red) and ATD-2 (blue) operations (computed over 29 APREQ-impacted flights)

6.2.2. CLT Simulation Day 2 Results (6/1/2016, North Flow)

The second scenario we describe involved the simulation of CLT airport arrival and departure traffic on 06/01/2016 during the 1000-1500 UTC timeframe. This simulation timeframe covers CLT departure banks # 2, 3 and 4.

6.2.2.1. Simulation Scenario Description

CLT was under the North-flow runway configuration during the selected simulation time-period, with departures operating on runways 36C and 36R, and arrivals operating on runways 36L, 36R and 36C, as shown in **Figure 43**. Similar to runway 18C in the South-flow configuration simulation scenario described in Section 6.2.1, runways 36C and 36R were in a mixed-use mode. Unlike the South-flow configuration, the virtually intersecting runway 23/5 was not used for

landings in this configuration. It was instead used as a taxiway for departure flights going from Terminals D and E to departure runway 36C.

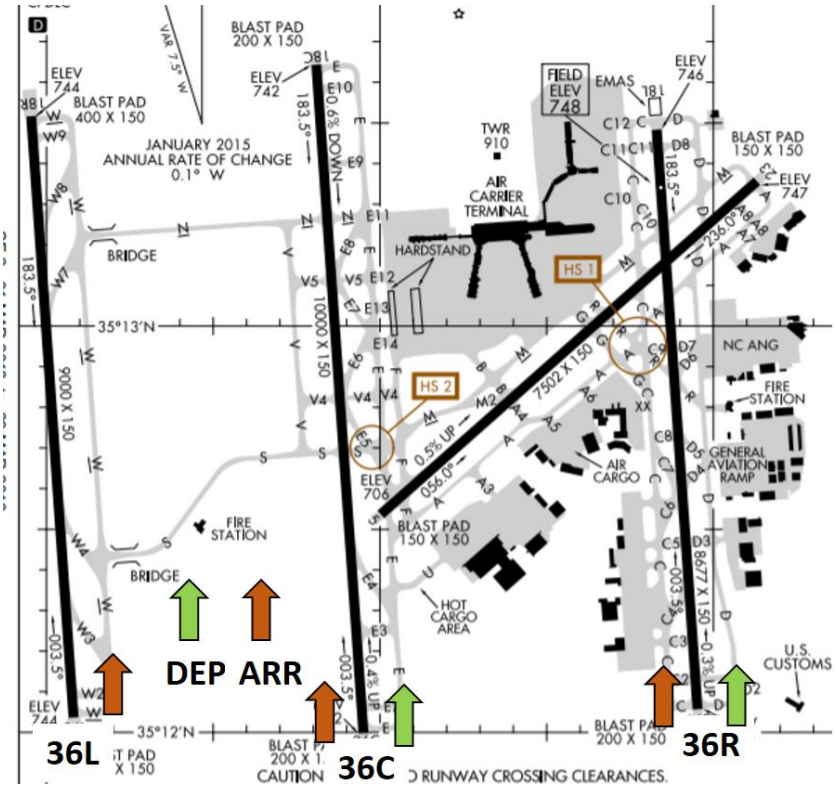

Figure 43. CLT North Flow Runway Configuration Runway Usage

The table below outlines the number of total departures and arrivals using the individual active runways during the simulated timeframe.

	36C	36R	36L	Operation Counts by Type
Departures	109	72	0	181
Arrivals	35	89	100	224
Total Ops Per Runway	144	161	100	405

The simulations also emulated the implementation of surface traffic flow management initiatives such as APREQs, miles-in-trail restrictions and Ground Delay Programs as described in Section 4.2. In this particular scenario, we simulated the following traffic management initiatives that were active during the 1000-1500 UTC timeframe on the actual 06/01/2016 day.

TMI Type	TMI Requesting Facility	Providing Facility	TMI Start	TMI End	Departures to
APREQ	ZDC	CLT	10:45	23:59	DCA
APREQ	ZDC	CLT	11:00	23:59	LGA
APREQ	ZTL	CLT	10:30	12:00	ORD

6.2.2.2. Benefits Results: Taxi-time Savings

Our simulation results for this scenario showed that the ATD-2 system saved around 9% of the total taxi-out time over all the departures, as shown in **Figure 44**. Similar level of taxi-out time savings (percentage-wise) were seen in the active movement area (AMA) taxi-out times as well as the ramp area taxi times.

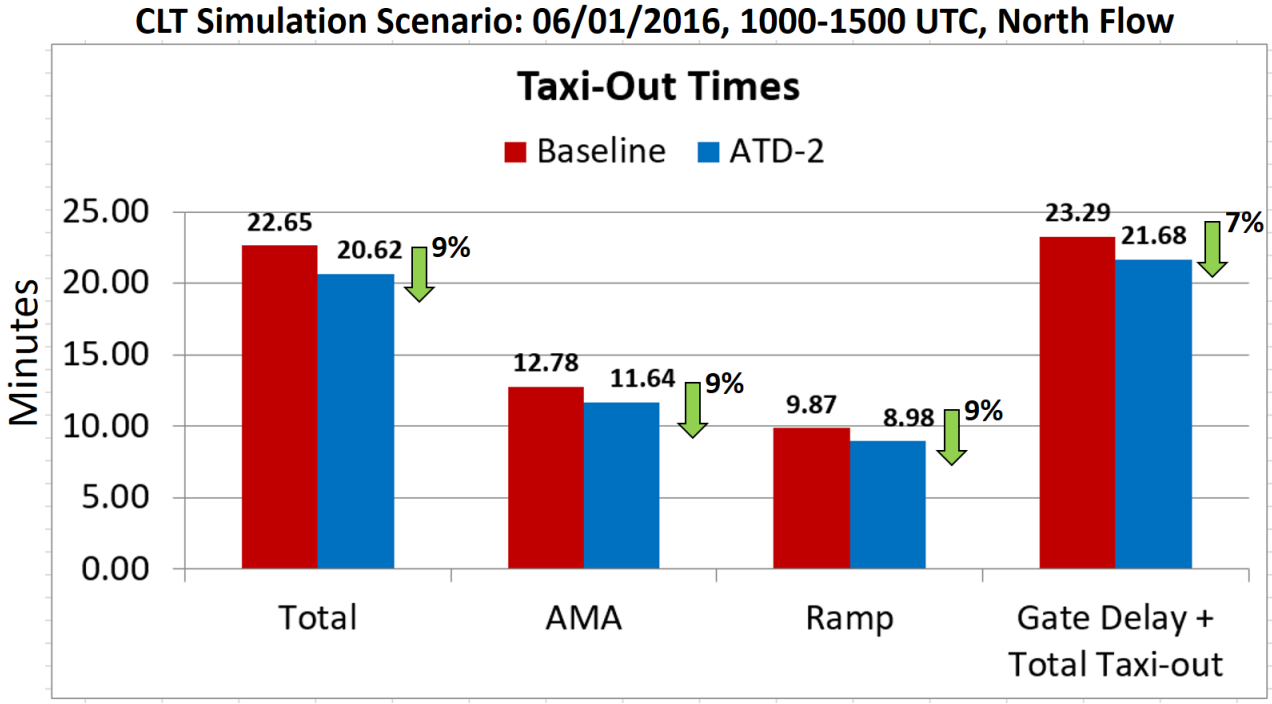

Figure 44. Taxi-Out Time Savings Benefits Estimated by Baseline VS ATD-2 Simulations for the 06/01/2016 1000-1500 UTC simulation scenario

Further, we also computed the total transit time for each departure consisting of the excess time spent at the gate in the ATD-2 simulation (because of the gate holds imposed by the ATD-2 system) and the taxi transit from gate pushback to runway takeoff. This total transit time metric is the fourth pair of bars shown in **Figure 44**. As seen from the figure, with the ATD-2 system there is a 7% drop in the total transit time metric on an average.

Further, we analyzed the impact of ATD-2 departure metering on arrival taxi-in times. **Figure 45** shows that with the ATD-2 system operating, there was a slight drop in the taxi-in times. As discussed above, we have decided to account for arrival taxi-in savings benefit in our overall, ATD-2 benefits computation as a separate component (which can be taken out of the final benefits numbers if necessary). As the reader will see in Sections 8 and 10, we present two versions of the overall ATD-2 system benefits, one including the arrival taxi-in savings benefits and one excluding them.

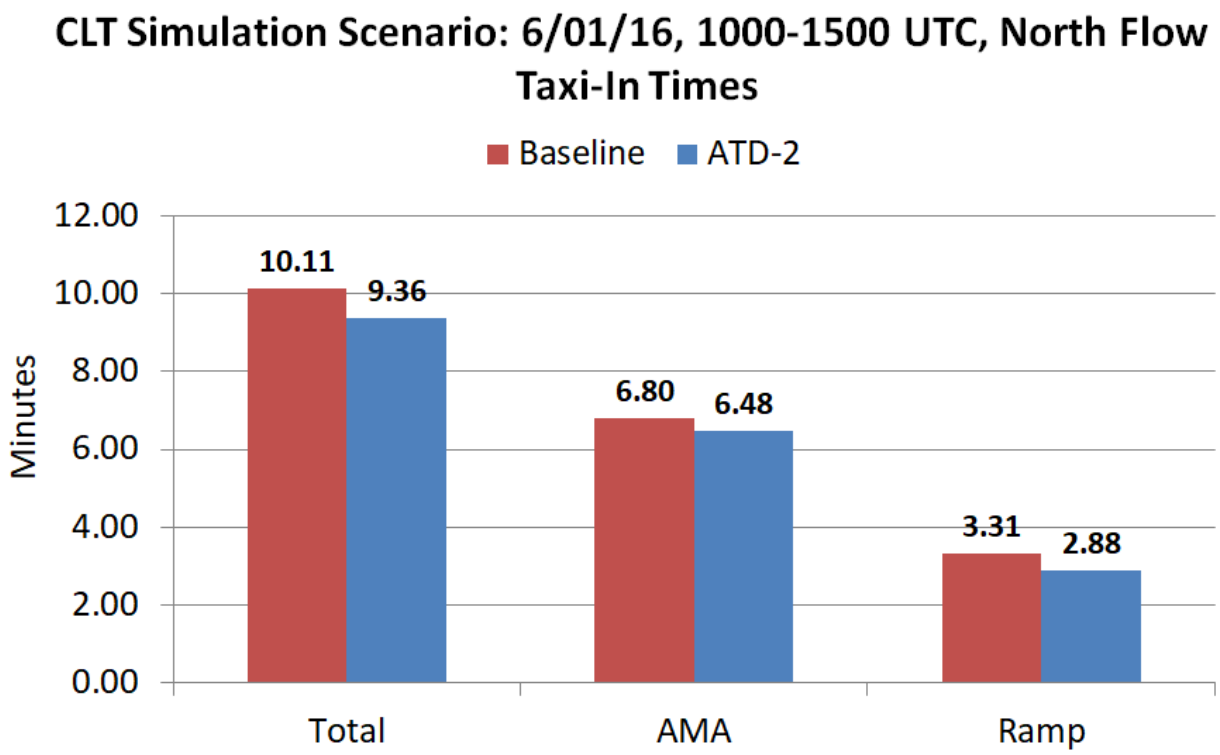

Figure 45. Taxi-In Time Savings Benefits Estimated by Baseline VS ATD-2 Simulations for the 06/01/2016 1000-1500 UTC simulation scenario

6.2.2.3. Analysis of On-Time Performance for Departure Flights

An important consideration for user-acceptance of the ATD-2 system is the question of what impact do the ATD-2 gate delays have on the overall On time performance of the airport in terms of late or early runway takeoff times. In relation to this aspect, we analyzed the runway takeoff time difference for each departure flight between the baseline simulation (current-day procedures) and the ATD-2 simulation (departure metering procedures). **Figure 46** shows the result of this analysis. The right half of this figure shows a histogram of runway takeoff time differences per flight (ATD-2 simulation takeoff time – Baseline simulation takeoff time). As seen from the figure, a big majority of the flights (~70%) took off either at the same time or earlier in the ATD-2 operations, whereas 30% of the flights took off later as compared to the baseline simulation. Moreover, out of the 30% flights departing late in the ATD-2 simulation, around half of them departed less than 2 minutes late than their counterpart departure in the ATD-2 simulation.

This demonstrates that the ATD-2 system had a positive impact on the On time performance of the airport, in general, but there were some flights that took off later than their baseline runway takeoff time. In general, if bringing the number of flights that takeoff later than baseline down (closer to zero) is of high importance to the airlines, then there are tools/settings available in the ATD-2 system, which can be modified to reduce the negative impact on certain flights. These tools/ settings include the optimal selection of the ATD-2 Tactical Surface Scheduler's taxi delay buffer parameter as well as modifications to how the ATD-2 Scheduler estimates earliest runway usage times for departure flights for scheduling purposes as well as how it back-computes gate delays

from the target runway takeoff times. But, before making these changes in the operational ATD-2 system, more simulation-based sensitivity tests are required to assess multiple alternatives and select the best.

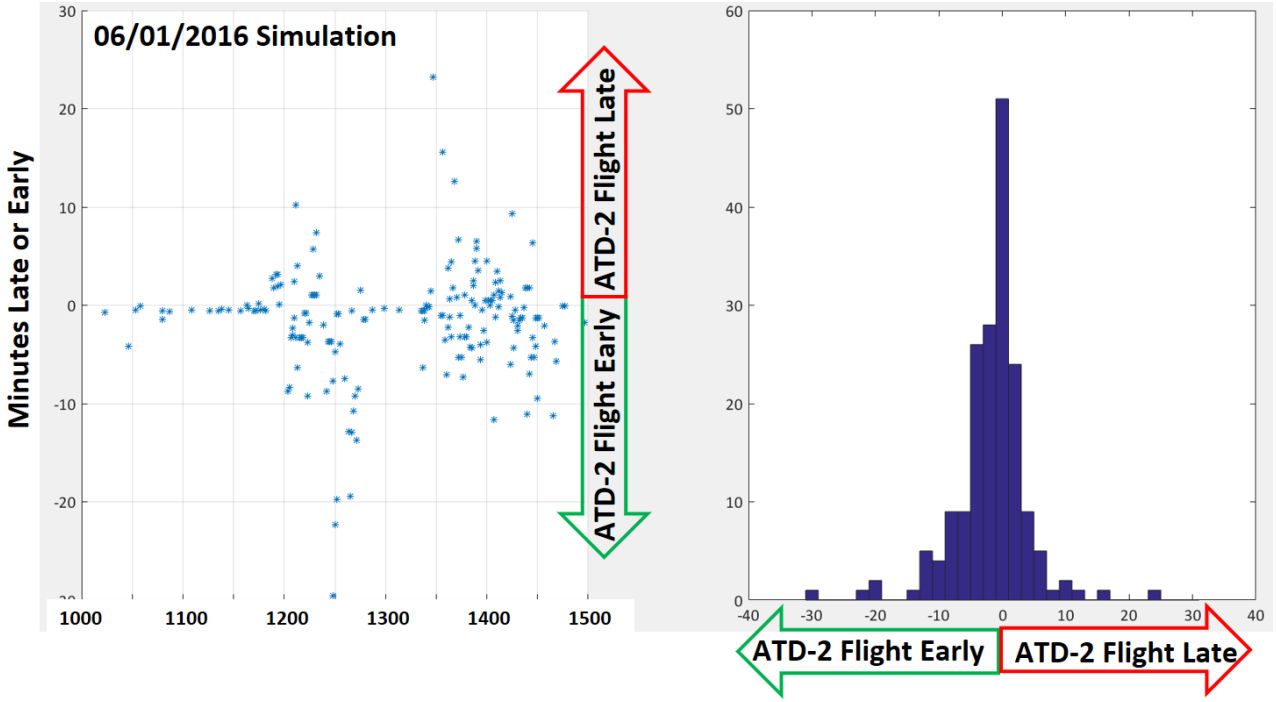

Figure 46. Analysis of On-Time Runway Takeoff Performance – Baseline VS ATD-2

Further, we also computed the percentage of departure flights in the baseline and ATD-2 simulations that had taxi out times within the taxi-out budget times provided by American Airlines to NASA. **Figure 47** shows the histograms of total taxi-out time per flight minus the corresponding AAL taxi-out budget, with the data for baseline simulation shown in the top-half (red bars) and the data for the ATD-2 simulation shown in the bottom half (blue bars). Our computations show that in the baseline simulation around 80% of the mainline and 69% of the regional flights took of with less than 15 minutes of delay as computed using SOBT and the airline budgeted taxi-out time, whereas in the case of ATD-2 operations these numbers were slightly higher 80% and 71%, respectively. Moreover, the percentage of mainline and regional flights, which had shorter taxi-out times than the budgeted taxi-out times, was also higher in the ATD-2 simulations as compared to baseline. This data demonstrates that the ATD-2 system had a slightly beneficial impact on the airport's on time performance.

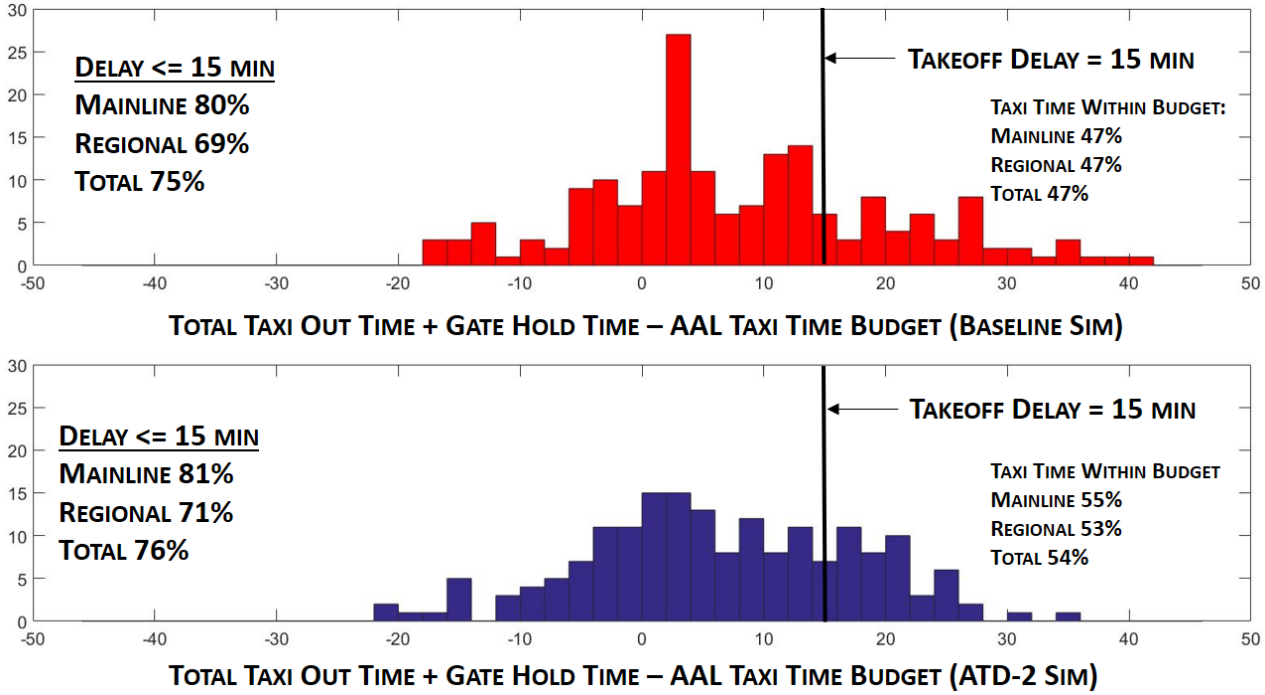

Figure 47. ATD-2 system had a beneficial impact on the airport's on time performance as per an analysis of Total Taxi-out Times as compared to AAL Taxi Out Time budget

6.2.2.4. Analysis of ATD-2's Impact on Airport Departure Throughput

Our simulation results show that the ATD-2 system did not have a major negative or positive impact on the overall airport throughput. **Figure 48** shows the cumulative airport throughput (i.e., the number of departures that have taken of at time 't') throughout the simulation timeframe. As seen from the figure, the baseline cumulative airport throughput line (red dashed line) falls either on or below the ATD-2 cumulative airport throughput line (blue solid line) for most of the simulation timeframe, with only a few places where it goes above the blue line by 1-2 departure aircraft. This demonstrates that the ATD-2 system does not have a negative impact on the airport's throughput despite prescribing gate holds.

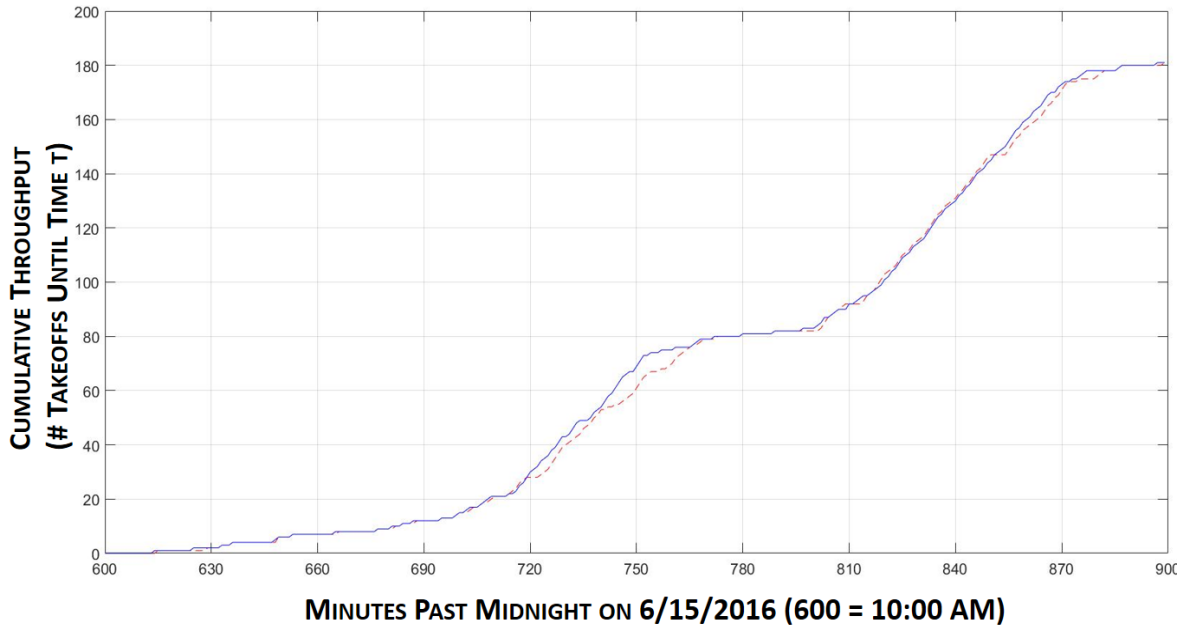

Figure 48. Cumulative airport throughput (baseline sim: red dashed line; ATD-2 sim: blue solid line) shows very little impact of ATD-2 gate holds on departure throughput

Figure 49 shows the cumulative departure throughputs separately for the two active departure runways (36C and 36R), again demonstrating that the ATD-2 system had very little impact on the individual runway throughputs.

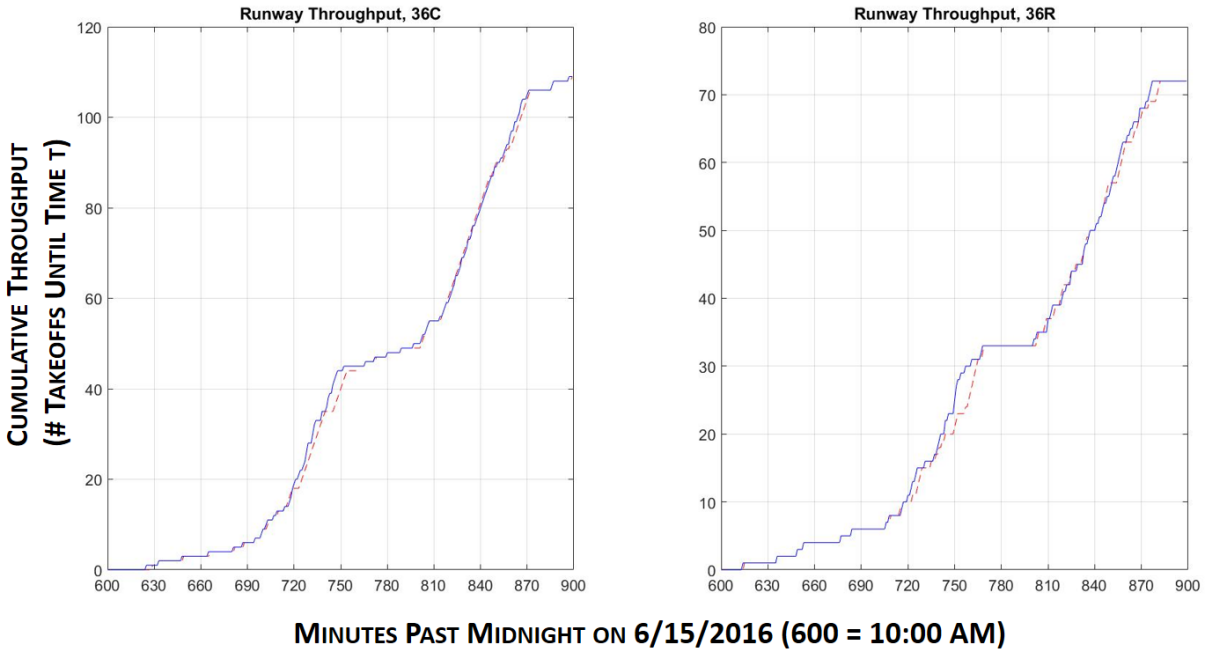

Figure 49. Cumulative airport throughput in the baseline simulation (red dashed line) and the ATD-2 simulation (blue solid line) shown for two departure runways separately

6.2.2.5. Simulation Validation

This section presents results from comparing simulation outputs with operational metrics from real operational data on the same historical day, as well as with a distribution of the same operational metrics computed over a set of similar days over a period of three months. The left-hand side of **Figure 50** shows the comparison of takeoff counts per 15-minute bin over the duration of the simulation, with the simulated counts shown by the red line, the actual counts on the day of operations shown by the blue line, and a region covering the 10-th to 90-th percentile takeoff counts per 15-minute bin over similar historical time-bins. Similar time-bins were chosen based on the detection of the same active runway configuration as the simulated configuration in those time-bins. For example, for the 12:30-12:45 UTC bin, we identified all 12:30-12:45 UTC bins over a period of three months (May-July 2016). Out of these bins, we identified those bins during which CLT had a North-flow runway configuration active. These identified same-configuration bins were used to compute the 10-th and 90-th percentile runway takeoff counts.

As seen from the left-hand side of **Figure 50**, the simulated takeoff counts follow the general trend of the actual runway takeoff counts, with three departure banks clearly visible. The discrepancies between simulated versus actual counts at the beginning and end of the simulation time-period can be attributed to the fact that we only included flights that pushed back after 10:00 UTC and before 15:00 UTC in the simulation. By doing so, we missed some of the departure flights at either end of the simulation time-period.

The right-hand side of **Figure 50** shows similar plot for the simulated versus actual gate out counts. Again, we see that the simulation followed the general trend of the actual counts with discrepancies at the beginning and end of the simulation timeframe attributed to flights that were by design not included in the simulation set.

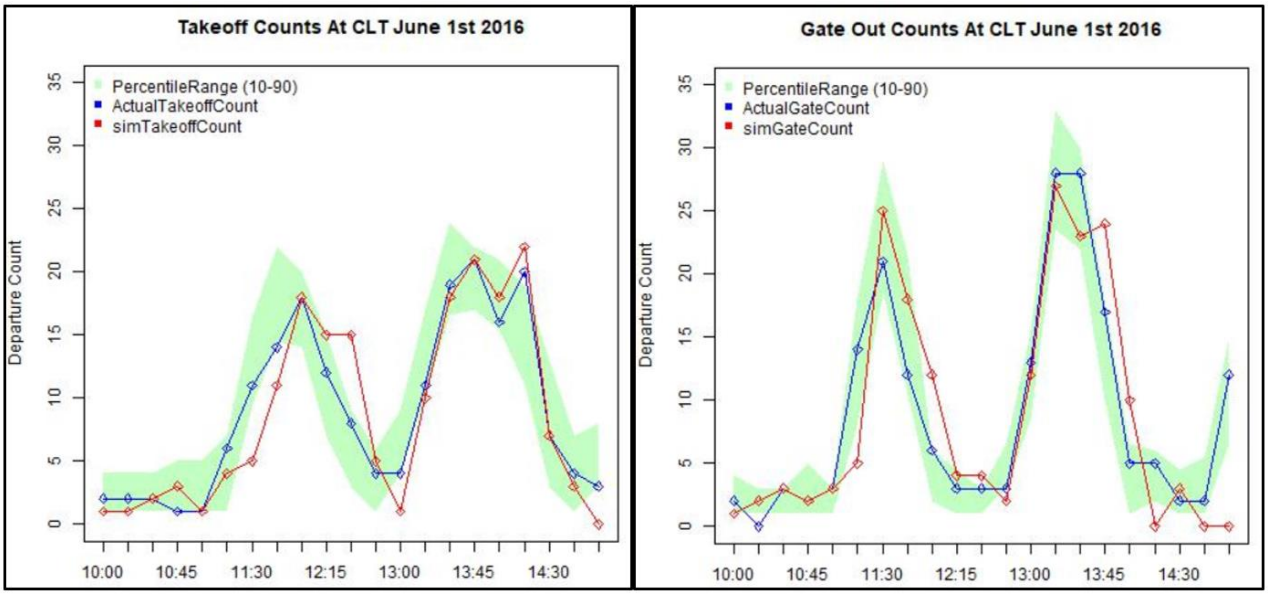

Figure 50. Runway Off and Gate Out Counts Validation – Simulation Versus Real Operations

Further, we also validated the taxi-out times by comparing simulated times against real historical operational taxi-out times from the same day as well as with a distribution of taxi-out times over

similar days. **Figure 51** shows the comparison of simulated and actual taxi-out times, with AMA taxi-out time comparison showed in the left half of the figure and the total (AMA + Ramp) taxi-out time comparison shown in the right half of the figure. As seen from the figures, the taxi-out times do not match very closely, but simulated taxi-out times follow the general trend of the actual observed simulated taxi-times with a couple of peaks visible in both simulated and actual data. The discrepancies at the beginning and end of the simulation timeframe can again be attributed to the fact that we had excluded flights outside the 10:00-15:00 UTC timeframe from the simulation by design, whereas in the actual operations they appear in the taxi-out time plots. The discrepancies between actual and simulated taxi-out times outside the beginning and ending time-bins can be attributed to multiple factors including, erroneous actual Gate OUT time data, differences in the handling of departure takeoff clearances between actual operations and simulation (human local controller clearances may contain additional delays due to the fact that the local controller is handling multiple arrival and departure clearances at the same time), and differences in simulated versus actual ramp and spot merge handling.

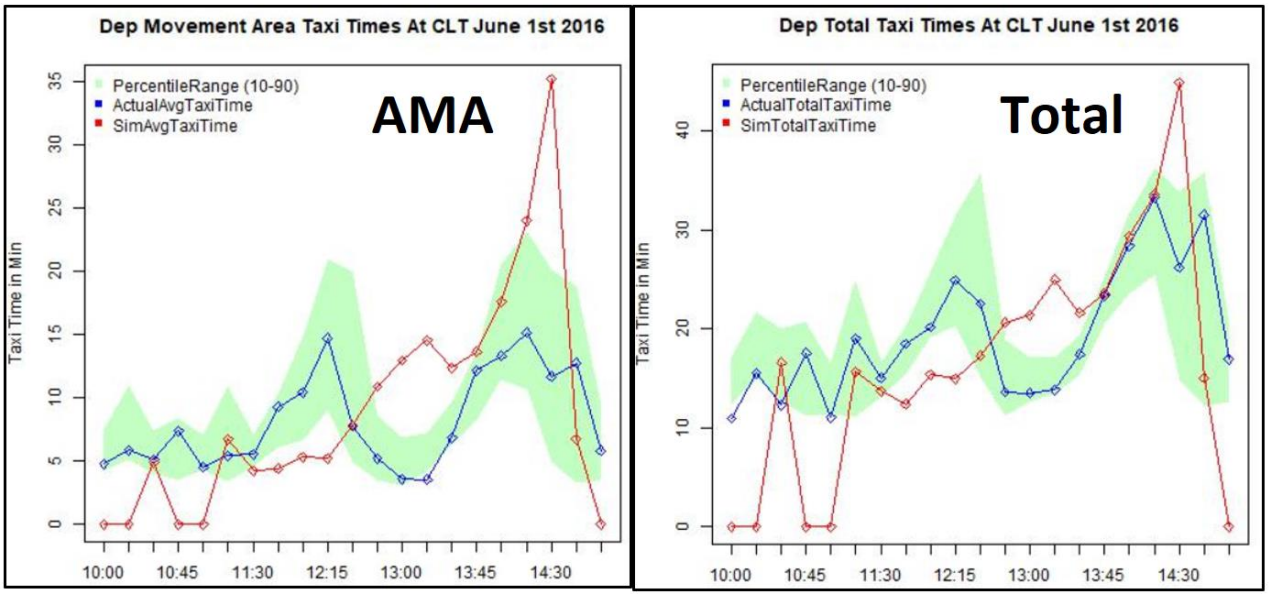

Figure 51. Taxi-Out Time Validation – Simulation Versus Real Operations

6.2.2.6. Analysis of Benefit Mechanism Contributions to ATD-2 Benefits

Analysis of simulation output data showed that three benefit mechanisms played a major role in providing taxi-out time savings. These were: (1) Demand throttling provided by Surface Departure Metering advisories (i.e., gate-holds); (2) Data exchange, especially more efficient and electronic coordination of APREQ restrictions; and (3) More predictable surface movements leading to better TMI compliance. We discuss each of these benefit mechanisms with supporting data analyses next.

Benefit Mechanism #1: Demand throttling provided by Surface Departure Metering advisories (i.e., gate-holds). As discussed above, our ATD-2 simulations included a full emulation of NASA's ATD-2 Tactical Surface Scheduler, which computed gate delays for departure flights in order to reduce taxi-out times but at the same time keeping sufficient pressure on the departure

runways. **Figure 52** shows that gate delay difference (i.e., ATD-2 simulation Gate OUT Time – Baseline simulation Gate OUT time) for each simulated departure flight. The right half of the figure shows a histogram of gate delay differences. We can see that the ATD-2 scheduler added a significant amount of gate delays over and above the baseline simulation. In the left half of the figure we show the gate delay difference plotted along the simulation timeline. This plot shows that the ATD-2 scheduler allocated majority of the gate delays during the time-periods when the departure demand on the CLT runways was at its peak, i.e., at or near the peaks of the two major departure banks included in the simulation. There are some gate delay difference points below the zero line in the plot on the left. These were flights that received higher gate delays in the baseline simulation because of active APREQs to their destination airports. Here also, we see that the ATD-2 scheduler handled these flights with smaller gate delays than in the baseline simulation. This was an effect of more efficient coordination with the receiving Center, which included sending more accurate runway takeoff time estimates to the Center, and after the Center sends back the controlled runway release time computing the required gate release time using a more accurate taxi-out time estimate. This benefit mechanism is discussed later. For the demand throttling benefit mechanism that we are discussing here, it would suffice to observe that the ATD-2 scheduler correctly allocated gate delays during the especially busy peak time-periods.

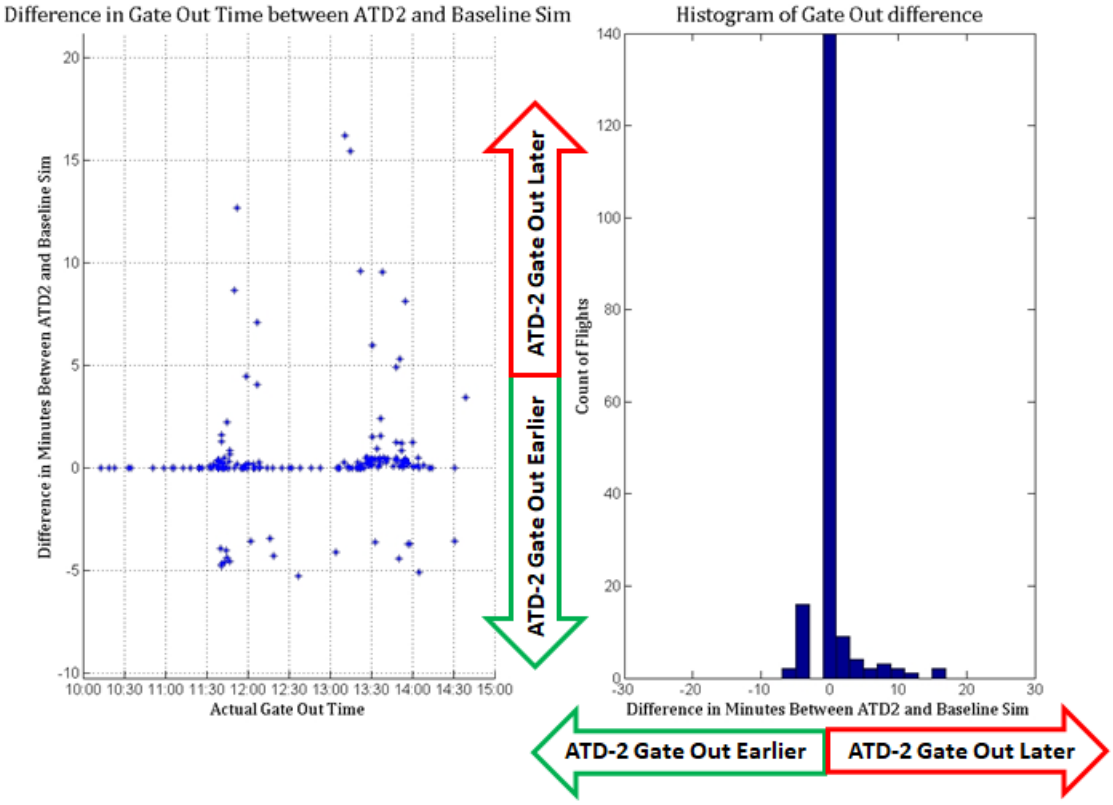

Figure 52. Gate Delay Difference, ATD-2 Operations – Baseline Operations

The beneficial effect that these tactical gate delays had on surface congestion can be seen in **Figure 53**. This figure plots the difference in Taxi-out Times (ATD-2 – Baseline) as a function of the difference in departure queue lengths experienced by the respective flights in the ATD-2 and Baseline simulations. As seen from the figure, ~55% of the flights experienced smaller departure

queue lengths, a result of the demand throttling provided by the tactical scheduler allocated gate delays and as a result experienced shorter taxi-out times. Moreover, an additional ~15% flights experienced slightly longer queues in the ATD-2 operations, but still managed to have smaller taxi-out times. In the case of these flights, although there were more flights ahead of them in the departure queue when they reached the spot, the runway takeoff times for those flights were sufficiently spaced out as a result of the gate delays and hence the flight was able to take off after spending a smaller time in taxi. Around 18% of the flights experienced longer queues than the baseline simulation and as a result experienced longer taxi-out times. Further around 12% flights experienced shorter queues, yet had longer taxi-out times. These longer taxi-out times are an indication that the ATD-2 scheduler settings in the simulations as well as in the field may need fine tuning. As discussed above, future efforts are necessary to assess different settings and algorithmic alternatives (e.g., taxi-out time prediction methods) in a fast-time simulation environment for optimizing the performance of the ATD-2 system in the field.

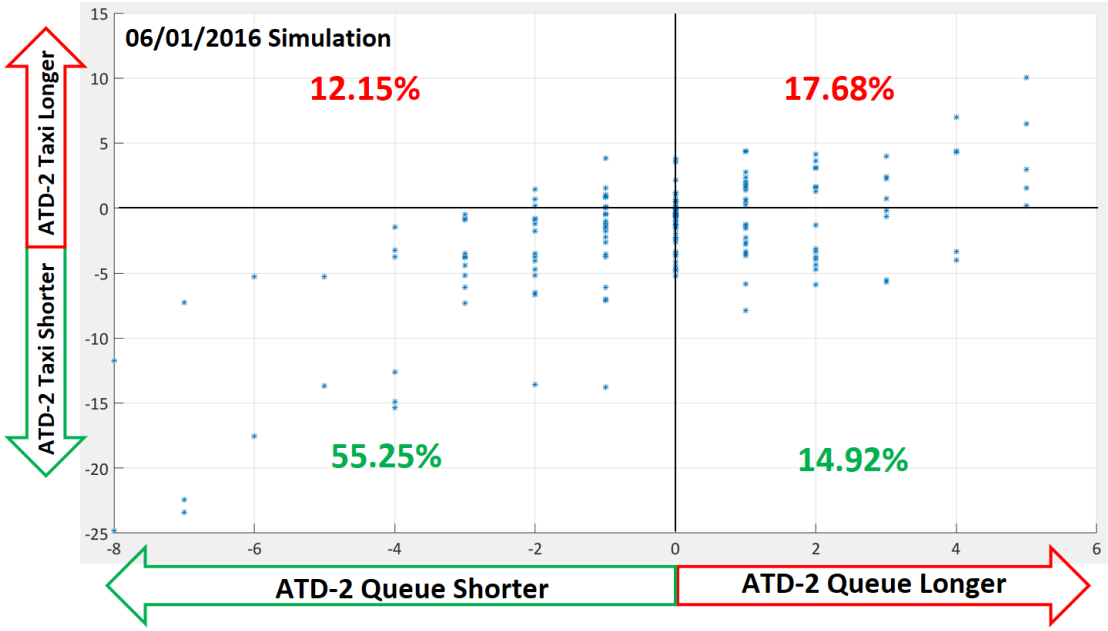

Figure 53. Taxi Out Time Difference (ATD-2 – Baseline) plotted as a function of Difference in Departure Queue Lengths Experienced by Flights at the Spot (ATD-2 – Baseline)

In summary, the demand throttling provided by ATD-2 Tactical Surface Scheduler-imposed gate delays contributed towards reducing the taxi-out times for departure flights in general. Next, we discuss another benefit mechanism, which we found especially beneficial for APREQ-impacted departure flights.

Benefit Mechanism # 2: Data exchange for APREQ Coordination. As discussed above, our simulation platform models the full data exchange process for APREQ flights including both, the current-day procedures as modeled in the baseline simulations and the ATD-2 electronic negotiation, accurate takeoff time estimate communication to the Center, and preferential scheduling modeled in the ATD-2 simulations. The effect of differences in handling the APREQ flights can be clearly seen in **Figure 54**. As seen from the figure, APREQ-impacted flights benefited the most from the ATD-2 system. We see a drop of around 4.5 minutes on an average in their taxi-out times and around 40% drop in their taxi-out time standard deviation, as compared to

the baseline simulation. These same statistics for all departure flights are a drop of 2 minutes on an average in the taxi-out times and a 25% drop in the standard deviation. Whereas, for non-APREQ flights the respective statistics are only a 1.6 minute taxi-out time drop on an average and only a 20% drop in the taxi-out time standard deviation. This clearly shows that the ATD-2 system handled the APREQ flights much more efficiently than the current-day procedures. Next, we will discuss an additional related benefit mechanism – higher TMI compliance.

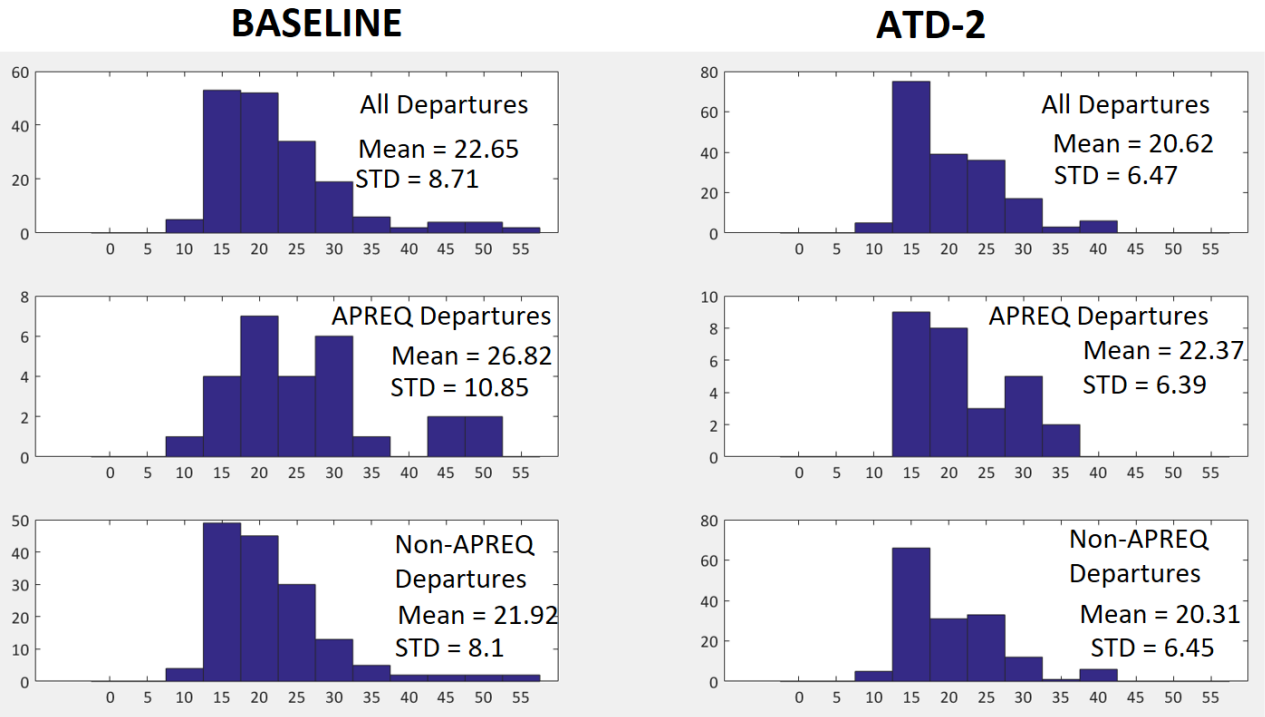

Figure 54. Taxi-Out Times (Mean and Variance) for All, APREQ and Non-APREQ flights for Baseline and ATD-2 Operations

Benefit Mechanism #3: Higher TMI Compliance. As a result of the modeled ATD-2 process for handling APREQ flights we saw only a slightly tighter compliance with APREQ runway release times for departure flights in our ATD-2 simulations as compared to the baseline simulations. **Figure 55** shows the counts of APREQ-impacted departure flights taking off within different timeframes as compared to their respective APREQ runway release time. In general, only one out of the 27 APREQ-impacted flights took off within the prescribed +2/-1 minute window in the ATD-2 simulation, with none departing in that window in the baseline simulation. Also, more flights departed within 15 minutes on either side of the APREQ runway release time in the ATD-2 simulation as compared to the baseline simulation.

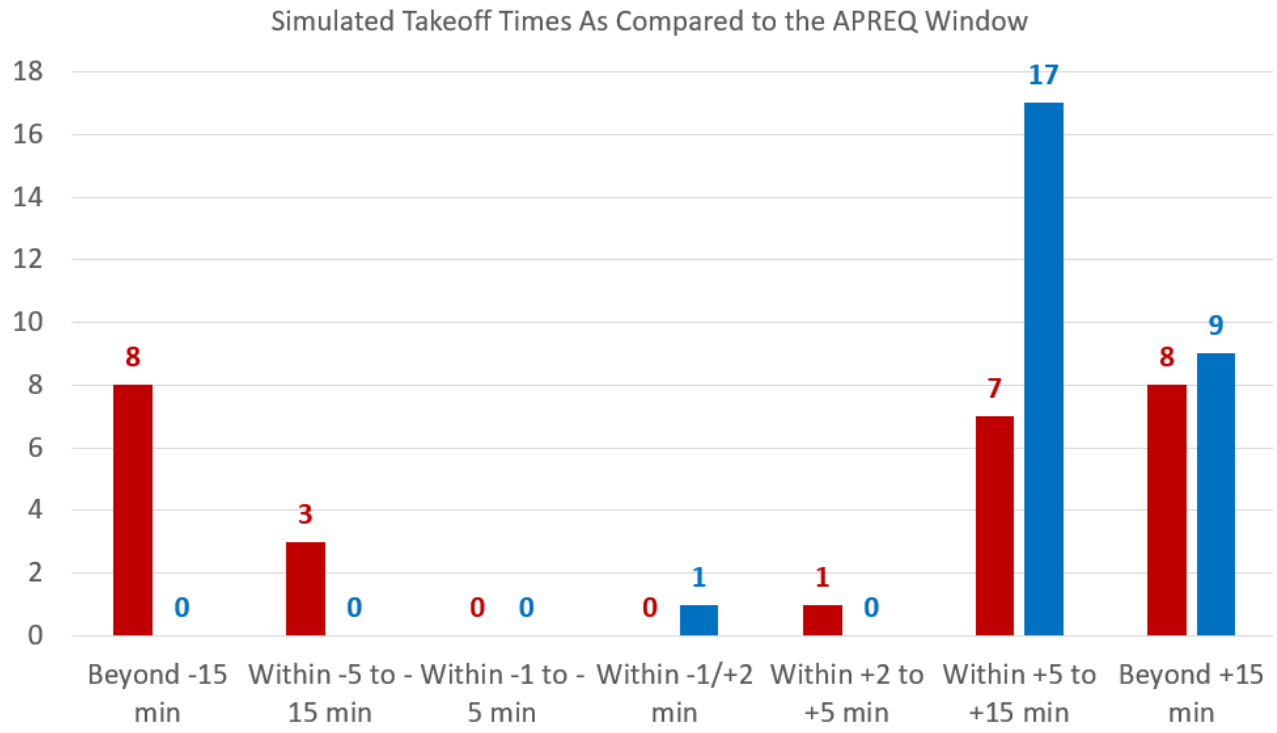

Figure 55. APREQ compliance for simulated baseline (red) and ATD-2 (blue) operations (computed over 27 APREQ-impacted flights)

6.3. DFW Simulations Details

6.3.1. DFW Simulation Day 1 Results (5/12/2016, East Flow)

The first DFW scenario we describe involved the simulation of DFW airport arrival and departure traffic on 05/12/2016 during the 1000-1700 UTC timeframe.

6.3.1.1. Simulation Scenario Description

DFW was under the East-flow runway configuration during the selected simulation time-period, with departures operating on runways 35L and 36R, and arrivals operating on runways 36L, 35R, 35C and 31R, as shown in **Figure 56**.

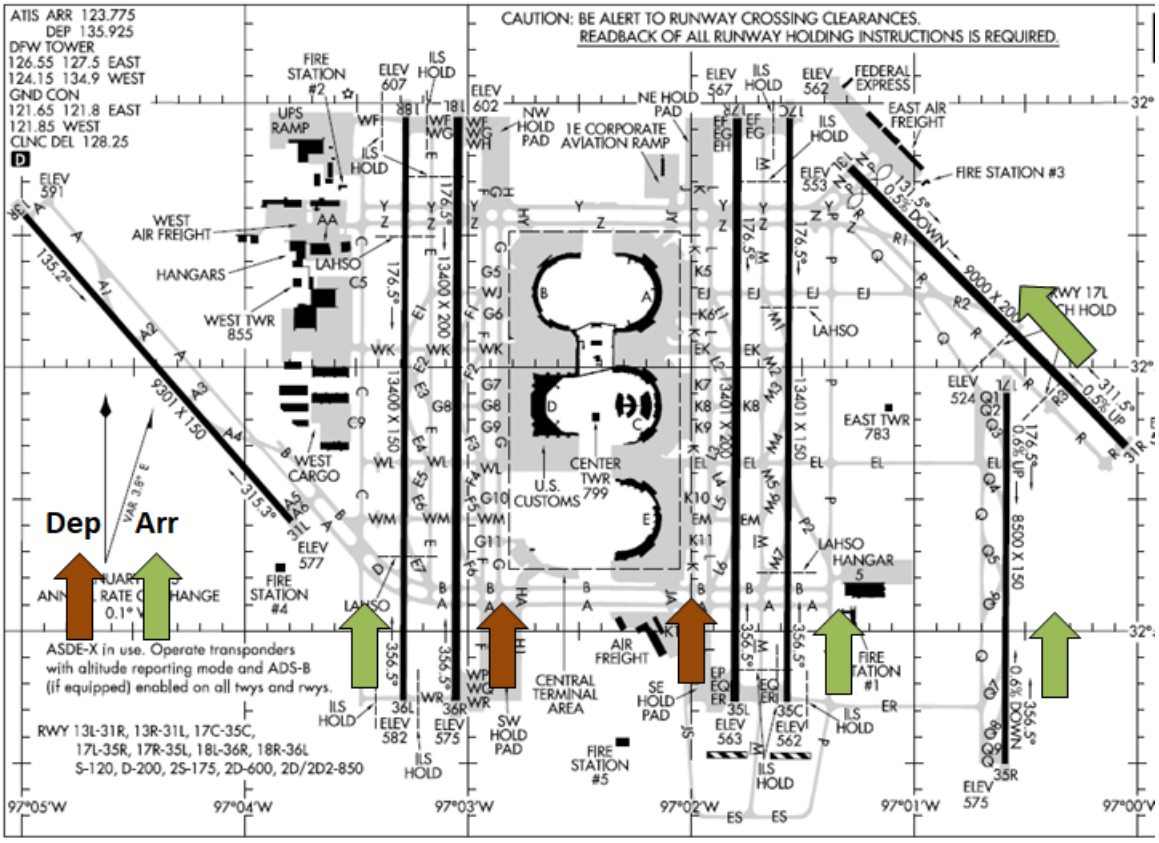

Figure 56. DFW East Flow Runway Configuration Runway Usage

The table below outlines the number of total departures and arrivals using the individual active runways during the simulated timeframe.

	36L	36R	35L	35C	35R	31R	Operation Counts by Type
Departures	0	138	165	0	0	0	303
Arrivals	125	0	0	131	45	5	306
Total Ops Per Runway	125	138	165	131	45	5	609

The simulations also emulated the implementation of surface traffic flow management initiatives such as APREQs, miles-in-trail restrictions and Ground Delay Programs as described in Section 4.2. In this particular scenario, we simulated the following traffic management initiatives that were active during the 1000-1700 UTC timeframe on the actual 05/12/2016 day.

TMI Type	TMI Requesting Facility	Providing Facility	TMI Start	TMI End	Departures to
MIT, 20	ZHU	ZFW	13:45	14:45	HOU
MIT, 10	ZFW	DFW	13:45	14:45	HOU, over Southern

					Departure Fixes

6.3.1.2. Benefits Results: Taxi-time Savings

Our simulation results for this scenario showed that the ATD-2 system saved around 8% of the total taxi-out time over all the departures, as shown in **Figure 57**. Slightly higher taxi-out time savings (percentage-wise), of 10% were seen in the AMA taxi-out times and lower (5%) savings in the ramp area taxi out times.

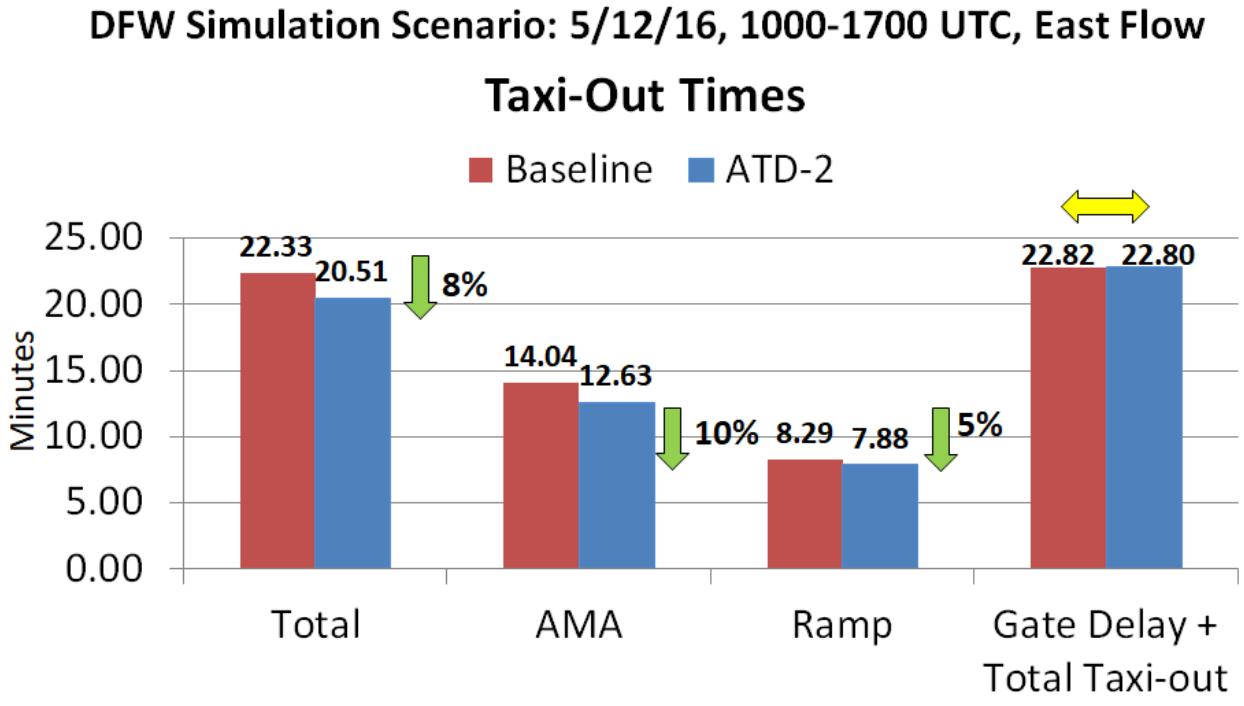

Figure 57. Taxi-Out Time Savings Benefits Estimated by Baseline VS ATD-2 Simulations for the 05/12/2016 1000-1700 UTC simulation scenario

Further, we also computed the total transit time for each departure consisting of the excess time spent at the gate in the ATD-2 simulation (i.e., ATD-2 system imposed gate delay) and the taxi transit from gate pushback to runway takeoff. This total transit time metric is the fourth pair of bars shown in **Figure 57**. As seen from the figure, with the ATD-2 system there is no change in the total transit time metric on an average.

We also analyzed the impact of ATD-2 departure metering on arrival taxi-in times. **Figure 58** shows that with the ATD-2 system operating there was a slight increase in the taxi-in times. However, this negative impact on arrival taxi-in times motivates the need for fine tuning of the ATD-2 scheduling algorithm as tailored to the DFW airport. More specifically, DFW consists of two pairs of parallel runways with the inboard runway used for departures and outboard runway for arrivals. There is a dependency between landings on the outboard runway and takeoffs in the inboard runway, and there needs to be more analysis for fine tuning how the ATD-2 scheduler handles minimum separations to model this dependency.

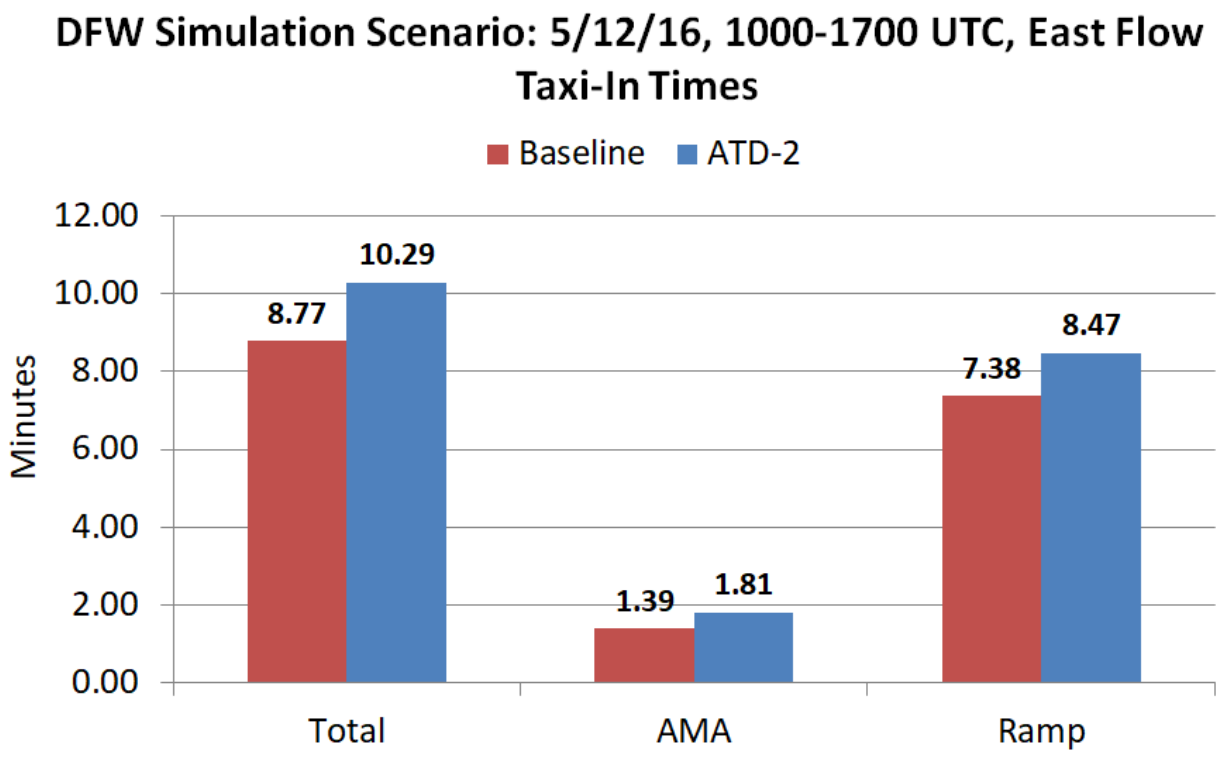

Figure 58. Taxi-In Time Savings Benefits Estimated by Baseline VS ATD-2 Simulations for the 05/12/2016 1000-1700 UTC simulation scenario

6.3.1.3. Analysis of On-Time Performance for Departure Flights

We analyzed the runway takeoff time difference for each departure flight between the baseline simulation (current-day procedures) and the ATD-2 simulation (departure metering procedures). **Figure 59** shows the results of this analysis. The right half of this figure shows a histogram of runway takeoff time differences per flight (ATD-2 simulation takeoff time – Baseline simulation takeoff time). As seen from the figure, a big majority of the flights (~60%) took off either at the same time or earlier in the ATD-2 operations, whereas 40% of the flights took off later as compared to the baseline simulation. Moreover, out of the 40% flights departing late in the ATD-2 simulation, around one third of them departed less than 2 minutes late than their counterpart departure in the ATD-2 simulation.

This demonstrates that the ATD-2 system had a slightly positive impact on the On time performance of the airport, in general, but there were some flights that took off later than their baseline runway takeoff time. In general, if bringing the number of flights that takeoff later than baseline down (closer to zero) is of high importance to the airlines, then there are tools/settings available in the ATD-2 system, which can be modified to reduce the negative impact on certain flights. These tools/ settings include the optimal selection of the ATD-2 Tactical Surface Scheduler's taxi delay buffer parameter as well as modifications to how the ATD-2 Scheduler estimates earliest runway usage times for departure flights for scheduling purposes as well as how it back-computes gate delays from the target runway takeoff times. But, before making these

changes in the operational ATD-2 system, more simulation-based sensitivity tests are required to assess multiple alternatives and select the best.

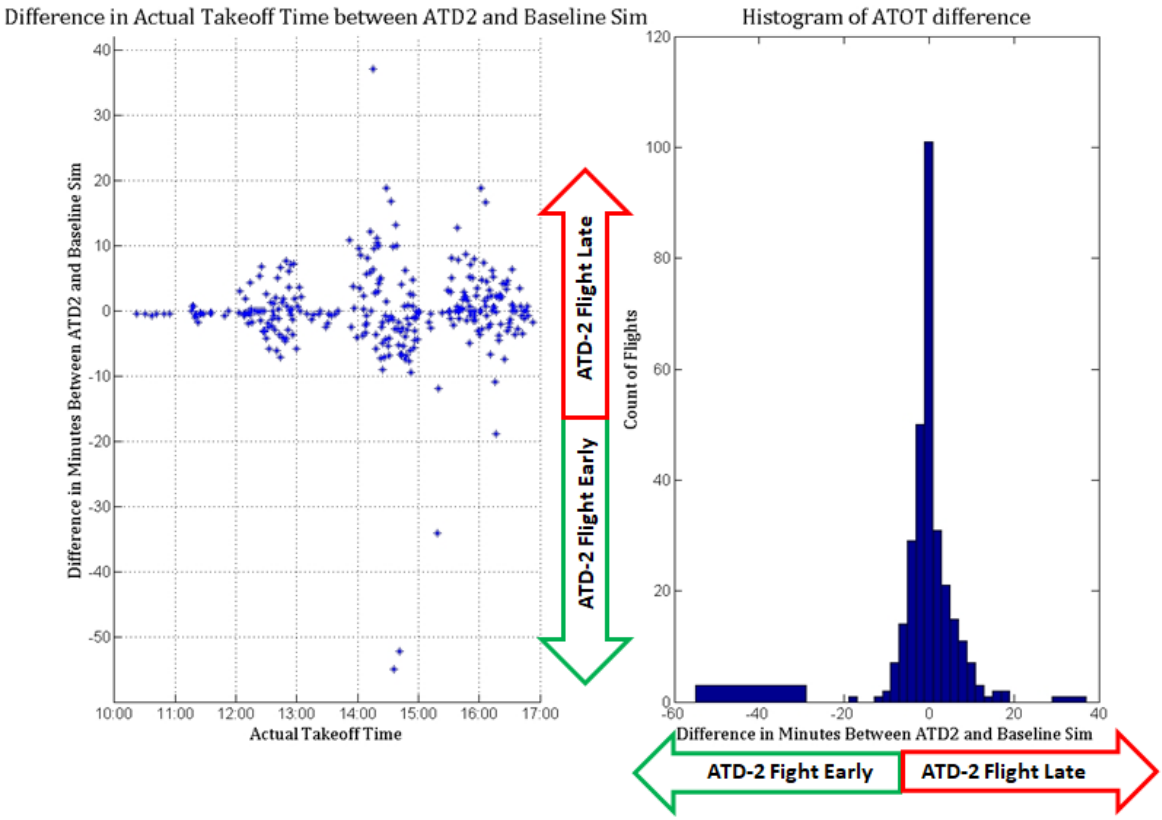

Figure 59. Analysis of On-Time Runway Takeoff Performance – Baseline VS ATD-2

6.3.1.4. Analysis of ATD-2's Impact on Airport Departure Throughput

Our simulation results show that the ATD-2 system did not have a major negative or positive impact on the overall airport throughput. **Figure 60** shows the cumulative airport throughput (i.e., the number of departures that have taken of at time 't') throughout the simulation timeframe. As seen from the figure, the baseline cumulative airport throughput line (red dashed line) falls either on or below the ATD-2 cumulative airport throughput line (blue solid line) for most of the simulation timeframe, with only a few places where it goes above the blue line by 1-2 departure aircraft. This demonstrates that the ATD-2 system does not have a major negative impact on the airport's throughput despite prescribing gate holds.

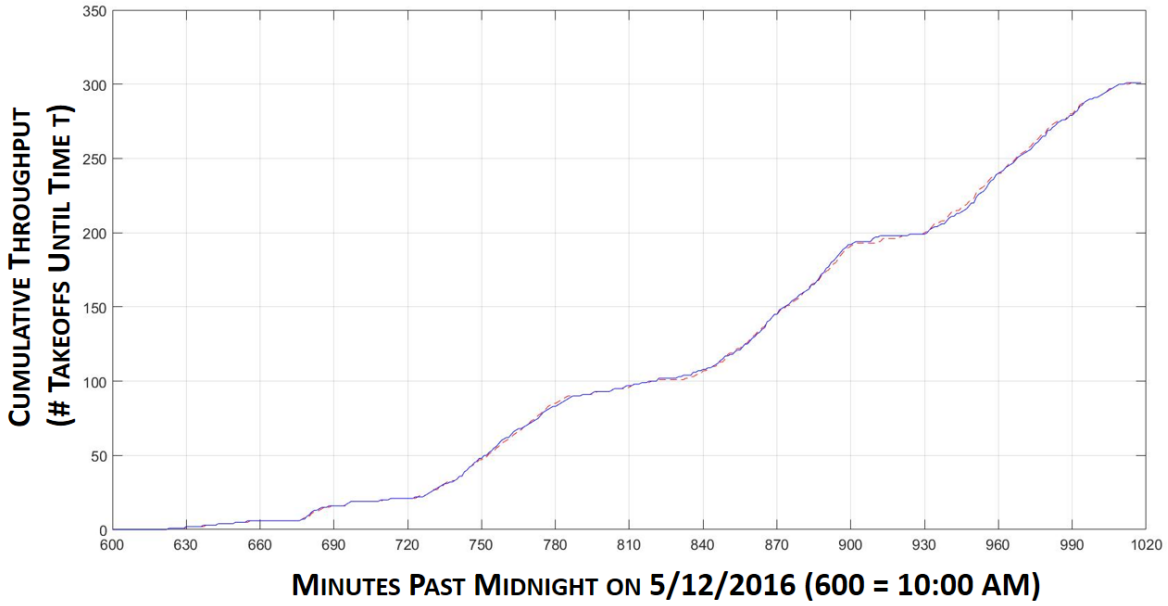

Figure 60. Cumulative airport throughput (baseline sim: red dashed line; ATD-2 sim: blue solid line) shows very little impact of ATD-2 gate holds on departure throughput

Figure 61 shows the cumulative departure throughputs separately for the two active departure runways (35L and 36R), again demonstrating that the ATD-2 system had very little impact on the individual runway throughputs.

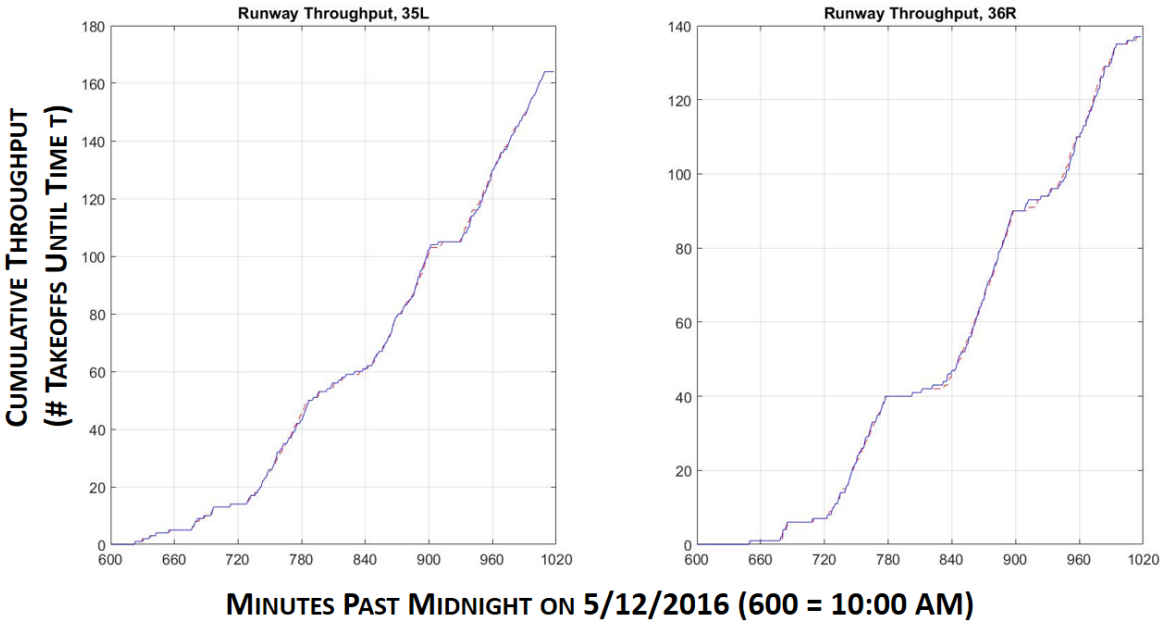

Figure 61. Cumulative airport throughput in the baseline simulation (red dashed line) and the ATD-2 simulation (blue solid line) shown for two departure runways separately

6.3.1.5. Simulation Validation

This section presents results from comparing simulation outputs with operational metrics from real operational data on the same historical day, as well as with a distribution of the same operational metrics computed over a set of similar days over a period of three months. The left-hand side of **Figure 62** shows the comparison of takeoff counts per 15-minute bin over the duration of the simulation, with the simulated counts shown by the red line, the actual counts on the day of operations shown by the blue line, and a region covering the 10-th to 90-th percentile takeoff counts per 15-minute bin over similar historical time-bins. Similar time-bins were chosen based on the detection of the same active runway configuration as the simulated configuration in those time-bins. For example, for the 16:30-16:45 UTC bin, we identified all 16:30-16:45 UTC bins over a period of three months (May-July 2016). Out of these bins, we identified those bins during which DFW had an East-flow runway configuration active. These identified same-configuration bins were used to compute the 10-th and 90-th percentile runway takeoff counts.

As seen from the left-hand side of **Figure 62**, the simulated takeoff counts follow the general trend of the actual runway takeoff counts, with three departure banks clearly visible. The discrepancies between simulated versus actual counts at the beginning and end of the simulation time-period can be attributed to the fact that we only included flights that pushed back after 10:00 UTC and before 17:00 UTC in the simulation. By doing so, we missed some of the departure flights at either end of the simulation time-period.

The right-hand side of **Figure 62** shows similar plot for the simulated versus actual gate out counts. Again, we see that the simulation followed the general trend of the actual counts with discrepancies at the beginning and end of the simulation timeframe attributed to flights that were by design not included in the simulation set.

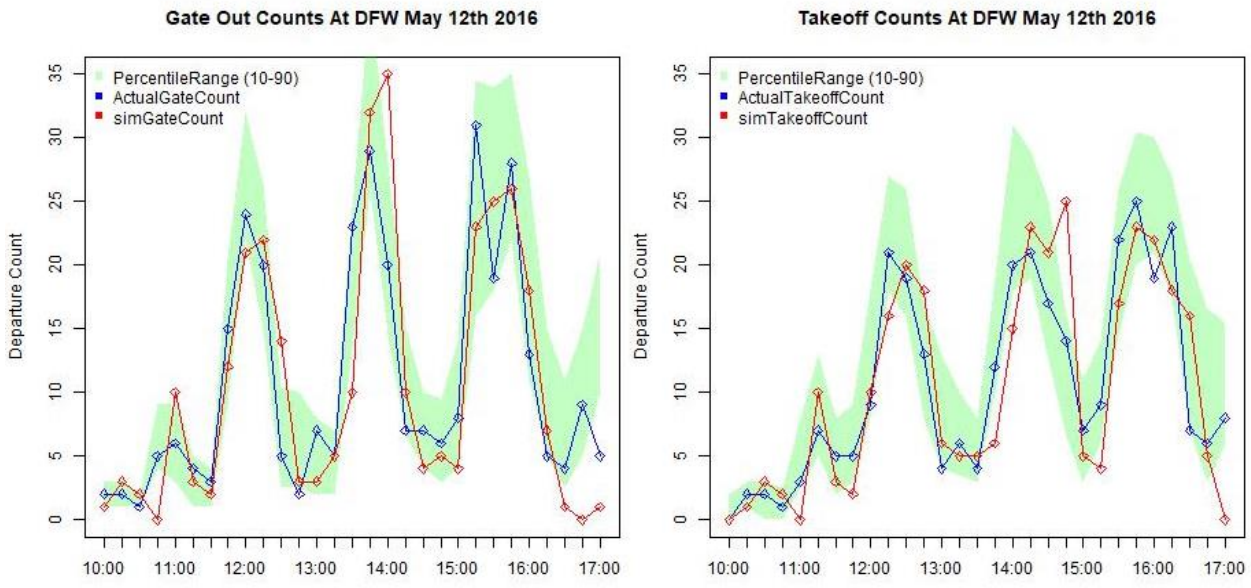

Figure 62. Runway Off and Gate Out Counts Validation – Simulation Versus Real Operations

Further, we also validated the taxi-out times by comparing simulated times against real historical operational taxi-out times from the same day as well as with a distribution of taxi-out times over

similar days. **Figure 63** shows the comparison of simulated and actual taxi-out times, with AMA taxi-out time comparison showed in the left half of the figure and the total (AMA + Ramp) taxi-out time comparison shown in the right half of the figure. As seen from the figures, the taxi-out times do not match very closely, but simulated taxi-out times follow the general trend of the actual observed simulated taxi-times with a couple of peaks visible in both simulated and actual data. The discrepancies at the beginning and end of the simulation timeframe can again be attributed to the fact that we had excluded flights outside the 10:00-17:00 UTC timeframe from the simulation by design, whereas in the actual operations they appear in the taxi-out time plots. The discrepancies between actual and simulated taxi-out times outside the beginning and ending time-bins can be attributed to multiple factors including, erroneous actual Gate OUT time data, differences in the handling of departure takeoff clearances between actual operations and simulation (human local controller clearances may contain additional delays due to the fact that the local controller is handling multiple arrival and departure clearances at the same time), and differences in simulated versus actual ramp and spot merge handling.

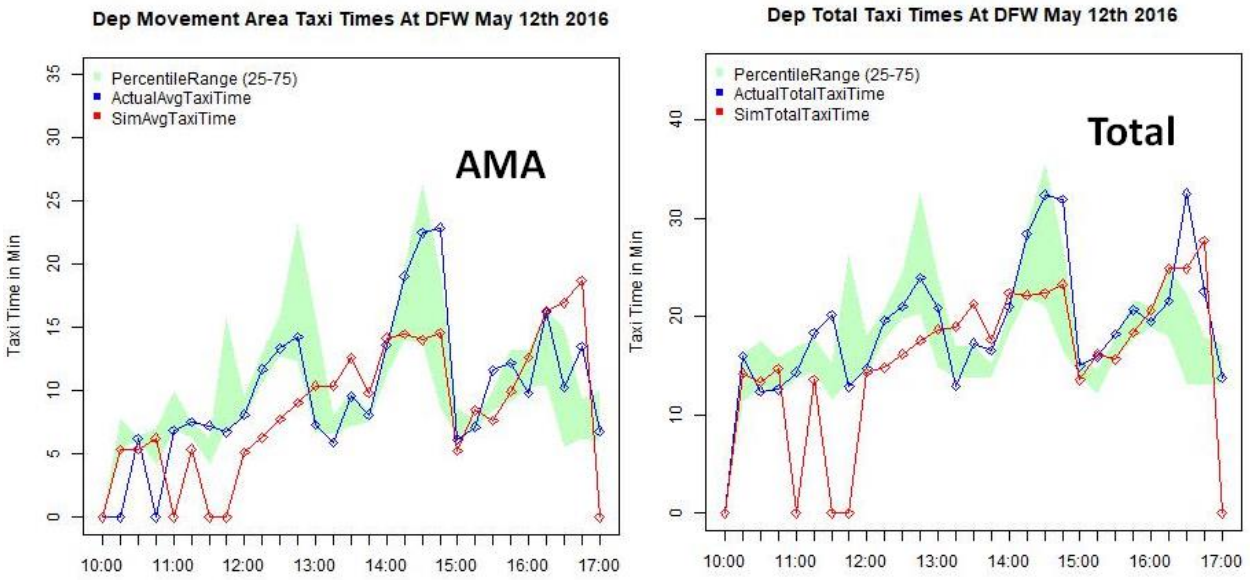

Figure 63. Taxi-Out Time Validation – Simulation Versus Real Operations

6.3.1.6. Analysis of Benefit Mechanism Contributions to ATD-2 Benefits

Analysis of simulation output data showed that two benefit mechanisms played a major role in providing taxi-out time savings. These were: (1) Demand throttling provided by Surface Departure Metering advisories (i.e., gate-holds) and (2) Data exchange and scheduling for TMI Coordination. We discuss each of these benefit mechanisms with supporting data analyses next.

Benefit Mechanism #1: Demand throttling provided by Surface Departure Metering advisories (i.e., gate-holds). As discussed above, our ATD-2 simulations included a full emulation of NASA's ATD-2 Tactical Surface Scheduler, which computed gate delays for departure flights in order to reduce taxi-out times but at the same time keeping sufficient pressure on the departure runways. **Figure 64** shows that gate delay difference (i.e., ATD-2 simulation Gate OUT Time – Baseline simulation Gate OUT time) for each simulated departure flight. The right half of the

figure shows a histogram of gate delay differences. We can see that the ATD-2 scheduler added a significant amount of gate delays over and above the baseline simulation. In the left half of the figure we show the gate delay difference plotted along the simulation timeline. This plot shows that the ATD-2 scheduler allocated majority of the gate delays during the time-periods when the departure demand on the DFW runways was at its peak, i.e., at or near the peaks of the three major departure banks included in the simulation. There are some gate delay difference points below the zero line in the plot on the left. These were flights that received higher gate delays in the baseline simulation because of active MITs to their destination airports. Here also, we see that the ATD-2 scheduler handled these flights with smaller gate delays than in the baseline simulation. This was an effect of more efficient coordination with the receiving Center, which included sending more accurate runway takeoff time estimates to the Center, and after the Center sends back the controlled runway release time computing the required gate release time using a more accurate taxi-out time estimate. This benefit mechanism is discussed later. For the demand throttling benefit mechanism that we are discussing here, it would suffice to observe that the ATD-2 scheduler correctly allocated gate delays during the especially busy peak time-periods.

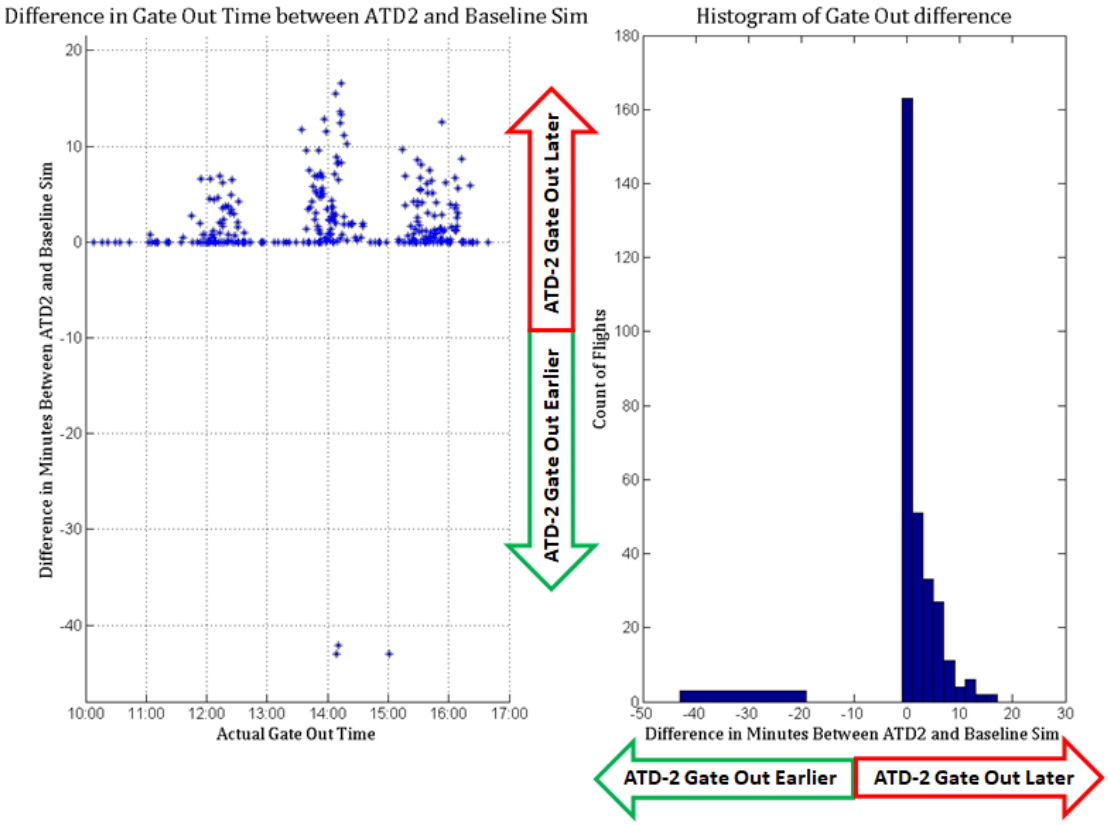

Figure 64. Gate Delay Difference, ATD-2 Operations – Baseline Operations

The beneficial effect that these tactical gate delays had on surface congestion can be seen in **Figure 65**. This figure plots the difference in Taxi-out Times (ATD-2 – Baseline) as a function of the difference in departure queue lengths experienced by the respective flights in the ATD-2 and Baseline simulations. As seen from the figure, ~56% of the flights experienced smaller departure queue lengths, a result of the demand throttling provided by the tactical scheduler allocated gate delays and as a result experienced shorter taxi-out times. Moreover, an additional ~20% flights

experienced slightly longer queues in the ATD-2 operations, but still managed to have smaller taxi-out times. In the case of these flights, although there were more flights ahead of them in the departure queue when they reached the spot, the runway takeoff times for those flights were sufficiently spaced out as a result of the gate delays and hence the flight was able to take off after spending a smaller time in taxi. Around 6% of the flights experienced longer queues than the baseline simulation and as a result experienced longer taxi-out times, which is an indication that the ATD-2 scheduler settings may need fine tuning.

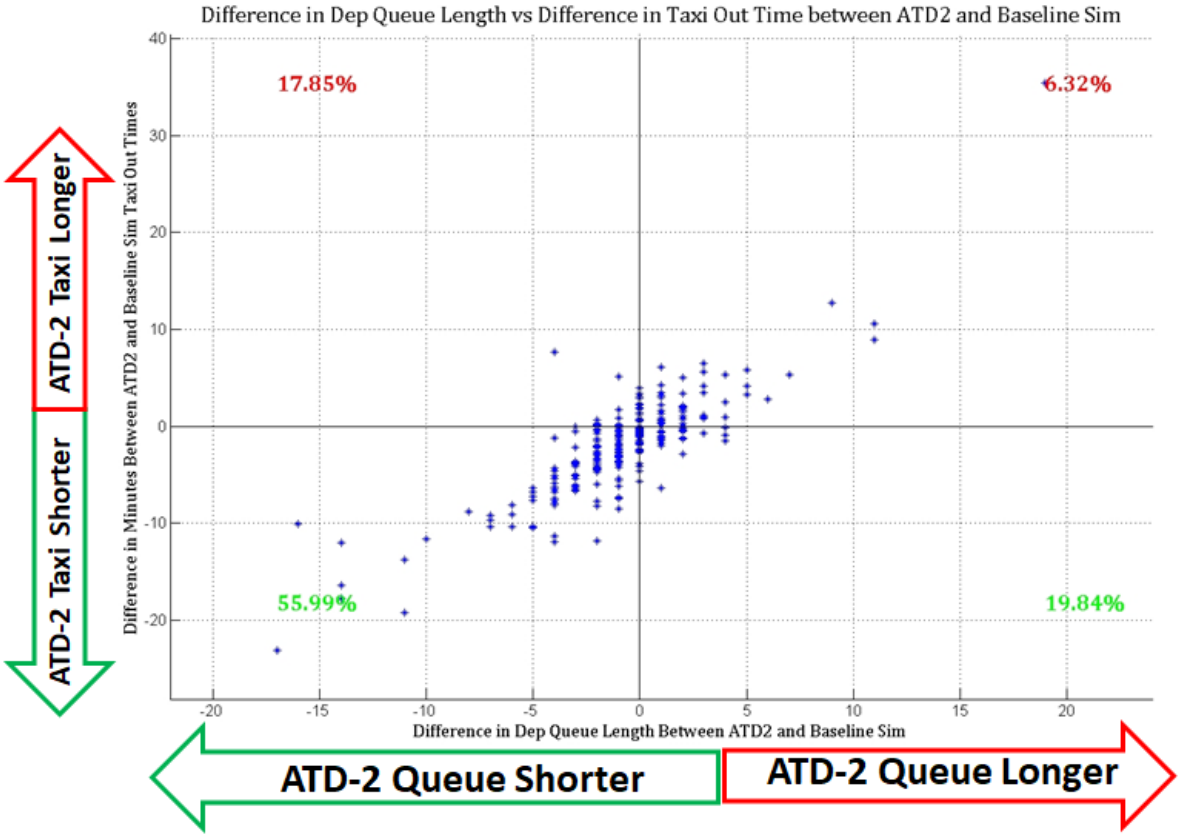

Figure 65. Taxi Out Time Difference (ATD-2 – Baseline) plotted as a function of Difference in Departure Queue Lengths Experienced by Flights at the Spot (ATD-2 – Baseline)

In summary, the demand throttling provided by ATD-2 Tactical Surface Scheduler-imposed gate delays contributed towards reducing the taxi-out times for departure flights in general. Next, we discuss another benefit mechanism, which we found especially beneficial for TMI-impacted departure flights.

Benefit Mechanism # 2: Data exchange and scheduling for TMI Coordination. Our simulation platform models the full data exchange and scheduling process for APREQ, EDCT, and MIT-impacted flights. The effect of differences in handling these TMI-impacted flights can be clearly seen in **Figure 66**. TMIs active in the case of DFW simulations included MIT restrictions on departure-fixes as well as EDCTs on flights going to impacted destinations (see the Table of TMIs in Section 6.3.1.1). As seen from **Figure 66**, TMI-impacted flights benefited about the same amount as other flights from the ATD-2 system on this day. We see a drop of around 1.8 minutes on an average in their taxi-out times. In terms of predictability of taxi out times, we see a ~9%

drop in taxi-out time standard deviation over all flights, as compared to the baseline simulation, but only a 2% drop for TMI-impacted flights. This shows that the ATD-2 system handled the TMI-impacted flights more efficiently than the current-day procedures, but was not able to increase the predictability of taxi out times for TMI-impacted flights.

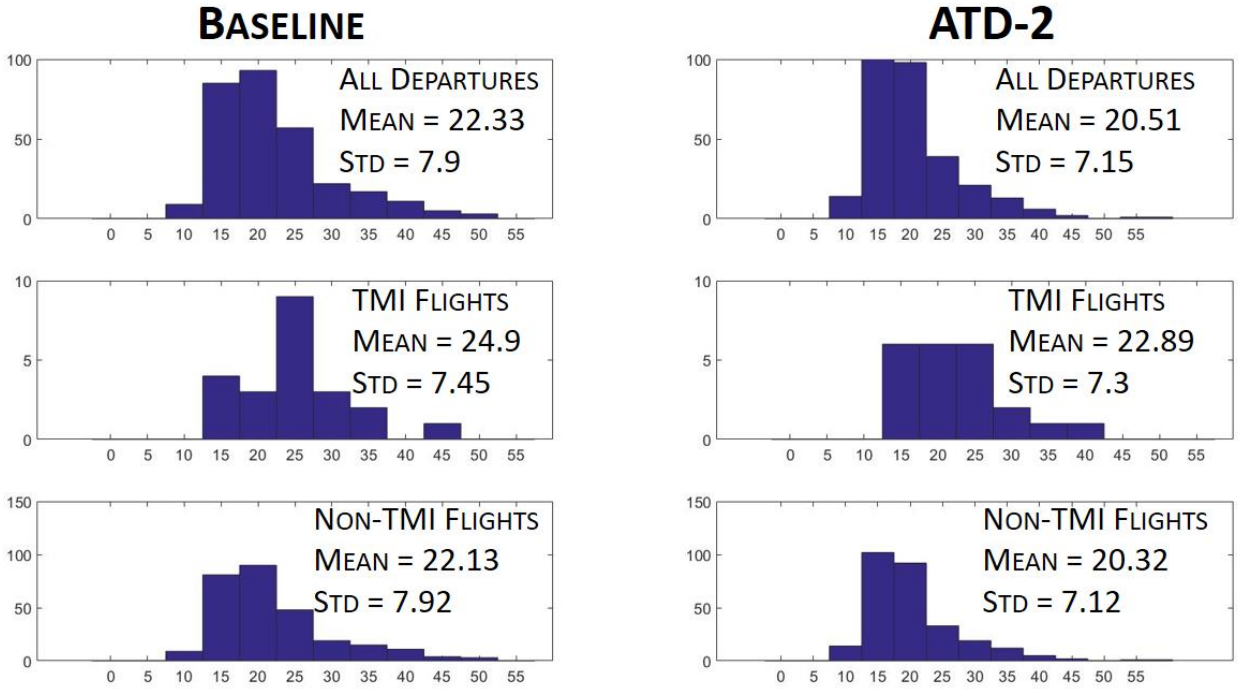

Figure 66. Taxi-Out Times (Mean and Variance) for All, TMI-Impacted and Non-TMI-Impacted flights for Baseline and ATD-2 Operations

6.3.2. DFW Simulation Day 2 Results (6/3/2016, West Flow)

The second DFW scenario we describe involved the simulation of DFW airport arrival and departure traffic on 06/03/2016 during the 1500-2100 UTC timeframe.

6.3.2.1. Simulation Scenario Description

DFW was under the West-flow runway configuration during the selected simulation time-period, with departures operating on runways 18L, 17R and 13L, and arrivals operating on runways 17L, 18R, 17C and 13R, as shown in **Figure 67**.

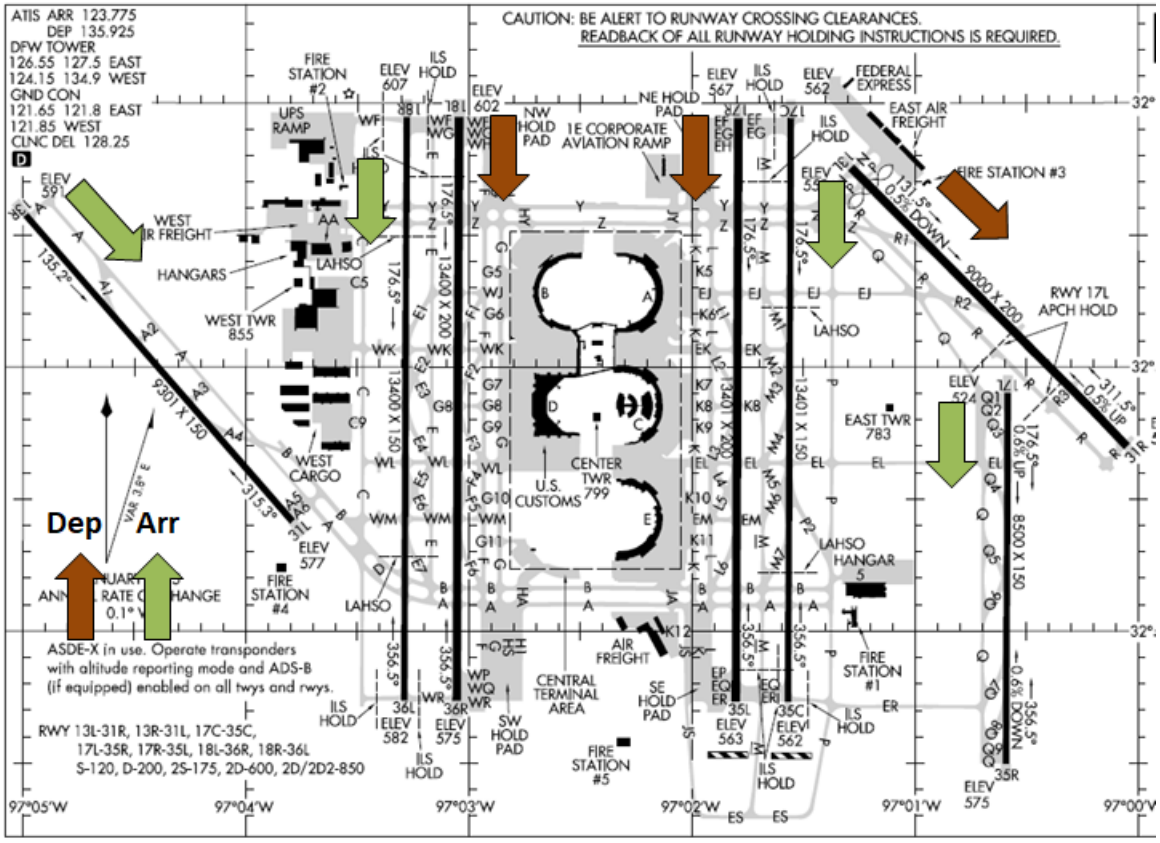

Figure 67. DFW West Flow Runway Configuration Runway Usage

The table below outlines the number of total departures and arrivals using the individual active runways during the simulated timeframe.

	18L	18R	17L	17C	17R	13L	13R	Operation Counts by Type
Departures	174	0	0	0	206	2	0	382
Arrivals	0	135	49	138	0	0	3	325
Total Ops Per Runway	174	135	49	138	206	2	3	707

The simulations also emulated the implementation of surface traffic flow management initiatives such as APREQs, miles-in-trail restrictions and Ground Delay Programs as described in Section 4.2. In this particular scenario, we simulated the following traffic management initiatives that were active during the 1500-2100 UTC timeframe on the actual 06/03/2016 day.

TMI Type/ Size	TMI Requesting Facility	Providing Facility	TMI Start	TMI End	Departures to
MIT, 15	ZHU	ZFW	18:00	23:59	IAH/HOU

MIT, 8	ZFW	DFW	18:00	23:59	IAH/HOU, via Southern Departure Fixes
MIT, 25	ZME	ZFW	19:00	20:15	ORD
MIT, 10	ZFW	DFW	19:00	20:15	ORD, on Northern Departure Fixes

6.3.2.2. Benefits Results: Taxi-time Savings

Our simulation results for this scenario showed that the ATD-2 system saved around 8% of the total taxi-out time over all the departures, as shown in **Figure 68**. Similar taxi-out time savings (percentage-wise) were seen in the active movement area (AMA) taxi-out times as well as the ramp taxi times.

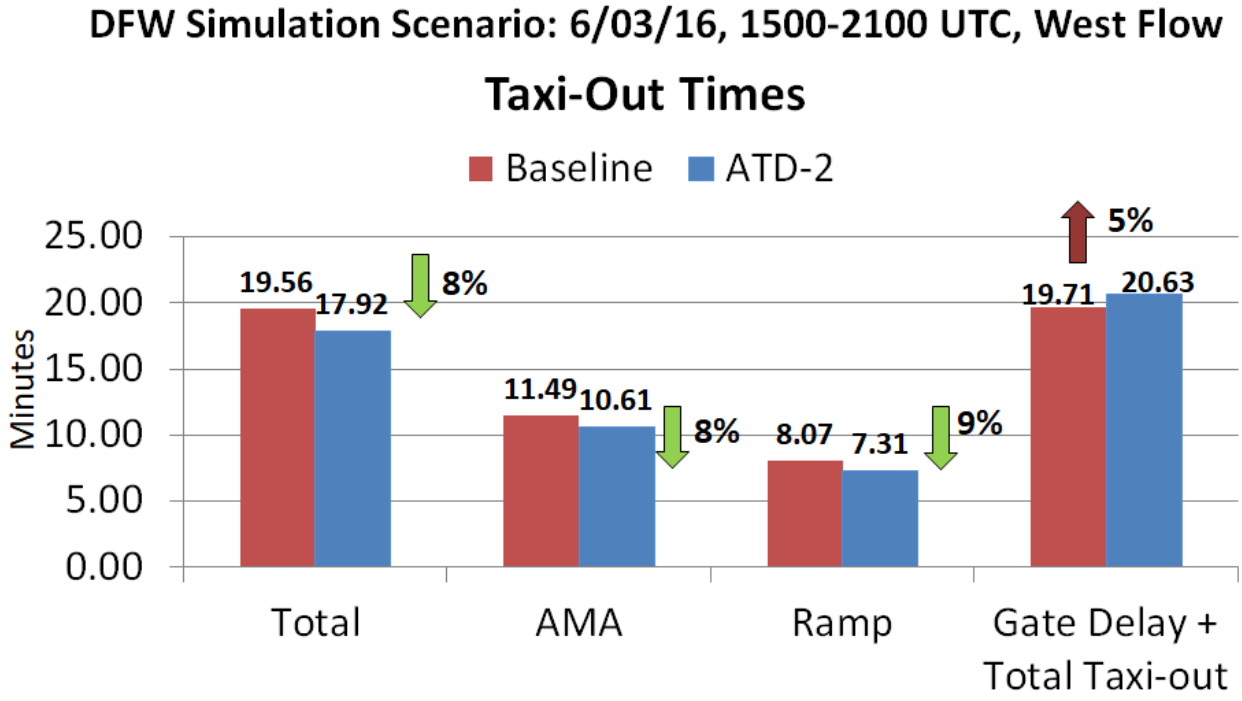

Figure 68. Taxi-Out Time Savings Benefits Estimated by Baseline VS ATD-2 Simulations for the 06/03/2016 1500-2100 UTC simulation scenario

Further, we also computed the total transit time for each departure consisting of the excess time spent at the gate in the ATD-2 simulation (i.e., ATD-2 system imposed gate delay) and the taxi transit from gate pushback to runway takeoff. This total transit time metric is the fourth pair of bars shown in **Figure 68**. As seen from the figure, with the ATD-2 system there is a 5% increase in the total transit time metric on an average for this simulation day. This points to the need for further fine tuning of the ATD-2 scheduling algorithm as tailored to DFW scheduling constraints.

We also analyzed the impact of ATD-2 departure metering on arrival taxi-in times. **Figure 69** shows that with the ATD-2 system operating there was a slight increase in the taxi-in times. Again, this warrants further simulation based sensitivity analysis to assess fine tuning changes to the ATD-2 scheduling algorithm for fitting it to DFW constraints.

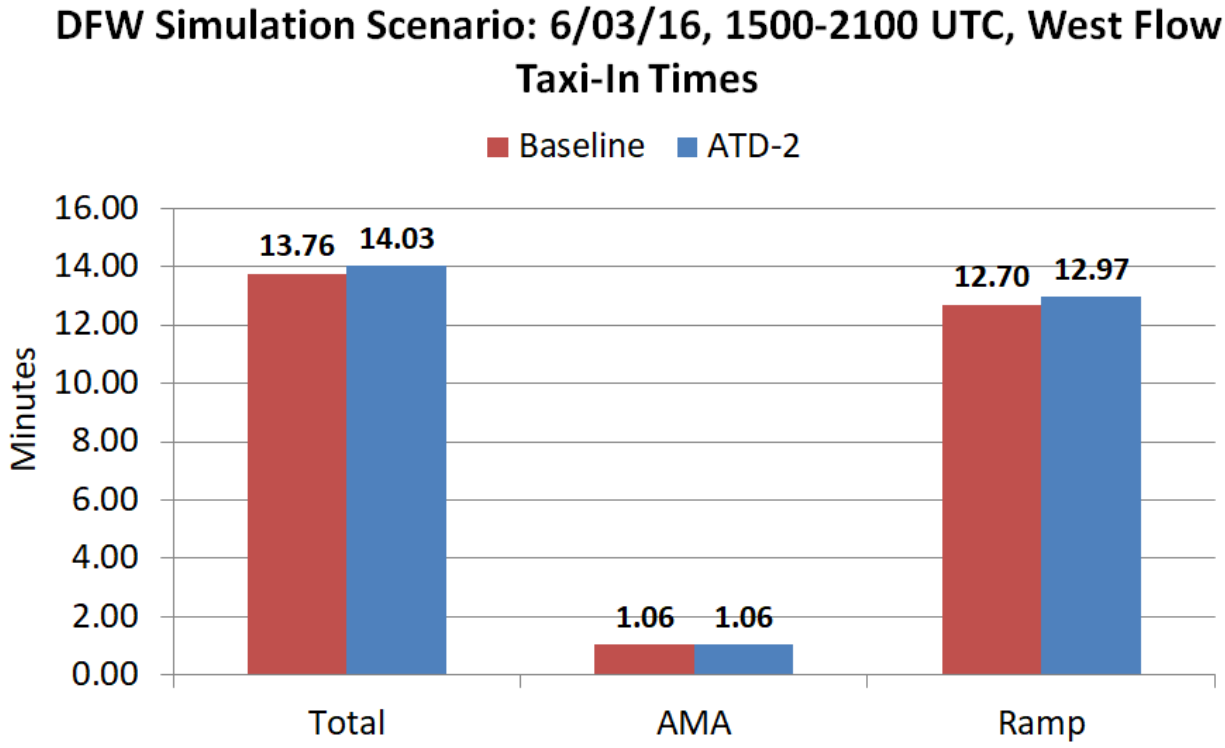

Figure 69. Taxi-In Time Savings Benefits Estimated by Baseline VS ATD-2 Simulations for the 06/03/2016 1500-2100 UTC simulation scenario

6.3.2.3. Analysis of On-Time Performance for Departure Flights

An important consideration for user-acceptance of the ATD-2 system is the question of what impact do the ATD-2 gate delays have on the overall On time performance of the airport in terms of late or early runway takeoff times. In relation to this aspect, we analyzed the runway takeoff time difference for each departure flight between the baseline simulation (current-day procedures) and the ATD-2 simulation (departure metering procedures). **Figure 70** shows the results of this analysis. The right half of this figure shows a histogram of runway takeoff time differences per flight (ATD-2 simulation takeoff time – Baseline simulation takeoff time). As seen from the figure, a big majority of the flights (~60%) took off either at the same time or earlier in the ATD-2 operations, whereas 40% of the flights took off later as compared to the baseline simulation. However, as seen from the figure there were a lot of highly delayed departures in the DFW ATD-2 simulation as compared to the baseline simulation. As mentioned above, this warrants further simulation based analysis to assess fine tuning changes to the ATD-2 algorithm in order to reduce the negative impacts of ATD-2 scheduling on the on time performance of the airport.

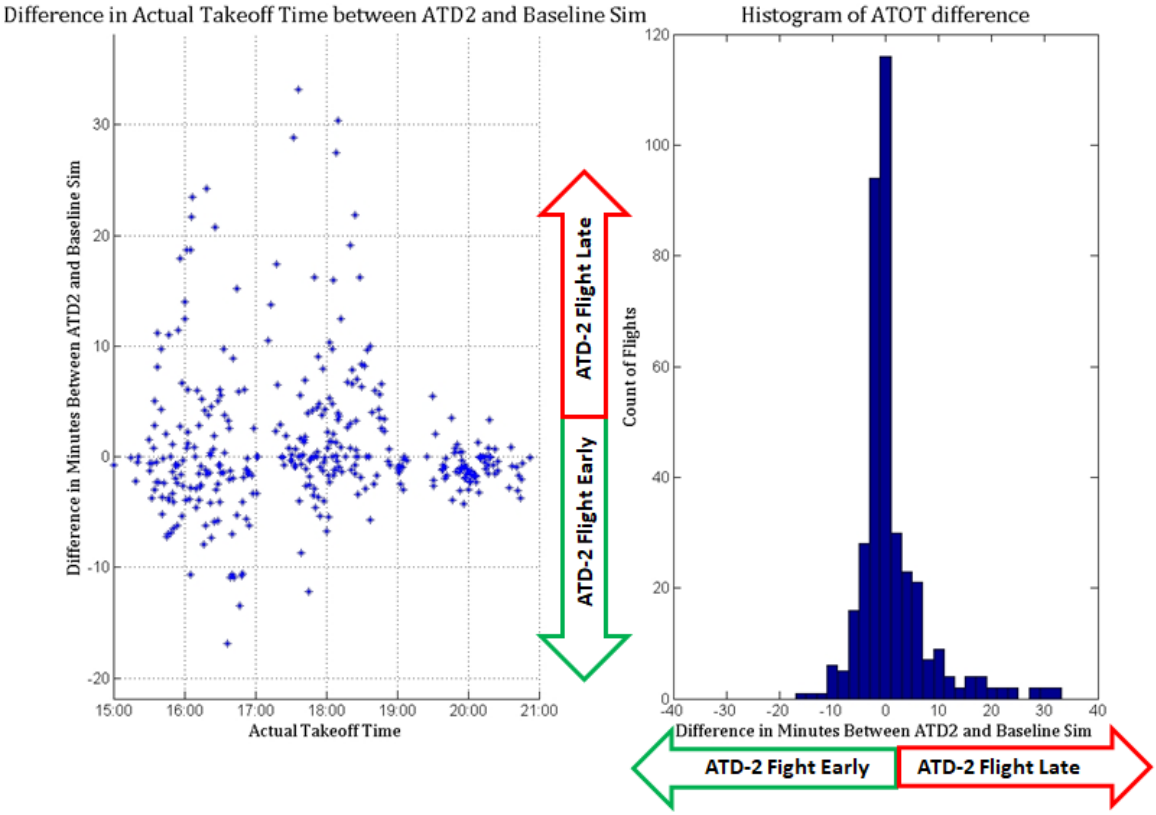

Figure 70. Analysis of On-Time Runway Takeoff Performance – Baseline VS ATD-2

6.3.2.4. Analysis of ATD-2's Impact on Airport Departure Throughput

Our simulation results show that the ATD-2 system had a minor negative impact on the overall airport throughput. **Figure 71** shows the cumulative airport throughput (i.e., the number of departures that have taken of at time 't') throughout the simulation timeframe. As seen from the figure, the baseline cumulative airport throughput line (red dashed line) fell either on or below the ATD-2 cumulative airport throughput line (blue solid line), except for an extended time in the middle part of the simulation, where the blue line lagged the red line by > 5 departure aircraft. This demonstrates that the ATD-2 scheduling algorithm needs fine tuning for fitting the constraints and operating characteristics at DFW.

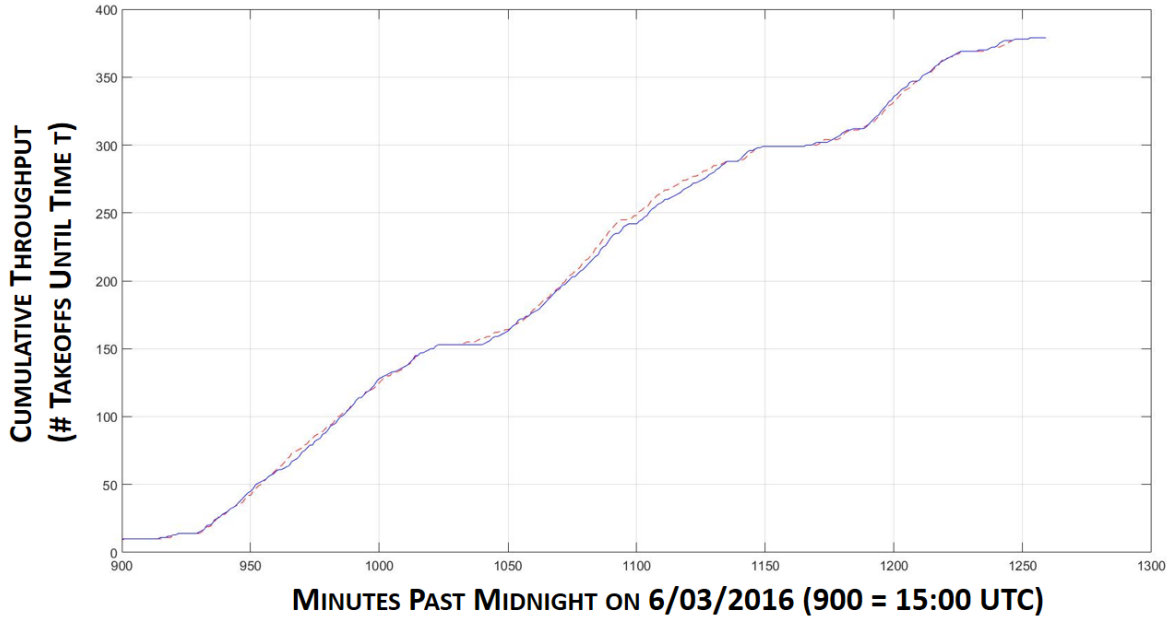

Figure 71. Cumulative airport throughput (baseline sim: red dashed line; ATD-2 sim: blue solid line) shows very little impact of ATD-2 gate holds on departure throughput

Figure 72 shows the cumulative departure throughputs separately for the two active departure runways (17R and 18L), again demonstrating that the ATD-2 system had a negative impact on the individual runway throughputs.

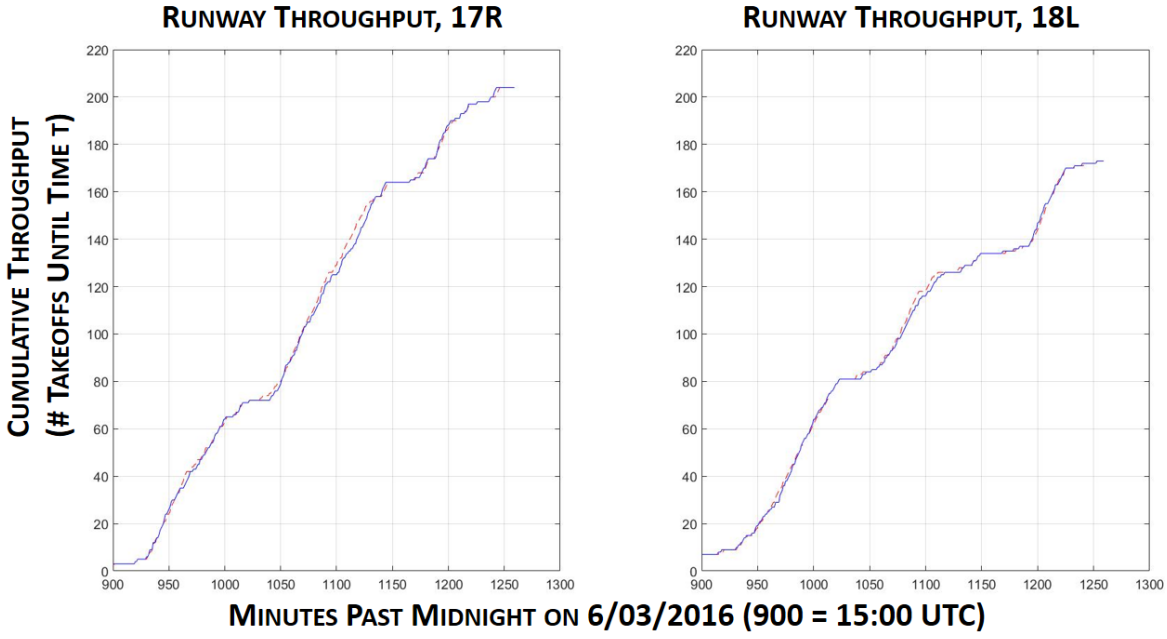

Figure 72. Cumulative airport throughput in the baseline simulation (red dashed line) and the ATD-2 simulation (blue solid line) shown for two departure runways separately

6.3.2.5. Simulation Validation

This section presents results from comparing simulation outputs with operational metrics from real operational data on the same historical day, as well as with a distribution of the same operational metrics computed over a set of similar days over a period of three months. The left-hand side of **Figure 73** shows the comparison of takeoff counts per 15-minute bin over the duration of the simulation, with the simulated counts shown by the red line, the actual counts on the day of operations shown by the blue line, and a region covering the 10-th to 90-th percentile takeoff counts per 15-minute bin over similar historical time-bins. Similar time-bins were chosen based on the detection of the same active runway configuration as the simulated configuration in those time-bins. For example, for the 16:30-16:45 UTC bin, we identified all 16:30-16:45 UTC bins over a period of three months (May-July 2016). Out of these bins, we identified those bins during which DFW had a West-flow runway configuration active. These identified same-configuration bins were used to compute the 10-th and 90-th percentile runway takeoff counts.

As seen from the left-hand side of **Figure 73**, the simulated takeoff counts follow the general trend of the actual runway takeoff counts, with three departure banks clearly visible. The discrepancies between simulated versus actual counts at the beginning and end of the simulation time-period can be attributed to the fact that we only included flights that pushed back after 15:00 UTC and before 21:00 UTC in the simulation. By doing so, we missed some of the departure flights at either end of the simulation time-period.

The right-hand side of **Figure 73** shows similar plot for the simulated versus actual gate out counts. Again, we see that the simulation followed the general trend of the actual counts with discrepancies at the beginning and end of the simulation timeframe attributed to flights that were by design not included in the simulation set.

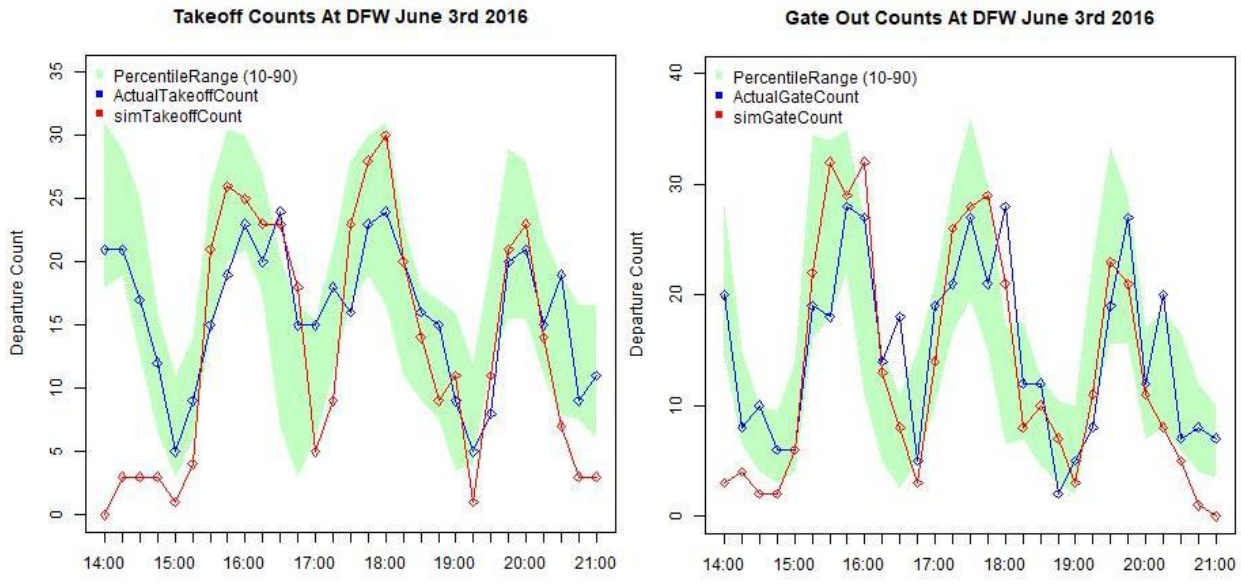

Figure 73. Runway Off and Gate Out Counts Validation – Simulation Versus Real Operations

Further, we also validated the taxi-out times by comparing simulated times against real historical operational taxi-out times from the same day as well as with a distribution of taxi-out times over

similar days. **Figure 74** shows the comparison of simulated and actual taxi-out times, with AMA taxi-out time comparison showed in the left half of the figure and the total (AMA + Ramp) taxi-out time comparison shown in the right half of the figure. As seen from the figures, the taxi-out times do not match very closely, but simulated taxi-out times follow the general trend of the actual observed simulated taxi-times with a couple of peaks visible in both simulated and actual data. The discrepancies at the beginning and end of the simulation timeframe can again be attributed to the fact that we had excluded flights outside the 15:00-21:00 UTC timeframe from the simulation by design, whereas in the actual operations they appear in the taxi-out time plots. The discrepancies between actual and simulated taxi-out times outside the beginning and ending time-bins can be attributed to multiple factors including, erroneous actual Gate OUT time data, differences in the handling of departure takeoff clearances between actual operations and simulation (human local controller clearances may contain additional delays due to the fact that the local controller is handling multiple arrival and departure clearances at the same time), and differences in simulated versus actual ramp and spot merge handling.

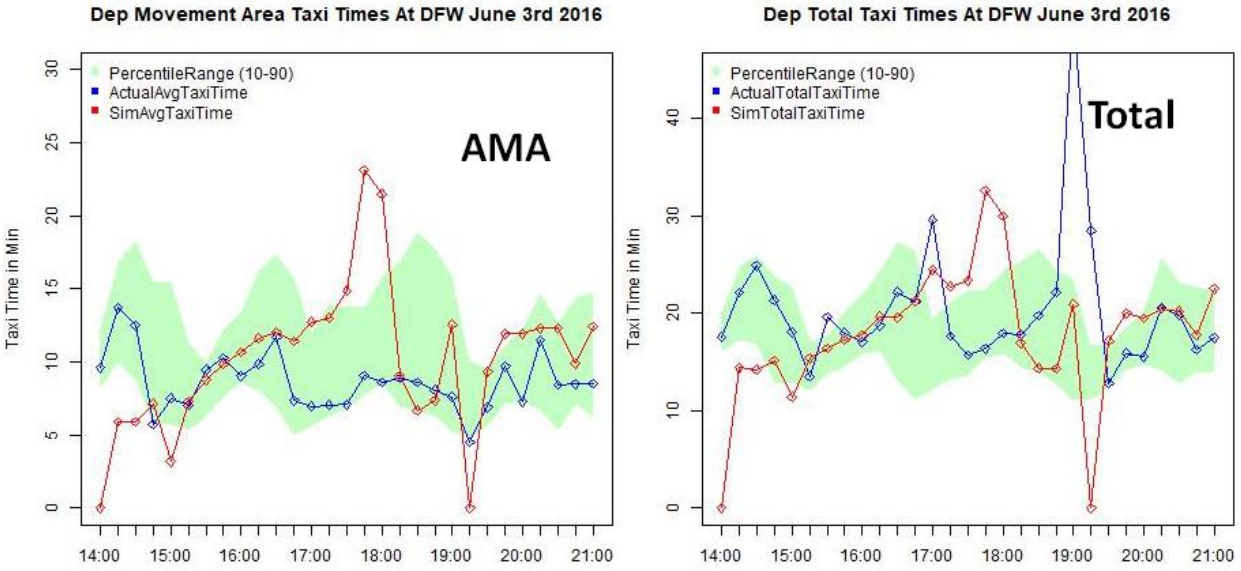

Figure 74. Taxi-Out Time Validation – Simulation Versus Real Operations

6.3.2.6. Analysis of Benefit Mechanism Contributions to ATD-2 Benefits

Analysis of simulation output data showed that two benefit mechanisms played a major role in providing taxi-out time savings. These were: These were: (1) Demand throttling provided by Surface Departure Metering advisories (i.e., gate-holds) and (2) Data exchange and scheduling for TMI Coordination.

Benefit Mechanism #1: Demand throttling provided by Surface Departure Metering advisories (i.e., gate-holds). As discussed above, our ATD-2 simulations included a full emulation of NASA's ATD-2 Tactical Surface Scheduler, which computed gate delays for departure flights in order to reduce taxi-out times but at the same time keeping sufficient pressure on the departure runways. **Figure 75** shows that gate delay difference (i.e., ATD-2 simulation Gate OUT Time – Baseline simulation Gate OUT time) for each simulated departure flight. The right half of the

figure shows a histogram of gate delay differences. We can see that the ATD-2 scheduler added a significant amount of gate delays over and above the baseline simulation. In the left half of the figure we show the gate delay difference plotted along the simulation timeline. This plot shows that the ATD-2 scheduler allocated majority of the gate delays during the time-periods when the departure demand on the DFW runways was at its peak, i.e., at or near the peaks of the three major departure banks included in the simulation. There are some gate delay difference points below the zero line in the plot on the left. These were flights that received higher gate delays in the baseline simulation because of active MITs to their destination airports. Here also, we see that the ATD-2 scheduler handled these flights with smaller gate delays than in the baseline simulation. This was an effect of more efficient coordination with the receiving Center, which included sending more accurate runway takeoff time estimates to the Center, and after the Center sends back the controlled runway release time computing the required gate release time using a more accurate taxi-out time estimate. This benefit mechanism is discussed later. For the demand throttling benefit mechanism that we are discussing here, it would suffice to observe that the ATD-2 scheduler correctly allocated gate delays during the especially busy peak time-periods.

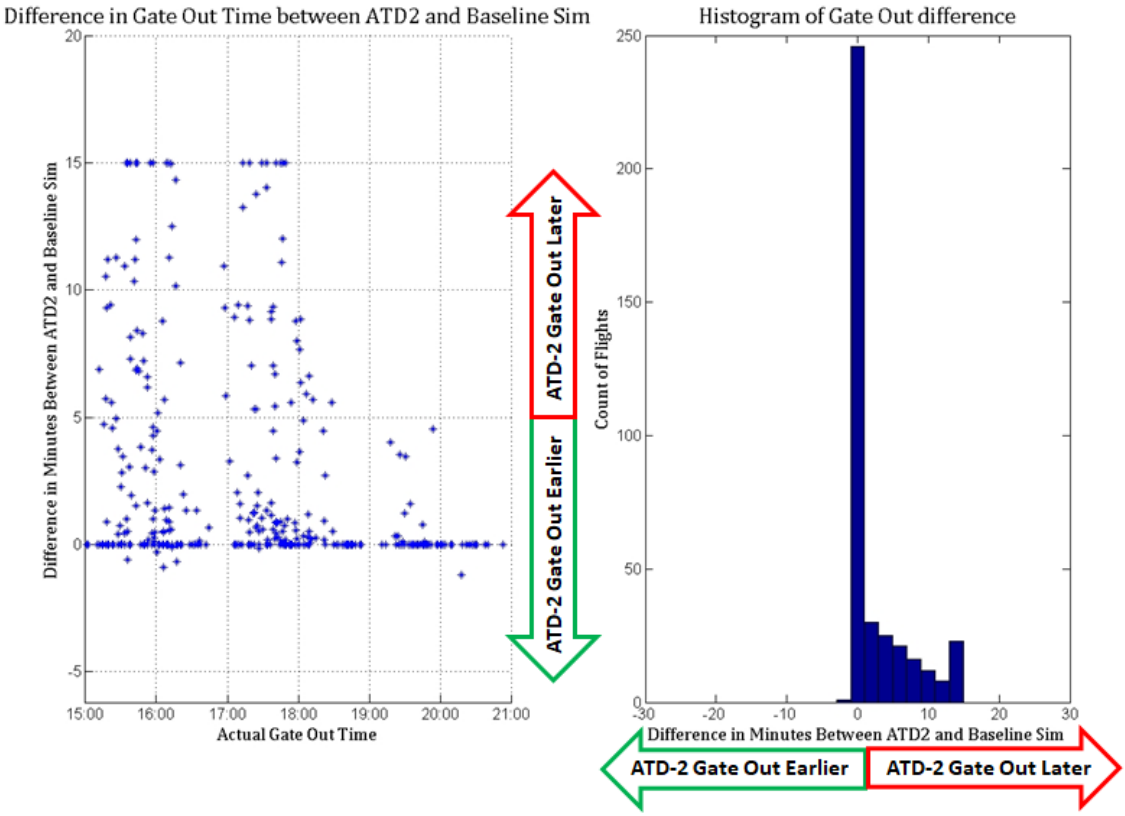

Figure 75. Gate Delay Difference, ATD-2 Operations – Baseline Operations

The beneficial effect that these tactical gate delays had on surface congestion can be seen in **Figure 76**. This figure plots the difference in Taxi-out Times (ATD-2 – Baseline) as a function of the difference in departure queue lengths experienced by the respective flights in the ATD-2 and Baseline simulations. As seen from the figure, ~53% of the flights experienced smaller departure queue lengths, a result of the demand throttling provided by the tactical scheduler allocated gate delays and as a result experienced shorter taxi-out times. Moreover, an additional ~23% flights

experienced slightly longer queues in the ATD-2 operations, but still managed to have smaller taxi-out times. In the case of these flights, although there were more flights ahead of them in the departure queue when they reached the spot, the runway takeoff times for those flights were sufficiently spaced out as a result of the gate delays and hence the flight was able to take off after spending a smaller time in taxi. Around 7% of the flights experienced longer queues than the baseline simulation and as a result experienced longer taxi-out times, which is an indication that the ATD-2 scheduler settings may need fine tuning. It is our opinion that future efforts to assess different settings and algorithmic alternatives (e.g., taxi-out time prediction methods) in a fast-time simulation environment will be highly beneficial for optimizing the performance of the ATD-2 system in the field.

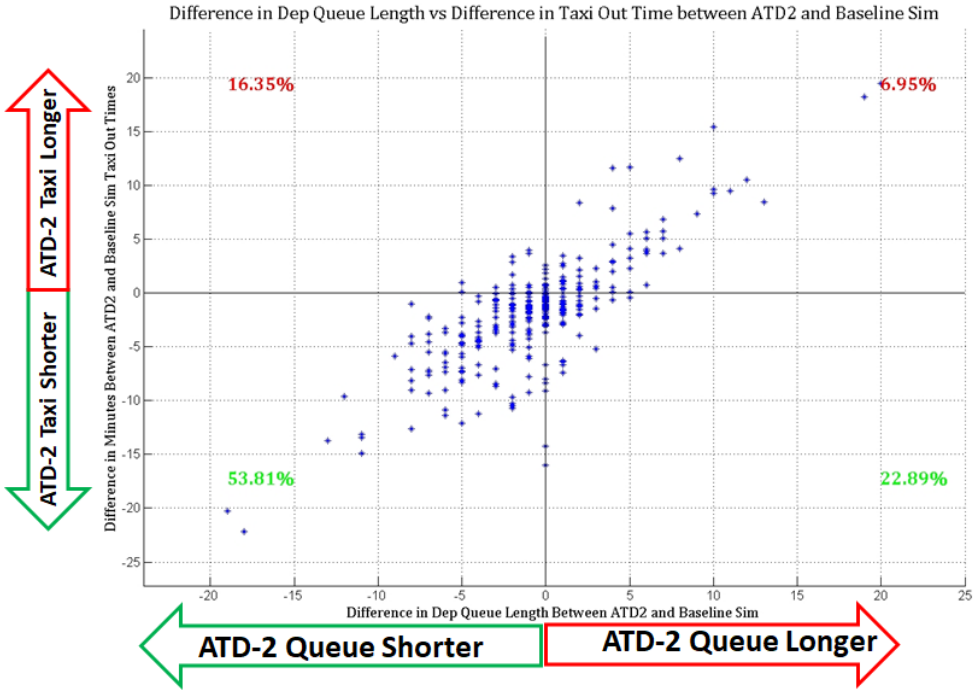

Figure 76. Taxi Out Time Difference (ATD-2 – Baseline) plotted as a function of Difference in Departure Queue Lengths Experienced by Flights at the Spot (ATD-2 – Baseline)

In summary, the demand throttling provided by ATD-2 Tactical Surface Scheduler-imposed gate delays contributed towards reducing the taxi-out times for departure flights in general. Next, we discuss another benefit mechanism, which we found especially beneficial for TMI-impacted departure flights.

Benefit Mechanism # 2: Data exchange and scheduling for TMI Coordination. Our simulation platform models the full data exchange and scheduling process for APREQ, EDCT, and MIT-impacted flights. The effect of differences in handling these TMI-impacted flights can be clearly seen in **Figure 77**. TMIs active in the case of DFW simulations included MIT restrictions on departure-fixes as well as EDCTs on flights going to impacted destinations (see Table of TMIs in Section 6.2.2.1). As seen from **Figure 77**, ATD-2 scheduling and data exchange was able to reduce the taxi-out times for TMI-impacted flights as well as other flights, but was not able to reduce the variance in the TMI flights' taxi out times. This points to the need for fine tuning the ATD-2 scheduling algorithm to fit the DFW constraints and operational features.

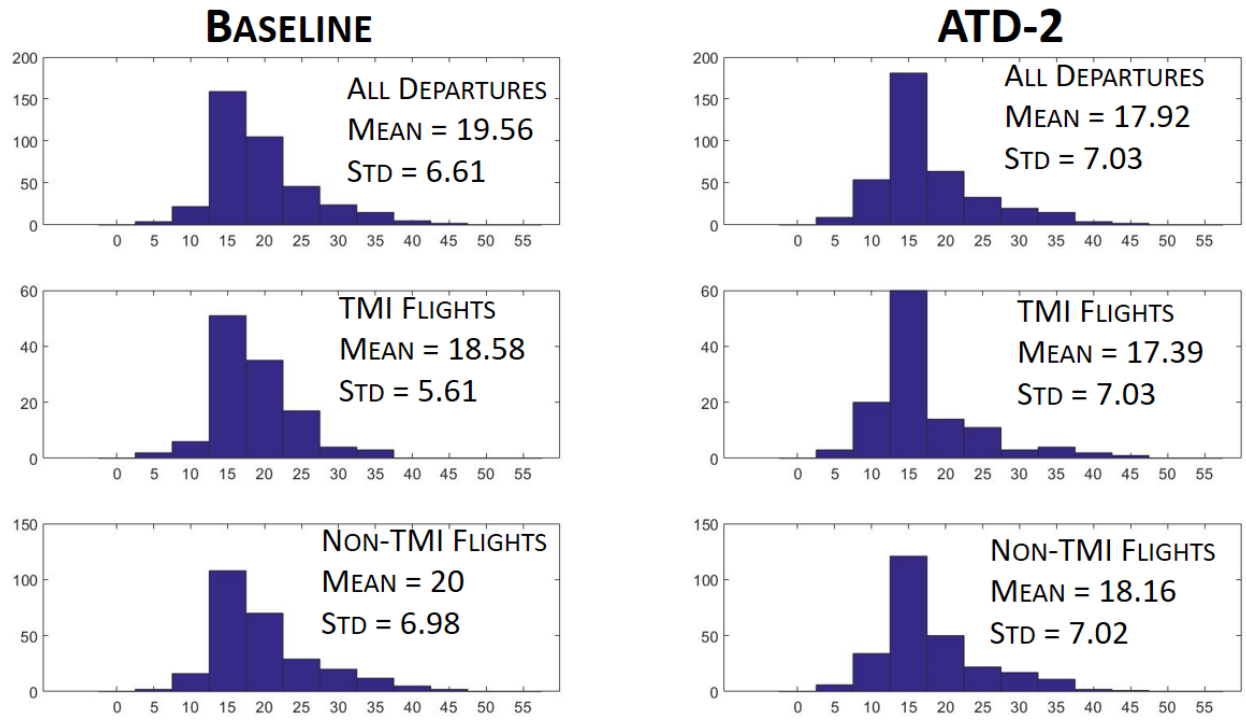

Figure 77. Taxi-Out Times (Mean and Variance) for All, TMI-impacted and Non-TMI-impacted flights for Baseline and ATD-2 Operations

6.4. EWR Simulations Details

6.4.1. EWR Simulation Day 1 Results (7/21/2016, South Flow)

The first EWR scenario we describe involved the simulation of EWR airport arrival and departure traffic on 07/21/2016 during the 0800-1800 UTC timeframe.

6.4.1.1. Simulation Scenario Description

EWR was under the South-flow runway configuration during the selected simulation time-period, with departures operating on runway 22R, and arrivals operating on runways 22L, 22R and 29 as shown in **Figure 78**.

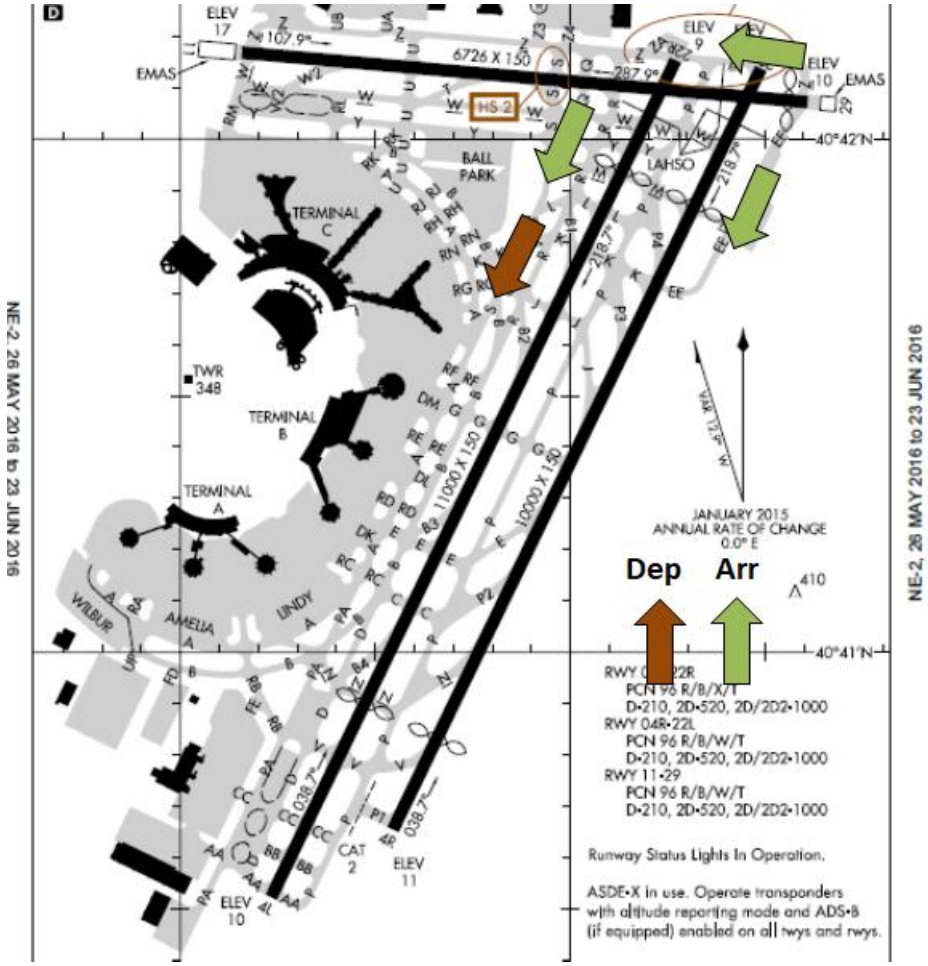

Figure 78. EWR South Flow Runway Configuration Runway Usage

The table below outlines the number of total departures and arrivals using the individual active runways during the simulated timeframe.

	22L	22R	29	Operation Counts by Type
Departures	0	287	0	287
Arrivals	245	15	1	261
Total Ops Per Runway	245	392	1	548

The simulations also emulated the implementation of surface traffic flow management initiatives such as APREQs, miles-in-trail restrictions and Ground Delay Programs as described in Section 4.2. In this particular scenario, we simulated the following traffic management initiatives that were active during the 0800-1800 UTC timeframe on the actual 07/21/2016 day.

TMI Type, Size	TMI Requesting Facility	Providing Facility	TMI Start	TMI End	Departures to
MINIT, 9	N90	EWR	10:00	13:00	ORD, over COATE departure fix
MINIT, 8	N90	EWR	13:00	14:15	DTW, over North departure fixes
MINIT, 8	N90	EWR	14:15	16:15	ORD, over COATE departure fix
MINIT, 6	N90	EWR	14:15	19:12	CLT, over BIGGY and LANNA
MINIT, 7	N90	EWR	17:00	19:11	DCA, over BIGGY
MINIT, 8	N90	EWR	16:30	19:00	ORD, over all departure fixes
GDP, average delay 56 minutes	ATCSCC	Airports in all Contiguous US Centers	12:57	16:08	SFO

6.4.1.2. Benefits Results: Taxi-time Savings

Our simulation results for this scenario showed that the ATD-2 system saved around 6% of the total taxi-out time over all the departures, as shown in **Figure 79**. Similar taxi-out time savings (percentage-wise) were seen in the AMA taxi-out times while the ramp taxi times saw a small reduction.

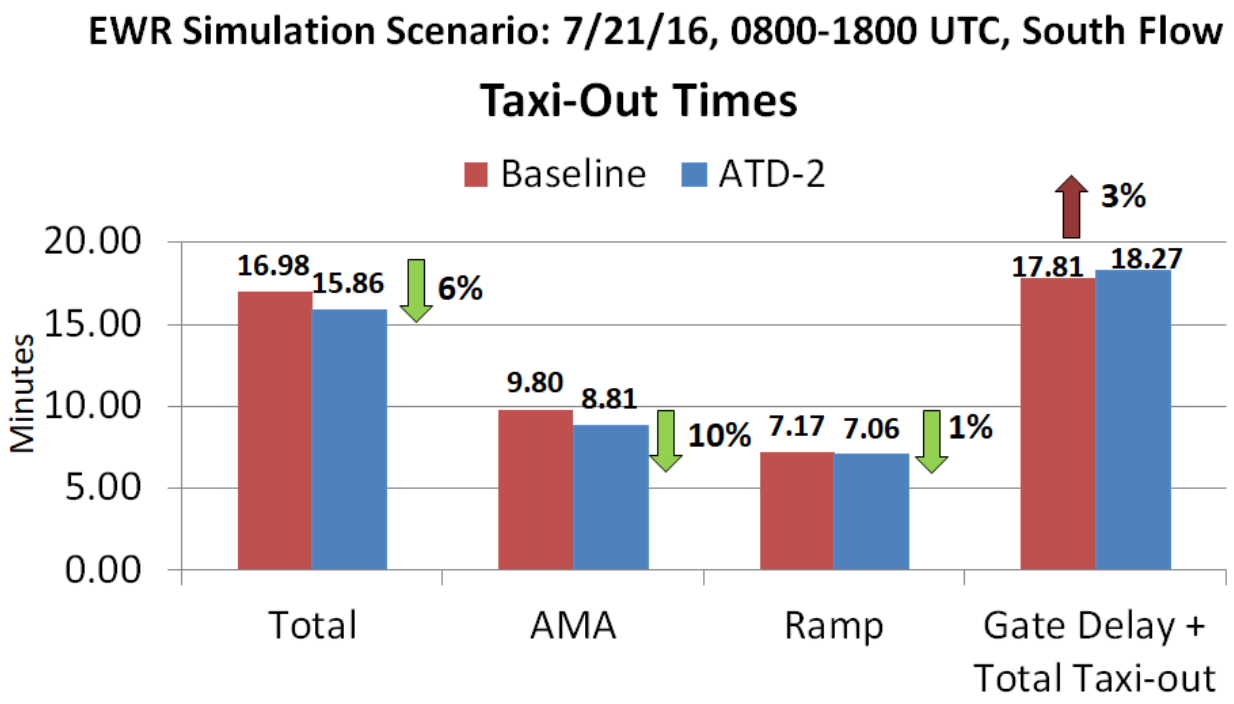

Figure 79. Taxi-Out Time Savings Benefits Estimated by Baseline VS ATD-2 Simulations for the 07/21/2016 0800-1800 UTC simulation scenario

Further, we also computed the total transit time for each departure consisting of the excess time spent at the gate in the ATD-2 simulation (i.e., ATD-2 system imposed gate delay) and the taxi transit from gate pushback to runway takeoff. This total transit time metric is the fourth pair of bars shown in **Figure 79**. As seen from the figure, with the ATD-2 system there is a 3% increase in the total transit time metric on an average for this simulation day.

We also analyzed the impact of ATD-2 departure metering on arrival taxi-in times. **Figure 80** shows that with the ATD-2 system operating there was a slight increase in the taxi-in times.

As in the case of DFW, these negative impacts on total transit times and taxi-in times warrant evaluation of fine tuning adjustments to the ATD-2 scheduling algorithm as tailored to EWR.

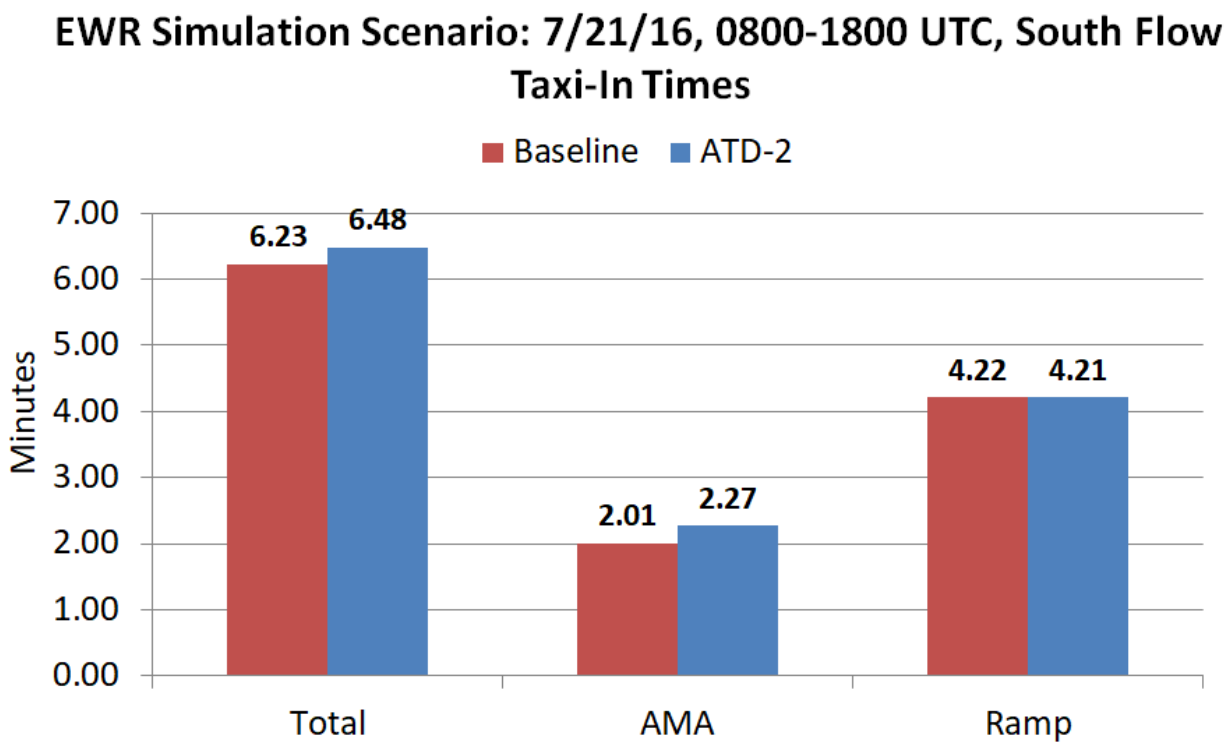

Figure 80. Taxi-In Time Savings Benefits Estimated by Baseline VS ATD-2 Simulations for the 07/21/2016 0800-1800 UTC simulation scenario

6.4.1.3. Analysis of On-Time Performance for Departure Flights

An important consideration for user-acceptance of the ATD-2 system is the question of what impact do the ATD-2 gate delays have on the overall On time performance of the airport in terms of late or early runway takeoff times. In relation to this aspect, we analyzed the runway takeoff time difference for each departure flight between the baseline simulation (current-day procedures) and the ATD-2 simulation (departure metering procedures). **Figure 81** shows the results of this analysis. The right half of this figure shows a histogram of runway takeoff time differences per flight (ATD-2 simulation takeoff time – Baseline simulation takeoff time). As seen from the figure, a big majority of the flights (~60%) took off either at the same time or earlier in the ATD-2 operations, whereas 40% of the flights took off later as compared to the baseline simulation. Moreover, out of the 40% flights departing late in the ATD-2 simulation, around half of them departed less than 2 minutes late than their counterpart departure in the ATD-2 simulation.

This demonstrates that the ATD-2 system had a positive impact on the On time performance of the airport, in general, but there were some flights that took off later than their baseline runway takeoff time. In general, if bringing the number of flights that takeoff later than baseline down (closer to zero) is of high importance to the airlines, then there are tools/settings available in the ATD-2 system, which can be modified to reduce the negative impact on certain flights. These tools/ settings include the optimal selection of the ATD-2 Tactical Surface Scheduler's taxi delay buffer parameter as well as modifications to how the ATD-2 Scheduler estimates earliest runway usage times for departure flights for scheduling purposes as well as how it back-computes gate delays

from the target runway takeoff times. But, before making these changes in the operational ATD-2 system, more simulation-based sensitivity tests are required to assess multiple alternatives and select the best.

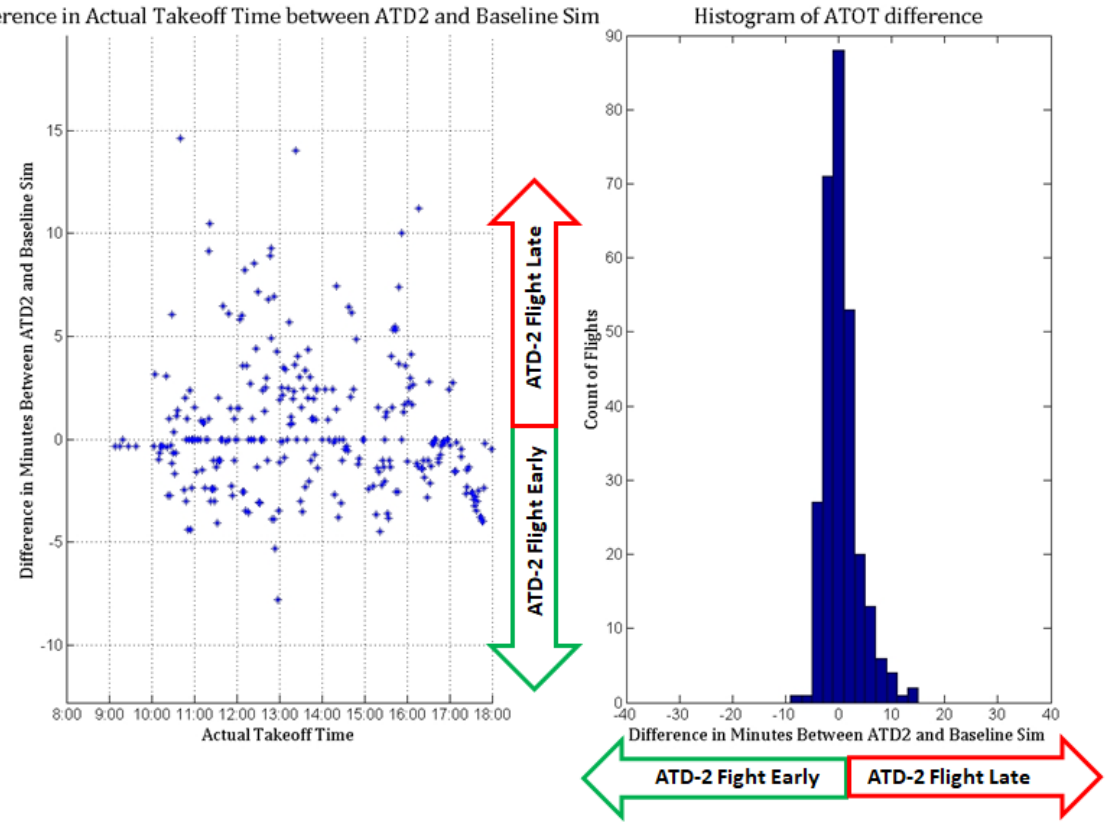

Figure 81. Analysis of On-Time Runway Takeoff Performance – Baseline VS ATD-2

6.4.1.4. Analysis of ATD-2's Impact on Airport Departure Throughput

Our simulation results show that the ATD-2 system had a minor negative impact on the overall airport throughput. **Figure 82** shows the cumulative airport throughput (i.e., the number of departures that have taken of at time 't') throughout the simulation timeframe. As seen from the figure, the baseline cumulative airport throughput line (red dashed line) fell either on or below the ATD-2 cumulative airport throughput line (blue solid line), for most of the simulation timeframe, except for a few time-periods where the blue line lagged the red line by ~1-2 departure aircraft. This demonstrates that the ATD-2 scheduling algorithm had practically no negative or positive impact on the airport departure throughput despite gate hold-backs. There was only one departure runway modeled (22R), so there is no need for looking at individual runway throughputs separately.

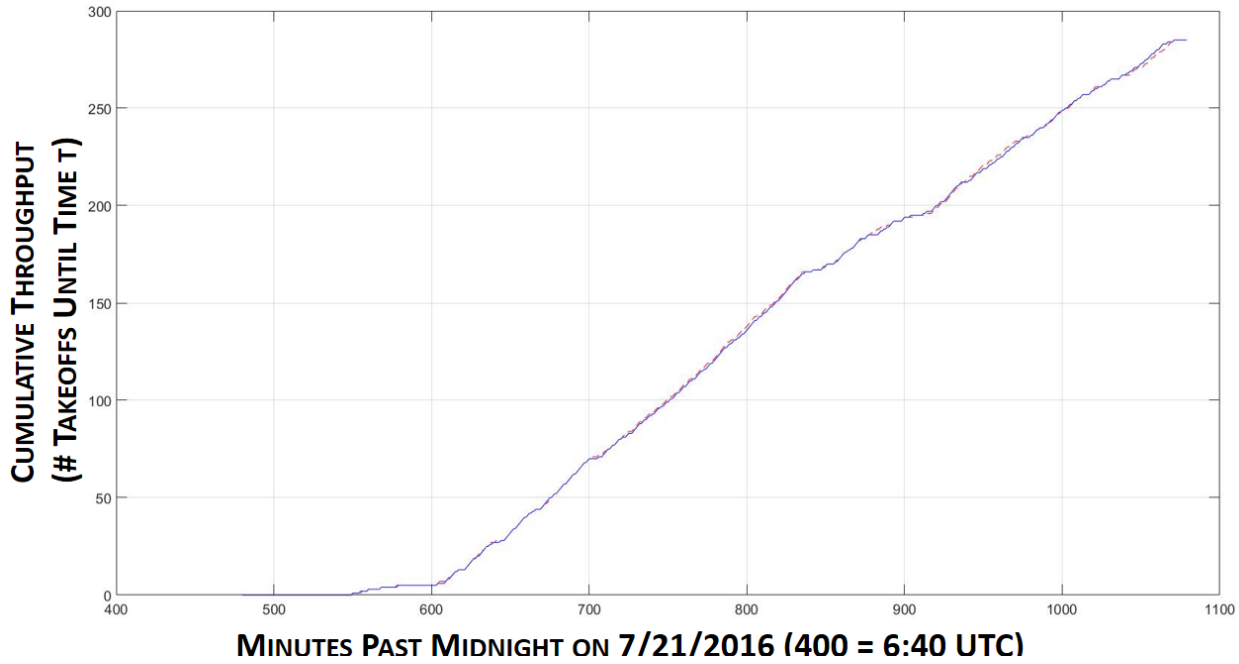

Figure 82. Cumulative airport throughput (baseline sim: red dashed line; ATD-2 sim: blue solid line) shows very little impact of ATD-2 gate holds on departure throughput

6.4.1.5. Simulation Validation

This section presents results from comparing simulation outputs with operational metrics from real operational data on the same historical day, as well as with a distribution of the same operational metrics computed over a set of similar days over a period of three months. The left-hand side of **Figure 83** shows the comparison of takeoff counts per 15-minute bin over the duration of the simulation, with the simulated counts shown by the red line, the actual counts on the day of operations shown by the blue line, and a region covering the 10-th to 90-th percentile takeoff counts per 15-minute bin over similar historical time-bins. Similar time-bins were chosen based on the detection of the same active runway configuration as the simulated configuration in those time-bins. For example, for the 16:30-16:45 UTC bin, we identified all 16:30-16:45 UTC bins over a period of three months (May-July 2016). Out of these bins, we identified those bins during which EWR had a South-flow runway configuration active. These identified same-configuration bins were used to compute the 10-th and 90-th percentile runway takeoff counts.

As seen from the left-hand side of **Figure 83**, the simulated takeoff counts follow the general trend of the actual runway takeoff counts, with three departure banks clearly visible. The discrepancies between simulated versus actual counts at the beginning and end of the simulation time-period can be attributed to the fact that we only included flights that pushed back after 08:00 UTC and before 18:00 UTC in the simulation. By doing so, we missed some of the departure flights at either end of the simulation time-period.

The right-hand side of **Figure 83** shows similar plot for the simulated versus actual gate out counts. Again, we see that the simulation followed the general trend of the actual counts with discrepancies at the beginning and end of the simulation timeframe attributed to flights that were by design not included in the simulation set.

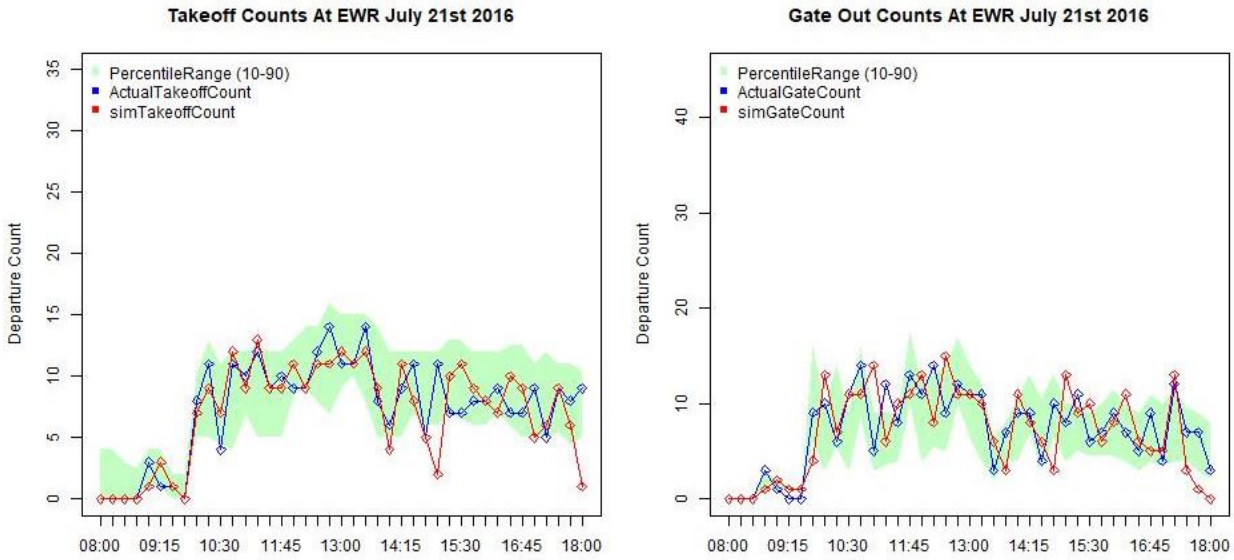

Figure 83. Runway Off and Gate Out Counts Validation – Simulation Versus Real Operations

Further, we also validated the taxi-out times by comparing simulated times against real historical operational taxi-out times from the same day as well as with a distribution of taxi-out times over similar days. **Figure 84** shows the comparison of simulated and actual taxi-out times, with AMA taxi-out time comparison showed in the left half of the figure and the total (AMA + Ramp) taxi-out time comparison shown in the right half of the figure. As seen from the figures, the taxi-out times do not match very closely, but simulated taxi-out times follow the general trend of the actual observed simulated taxi-times with a couple of peaks visible in both simulated and actual data. The discrepancies at the beginning and end of the simulation timeframe can again be attributed to the fact that we had excluded flights outside the 08:00-18:00 UTC timeframe from the simulation by design, whereas in the actual operations they appear in the taxi-out time plots. The discrepancies between actual and simulated taxi-out times outside the beginning and ending time-bins can be attributed to multiple factors including, erroneous actual Gate OUT time data, differences in the handling of departure takeoff clearances between actual operations and simulation (human local controller clearances may contain additional delays due to the fact that the local controller is handling multiple arrival and departure clearances at the same time), and differences in simulated versus actual ramp and spot merge handling. It can be noted, for the Movement Area taxi time plot, that there is a 2 hour section of time where the actual taxi time is 0. This is due to an availability gap in the processing of our ASDE-X data source.

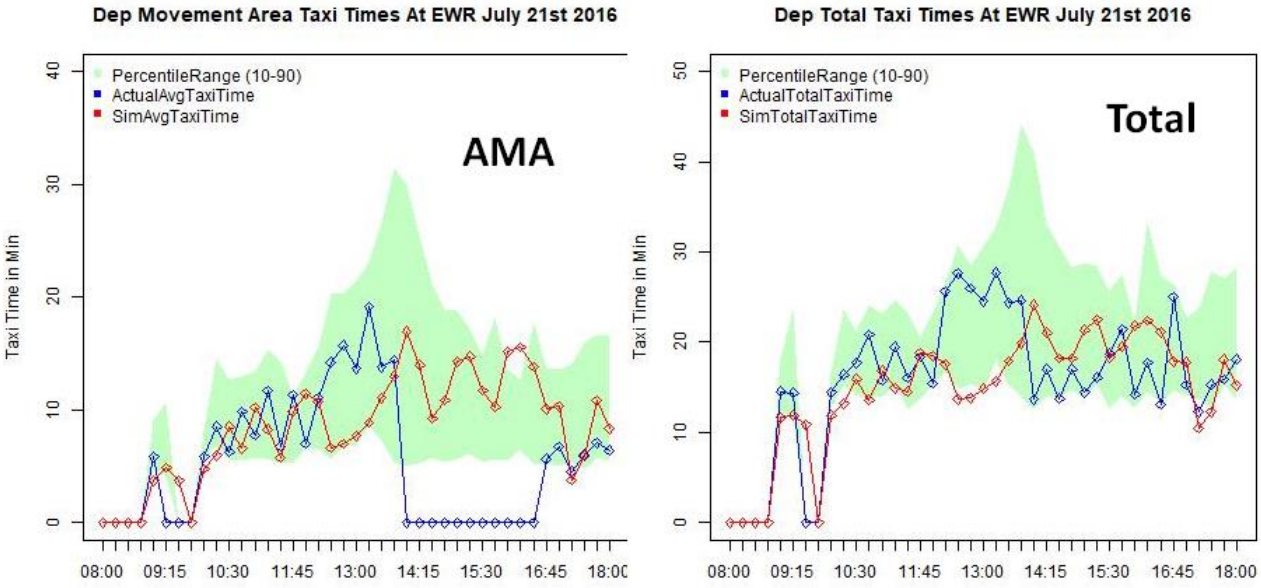

Figure 84. Taxi-Out Time Validation – Simulation Versus Real Operations. (Note: an availability gap in ASDE-X data prevented us from computing AMA historical taxi-out times for a period of the simulation, which is the reason for zero taxi-out times in the right-half)

6.4.1.6. Analysis of Benefit Mechanism Contributions to ATD-2 Benefits

Analysis of simulation output data showed that two benefit mechanisms played a major role in providing taxi-out time savings. These were: (1) Demand throttling provided by Surface Departure Metering advisories (i.e., gate-holds) and (2) Data exchange and scheduling for TMI Coordination. We discuss each of these benefit mechanisms with supporting data analyses next.

Benefit Mechanism #1: Demand throttling provided by Surface Departure Metering advisories (i.e., gate-holds). As discussed above, our ATD-2 simulations included a full emulation of NASA's ATD-2 Tactical Surface Scheduler, which computed gate delays for departure flights in order to reduce taxi-out times but at the same time keeping sufficient pressure on the departure runways. **Figure 85** shows that gate delay difference (i.e., ATD-2 simulation Gate OUT Time – Baseline simulation Gate OUT time) for each simulated departure flight. The right half of the figure shows a histogram of gate delay differences. We can see that the ATD-2 scheduler added a significant amount of gate delays over and above the baseline simulation. In the left half of the figure we show the gate delay difference plotted along the simulation timeline. This plot shows that the ATD-2 scheduler allocated majority of the gate delays during the time-periods when the departure demand on the EWR runways was at its peak, i.e., at or near the peaks of the two major departure banks included in the simulation. There are some gate delay difference points below the zero line in the plot on the left. These were flights that received higher gate delays in the baseline simulation because of active MITs to their destination airports. Here also, we see that the ATD-2 scheduler handled these flights with smaller gate delays than in the baseline simulation. This was an effect of more efficient coordination with the receiving Center, which included sending more accurate runway takeoff time estimates to the Center, and after the Center sends back the controlled runway release time computing the required gate release time using a more accurate

taxi-out time estimate. This benefit mechanism is discussed later. For the demand throttling benefit mechanism that we are discussing here, it would suffice to observe that the ATD-2 scheduler correctly allocated gate delays during the especially busy peak time-periods.

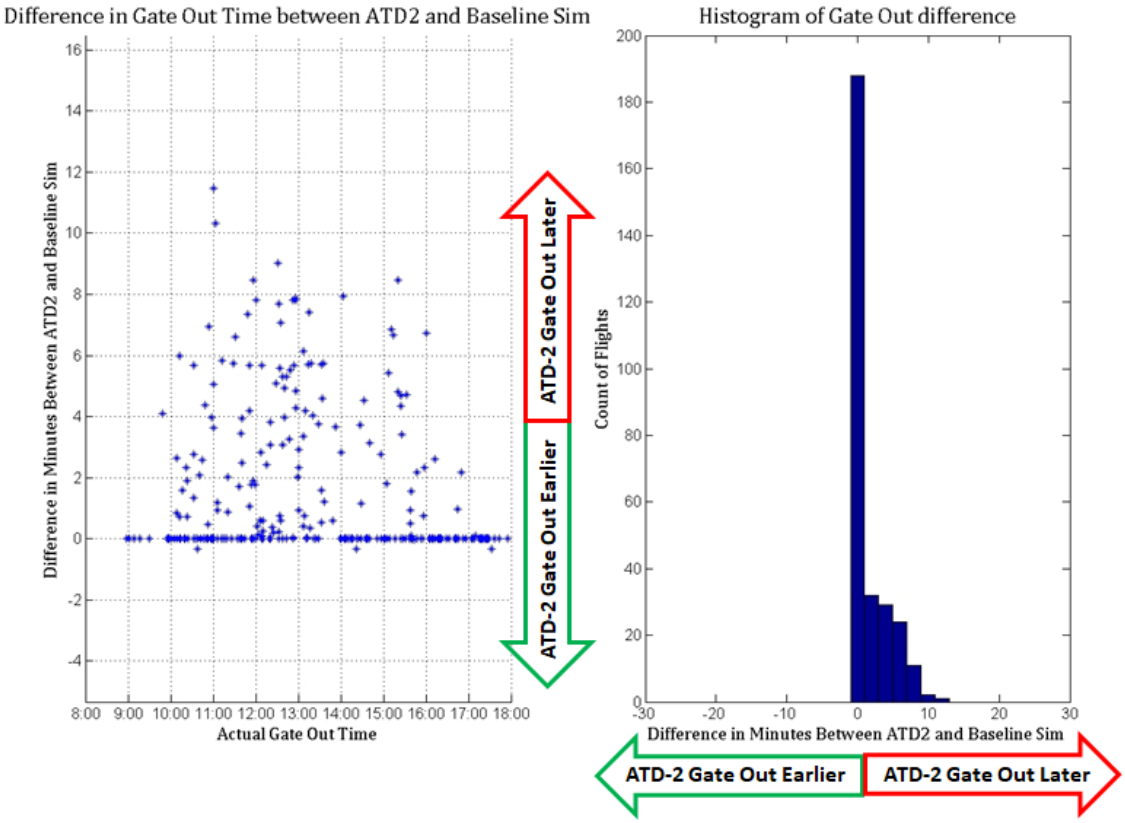

Figure 85. Gate Delay Difference, ATD-2 Operations – Baseline Operations

The beneficial effect that these tactical gate delays had on surface congestion can be seen in **Figure 86**. This figure plots the difference in Taxi-out Times (ATD-2 – Baseline) as a function of the difference in departure queue lengths experienced by the respective flights in the ATD-2 and Baseline simulations. As seen from the figure, ~63% of the flights experienced smaller departure queue lengths, a result of the demand throttling provided by the tactical scheduler allocated gate delays and as a result experienced shorter taxi-out times. Moreover, an additional ~16% flights experienced slightly longer queues in the ATD-2 operations, but still managed to have smaller taxi-out times. In the case of these flights, although there were more flights ahead of them in the departure queue when they reached the spot, the runway takeoff times for those flights were sufficiently spaced out as a result of the gate delays and hence the flight was able to take off after spending a smaller time in taxi. Around 4% of the flights experienced longer queues than the baseline simulation and as a result experienced longer taxi-out times, which is an indication that the ATD-2 scheduler settings may need fine tuning. It is our opinion that future efforts to assess different settings and algorithmic alternatives (e.g., taxi-out time prediction methods) in a fast-time simulation environment will be highly beneficial for optimizing the performance of the ATD-2 system in the field.

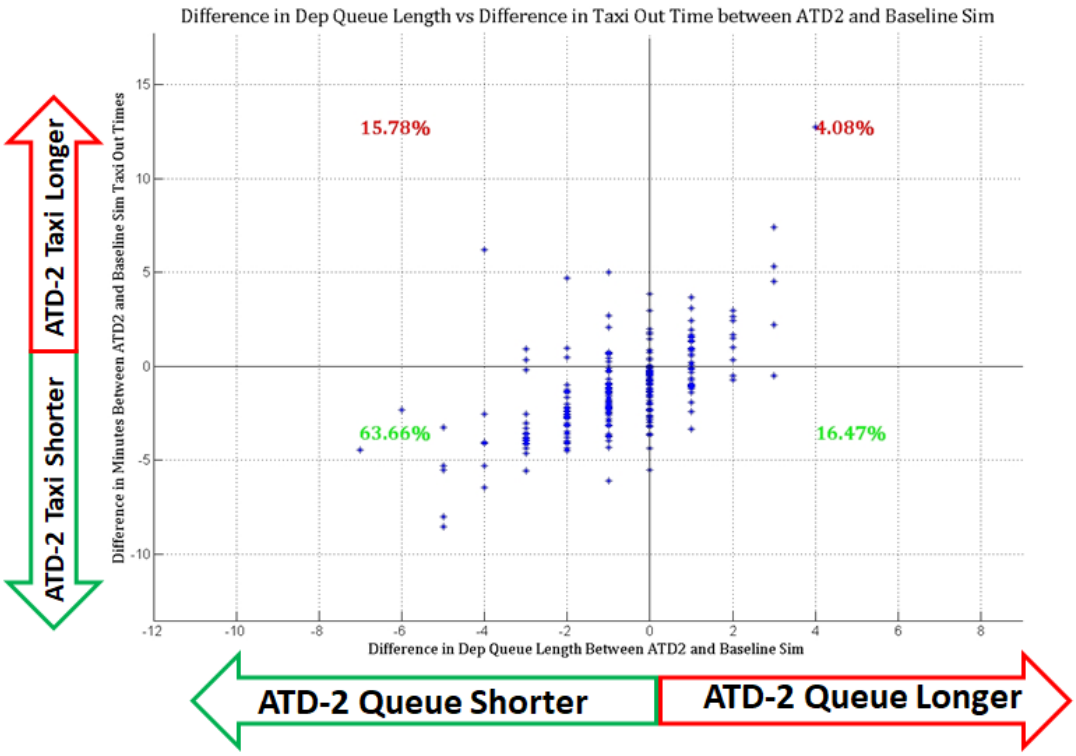

Figure 86. Taxi Out Time Difference (ATD-2 – Baseline) plotted as a function of Difference in Departure Queue Lengths Experienced by Flights at the Spot (ATD-2 – Baseline)

In summary, the demand throttling provided by ATD-2 Tactical Surface Scheduler-imposed gate delays contributed towards reducing the taxi-out times for departure flights in general. Next, we discuss another benefit mechanism, which we found especially beneficial for TMI-impacted departure flights.

Benefit Mechanism # 2: Data exchange and scheduling for TMI Coordination. Our simulation platform models the full data exchange and scheduling process for APREQ, EDCT, and MIT-impacted flights. The effect of differences in handling these TMI-impacted flights can be clearly seen in **Figure 87**. TMIs active in the case of EWR simulations included MIT restrictions on departure-fixes as well as EDCTs on flights going to impacted destinations (see Table in Section 6.4.1.1). As seen from the figure, ATD-2 scheduling and data exchange was able to reduce the taxi-out times for TMI-impacted flights as well as other flights, but was not able to reduce the variance in the TMI flights' taxi out times. This points to the need for fine tuning the ATD-2 scheduling algorithm to fit the EWR constraints and operational features.

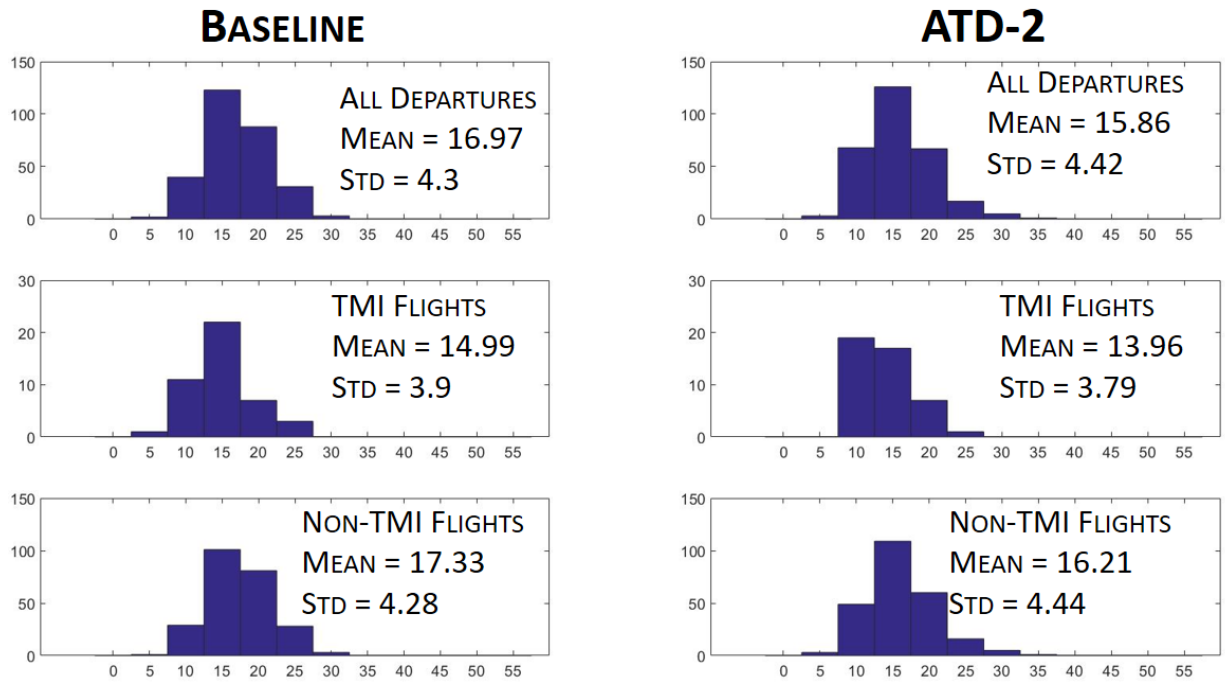

Figure 87. Taxi-Out Times (Mean and Variance) for All, TMI-impacted and Non-TMI-impacted flights for Baseline and ATD-2 Operations

6.4.2. EWR Simulation Day 2 Results (7/29/2016, North Flow)

The second EWR scenario we describe involved the simulation of EWR airport arrival and departure traffic on 07/29/2016 during the 0900-1800 UTC timeframe.

6.4.2.1. Simulation Scenario Description

EWR was under the North-flow runway configuration during the selected simulation time-period, with departures operating on runway 04L, and arrivals operating on runways 04L, 04R and 11 as shown in **Figure 88**.

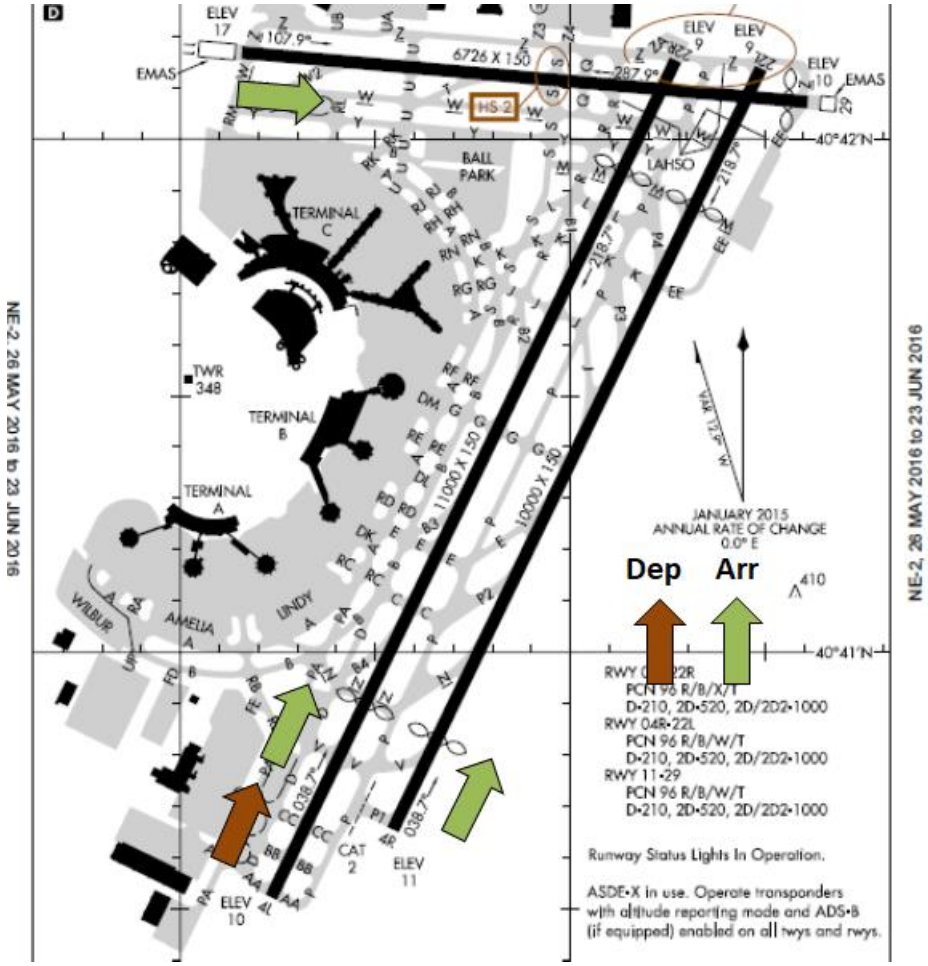

Figure 88. EWR North Flow Runway Configuration Runway Usage

The table below outlines the number of total departures and arrivals using the individual active runways during the simulated timeframe.

	04L	04R	11	Operation Counts by Type
Departures	261	0	0	261
Arrivals	6	204	8	218
Total Ops Per Runway	267	204	8	479

The simulations also emulated the implementation of surface traffic flow management initiatives such as APREQs, miles-in-trail restrictions and Ground Delay Programs as described in Section 4.2. In this particular scenario, we simulated the following traffic management initiatives that were active during the 0900-1800 UTC timeframe on the actual 07/29/2016 day.

TMI Type, Size	TMI Requesting Facility	Providing Facility	TMI Start	TMI End	Departures to
MINIT, 7	N90	EWR/LGA	10:15	11:45	CLT, over BIGGY
MINIT, 8	N90	EWR	10:00	15:30	ORD, over COATE
MINIT, 8	N90	EWR	12:15	16:30	CLT, over all departure fixes
MINIT, 5	N90	EWR/LGA	11:15	13:30	All departures over WHITE
MINIT, 6	N90	EWR/LGA	11:45	13:40	All departures over BIGGY
MINIT, 8	N90	EWR/LGA	14:00	15:00	DTW, over GAYEL
MINIT, 5	N90	EWR/LGA	13:30	20:00	All departures over North gates
MINIT, 5	N90	EWR/LGA	13:30	15:00	All departures over WHITE
MINIT, 8	N90	EWR/LGA	14:20	15:30	All departures over PARKE
MINIT, 7	N90	EWR/LGA	14:20	15:30	All departures over ZIMMZ
MINIT, 6	N90	EWR/LGA	17:15	20:15	CLT, over BIGGY

6.4.2.2. Benefits Results: Taxi-time Savings

Our simulation results for this scenario showed that the ATD-2 system saved around 7% of the total taxi-out time over all the departures, as shown in **Figure 89**. Similar taxi-out time savings (percentage-wise) were seen in the AMA taxi-out times and the ramp taxi times.

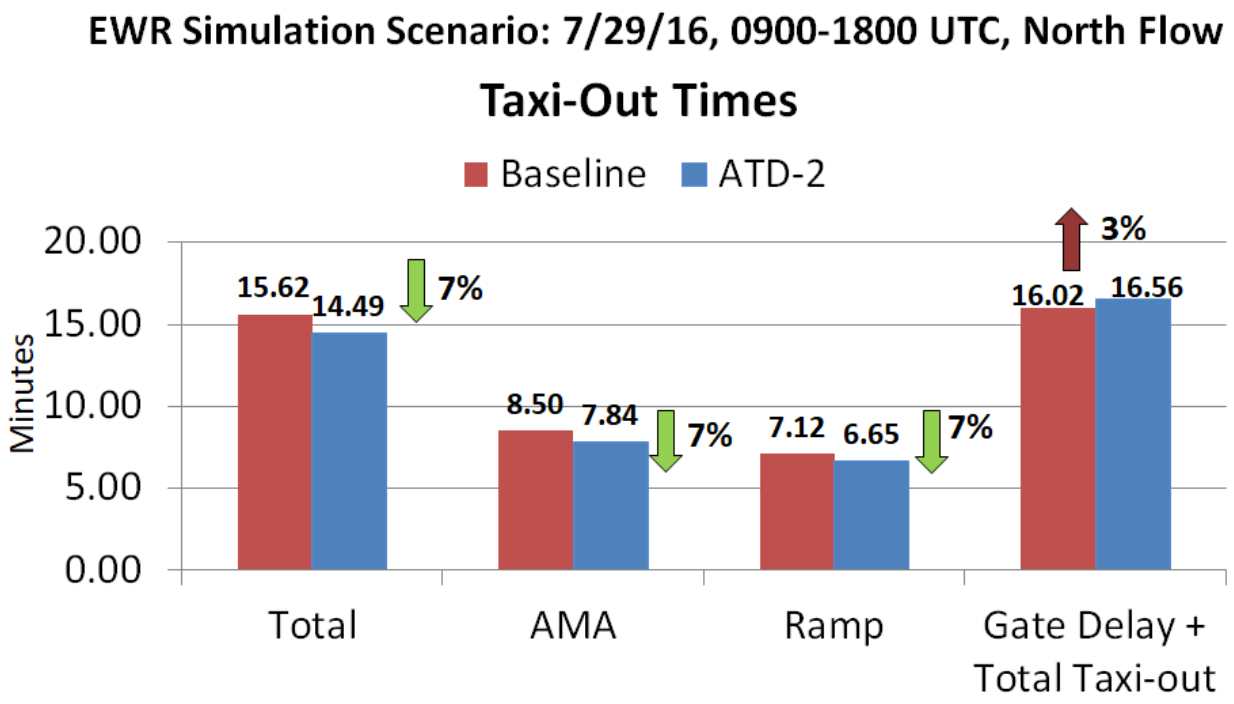

Figure 89. Taxi-Out Time Savings Benefits Estimated by Baseline VS ATD-2 Simulations for the 07/29/2016 0900-1800 UTC simulation scenario

Further, we also computed the total transit time for each departure consisting of the excess time spent at the gate in the ATD-2 simulation (i.e., ATD-2 system imposed gate delay) and the taxi transit from gate pushback to runway takeoff. This total transit time metric is the fourth pair of bars shown in **Figure 89**. As seen from the figure, with the ATD-2 system there is a 3% increase in the total transit time metric on an average for this simulation day.

We also analyzed the impact of ATD-2 departure metering on arrival taxi-in times. **Figure 90** shows that with the ATD-2 system operating there was no change in the taxi-in times.

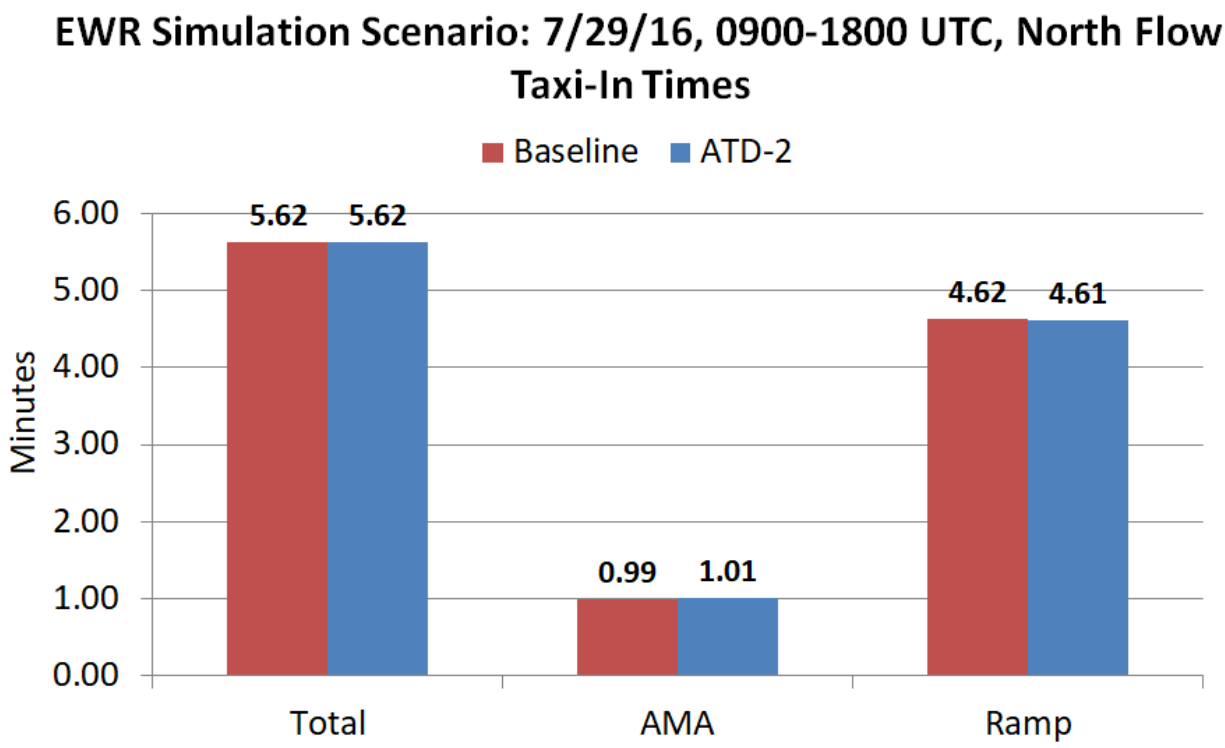

Figure 90. Taxi-In Time Savings Benefits Estimated by Baseline VS ATD-2 Simulations for the 07/29/2016 0900-1800 UTC simulation scenario

6.4.2.3. Analysis of On-Time Performance for Departure Flights

An important consideration for user-acceptance of the ATD-2 system is the question of what impact do the ATD-2 gate delays have on the overall On time performance of the airport in terms of late or early runway takeoff times. In relation to this aspect, we analyzed the runway takeoff time difference for each departure flight between the baseline simulation (current-day procedures) and the ATD-2 simulation (departure metering procedures). **Figure 91** shows the results of this analysis. The right half of this figure shows a histogram of runway takeoff time differences per flight (ATD-2 simulation takeoff time – Baseline simulation takeoff time). As seen from the figure, a big majority of the flights (~60%) took off either at the same time or earlier in the ATD-2 operations, whereas 40% of the flights took off later as compared to the baseline simulation. Moreover, out of the 40% flights departing late in the ATD-2 simulation, around one quarter of them departed less than 2 minutes late than their counterpart departure in the ATD-2 simulation.

This demonstrates that the ATD-2 system had a positive impact on the On time performance of the airport, in general, but there were some flights that took off later than their baseline runway takeoff time. In general, if bringing the number of flights that takeoff later than baseline down (closer to zero) is of high importance to the airlines, then there are tools/settings available in the ATD-2 system, which can be modified to reduce the negative impact on certain flights. These tools/ settings include the optimal selection of the ATD-2 Tactical Surface Scheduler's taxi delay buffer parameter as well as modifications to how the ATD-2 Scheduler estimates earliest runway usage times for departure flights for scheduling purposes as well as how it back-computes gate delays

from the target runway takeoff times. But, before making these changes in the operational ATD-2 system, more simulation-based sensitivity tests are required to assess multiple alternatives and select the best.

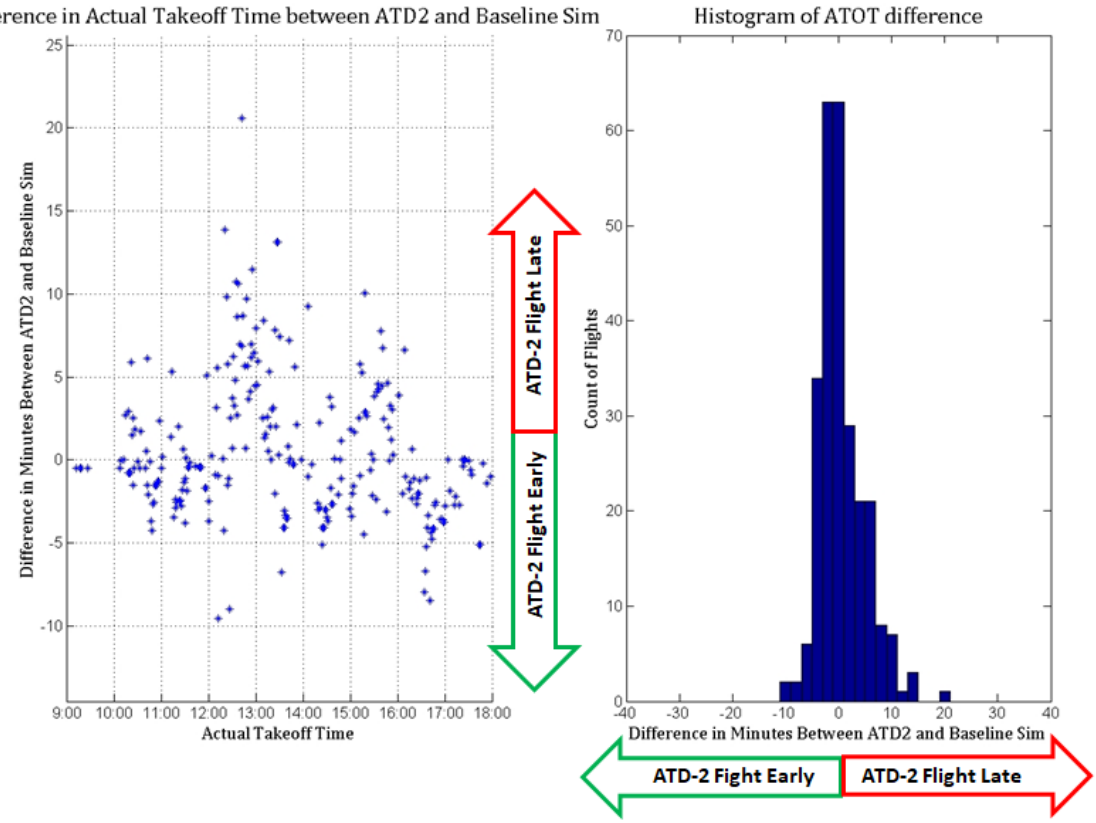

Figure 91. Analysis of On-Time Runway Takeoff Performance – Baseline VS ATD-2

6.4.2.4. Simulation Validation

This section presents results from comparing simulation outputs with operational metrics from real operational data on the same historical day, as well as with a distribution of the same operational metrics computed over a set of similar days over a period of three months. The left-hand side of **Figure 92** shows the comparison of takeoff counts per 15-minute bin over the duration of the simulation, with the simulated counts shown by the red line, the actual counts on the day of operations shown by the blue line, and a region covering the 10-th to 90-th percentile takeoff counts per 15-minute bin over similar historical time-bins. Similar time-bins were chosen based on the detection of the same active runway configuration as the simulated configuration in those time-bins. For example, for the 16:30-16:45 UTC bin, we identified all 16:30-16:45 UTC bins over a period of three months (May-July 2016). Out of these bins, we identified those bins during which EWR had a North-flow runway configuration active. These identified same-configuration bins were used to compute the 10-th and 90-th percentile runway takeoff counts.

As seen from the left-hand side of **Figure 92**, the simulated takeoff counts follow the general trend of the actual runway takeoff counts, with three departure banks clearly visible. The discrepancies between simulated versus actual counts at the beginning and end of the simulation time-period can be attributed to the fact that we only included flights that pushed back after 09:00 UTC and before

18:00 UTC in the simulation. By doing so, we missed some of the departure flights at either end of the simulation time-period.

The right-hand side of **Figure 92** shows similar plot for the simulated versus actual gate out counts. Again, we see that the simulation followed the general trend of the actual counts with discrepancies at the beginning and end of the simulation timeframe attributed to flights that were by design not included in the simulation set.

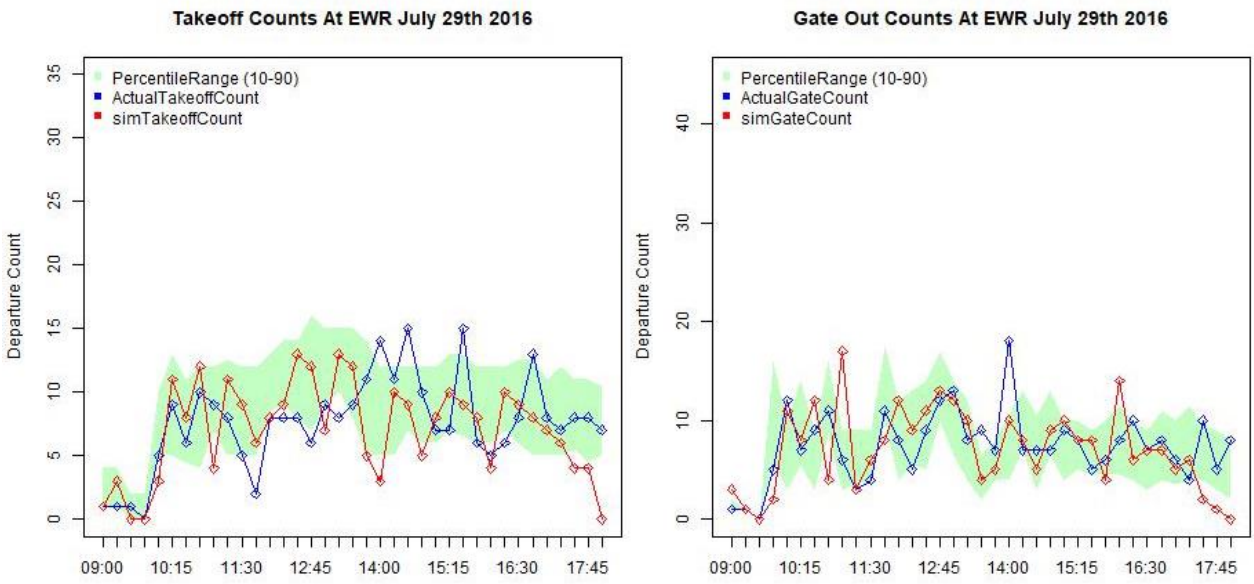

Figure 92. Runway Off and Gate Out Counts Validation – Simulation Versus Real Operations

Further, we also validated the taxi-out times by comparing simulated times against real historical operational taxi-out times from the same day as well as with a distribution of taxi-out times over similar days. **Figure 93** shows the comparison of simulated and actual taxi-out times, with AMA taxi-out time comparison showed in the left half of the figure and the total (AMA + Ramp) taxi-out time comparison shown in the right half of the figure. As seen from the figures, the taxi-out times do not match very closely, but simulated taxi-out times follow the general trend of the actual observed simulated taxi-times with a couple of peaks visible in both simulated and actual data. The discrepancies at the beginning and end of the simulation timeframe can again be attributed to the fact that we had excluded flights outside the 09:00-18:00 UTC timeframe from the simulation by design, whereas in the actual operations they appear in the taxi-out time plots. The discrepancies between actual and simulated taxi-out times outside the beginning and ending time-bins can be attributed to multiple factors including, erroneous actual Gate OUT time data, differences in the handling of departure takeoff clearances between actual operations and simulation (human local controller clearances may contain additional delays due to the fact that the local controller is handling multiple arrival and departure clearances at the same time), and differences in simulated versus actual ramp and spot merge handling.

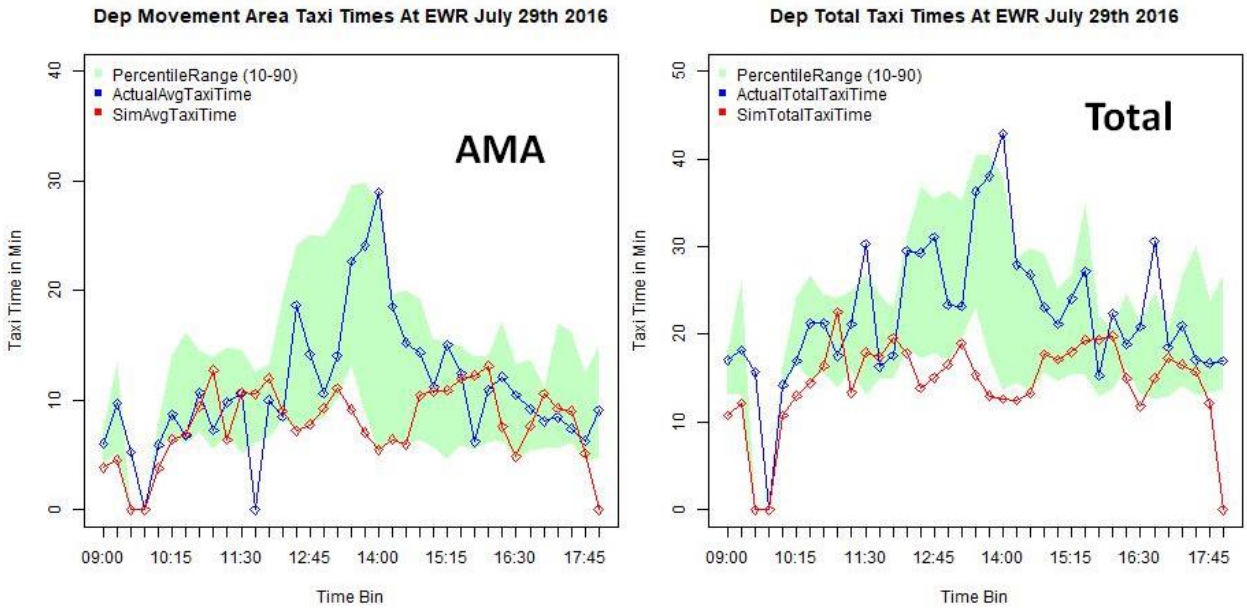

Figure 93. Taxi-Out Time Validation – Simulation Versus Real Operations

6.4.2.5. Analysis of Benefit Mechanism Contributions to ATD-2 Benefits

Analysis of simulation output data showed that two benefit mechanisms played a major role in providing taxi-out time savings. These were: (1) Demand throttling provided by Surface Departure Metering advisories (i.e., gate-holds) and (2) Data exchange and scheduling for TMI Coordination.

Benefit Mechanism #1: Demand throttling provided by Surface Departure Metering advisories (i.e., gate-holds). As discussed above, our ATD-2 simulations included a full emulation of NASA's ATD-2 Tactical Surface Scheduler, which computed gate delays for departure flights in order to reduce taxi-out times but at the same time keeping sufficient pressure on the departure runways. **Figure 94** shows that gate delay difference (i.e., ATD-2 simulation Gate OUT Time – Baseline simulation Gate OUT time) for each simulated departure flight. The right half of the figure shows a histogram of gate delay differences. We can see that the ATD-2 scheduler added a significant amount of gate delays over and above the baseline simulation. In the left half of the figure we show the gate delay difference plotted along the simulation timeline. This plot shows that the ATD-2 scheduler allocated majority of the gate delays during the time-periods when the departure demand on the EWR runways was at its peak, i.e., at or near the peaks of the two major departure banks included in the simulation. There are some gate delay difference points below the zero line in the plot on the left. These were flights that received higher gate delays in the baseline simulation because of active MITs to their destination airports. Here also, we see that the ATD-2 scheduler handled these flights with smaller gate delays than in the baseline simulation. This was an effect of more efficient coordination with the receiving Center, which included sending more accurate runway takeoff time estimates to the Center, and after the Center sends back the controlled runway release time computing the required gate release time using a more accurate taxi-out time estimate. This benefit mechanism is discussed later. For the demand throttling benefit mechanism that we are discussing here, it would suffice to observe that the ATD-2 scheduler correctly allocated gate delays during the especially busy peak time-periods.

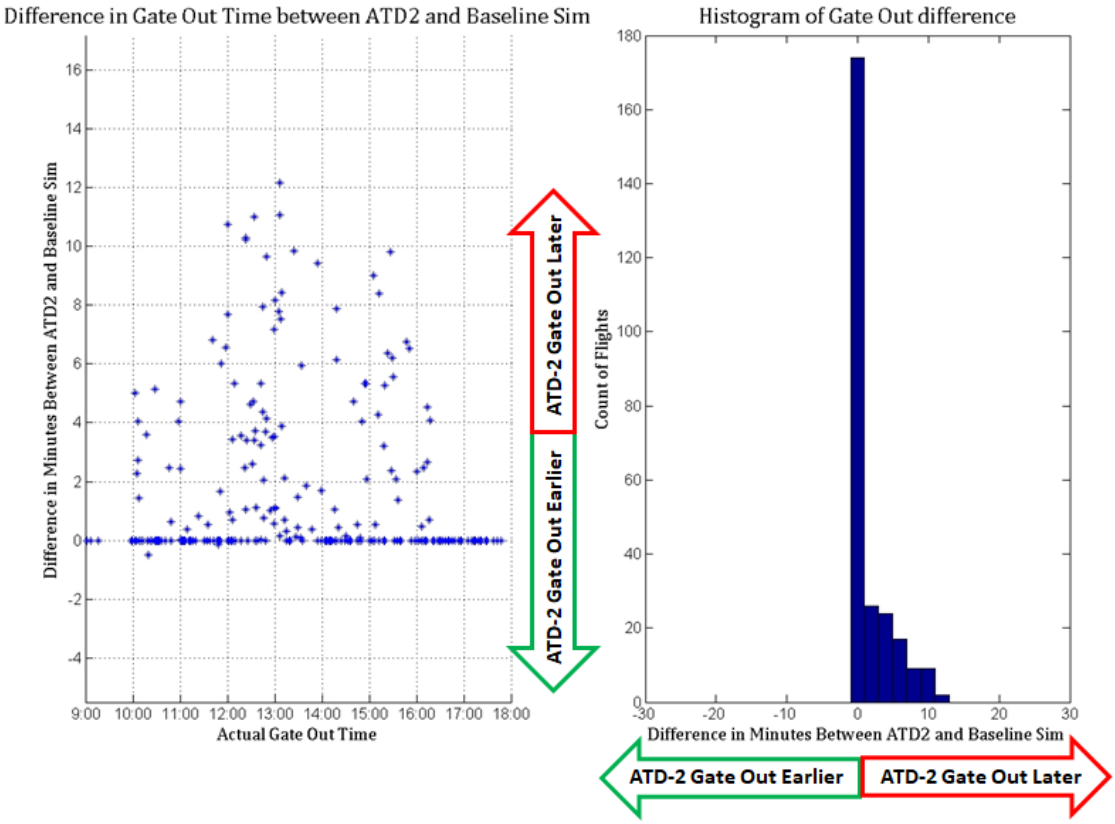

Figure 94. Gate Delay Difference, ATD-2 Operations – Baseline Operations

The beneficial effect that these tactical gate delays had on surface congestion can be seen in **Figure 95**. This figure plots the difference in Taxi-out Times (ATD-2 – Baseline) as a function of the difference in departure queue lengths experienced by the respective flights in the ATD-2 and Baseline simulations. As seen from the figure, ~50% of the flights experienced smaller departure queue lengths, a result of the demand throttling provided by the tactical scheduler allocated gate delays and as a result experienced shorter taxi-out times. Moreover, an additional ~23% flights experienced slightly longer queues in the ATD-2 operations, but still managed to have smaller taxi-out times. In the case of these flights, although there were more flights ahead of them in the departure queue when they reached the spot, the runway takeoff times for those flights were sufficiently spaced out as a result of the gate delays and hence the flight was able to take off after spending a smaller time in taxi. Around 6% of the flights experienced longer queues than the baseline simulation and as a result experienced longer taxi-out times, which is an indication that the ATD-2 scheduler settings may need fine tuning. It is our opinion that future efforts to assess different settings and algorithmic alternatives (e.g., taxi-out time prediction methods) in a fast-time simulation environment will be highly beneficial for optimizing the performance of the ATD-2 system in the field.

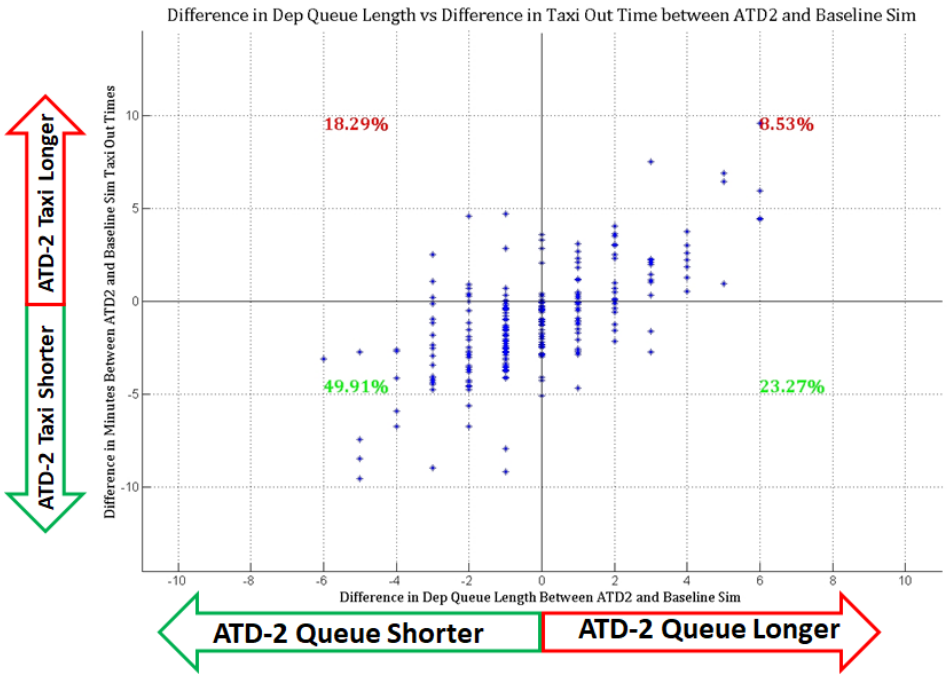

Figure 95. Taxi Out Time Difference (ATD-2 – Baseline) plotted as a function of Difference in Departure Queue Lengths Experienced by Flights at the Spot (ATD-2 – Baseline)

In summary, the demand throttling provided by ATD-2 Tactical Surface Scheduler-imposed gate delays contributed towards reducing the taxi-out times for departure flights in general. Next, we discuss another benefit mechanism, which we found especially beneficial for TMI-impacted departure flights.

We saw results similar to the EWR 7/21/2016 simulation for the second benefit mechanism.

6.5. Simulation-based Sensitivity Tests

In addition to the baseline versus ATD-2 operations simulations for multiple simulation days per airport, we also conducted three simulation-based sensitivity studies. These studies were the following:

1. Simulation study to assess the effects of each departure flight pushing back at exactly its Scheduled Off Block Time, focused on the CLT North Flow configuration
2. Simulation study to assess the benefits of adding Phase II functionality: Strategic Scheduler for optimum queue delay buffer parameter setting, focused on the relatively more challenging CLT South Flow configuration, and
3. Leverage a past simulation study to assess the benefits of adding Phase III Integrated Airspace Scheduling capability, focused on the New York airspace

6.5.1. Sensitivity study # 1: Effect of departure flights pushing back at their SOBTs

This sensitivity test looked at the impact of departure flights leaving their gates at exactly their SOBTs. Note that in all the simulations described so far we had added historical-data driven perturbations to the SOBTs to compute EOBTs and then Push Ready Times by perturbing the

EOBTs. In those simulations flights left their gates at their respective Push Ready Times, or at delayed times as per ATD-2 scheduler-computed TOBTs.

We conducted a separate sensitivity test simulation to check if pushback at SOBT will add more congestion and lead to additional taxi-out delays. For this sensitivity test, we ran the CLT North Flow, 5/6/2016 simulation scenario through the simulation platform, only this time we set the Push Ready Times equal to SOBTs. In other words, the flights were ready to pushback at their SOBTs.

Figure shows the comparison of taxi-out times for two scenarios – in red we show the taxi-times for the baseline simulation with flights being ready to pushback at the perturbed Push Ready Times; in blue we show the taxi-times for the baseline simulation with flights being ready to pushback at their SOBTs. We saw that having everyone pushback at their SOBTs added around 2% additional total taxi-out time, 6% additional AMA taxi-out time and 2% additional total transit time (gate-hold plus taxi-out time). There was a 3% reduction observed in the ramp area taxi-out times.

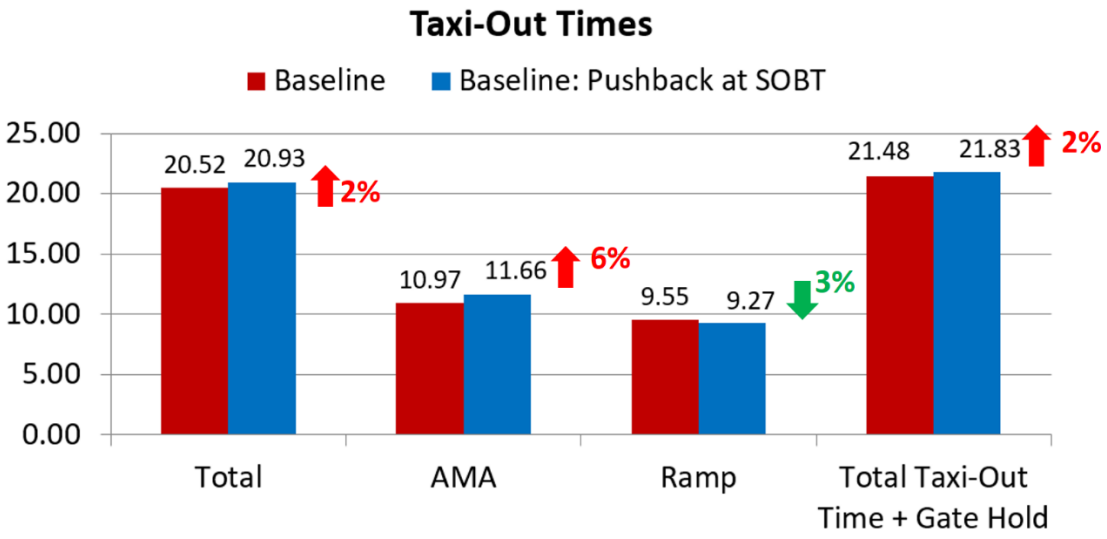

Figure 96. Sensitivity test shows that having flights pushback at their SOBTs will lead to ~2% increase in average total (AMA + ramp) taxi-out times

6.5.2. Sensitivity study #2: Effect of Phase II ATD-2 Strategic Scheduler on CLT operations

In this sensitivity study we assessed the added benefits of Phase II ATD-2 Strategic Scheduler on top of the Phase I ATD-2 Tactical Surface Scheduler. Phase II Strategic departure metering will provide the airlines and the ATCT controllers, as well as receiving Center traffic managers, with a reliable estimate of expected future departure traffic flows. This will enable the decision-makers to wisely choose the settings for ground departure metering programs such as metering start/end times and Taxi Delay Buffer values, as well as airspace TMI restrictions such as APREQs and MITs. The key metric that the Strategic Scheduler will provide to decision makers is an estimate of the expected Excess Taxi-out Time under different future settings of a departure metering program.

In our study we simulated the CLT North Flow, 6/2/2016 simulation scenario under the following three conditions:

- Condition # 1: Baseline (current-day) operations without any metering
- Condition # 2: ATD-2 operations with a choice of a static 5 minute Taxi Delay Buffer throughout the simulation timeframe
- Condition #3: ATD-2 operations with Taxi Delay Buffer values chosen based on the Strategic Scheduler estimates of future expected excess taxi-out time values

Figure X shows plots of Excess Taxi-Out Times per departure flight as a function of the simulated takeoff time, for the three conditions described above. The left-most plot, showing excess taxi-out times for departure flights when departure metering is OFF, shows high excess taxi-out times during the 13:00 to 14:00 UTC time period, with smaller (< 5 minutes) excess taxi-out times at other times in the simulation timeframe. The middle plot, showing excess taxi-out times for departure flights with ATD-2 departure metering ON but using a static 5 minute Taxi Delay Buffer, shows that the ATD-2 scheduler was successful in somewhat reducing the taxi-out times, but there are still a lot of flights with excess taxi-out times between 5 to 20 minutes; and that there is significant room for improvement by carefully selecting appropriate Taxi Delay Buffers during specific time periods. In the right-most plot, we show results from a Phase II ATD-2 system simulation where Strategic Scheduling was first applied to estimate excess taxi-out times, identify that large excess taxi-out times are expected during 13:00 to 14:00 UTC, and then accordingly design the Taxi Delay Buffer of 2 minutes during the 12:30 to 14:00 UTC timeframe and 5 minutes outside it (as shown on the figure). The right-most excess taxi-out times plot shows that the Phase II ATD-2 system successfully reduced the excess taxi-out time for a majority of the flights, with only two flights having excess taxi-out times greater than 10 minutes now. There are still a lot of flights with excess taxi-out times between 5 and 10 minutes. This inefficiency can be handled by fine tuning the ATD-2 scheduling algorithm in the future.

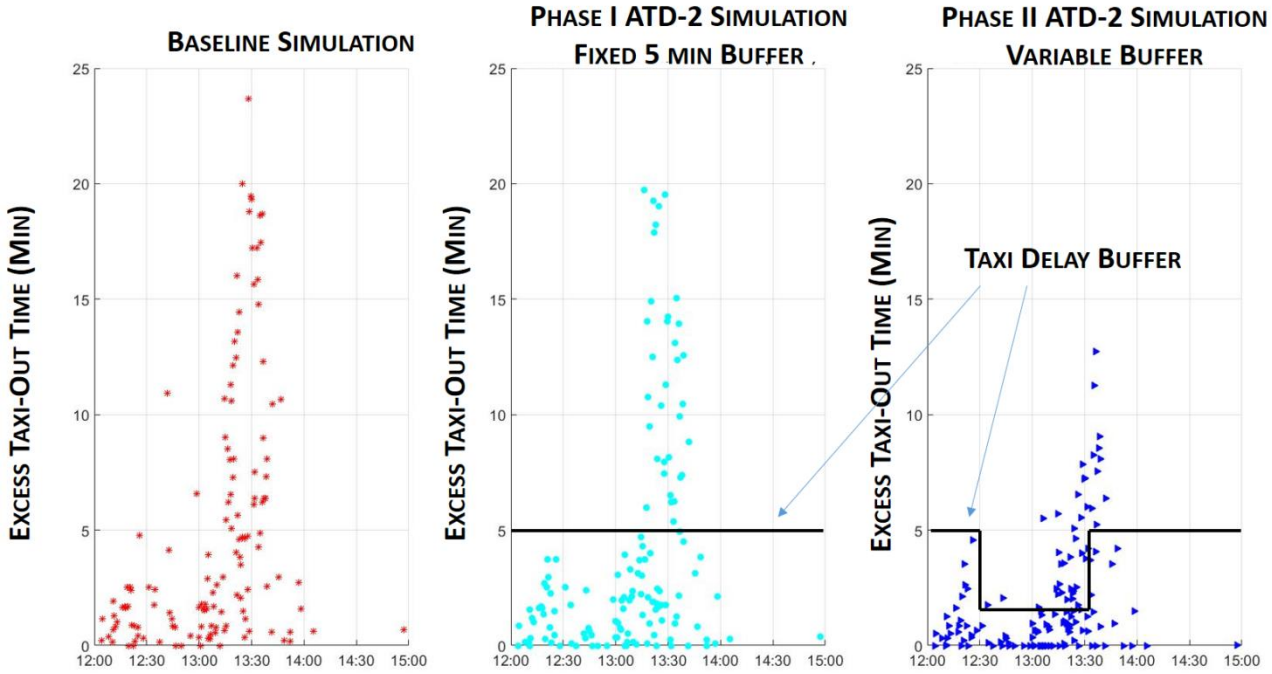

Figure 97. Phase II ATD-2 system showed significant taxi-delay savings benefit over the Phase I ATD-2 system

6.5.3. Sensitivity Study # 3: Phase III Hierarchical Multi-airport Airspace Scheduling

This sensitivity study leveraged a past research effort performed by our team members [SL14]. This past effort studied the impact of implementing a hierarchical airspace-surface scheduling system at the New York TRACON. As shown in **Figure 98**, this hierarchical system consists of a metroplex Departure Manager (mDMAN) that inputs external departure constraints and fix crossing schedules for all New York TRACON departures and develops Target Takeoff Times (TTOTs) for departures from all underlying airports. For each major airport (JFK, EWR, LGA, TEB), TTOTs are sent to that airport's dedicated Surface Manager (SMAN) whereas for less-equipped airports the TTOTs are communicated to the ATCTs who are responsible for adhering to them. For the major airports, the SMAN computes Target Movement Area Entry Times (TMATs) and perhaps also Target Off Block Times (TOBTs) that adhere to the mDMAN TTOTs and at the same time balance the airports departure and arrival demand to the runway system capacity.

In addition to computing TTOTs, the mDMAN also computes departure route reallocations for balancing the traffic demand on busy departure fixes in the metroplex.

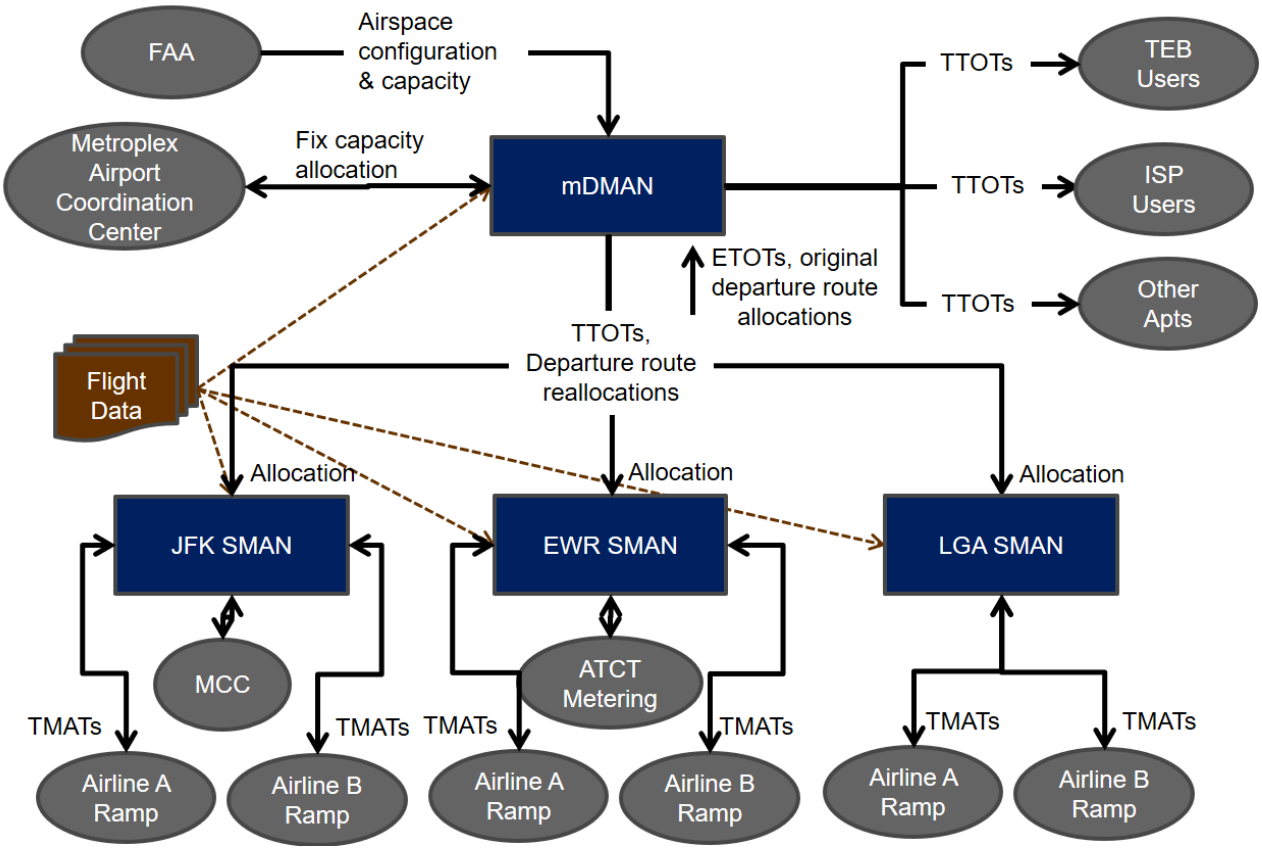

Figure 98. Hierarchical Surface-Airspace Scheduling Architecture for New York TRACON

The past research effort conducted a simulation-based study to assess the benefits of implementing such a hierarchical scheduling system at New York. As shown in **Figure 99**, our simulations showed that on an average scheduling can save around 1.5 minutes of taxi and airborne delay per departure without re-routing and if re-routing was also used then it could save around 3.4 minutes of taxi and airborne delay.

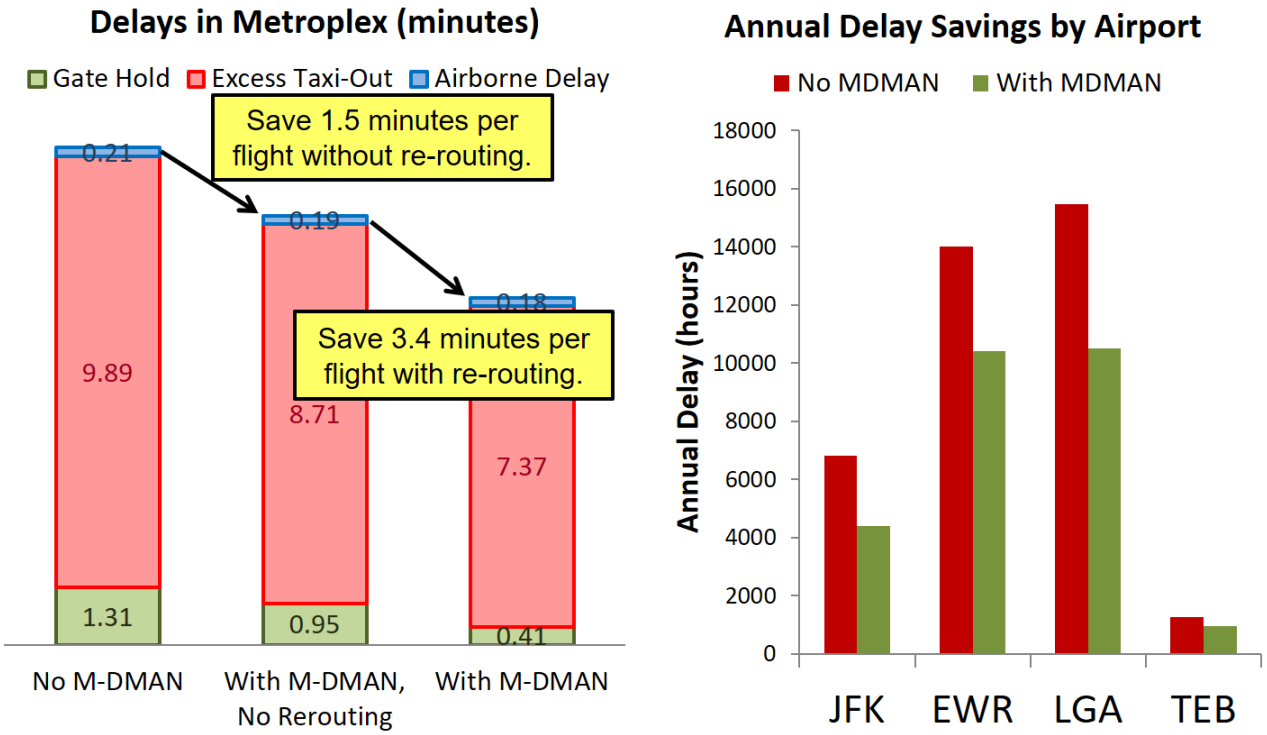

Figure 99. Simulations showed significant taxi and airborne delay savings potential for a hierarchical multi-airport departure metering solution at the New York TRACON

Figure 100 shows that there is significant reduction in taxi-out times with the variable taxi delay buffer in the Phase II ATD-2 system as compared to the Phase I ATD-2 system.

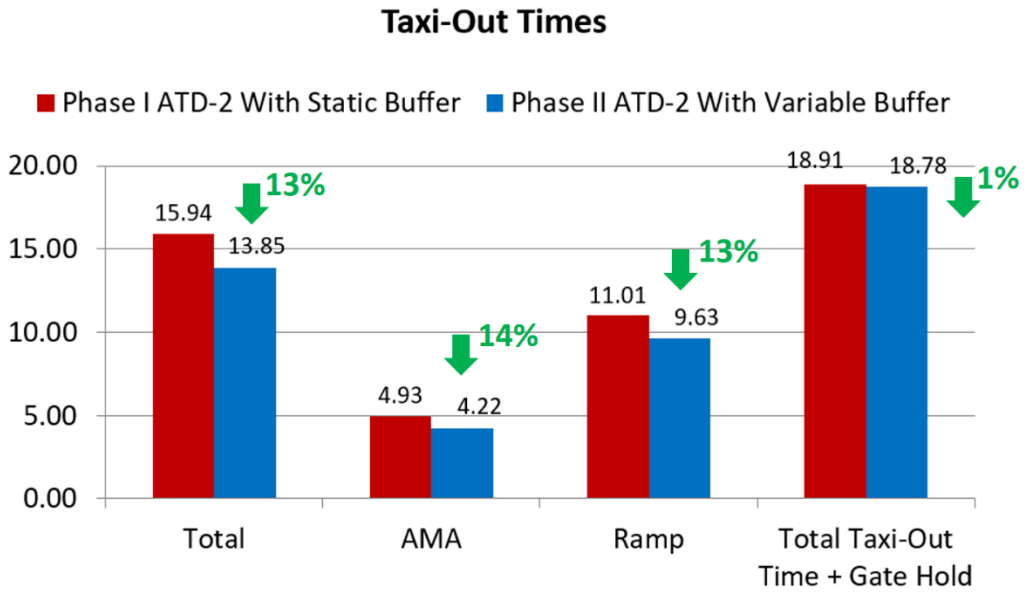

Figure 100. Sensitivity test shows that Phase II ATD-2 system can add significant benefits on top of the Phase I ATD-2 system

6.6. Lessons Learned from High-fidelity Simulations

Section 6.1 presented numerical data on the key benefit metric computed from the high-fidelity simulations (taxi-out time savings). Sections 6.2-6.4 presented more details in terms of deeper dive into the benefits, impacts on ON-time performance and airport throughput, validation of simulation models, as well as apportioning the benefits to individual benefit mechanisms. This section summarizes the key lessons from high-fidelity simulations.

Although our simulations demonstrated that significant benefits can be obtained by implementing the ATD-2 system at the three study airports, they also showed that there is room for enhancing ATD-2's benefits potential by improving the ATD-2 scheduling algorithms, data exchange processes, and traffic flow management procedures. The main lessons learned from the high-fidelity simulations in this respect were the following:

(1) Accuracy of the Earliest Runway Usage Time (ERUT) estimates provided to the ATD-2 Surface Tactical Scheduler has a significant impact on the performance of the departure operations. Accuracy of Earliest Off Block Times (EOBTs) received from the airlines has a significant influence on the ERUT accuracy. Taxi-out Time estimate accuracy is another big influencing factor. The impact of ERUT uncertainty is especially large during time-periods when a mixed-use runway (e.g., 18C or 36C/36R at CLT) or the arrival runway among a pair of parallel dependent runways (e.g., 35L-35C pair at DFW, 22L-22R pair at EWR) is experiencing heavy arrival throughput. In these situations, if the scheduler gets the ERUT for departures even slightly wrong, then a small error may be enough to put the departure behind a batch of arrivals in the scheduler timeline, causing excess gate delays. In fact, ERUT uncertainty has a significantly larger impact on departure metering operations at airports like DFW and EWR where a runway is not shared between arrivals and departures, but there is dependency between arrival and departure operations on parallel runways (the arrival runway in this case receives more sustained flow of arrivals). At these airports, the ATD-2 scheduling algorithm and ERUT estimation process may need to be modified to obtain the maximum benefit.

(2) The ATD-2 method of using a single Desired Excess Queue Time parameter for each departure runway can be improved to better manage the uncertainty in taxi-out transit times. Taxi transit time uncertainty varies depending upon the gate-runway pair for the flight. It may be worthwhile testing out an alternative methodology for back-computing the Target Off Block Time (TOBT) from the Target Takeoff Time (TTOT) using gate-runway pair dependent Desired Excess Queue Time estimate.

(3) Certain runway configurations present unique scheduling challenges. For example, the CLT South-flow configuration is especially challenging because of the proximity of the ramp exit points to the runway departure ends. In our simulations, although we did see positive taxi-out time savings for CLT South-flow configuration simulations, the savings were smaller than the respective savings in CLT North-flow simulations. Besides, when gate delays were added to the taxi-out times to account for the full transit time, the savings were even further reduced. Moreover, long queues extending back into the ramp areas were frequently observed in the CLT South-flow simulations even under active ATD-2 departure metering.

(4) Prioritization rules in the ATD-2 scheduling algorithm sometimes cause big jumps in gate delays, especially near the time-points where a departure flight moves from "Uncertain" to "Planned" status and from "Planned" to "Ready" status in the scheduling hierarchy. In some cases, complex interactions between individual flight EOBT or Push Ready times and the prioritization rules cause certain flights to be penalized by excessive gate delays.

(5) For EWR, a single airport metering solution may not work. A multi-airport ATD-2 system, where departure metering is performed in a hierarchical manner, is recommended. For example, departure-fix de-confliction performed at the TRACON level by an Airspace Scheduler with individual Surface Schedulers at each major New York airport performing airport-level departure metering, and takeoff time constraints imposed by the Airspace Scheduler on the Surface Schedulers. The DFW airspace may also benefit from such a hierarchical scheduling framework.

This concludes our discussion of results from the high-fidelity simulations. After completing the simulations, performance metrics and other data were sent to the downstream tasks that performed extrapolation of benefits to the nationwide benefits and annualized benefits, as well as converted the time savings to monetized savings on a nationwide and annualized scale. **Figure 101** shows the inter-relationship between the high-fidelity simulation task and the downstream extrapolation/ monetization tasks. The next two sections (Sections 7 and 8) discuss the extrapolation and monetization tasks.

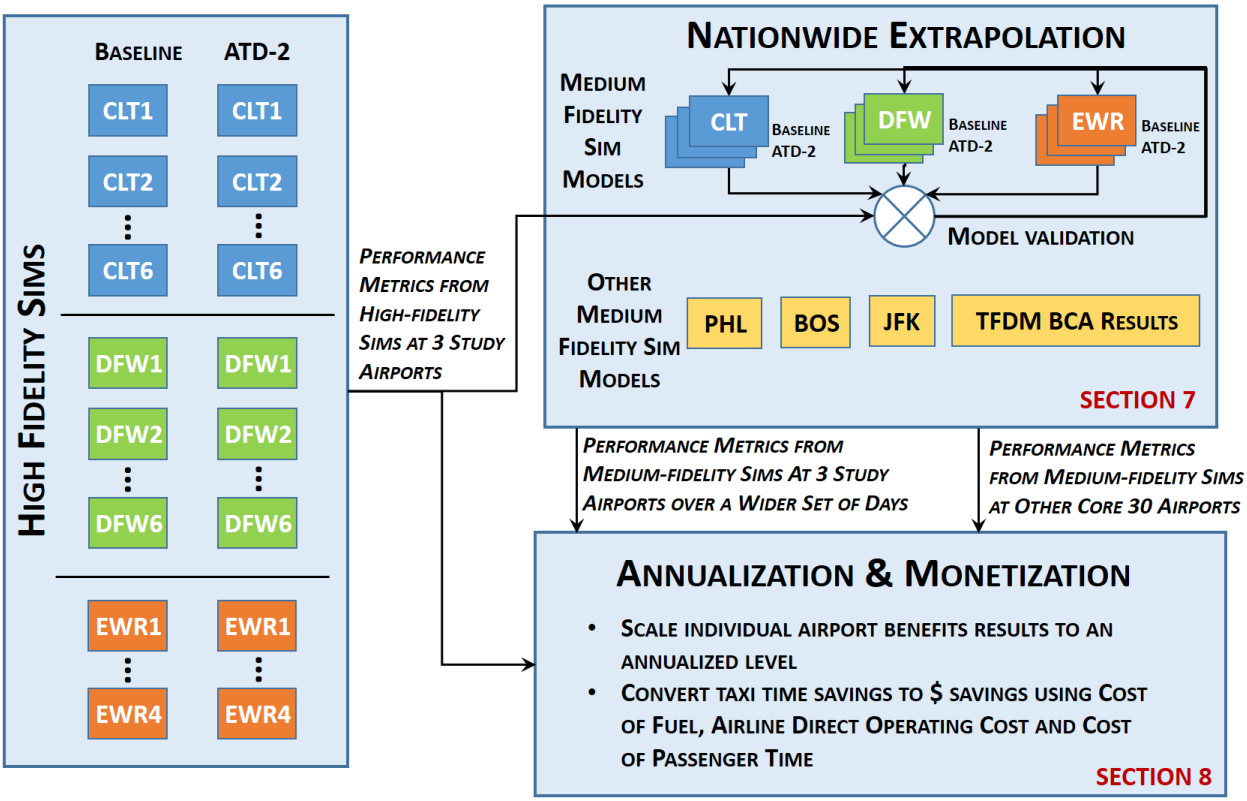

Figure 101. Inter-relationship between the high-fidelity simulation and downstream extrapolation/monetization tasks

7. BENEFITS EXTRAPOLATION TO NATIONWIDE BENEFITS

7.1. Medium-Fidelity Queuing Network Models

The generalization to a wider range of airports involved the development of medium-fidelity queuing network models for the major airports. These models focused on modeling the aggregate queuing behavior at the runway thresholds and, when needed, the ramp areas. These models considered major flows/configurations, and the number of departure runway servers needed. We also implemented the ATD-2 logic within the queueing network simulation environments. In order to draw comparisons to the SOSS simulations, we describe the models for CLT, EWR and DFW in detail, along with their validation. We then present the benefits from ATD-2 departure metering, as evaluated by the medium-fidelity models, and compare them with the SOSS simulations of the same when possible.

7.1.1. CLT queuing network models

7.1.1.1. North-Flow configuration

We first consider CLT in the North-Flow configuration. Figure 102 shows the layout of CLT in this configuration, along with the locations of various queues. It also shows the resulting queuing network model that we use to predict and simulate taxi operations.

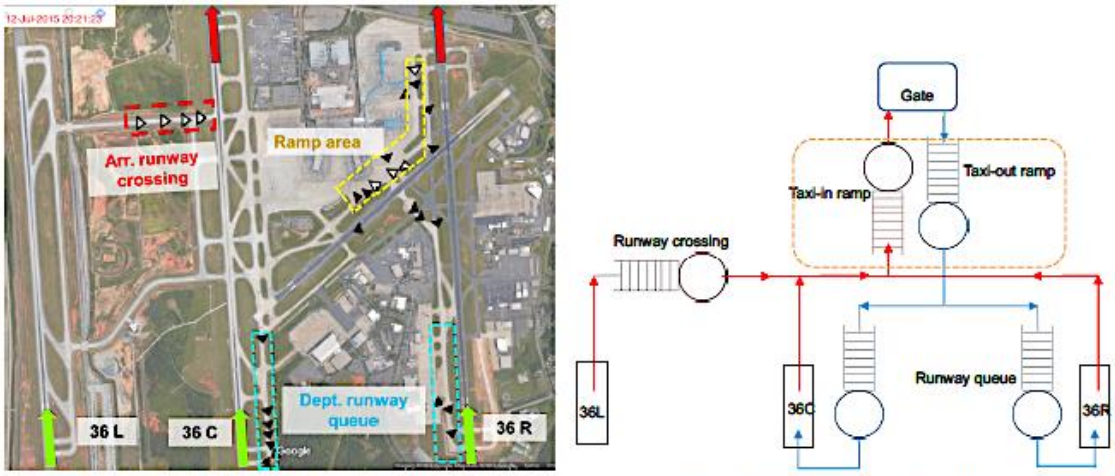

(a) Airport layout with a snapshot of aircraft positions (b) Queuing network representation

Figure 102. (a) Airport layout for Charlotte Douglas International airport (CLT) in the North-Flow. Flights taxiing-in and taxiing-out are represented by gray and black triangles, respectively. The ramp queues and departure runway queues are shown in yellow and cyan, respectively. The taxi-in runway crossing queue is shown in red. Departure runways are indicated with red arrows and arrival runways with green arrows. (b) Queuing network model for the airport surface, the taxi-in queues shown in red and taxi-out queues shown in blue.

The service rates for the queue servers are determined from operational data. In particular, the service rates for the taxi-out (and taxi-in) ramp servers are conditioned on the taxi-in (and taxi-out) ramp queue lengths, in order to reflect the interactions between arrivals and departures in the ramp area. The service times of the departure runway servers are each conditioned on the number of arrivals on that runway, in addition to the prevailing meteorological conditions. Finally, active runway crossings at CLT occur at two points on the runway close to one another. We treat them as

two parallel, independent servers. The distribution of time between two successive crossings is learned from data, using intervals which had a non-zero runway crossing queue length.

We validate the model by considering its performance in predicting baseline (current) operations. The results of this validation are shown in **Table 22**.

Time (minutes)	Gate-to-spot	Spot-to-runway	Taxi-out	Taxi-in
Mean value	9.7	10.5	20.2	10.2
Mean error	-0.3	1.0	0.7	0.5

Table 22. Validation of North-Flow queuing model of CLT using simulation of baseline operations. The test set comprised of 14,122 departures and 16,383 arrivals.

Figure 103 shows the different queue length predictions and actual values for a particular day (June 25, 2016).

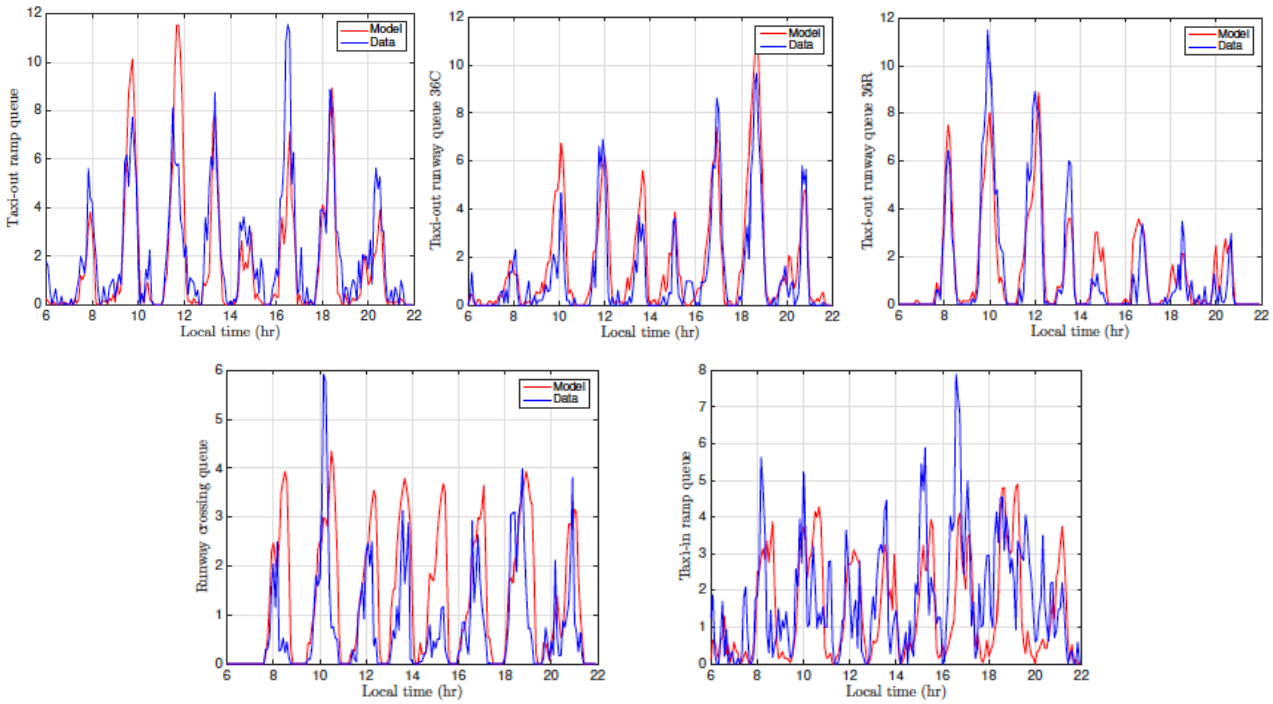

Figure 103. (Clockwise, from top left) Actual and modeled taxi-out ramp queue, runway queues for 36 C and 36R, taxi-in ramp queue, and runway crossing queue lengths on 6/25/2016.

7.1.1.2. South-Flow configuration

We use a similar modeling approach for CLT in the South-Flow configuration. **Figure 104** shows the layout of CLT in this configuration, along with the locations of various queues. It also shows the resulting queuing network model that we use to predict and simulate taxi operations.

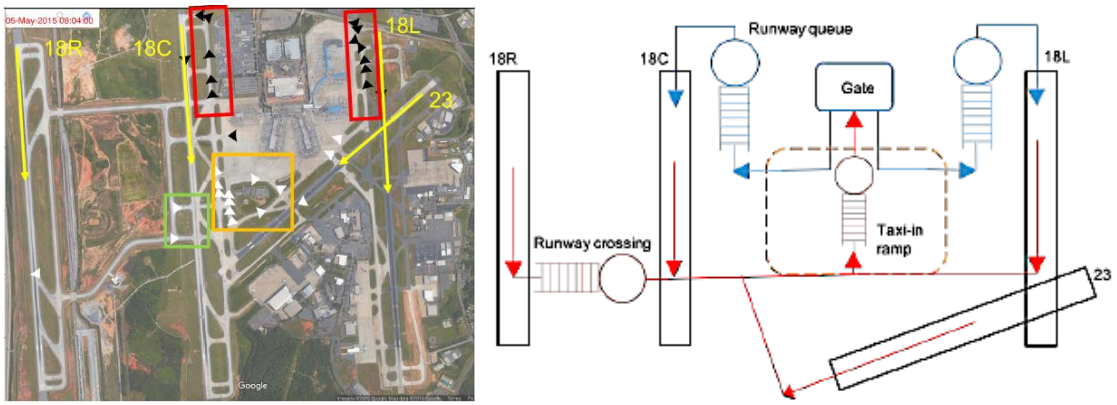

Figure 104. (a) Airport layout for CLT in the South-Flow. The flights taxiing-in and those taxiing-out are represented by white and black triangles, respectively. The ramp queues and departure runway queues are orange and red, respectively. The taxi-in runway crossing queue is shown in green. (b) Queuing network model for the airport surface.

In particular, taxi-in flights in this configuration queue-up on the active movement area before entering the ramp area. Secondly, the departure runway queue for 18L regularly spills into the ramp area. The arrivals landing on 18R need to cross the departure runway (18C), leading to

a runway crossing queue. The arrivals on the cross runway (23) are synchronized with the takeoffs on 18L in a way that leads to a small impact on the departures. The departure runway service time distribution for 18L is modelled as a function of the weather (VMC/IMC), and the number of landings on the departure and crossing runways in a given time period.

We validate the model by considering its performance in predicting baseline (current) operations. The results of this validation are shown in **Table 23**.

Time (minutes)	Taxi-out	Taxi-in
Mean value	19.7	11.6
Mean error	-0.8	0.3

Table 23. Validation of South-Flow queuing model of CLT using simulation of baseline operations. The test set comprised of 7,069 departures and 7,499 arrivals.

7.1.1.3. Simulation of ATD-2 metering at CLT

We simulate the ATD-2 logic within our queuing network models over a three-month period between May-July 2016. We consider days which were predominantly in a single "flow", and for which ASDE-X data was mostly available. The simulations therefore span 35 days in the North-Flow and 20 days in the South-Flow. We also consider the effect of the "excess queue parameter" on the impacts of metering. This variation is shown in **Table 24**.

Excess queue parameter →	**4 min**	**6 min**	**8 min**	**10 min**	**12 min**
Mean hold time over all flights	**4.0**	**2.9**	**2.1**	**1.5**	**1.1**
Fraction of flights held	0.7	0.6	0.5	0.4	0.3

Mean hold time of flights held	5.4	4.7	4.3	4.1	3.7
Fraction of flights held >2 min	0.6	0.4	0.3	0.3	0.2
Mean hold time of flights held > 2min	6.6	6.1	5.7	5.5	5.2
Taxi-out time reduction	**2.8**	**2.6**	**2.1**	**1.6**	**1.2**
% Taxi-out time reduction	**13.2%**	**12.3%**	**9.8%**	**7.5%**	**5.7%**
Mean change in OFF time	1.1	0.3	0.0	-0.1	-0.1

Table 24. Variation of impacts of ATD-2 on CLT North-Flow operations (15,718 departures) with the excess queue parameter. The analysis suggests that a value of 8 min provides the right balance between congestion and runway utilization, resulting in taxi-out time savings that are commensurate with the hold times, and not adversely impacting the takeoff times.

As mentioned earlier, SOSS was used to conduct high-fidelity simulations of the baseline and ATD-2 operations on three days in the CLT North-Flow, namely, 5/6/2016, 5/31/2016, and 6/1/2016. **Figure 105** shows the comparisons of the baseline and ATD-2 simulations, in terms of baseline taxi-out times, metering gate hold times, and taxi-out time savings from ATD-2, using both the queuing model and SOSS.

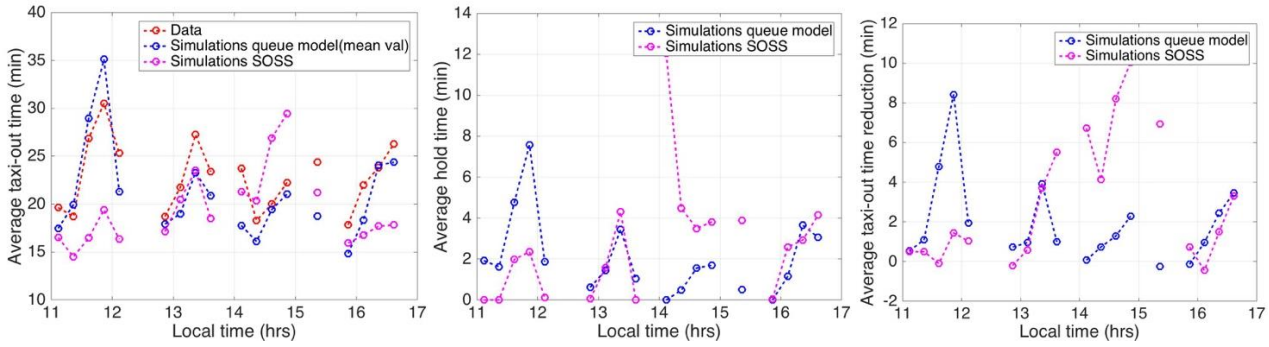

Figure 105. Comparisons of baseline and ATD-2 metering simulations using the queuing network models and SOSS at CLT in the North-Flow, excess queue parameter of 8 min. (Left) The baseline simulations also show comparisons of the average taxi-out time from the queuing model and SOSS simulations to actual data. (Center) Comparison of gate hold times, and (Right) Comparison of taxi-out time reductions.

Excess queue parameter →	**5 min**
Mean hold time over all flights	**2.1**
Fraction of flights held	0.6
Mean hold time of flights held	3.7
Fraction of flights held >2 min	0.4
Mean hold time of flights held > 2min	5.2
Taxi-out time reduction	**2.0**
% Taxi-out time reduction	**10.7%**

Mean change in OFF time	0.1

Table 25. Impacts of ATD-2 on CLT South-Flow (7,069 dep), excess queue parameter of 5 min.

SOSS was used to conduct high-fidelity simulations of the baseline and ATD-2 operations on three days in the CLT South-Flow, namely, 5/17/2016, 6/2/2016, and 6/15/2016. **Figure 106** shows the comparisons of the baseline and ATD-2 simulations, in terms of baseline taxi-out times, metering gate hold times, and taxi-out time savings from ATD-2, using both the queuing model and SOSS.

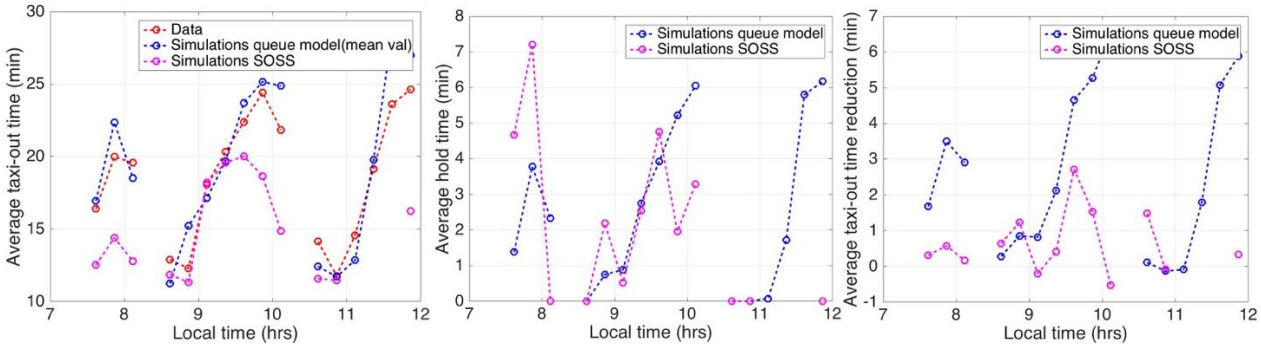

Figure 106. Comparisons of baseline and ATD-2 metering simulations using the queuing models and SOSS at CLT in the South-Flow, excess queue parameter of 5 min. (Left) Baseline simulations. (Center) Comparison of gate hold times, and (Right) Comparison of taxi-out time reductions.

7.1.1. EWR queuing network models

The queuing model for taxi-out operations at EWR in the North-Flow consists of a single queue for the departure runway. Since the data suggests that unlike CLT (where departures spend nearly 50% of the taxi-out time in the ramp), departures in EWR spend much less time in the ramp area, we do not explicitly model the ramp server. The service time for the departure runway system is conditioned on the number of arrivals on the runway and weather condition (VMC/IMC), and learned from data. A very similar model (with different service time distributions) is identified for the South-Flow at EWR.

Figure 107. (Left) Airport layout for EWR in North-Flow; (Center) Taxi-in and taxi-out trajectories in the North-Flow, and (Right) Airport layout in the South-Flow.

We validate the model by considering its performance in predicting baseline (current) operations. The results of this validation are shown in **Table 26**.

Time (minutes)	**North-Flow**		**South-Flow**	
	Taxi-out (9,251 flts)	**Taxi-in** (8,123 flts)	**Taxi-out** (16,349 flts)	**Taxi-in** (15,753 flts)
Mean value	21.3	9.4	20.1	9.4
Mean error	0.2	-0.1	0.6	-0.5

Table 26. Validation of queuing models of EWR using simulations of baseline operations.

7.1.1.1. Simulation of ATD-2 metering at EWR

We simulate the ATD-2 logic within our queuing network models over a three-month period between May-July 2016. We consider days on which EWR was predominantly in a single configuration/flow, and for which ASDE-X data was mostly available. The simulations therefore span 40 days in the North-Flow and 48 days in the South-Flow. We consider excess queue parameters of 8 min and 15 min in the North-Flow, to evaluate the impacts (**Table 27**). We choose a value of 15 min in the remaining simulations in order to enable comparisons with SOSS, but note that an excessive queue parameter of 8 min could yield significantly more taxi-out time savings without adversely impacting the runway utilization.

Excess queue parameter →	**8 min**	**15 min**
Mean hold time over all flights	**1.4**	**0.3**
Fraction of flights held	0.3	0.1
Mean hold time of flights held	4.1	3.8
Fraction of flights held >2 min	0.2	0.1
Mean hold time of flights held > 2min	5.7	5.4

Taxi-out time reduction	**1.2**	**0.1**
% Taxi-out time reduction	**5.8%**	**0.6%**
Mean change in OFF time	0.2	0.2

Table 27. Variation of impacts of ATD-2 on EWR North-Flow operations (9,251 departures) with the excess queue parameter.

As mentioned earlier, SOSS was used to conduct high-fidelity simulations of the baseline and ATD-2 operations on two days in the EWR North-Flow, namely, 5/6/2016 and 7/29/2016. **Figure 108** shows the comparisons of the baseline and ATD-2 simulations, in terms of baseline taxi-out times, metering gate hold times, and taxi-out time savings from ATD-2, using both the queuing model and SOSS. **Table 28** shows the expected impacts of ATD-2 on South-Flow operations.

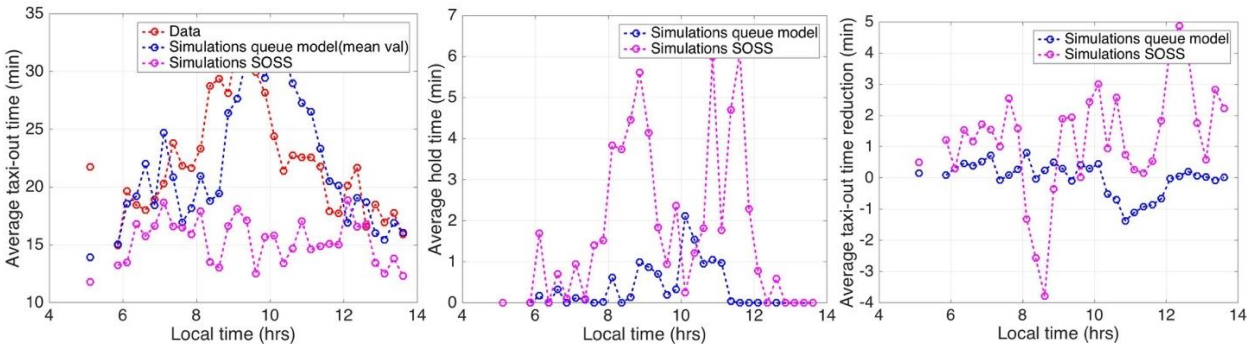

Figure 108. Comparisons of baseline and ATD-2 metering simulations using the queuing network models and SOSS at EWR in the North-Flow on 7/29/2016, excess queue parameter of 15 min. (Left) The baseline simulations also show comparisons of the average taxi-out time from the queuing model and SOSS simulations to actual data. (Center) Comparison of gate hold times, and (Right) Comparison of taxi-out time reductions.

Excess queue parameter →	**12 min**
Mean hold time over all flights	**0.4**
Fraction of flights held	0.2
Mean hold time of flights held	2.5
Fraction of flights held >2 min	0.1
Mean hold time of flights held > 2min	4.3
Taxi-out time reduction	**0.4**
% Taxi-out time reduction	**2.0%**
Mean change in OFF time	0.0

Table 28. Impacts of ATD-2 on EWR South-Flow (7,069 dep), excess queue parameter of 12 min.

7.1.2. DFW queuing network models

South-Flow is the primary runway configuration at DFW. The airport operated in South-Flow for around 80% of the time during May-July 2016. The queuing models for taxi-out operations at DFW consist of a single queue for each departure runway. The parameters for the queue model were conditioned on the prevailing weather conditions (VMC/IMC), and determined using data from May-June 2016. The mean time for each runway-gate combination was used to predict the taxi-in times. We validate the models by considering their performance in predicting baseline (current) operations. The results of this validation are shown in **Table 29**.

Time (minutes)	North-Flow		South-Flow	
	Taxi-out (6,788 flts)	**Taxi-in** (6,349 flts)	**Taxi-out** (53,513 flts)	**Taxi-in** (51,577 flts)
Mean value	18.7	10.1	16.8	11.2
Mean error	-0.6	-0.0	0.0	0.23

Table 29. Validation of queuing models of DFW using simulations of baseline operations.

To enable comparisons with the SOSS simulations, we adopt an excess queue parameter of 10 min in North-Flow and 12 min in South-Flow. **Table 30** shows the expected impacts of ATD-2 from the queuing network simulations of the North and South Flows.

Excess queue parameter →	**N-Flow 10 min**	**S-Flow 12 min**
Mean hold time over all flights	**0.8**	**0.3**
Fraction of flights held	0.2	0.1
Mean hold time of flights held	3.7	2.9
Fraction of flights held >2 min	0.1	0.1
Mean hold time of flights held > 2min	5.2	4.7
Taxi-out time reduction	**0.8**	**0.4**
% Taxi-out time reduction	**4.2%**	**2.1%**
Mean change in OFF time	0.1	0

Table 30. Impacts of ATD-2 on DFW North-Flow (6,788 dep), excess queue parameter of 10 min, and South-Flow (53,513 dep) with an excess queue parameter of 12 min.

7.2. Simulated impact of ATD-2 on taxi-out time distributions

A key advantage of the medium-fidelity queueing network models is that they enable fast-time simulations of operations on a large number of days. **Figure 109**-**Figure 111** compare the taxi-out time distributions at CLT, EWR and DFW, with and without ATD-2. The benefits of ATD-2 are apparent from the leftward shift of the taxi-out time distributions, indicating a decrease in the number/proportion of flights with long taxi-out times. The figures also show that the most benefits are likely to be experienced at CLT (in both the North- and South-Flows), followed by DFW (especially in the North-Flow). Similar to the findings from the SOSS simulations, it appears that EWR may see the least benefits from ATD-2 metering. One reason for this is that the queuing

network models do not consider benefit mechanisms such as APREQ management and improved merges into the overhead stream, and the purely ground-based benefits of departure metering at EWR may be quite limited.

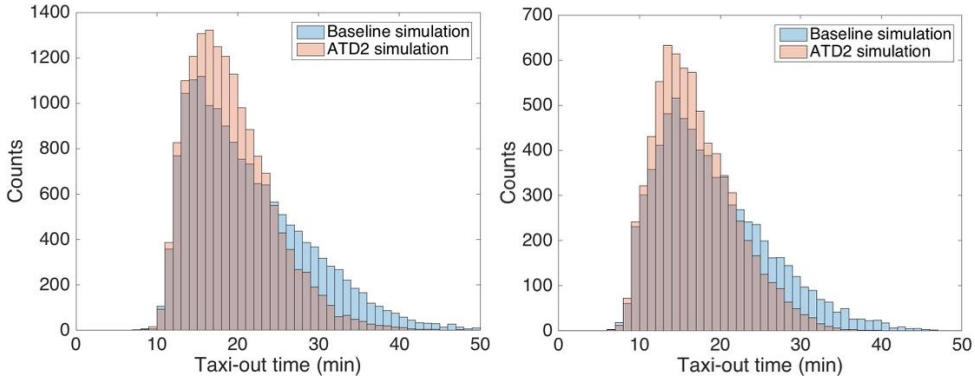

Figure 109. Estimated impact of ATD-2 on taxi-out time distributions at CLT in (Left) North and (Right) South Flows.

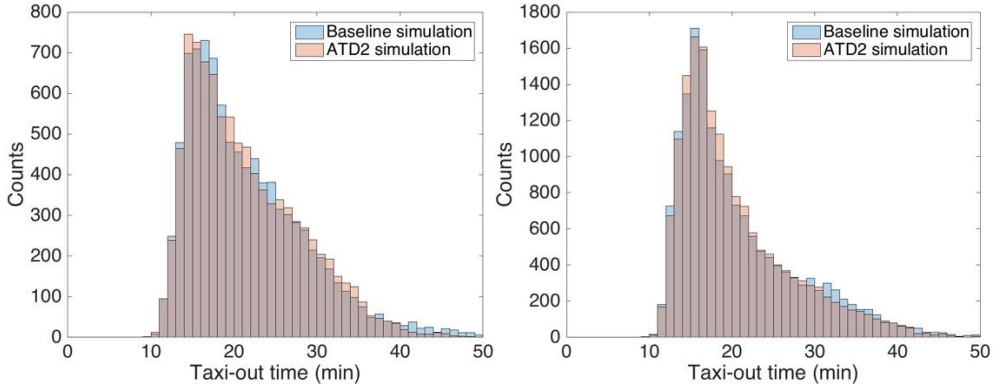

Figure 110. Estimated impact of ATD-2 on taxi-out time distributions at EWR in (Left) North and (Right) South Flows.

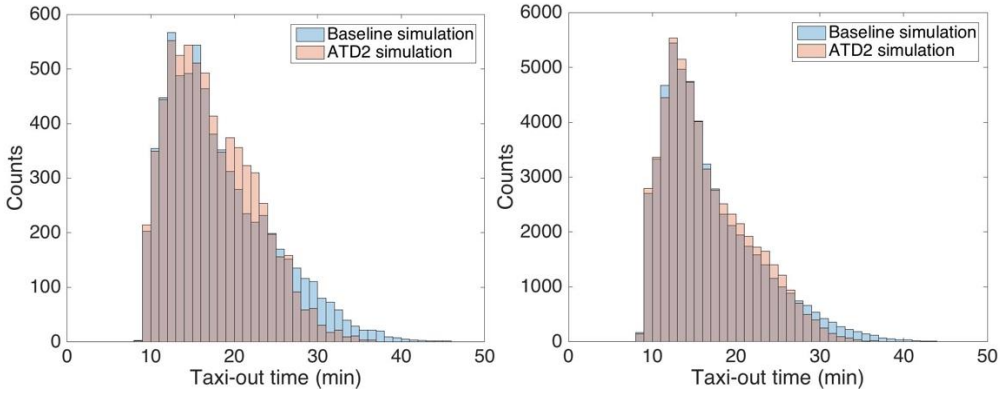

Figure 111. Estimated impact of ATD-2 on taxi-out time distributions at DFW in (Left) North and (Right) South Flows.

7.3. Translating queuing model benefits to SOSS benefits

As we have seen earlier, the SOSS simulations are higher-fidelity than the queuing model simulations, and models more refined benefits mechanisms (such as APREQs) than the queuing network models, which only reflect departure metering to alleviate surface congestion. Therefore, simulations of the same day (and underlying conditions) using the two different models can result in different estimates of taxi time reduction. **Table 31** shows the comparisons of the percentage reduction in taxi-out time estimated by the two approaches, for the same set of days that were used in the SOSS simulations. Using this table (and adopting the median scaling factor in order to minimize the impact of outliers), it appears that a factor of 1.9 may be used to approximate the taxi-out time benefits of a SOSS simulation, given those of a queuing model simulation.

Airport	Configuration	Date	% taxi-out time reduction				Scaling factor
			Queue model		SOSS		
CLT	North-Flow	5/06/2016	10.7	13.4	15.1	7.4	1.4
		5/31/2016	14.4		3.8		0.3
		6/01/2016	12.8		9.0		0.7
	South-Flow	5/17/2016	12.2		5.7		0.5
		6/02/2016	14.9		5.8		0.4
		6/15/2016	13.9		9.8		0.7
DFW	North-Flow	5/12/2016	5.6	1.4	8.2	9.5	1.5
		6/04/2016	1.3		14.0		10.5
	South-Flow	6/03/2016	0.6		8.4		13.1
		7/05/2016	1.4		10.6		7.7
		7/17/2016	4.6		10.7		2.3
		7/28/2016	0.5		6.4		11.7
EWR	North-Flow	5/06/2016	1.3	1.0	9.7	8.5	7.5
		7/29/2016	0.1		7.2		91.9
	South-Flow	7/03/2016	0.6		21.8		34.9
		7/21/2016	7.8		6.6		0.8
Median values			**5.1**		**8.7**		**1.9**

Table 31. Comparison of percentage taxi-out time reductions, as estimated by a queuing model and SOSS. The median scaling factor (that can be used to translate queuing model benefits to prospective SOSS benefits) is 1.9.

7.4. Extension to Other Major Airports

We leverage prior analysis of congestion that was developed in [SB14] to evaluate the pool of benefits from aggregate departure metering strategies such as N-Control [SSB14]. We present the aggregate analyses from [SB14], which determined the number of flights that departed when an airport was saturated (i.e., in congestion), the taxi-out times of flights in congestion, and the typical taxi-out times experienced by flights when the airport was at the saturation point. The difference between the aforementioned taxi-out times is a reflection of the potential taxi-out time reduction that may be achieved by operating the airport at close to the saturation point (thereby maintaining runway utilization).

Airport	Wx	% time in MC	Avg. taxi-out	Taxi-out @ saturation	Avg. taxi congestion	% reduction potential	% time congested	Total taxi-out time reduction potential
JFK	VMC	86	35.0	41.3	56.4	36.5%	31.5%	**12.5%**
	IMC	14	43.2	47.5	68.8	45.0%	40.9%	
EWR	VMC	83	28.1	38.0	51.9	36.5%	20.4%	**7.9%**
	IMC	17	31.0	35.2	50.3	43.0%	23.6%	
PHL	VMC	86	22.5	26.1	37.5	43.6%	27.2%	**14.3%**
	IMC	14	27.2	25.1	40.1	59.6%	48.7%	
BOS	VMC	84	19.9	25.0	34.5	37.9%	13.5%	**6.0%**
	IMC	16	21.6	25.5	37.2	45.7%	22.6%	

Table 32. Taxi-out time reduction potential for JFK, EWR, PHL and BOS, as estimated in [SB14].

For other core 30 FAA airports, results from the FAA's analysis of TFDM benefits at these airports were used as proxy estimates for ATD-2 benefits (see Table below).

Airport	DQM Benefits (annual)	Percent Total
ATL	$6,449,002	10.9%
BOS	$1,801,410	3.1%
BWI	$652,913	1.1%
CLT	$2,335,478	4.0%
DCA	$1,543,964	2.6%
DEN	$2,747,941	4.7%
DFW	$1,839,168	3.1%
DTW	$2,160,668	3.7%
EWR	$4,794,968	8.1%
FLL	$510,769	0.9%

IAD	$780,364	1.3%
IAH	$1,848,868	3.1%
JFK	$5,898,825	10.0%
LAS	$922,054	1.6%
LAX	$1,514,341	2.6%
LGA	$4,407,389	7.5%
MCO	$445,852	0.8%
MDW	$531,778	0.9%
MIA	$1,003,959	1.7%
MSP	$2,045,817	3.5%
ORD	$5,942,930	10.1%
PHL	$3,759,696	6.4%
PHX	$1,451,193	2.5%
SAN	$403,058	0.7%
SEA	$842,265	1.4%
SFO	$1,707,057	2.9%
SLC	$688,805	1.2%

Figure 112 shows the taxi-out time potential of TFDM at the 20 major airports, as previously estimated by MCR Federal [HM12]. For completeness, we also present, in Table 33, the relative percentage of annual TFDM benefits estimated at each of the major airports, as calculated by MCR. **Table 32Error! Reference source not found.** suggests that the benefits at JFK, EWR, PHL and LGA are 3.5, 2.4, 3.3 and 2.0 times those at BOS. On the other hand, the TFDM results in suggest that the benefits at JFK, EWR, PHL and LGA are 3.3, 2.7, 2.1 and 2.4 times those at BOS. We note that the TFDM results are based on a constant excess queue parameter of 6 min, while the values assumed in our medium-fidelity models are closer to (or even larger than) the "low benefit" numbers assumed in TFDM, except in the base of CLT where the values are closer to the "medium benefit" values (Figure 112).

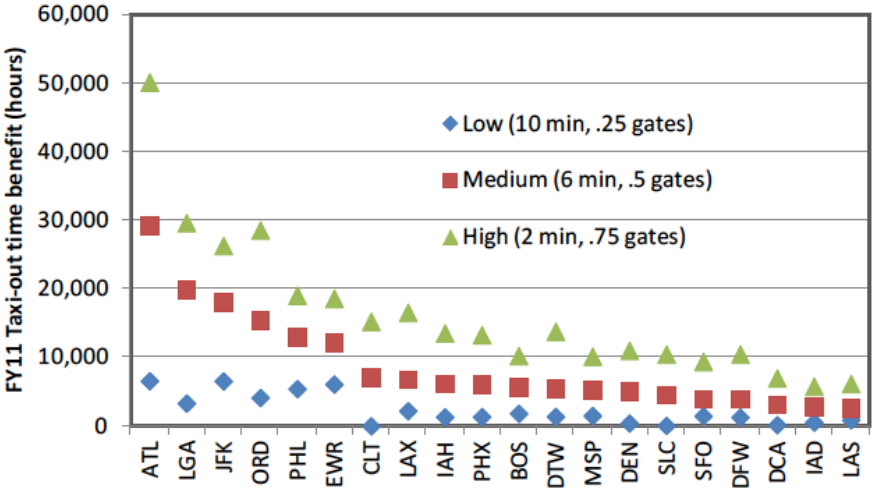

Figure 112. Taxi-out time benefits from TFDM surface metering (in hours) for the top 20 airports, as estimated by [HM12].

Apt.	% TFDM benefits	Normalized TFDM benefits	[SB10] & [Fornes15]	Med-fidelity benefits	SOSS scaling	Extrap. factor	% extrapolated benefit
ATL	10.9	1.3			1.9	2.6	**6.7%**
ORD	10.1	1.2			1.9	2.4	**6.2%**
JFK	10.0	1.2	1.5		1.9	2.9	**7.5%**
EWR	8.1	1.0	1.0	**1.0**	8.5	8.5	**22.3%**
LGA	7.5	0.9	0.8		1.9	1.6	**4.1%**
PHL	6.4	0.8	1.4		1.9	2.7	**7.0%**
DEN	4.7	0.6			1.9	1.1	**2.9%**
CLT	4.0	0.5		**3.2**	0.6	1.8	**4.6%**
DTW	3.7	0.5			1.9	0.9	**2.2%**
MSP	3.5	0.4			1.9	0.8	**2.1%**
IAH	3.1	0.4			1.9	0.7	**1.9%**
DFW	3.1	0.4		**0.9**	6.8	6.4	**16.9%**
BOS	3.1	0.4	0.4		1.9	0.8	**2.0%**
SFO	2.9	0.4			1.9	0.7	**1.8%**
DCA	2.6	0.3			1.9	0.6	**1.6%**
LAX	2.6	0.3			1.9	0.6	**1.6%**
PHX	2.5	0.3			1.9	0.6	**1.5%**
MIA	1.7	0.2			1.9	0.4	**1.0%**
LAS	1.6	0.2			1.9	0.4	**1.0%**
SEA	1.4	0.2			1.9	0.3	**0.9%**
IAD	1.3	0.2			1.9	0.3	**0.8%**
SLC	1.2	0.1			1.9	0.3	**0.7%**
BWI	1.1	0.1			1.9	0.3	**0.7%**
MDW	0.9	0.1			1.9	0.2	**0.6%**
FLL	0.9	0.1			1.9	0.2	**0.5%**
MCO	0.8	0.1			1.9	0.2	**0.5%**
SAN	0.7	0.1			1.9	0.2	**0.4%**

Table 33. Relative percentage of annual TFDM benefits estimated at each of the major airports, as calculated by MCR, assuming and excess queue parameter of 6 min; medium-fidelity model benefits relative to EWR; SOSS scaling factor (set to 1.9 for airports where not explicitly known from Table 33), the combined nationwide benefit extrapolation factor, and the resulting % total benefit corresponding to each airport.

7.5. Estimating NAS-Wide Network Impacts

Implementation of ATD-2 at an airport is likely to yield benefits elsewhere in the system. From previous sections, we can see that by improving departure throughput and avoiding surface gridlock at an airport with ATD-2, the departure delays at that airport are likely to decrease. However, due to the interconnected nature of the system, this decrease in departure delays will imply less propagation of delays to other airports in the system, compared to a situation without ATD-2. Similarly, another ATD-2 benefit mechanism, improved merging and sequencing into the overhead stream, will also result in better on-time arrival performance at destination airports, thereby decreasing delay propagation. Our approach to estimating these network effects will leverage our recent work on modeling air traffic delay propagation [GBJ16-1, GBJ16-2, GBJ16-3, GB17]. These models reflect the effect of delays at one airport on future (i.e., over the next few hours) delays at other airports. We will employ these models to estimate the effect of decreasing the departure delays at one airport (say, CLT) through the implementation of ATD-2, on the delays at other Core 30 airports. **Figure 113** shows the application of this methodology to evaluate the second-order, knock-on effects of ATD-2 implementation at CLT.

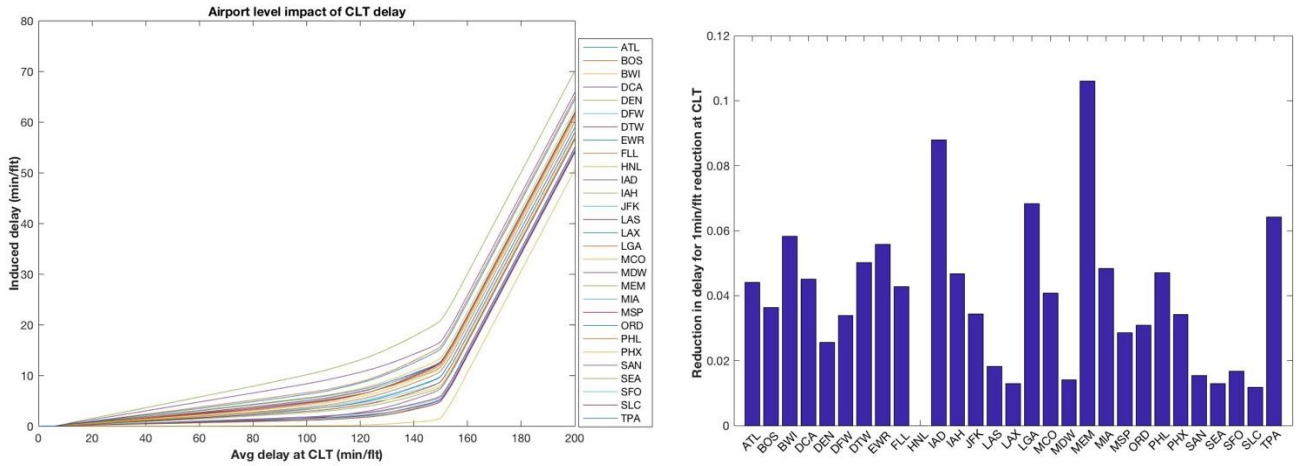

Figure 113. (Left) Estimated induced delay at various airports in the NAS, for different levels of departure delay at CLT. (Right) Slope of the middle region of the curves shown on the left, showing the expected reduction of departure delays at different airports, for a minute reduction of the departure delay at CLT. For example, a minute of departure delay reduction at CLT would potentially yield a departure delay reduction of about 0.045 min (or 3 sec) at PHL.

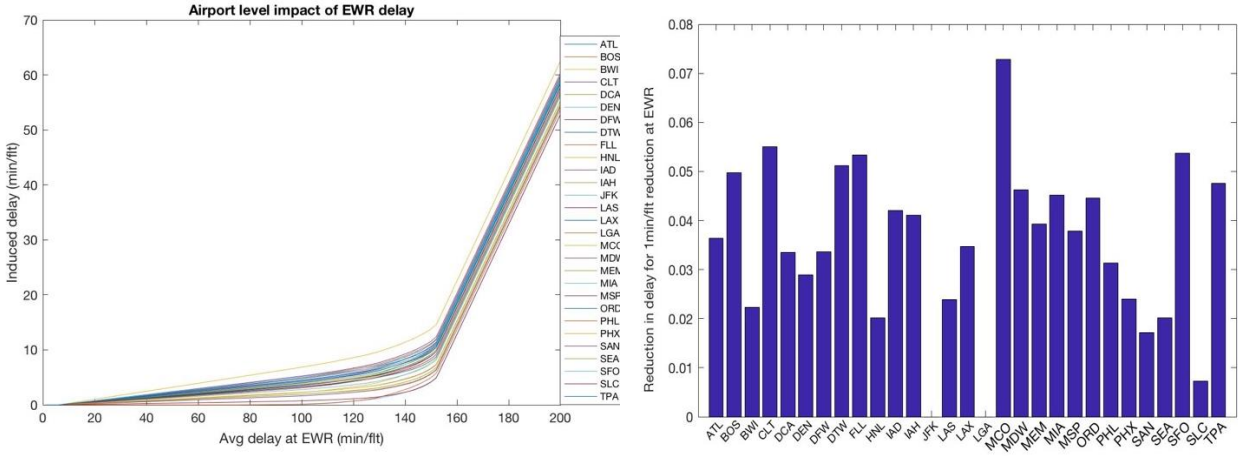

Figure 114. (Left) Estimated induced delay at various airports in the NAS, for different levels of departure delay at EWR. (Right) Slope of the middle region of the curves shown on the left, showing the expected reduction of departure delays at different airports, for a minute reduction of the departure delay at EWR.

8. BENEFITS EXTRAPOLATION TO ANNUALIZED AND MONETIZED BENEFITS

8.1.Benefits Monetization

After completion of the simulations – a combination of the high fidelity SOSS model and the medium fidelity MIT model – the results will be monetized using the standard methods provided by the FAA (economic factors) which include Airline Direct Operating Costs (ADOC), Passenger Value of Time (PVT) and fuel costs. Thus the DQM tool will move taxi-out delay to the gate resulting in fuel savings, while any increase in through-put will translate into delay reduction (measured by change in Off-Time), thus both ADOC and PVT. We will then combine with the Extrapolation to the core 30 airports and Annualization to estimate total benefits/year.

The monetization will be based on TFDM [FAA16] derived ADOC/PVT and Fuel values. This will provide a consistent comparison independent of variations in fuel and other economic values. These factors were approved during the TFDM final investment decision (FID). For the three airports modeled the factors are shown in **Table 34**. These values vary due to different fleet mix at the airport, which effects the number of enplanements/flight as well as the ADOC.

Airport	Fuel ($/hr)	PVT ($/hr)	ADOC ($/Hr)
CLT	$605.28	$3,844.69	$1,748.68
DFW	$645.45	$4,318.48	$1,865.14
EWR	$638.15	$4,220.87	$1,844.03

Table 34. Table Benefit Factors by Airport

Figure 115 shows the monetized benefits for each SOSS simulated airport. Note that CLT and DFW each have 6 simulated days and EWR 4. As you can see, there are 3 components to the benefits (ADOC, PVT, and Fuel). Only CLT, in these results has significant benefits in all three categories, while DFW has very little delay savings and EWR a smaller percentage. This chart shows the total across all the days simulated and extrapolated to a full day.

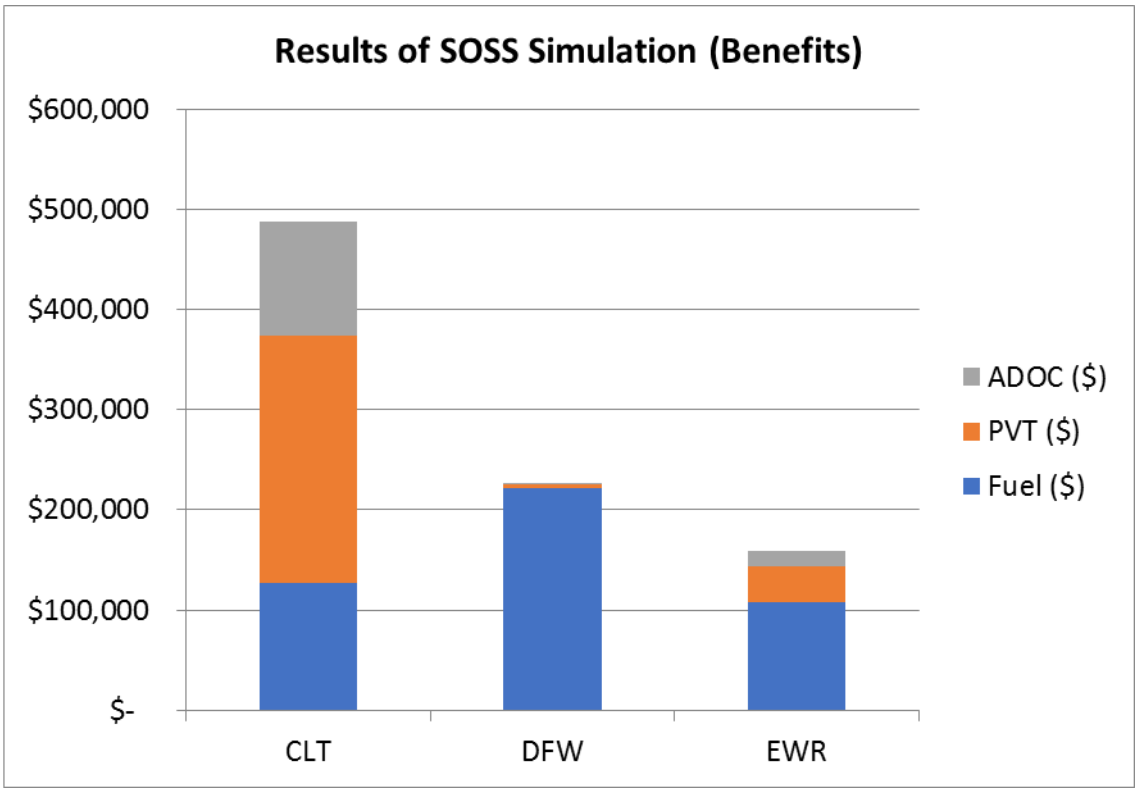

Figure 115, SOSS Simulated Benefits ($)

In order to calculate the fuel savings vs delay savings the following equation was applied to the results:

$$C_i = \{\min(t^0_{off}, t^i_{off}) - t^i_{out}\} * F_r + (t^i_{off} - t^o_{off}) * (A + P)$$

The cost C is an estimate of the cost for an ATD2 flight. The baseline would have no ADOC (A) or PVT (P). F_r is the cost of fuel/minute. Note that this value is relative to the minimum of the two "off" times (Baseline vs ATD-2). This is due to the occasions where ATD-2 has a later off-time and we don't want to double count (ADOC contains fuel as a subset). This cost is then subtracted from the baseline cost (Off – Out)* F_r to yield the net savings.

There is some indications that due to reduced congestion there may be some delay savings during the taxi-in phase of flight. The statistics and the medium fidelity model are inconclusive so for this report they are not included.

Table 35 shows the benefits results for each of the SOSS runs. As can be seen EWR has 3 days where the total benefits are Negative this is due to a significant number of flights with delayed Off-Times, thus a loss of ADOC and PVT. Even though the total taxi-out time reduction is significant, the value of ADOC and PVT far exceed simple fuel savings and thus drives the daily result negative. It is possible with alternate buffer times, reducing time at gate, there would be fewer times where the off-time is impacted.

Similar calculations were applied to the medium fidelity model.

Airport	Total (daily$)
CLT	$84,174
CLT	$20,967
CLT	$164,801
CLT	$40,400
CLT	$55,774
CLT	$120,870
DFW	$29,738
DFW	$139,937
DFW	-$66,742
DFW	$77,319
DFW	$46,547
DFW	$185
EWR	$234,096
EWR	-$19,145
EWR	-$39,850
EWR	-$16,780

Table 35, Benefits Results for Daily SOSS Runs

8.1.1. Example Calculation

To provide a more detailed context the following is an example of the benefits calculation for a single CLT simulation output

Baseline Flight: Taxi-Out Ready/Actual Out = 12:30 UTC

Off-Time = 12:52

Thus taxi-out time = 22 minutes

ATD-2 Flight: Taxi-Our Ready = 12:30

Actual Out =12:40

Off-Time=12:50

Thus Taxi-Time is 10 minute and 2 minutes early off

Cost for fuel in Baseline = 22 minutes*$10.09/min = $222

Cost for fuel in ATD-2 = 10*$10.09=$101

Cost for early off = (2 minutes*($64.08/min+$29.14/min) (PVT+ADOC) =$186

Savings for ATD-2 = $222-101-186 = -65 or a net change of $287

8.2. Benefits Annualization

In extrapolating the daily benefits to a full year (2016 in this case) a couple of methods were applied: 1) the selected dates were chosen because the weather and other factors indicated a fair number of "similar" days (see section X.X date selection). Thus 5/6/2016 at CLT was similar to 6 NAS days and 6/15/16 is similar to 16 days. This allows extrapolation to the similar days by simple multiplication with the number of similar days. This accounts for approximately 60 days in the year – some differences by airport. One can then extrapolate to a year by the simple expedient of multiplying by 366/n where n is the number of equivalent dates.

Using this method yields: CLT = $33.7M; DFW = $4.4M; EWR = $6.8M

Alternately we can extend the proxy of using taxi-out delay as a correlated factor (e.g., CLT 2016 taxi-out delay was ~1.7M minutes. The 6 SOSS days account for 39,000, thus an annual factor of 43.1. The benefits for the 6 days is $487,000 so the annual amount would be 43.1*487=$21M. Not a great comparison. DFW yields $12M and EWR $13.3M. The similar days method likely a more accurate method and for this report we combined the methods using a 60%/40% weighting. Thus CLT=$28,.6, DFW=$7.4M and EWR at $9.4M

Applying the extrapolation to the NAS from section 7, yields a NAS wide benefit of $300M/year. That is nearly 5 times larger than the TFDM estimate. This is primarily due to the high level of delay savings at CLT, resulting in CLT being 10 times larger than the TFDM estimate. **Figure 44** shows that on 6/1/16 date there was over 1 minute/flight of delay savings as well as reduced taxing time. From a benefits perspective that is very large due to the nature of delay (ADOC & PVT) savings.

Using the MIT medium fidelity model the results are all smaller than the SOSS results, as indicated in section 7. CLT is $3.5M modestly larger than the TFDM results of $2.3M, however DFW is much smaller at only $325,000 vs $1.8M in TFDM. EWR at $2M is somewhat smaller . When extrapolated to the NAS and applying the 1.9 factor for SOSS adjustments, yields $73M modestly larger than the $60M in TFDM for the mode of the distribution.

9. ATD-2 COSTS ANALYSIS

For this analysis the ATD-2 system was assumed to impact the existing TFDM program that has been baselined, but not implemented. The TFDM program was baselined in June-2016 after extensive cost analyses.

The TFDM cost estimate was developed over several years at the fourth WBS level (e.g., WBS 3.1.2.3). The costs were based on a combination of proposals from vendors and estimates based on size and type of the problem (e.g., DQM with SLOC and cost/SLOC). In addition the cost had uncertainty applies to various parameters to capture the lack of certainty in the values (e.g., salaries of SW engineers, number of SLOC, etc). The uncertainty was evaluated using monte-carlo techniques and then the output was created at a "high-confidence" level. High-Confidence at the FAA is generally an 80% confidence that the costs will be less-than the estimate 80% of the time. This is often called "Risk-Adjusted" and is done to be conservative and ensure success without the need for additional funds a majority of the time.

In developing the impact of ATD-2 on the baselined TFDM program 2 factors were assumed: 1) research done by NASA would reduce the parametric uncertainty in the cost estimate and 2) the research would guide the way to a lower point estimate (e.g., mean or mode of the risk distribution). Thus the technique was to simply reduce the variance and mode of the risk distributions assigned to the dominant WBS elements. The amount of change was based on discussions with cost and operational SMEs. In the end reduction of the relative max and min of the typically assigned triangular distribution was reduced by 5% and the point/mode of the distribution reduced by 2.5%. **Figure 116** displays the largest components of the F&E (Capital) costs. In addition it shows the magnitude of uncertainty assigned during the TFDM[FAA16] analysis.

For example Prime FTE for Software had an original risk distribution of 60%/100%/170% for the low/mode/high respectively. By applying the above adjustments this changes to 59.5%/97.5%/164%. This has the impact of reducing the 80th percentile of the cost from a 1.3 multiplier to1.22.

The cost model developed for TFDM is extremely complex with several hundred worksheets.

Over all the effect was to reduce the cost estimate by 3.5%. Note that this was applied only to the Capital (F&E) portion of the cost. No impact on the operating costs was assumed.

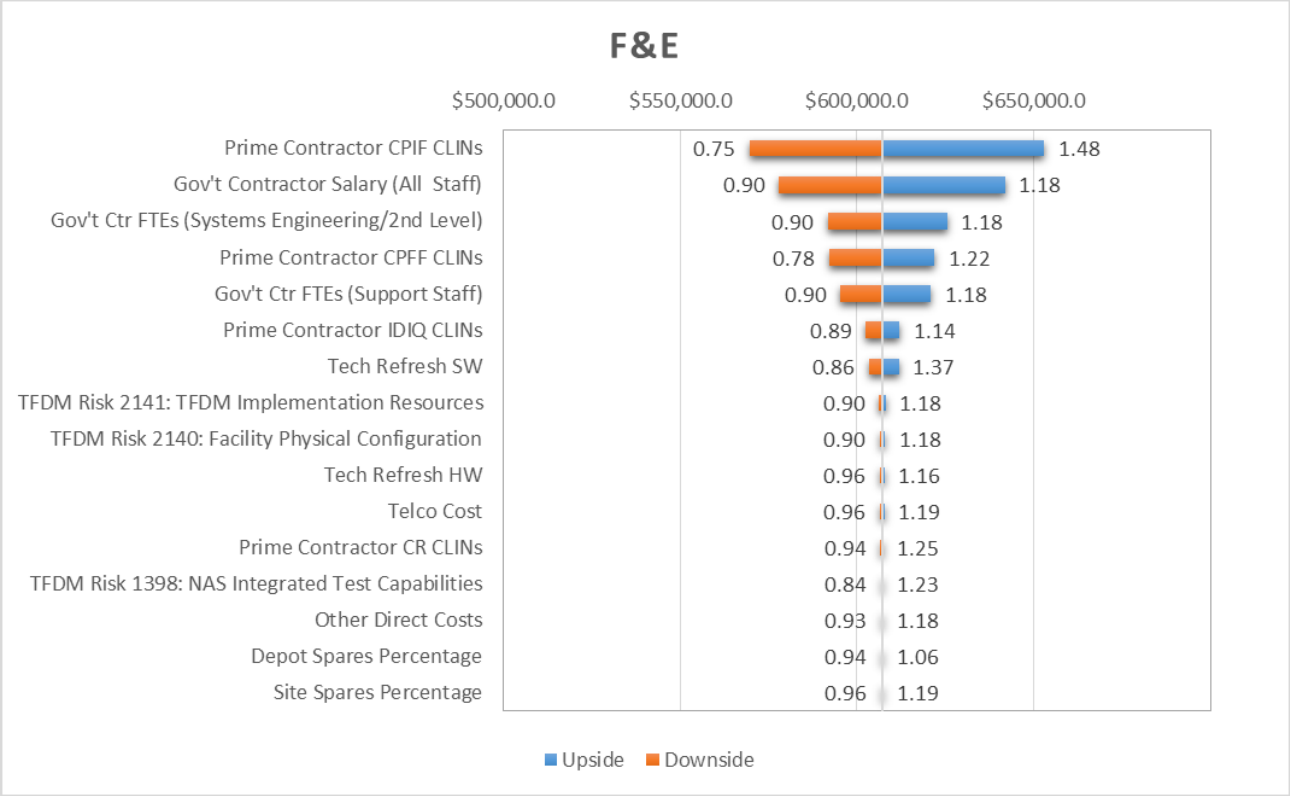

Figure 116, TFDM costs with major uncertainty

10. BENEFITS AND COSTS ANALYSIS SUMMARY

This section provides a self-contained summary of all the key technical tasks we conducted in support of generating high-fidelity benefits and costs estimates as well as presents the final benefits and costs comparison results.

First, we provide a brief summary of the overall technical approach. The project technical approach was as follows:

- We took a high-fidelity simulation based approach for analyzing the benefits of implementing the ATD-2 system at three carefully chosen airport sites – CLT, DFW, and EWR.
- We first analyzed the operational shortfalls related to departure operations management at these and other airports vis-à-vis the ATD-2 benefit mechanisms, which helped us identify key simulation modeling requirements for conducting a reliable benefits assessment using simulations.
- Next, we developed an integrated surface-airspace simulation platform that combined NASA's Surface Operations Simulator and Scheduler (SOSS) airport surface simulation platform with ATAC's Airspace Operations Simulator and Scheduler (AOSS) airspace simulation platform. In addition to simulation of departure airspace trajectories, AOSS also provided realistic modeling of the traffic flow management operations for handling departure TMI restrictions (including APREQs, EDCTs, and MITs) in both current-day operations and future operations under the management of the ATD-2 system.
- This high-fidelity simulation platform was employed to conduct baseline (current-day procedures) and ATD-2 (departure metering procedures) simulations for a set of carefully chosen simulation days and scenarios at the three airports.
- Results from high-fidelity simulations were used to compare ATD-2 operations against baseline operations and measure key performance metrics such as reduction in taxi-out times, impact on ON-time performance, impact on airport throughput, as well as in-depth analysis of individual benefit mechanisms.
- Outputs from the high-fidelity simulations were fed to downstream extrapolation tasks. One task addressed the nationwide extrapolation of ATD-2 benefits. In this task, we employed medium-fidelity queueing models at the three chosen airports to measure the ATD-2 benefits at a larger set of simulation days to aid annualization of benefits. In addition, medium-fidelity models were employed at three other airports (PHL, JFK and BOS) to estimate the benefits of implementing ATD-2 at these airports. Further, results from FAA's TFDM benefits analysis were leveraged to estimate the benefits of implementing the ATD-2 system at the rest of the core 30 FAA airports.
- Outputs from the high-fidelity and medium-fidelity simulations were then fed to the monetization and annualization task. This task monetized the taxi-out time savings as well as takeoff time savings by measuring their impact on fuel usage, airline direct operating costs and passenger travel times. Moreover, benefits from individual simulation days were scaled up by appropriate multiplication factors to obtain benefits at an annualized scale. These multiplication factors were generated by a meticulous year-long analysis of

historical weather, traffic demand-capacity imbalance, TMI impact and departure delay data at local and national levels.

- FAA-recommended methodologies were applied to estimate the cost of implementing the ATD-2 system at the FAA core 30 airports and to assess how much impact it will have on the cost of the FAA's TFDM program.
- Finally, the costs and benefits of implementing the ATD-2 system were weighed against each other and a return on investment analysis was conducted.

Next, we discuss the key outcomes from each of the main simulation, extrapolation and benefits-costs analysis tasks.

10.1. High Fidelity Simulation-based Benefits Estimates Summary for Selected Sites

From the benefits computation perspective, the key performance metric provided by high-fidelity simulations was the amount of taxi out time savings provided by ATD-2 for each simulation scenario. **Table 36** shows the summary taxi out time savings per simulated scenario in terms of the percentage saving over the average taxi out time in the baseline simulation observed over the duration of the simulation timeframe. Since we simulated only a part of each selected simulation day, we applied a full day multiplier to go from part-day benefits to full-day benefits. We developed this full-day multiplier by analyzing the real, historical observed taxi out delays during the simulation timeframe in comparison to the delays over the entire duration of the day. The last column of the table shows the full-day benefits.

Table 36. Summary Taxi Out Time Savings Results from Individual Simulation Scenarios

Airport	Simulation Day	Annualization Day Rank	Runway Config	Simulation Timeframe (UTC)	Taxi-Out Time Savings During Sim Time (%, min)	Full-Day Multiplier	Full-Day Benefits (min)
CLT	6/15/2016	1	South	1000-1600	9.82, 422	3.19	1,346
CLT	5/17/2016	2	South	0900-1700	5.71, 325	2.16	702
CLT	6/1/2016	3	North	1000-1500	8.97, 368	5.02	1,847
CLT	6/2/2016	4	South	1200-1500	5.85, 324	9.18	1,217
CLT	5/6/2016	5	North	1600-2100	15.13, 708	2.23	1,579
CLT	5/31/2016	7	North	1600-2100	3.8, 155	3.49	541
		CLT AVERAGE DAILY SAVING (~699 DEPARTURES PER DAY)=					1.72 MIN
DFW	5/12/2016	1	East	1000-1700	8.16, 551	2.4	1,322
DFW	6/4/2016	6	East	1700-2300	14, 869	2.54	2,207
DFW	6/3/2016	2	West	1500-2100	8.38, 626	3.34	2,091
DFW	7/5/2016	3	West	1500-2100	10.6, 728	2.57	1,871
DFW	7/17/2016	4	West	1000-1600	10.7, 511	3.05	1,559

DFW	7/28/2016	5	West	1000-1600	6.39, 289	4.16	1,202
		DFW AVERAGE DAILY SAVING (~905 DEPARTURES PER DAY)=					**1.89 MIN**
EWR	5/6/2016	3	North	1400-2000	9.7, 249	5.25	1,307
EWR	7/21/2016	1	South	0800-1800	6.55, 319	2.78	887
EWR	7/29/2016	2	North	0900-1800	7.24, 295	3.11	917
EWR	7/3/2016	5	South	0900-1600	21.69, 761	2.93	2,230
		EWR AVERAGE DAILY SAVING (~905 DEPARTURES PER DAY)=					**2.34 MIN**

As seen from the table (green highlight rows) and as summarized in **Figure 117** below, on an average, the ATD-2 system provided around 2 minutes of taxi-out time savings per departure at CLT and DFW. For EWR, the benefit was slightly above two minutes per departure flight.

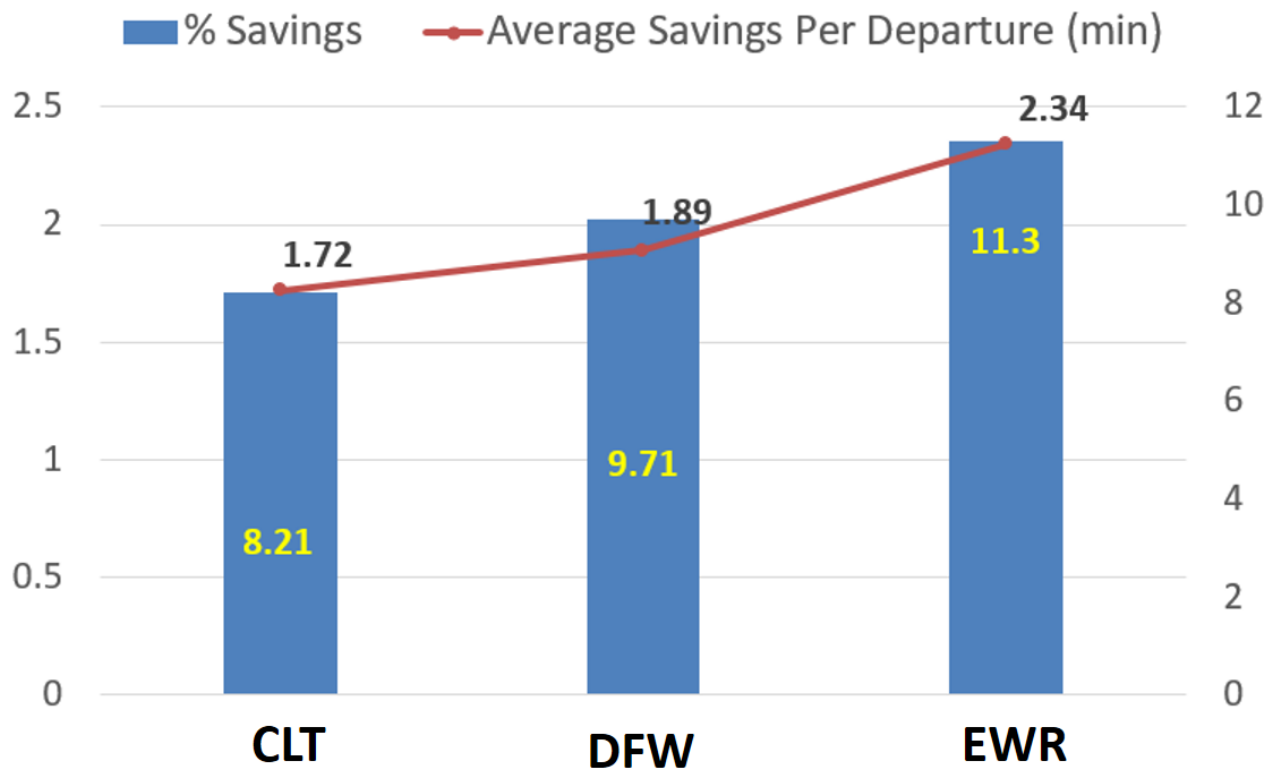

Figure 117. Percent and average per departure flight taxi-out time savings at the three airports, averaged over all the simulations per airport

10.2. Benefits Annualization and Monetization Summary

The overall ATD-2 benefits estimated from our simulations were estimated at $300M over the NAS. While larger than the TFDM-comparable portion of the benefits due to delay savings as well as fuel, this is not unexpected. With the lower value of delay savings found using the MIT medium fidelity model, we chose to use the average of the two sources.

By looking at the full technology lifecycle and extrapolating over the same years as used provided in the TFDM BCAR[FAA16] (thru 2045), this results in an overall lifecycle benefit of $3.5 Billion, significantly larger than the $1.2B claimed for TFDM in the Benefits basis of estimate and the BCAR. **Table 37** shows the summary of the benefits results from the TFDM BCAR.

Lifecycle Benefits (Risk Adjusted, FY2016 $ Millions)	
Benefit	
Reduced fuel burn through Departure Queue Management	$900 M
Increased opportunity for flight prioritization	$179 M
Increased opportunity to take CFR delay at gate	$15 M
Improved off-time compliance related to controlled departure times	$404 M
Improved runway load balancing (strategic)	$329 M
Improved runway load balancing (tactical)	$102 M
System consolidation and reduction in paper flight strips	$213 M
Reduced accidents related to strip mishandling	$46 M
Total	**$2,189 M**

Table 37. TFDM benefits

Adjusting **Table 37** for the ATD-2 results – assumed to apply to the "Reduced fuel through DQM" portion (note that from the BCAR it is somewhat smaller than the modeled $1.2B due to some final risk adjusting), yields $3.9B, as shown in **Table 38**. This is about a 77% increase.

Lifecycle Benefits (Risk Adjusted, FY2016 $ Millions)	
Benefit	
Reduced fuel burn through Departure Queue Management	$2,600 M
Increased opportunity for flight prioritization	$179 M
Increased opportunity to take CFR delay at gate	$15 M
Improved off-time compliance related to controlled departure times	$404 M
Improved runway load balancing (strategic)	$329 M
Improved runway load balancing (tactical)	$102 M
System consolidation and reduction in paper flight strips	$213 M
Reduced accidents related to strip mishandling	$46 M
Total	**$3,889 M**

Table 38, Adjusted benefits for ATD-2

10.3. Costs Analysis Summary

By reducing the risks in TFDM via better understanding the problem, we have estimated an overall cost reduction of 3.5%. In TFDM the cost was estimated at $1.3B in risk-adjusted TY$, thus the future costs due to ATD-2 would be $1.25B.

10.4. Final Benefits-Costs Analysis Results

The business case metrics – Benefit-to-Cost (B/C) ratio and Net Present Value (NPV) – were adjusted from the TFDM results. B/C can be calculated by using simple multipliers (B*B_ATD/(C*C_ATD) or B_TFDM*1.77/(C_TFDM*0.965) => (B/C)_TFDM*(1.77/0.965) which results in an increase of 83%. The B/C ratio for TFDM was estimated at 1.03, a barely breakeven estimate. With ATD-2 analysis this improved to a solid 1.9. Similarly the NPV goes from a minimal $17M to nearly $500M.

10.5. Conclusions and Proposed Future Work

This project developed and executed a high-fidelity simulation based approach for estimating the benefits and costs associated with implementing NASA's ATD-2 departure metering system at major national airports. Our simulation results and the subsequent extrapolation to national and annual levels showed that

- The ATD-2 system offers significant taxi-out time savings benefits at congested airports in the NAS, without having negative impact on taxi-in times, OFF time performance and airport throughput.
- The ATD-2 system provides $2.6 Billion in monetary benefits nationwide due to significant reduction in delay as well as gate hold time. The three primary simulated airports (CLT, DFW, EWR) had an annual total of 3.5 million minutes of reduced taxi-time and nearly 400 thousand minutes of early off times (delay savings). When extrapolated to the NAS this yields approximately $2.6B in monetary value.
- The ATD-2 benefits significantly outweigh the implementation costs.
- Incorporation of ATD-2 into the FAA's planned TFDM system deployments significantly improves the B/C ratio of the TFDM program.
- ATD-2 benefits could be enhanced through a number of identified mechanisms

Our simulations also demonstrated that there is room for enhancing ATD-2's benefits potential by improving the ATD-2 scheduling algorithms, data exchange processes, and traffic flow management procedures. The **key lessons learned** were the following: (1) Accurate estimation of earliest runway usage times and appropriate spacing of departure operations with interacting arrival operations on the runway system presents a challenge, especially at DFW and EWR where parallel dependent runway operations may hinder ATD-2 scheduling efficacy during time periods of heavy arrival traffic; (2) Taxi time uncertainty varies from flight to flight even for the same airport, and this variance obstructs efficient computation of Target Off Block Times (TOBTs) from Target Takeoff Times (TTOTs). There is a need for assessing complementary methods for managing this uncertainty, in addition to the existing method of using a non-zero Desired Excess Queue Time parameter; (3) Certain runway configurations present unique scheduling challenges, for example the South-flow configuration at CLT. There is a need for assessing ATD-2 scheduling algorithm modifications to optimize departure metering operations under such runway configurations; (4) Prioritization rules in the ATD-2 scheduling algorithm often result in big sequence jumps when a departure moves from "Uncertain" to "Planned" and from "Planned" to "Ready" status. These rules may need fine tuning and tailoring to address different operational demand-capacity conditions; (5) New York TRACON is a complex airspace with departure-fix merging being the most restrictive constraint on TRACON departures. Our past research recommends a multi-airport, hierarchical airspace-surface scheduling system instead of a single-airport ATD-2 system as a metering solution for New York airports. Further simulation-based evaluation of such a system is essential before it is deployed in the field.

In light of these key lessons learned from our simulations, we propose the following **future research paths** for conducting further simulation-based analysis of ATD-2 departure metering algorithms, data exchange processes, and traffic flow management procedures:

1) Simulation based assessment of algorithmic options for optimized handling of arrival-departure spacing, especially focused on mixed-use or dependent arrival-departure operations,
2) Simulation based assessment of algorithmic options for efficiently addressing the uncertainty in taxi-out times while back-computing TOBTs from TTOTs,
3) Simulation based assessment of alternative prioritization rules implementation within the ATD-2 scheduling algorithm,
4) Development of a concept of operations for a hierarchical airspace-surface scheduling system for busy metroplexes with departure fix merging constraints, such as New York TRACON and Dallas Fort Worth TRACON, and
5) Simulation based assessment of a hierarchical airspace-surface scheduling system for addressing departure fix merging constraints in conjunction with surface constraints and external departure restrictions.

11. REFERENCES AND CITATIONS

[ACJQ15] Aponso, B., Coppenbarger, R., Jung, Y., Quon, L., et al., "Identifying Key Issues and Potential solutions for Integrated Arrival, Departure, Surface Operations by Surveying Stakeholder Preferences," AIAA Aviation 2015 conference, June 2015.

[AK01] https://www.isr.umd.edu/NEXTOR/Conferences/200603_NAS_Performance/Session%203a_Klein%20NASATM%20Performance%20Indexes.pdf

[ASPM] FAA, Aviation System Performance Metrics, https://aspm.faa.gov/

[ATAC16] ATAC NRA Team, "Report Cataloging Shortfalls, ATD-2 Benefit Mechanisms, and Metrics," Task 1 report for NASA NRA titled *Benefit and Cost Assessment of Integrating Arrival, Departure, and Surface Operations with ATD-2,* submitted in November 2016.

[ATAC16-2] ATAC NRA Team, "NASA NRA Report Describing the Final Selection of Sites for Modeling and Simulation," Task 2 report for NASA NRA titled *Benefit and Cost Assessment of Integrating Arrival, Departure, and Surface Operations with ATD-2,* submitted in December 2016.

[ATAC17] ATAC NRA Team, "Report Describing the Models, Simulation Environment, and Assumptions for Benefits Assessment at Select Sites," Simulation environment description report for NASA NRA titled *Benefit and Cost Assessment of Integrating Arrival, Departure, and Surface Operations with ATD-2,* submitted in August 2017.

[ATAC17-2] ATAC NRA Team, "Base Year Report," Base Year report for NASA NRA titled *Benefit and Cost Assessment of Integrating Arrival, Departure, and Surface Operations with ATD-2,* submitted in September 2017.

[B17] Bagasol, L., "Tactical Scheduler," Presentation slides outlining scheduling, data-exchange, prioritization and spacing steps in NASA's ATD-2 Tactical Surface Scheduler.

[BB17] Badrinath S. and H. Balakrishnan. "Control of a Non-Stationary Tandem Queue Model of the Airport Surface," American Control Conference, May 2017.

[BTS16] Bureau of Transportation Statistics (BTS) website, http://www.transtats.bts.gov/airports.asp?pn=1, accessed on 12/29/2016.

[C17] Coppenbarger, R., "ATD-2 Benefit Metrics, Mechanisms, and Analyses," Presentation at the NASA ATD-2 Mini Workshop with ATAC NRA Team, NASA Ames, April 19, 2017.

[CCC17] Chevalley, E., Callantine, T., Coppenbarger, R., Multiple slide-decks and documents from meeting to discuss CLT and DFW airspace modeling between ATAC team and NASA.

[CE11] Capps, A. and Engelland, S.A., "Characterization of Tactical Departure Scheduling in the National Airspace System," AIAA-2011-6835, 11th AIAA Aviation Technology, Integration, and Operations (ATIO) Conference, Virginia Beach, VA, September 20–22, 2011.

[CJ16] Coppenbarger, R., Jung, Y., Malik, W., Chevalley, E., et. al., "Benefit Opportunities for Integrated Arrival Departure Surface Scheduling: A Study of Operations at Charlotte-Douglas International Airport," Digital Avionics Systems Conference, September 2016.

[DB10] Deonandan, I., and Balakrishnan, H., "Evaluation of Strategies for Reducing Taxi-out Emissions at Airports," *Proceedings of the AIAA Aviation Technology, Integration, and Operations (ATIO) Conference*, September 2010.

[ELR14] Eshow M., Lui M., and Ranjan S., "Architecture and Capabilities of a Data Warehouse for ATM Research" Digital Avionics Systems Conference (DASC), 2014 IEEE/AIAA 33rd, Hilton Head, SC, 2014.

[FAA01] http://aspmhelp.faa.gov/index.php/TFMSC

[FAA16] FAA, "Final Business Case for Terminal Flight Data Manager," FAA document, June 2016. FAA, "Final Business Case for Terminal Flight Data Manager," FAA document, June 2016.

[GB17] K. Gopalakrishnan and H. Balakrishnan. "A Comparative Analysis of Models for Predicting Delays in Air Traffic Networks," USA/Europe Air Traffic Management Seminar, June 2017.

[GBJ16-1] K. Gopalakrishnan, H. Balakrishnan and R. Jordan. "Deconstructing Delay Dynamics: An Air Traffic Delay Example," International Conference on Research in Air Transportation (ICRAT), June 2016.

[GBJ16-2] K. Gopalakrishnan, H. Balakrishnan and R. Jordan. "Clusters and Communities in Air Traffic Delay Networks," American Control Conference, July 2016.

[GBJ16-3] K. Gopalakrishnan, H. Balakrishnan and R. Jordan. "Stability of Networked Systems with Switching Topologies," IEEE Conference on Decision and Control, December 2016.

[I15] Idris, H., R., "Identification of Local and Propagated Queuing Effects at Major Airports", 15th AIAA Aviation Technology, Integration, and Operations Conference, AIAA AVIATION Forum, (AIAA 2015-2271)

[KC14] Kistler, M., Capps, A. and Engelland, S.A., "Characterization of Nationwide TRACON Departure Operations," AIAA-2014-2019, 14th AIAA Aviation Technology, Integration, and Operations (ATIO) Conference, Atlanta, GA, June 16–20, 2014.

[MB16] P. McFarlane and H. Balakrishnan. "Optimal Control of Airport Pushbacks in the Presence of Uncertainties," American Control Conference, July 2016.

[NASA15] NASA, "A Concept for Integrated Arrival/Departure/Surface (IADS) Traffic Management for the Metroplex," Airspace Technology Demonstration 2 (ATD-2) ConOps Synopsis (DRAFT), 2015.

[NASA16] NASA, "SOSS User Guide," NASA SOSS Simulation Team Document, November 2016.

[N16] NASA ATD-2 ConUse Team, "ATD-2 Concept of Use for Charlotte Douglas International Airport for Phase 1 Baseline Integrated Arrival, Departure, Surface (IADS) Demonstration," Working Paper Series.

[NASA17] NASA, "Truth Data Analysis," NASA ATD-2 Team Presentation, June 2017.

[SB14] I. Simaiakis and H. Balakrishnan. "Design and Simulation of Airport Congestion Control Algorithms," American Control Conference, June 2014.

[SB16] I. Simaiakis and H. Balakrishnan. "A Queuing Model of the Airport Departure Process," Transportation Science, Vol. 50, No. 1, pp. 94-109, February 2016.

[SL11] Stroiney, Steven, and Benjamin Levy. "Departure queue management benefits across many airports." In *Integrated Communications, Navigation and Surveilance Conference (ICNS), 2011*, pp. M5-1. IEEE, 2011.

[SS11] Stroiney, S., Saraf, A., Griffin, K., Levy, B., et al., "Airport Survey and Selection Report," Report prepared under NASA Prime Contract # NNA11AC50C, submitted December 16th, 2011.

[SL14] Saraf, A., Levy, B., Stroiney, S., Griffin, K., "Metroplex Departure Management," Final presentation for Saab Sensis R&D project.

[SSB14] I. Simaiakis, M. Sandberg and H. Balakrishnan. "Dynamic Control of Airport Departures: Algorithm Development and Field Evaluation," IEEE Transactions on Intelligent Transportation Systems, Vol. 15, No. 1, pp. 285-295, February 2014.

[WM13] Windhorst, R.D., Montoya, J.V., Zhu, Z., Gridnev, S., Griffin, K.J., Saraf, A., and Stroiney, S., "Validation of Simulations of Airport Surface Traffic with the Surface Operations Simulator and Scheduler," AIAA Aviation Technology, Integration, and Operations Conference, Los Angeles, CA, August 2013.

[Z15] Zhu, Z., "SOSS Runway Separation," NASA SOSS Simulation Team Document, February 2015.

[Z17] Zhifan Zhu, "ATD-2 Surface Tactical Scheduler Runway Separations and Weight Classes Data – ATD2AcTypes.csv and CLT_runway_separations.csv," Data provided to ATAC, September 25, 2017.

12. APPENDIX A (SIMULATION RESULTS DETAILS)

12.1. CLT Simulation Days

12.1.1. CLT Simulation Day 3 Results (6/02/2016, South Flow)

The first scenario we describe involved the simulation of CLT airport arrival and departure traffic on 06/02/2016 during the 1200-1500 UTC timeframe. During this day the airport was operating in the South flow configuration.

12.1.1.1. Benefits Results: Taxi-time Savings Charts

Our simulation results for this scenario showed that the ATD-2 system saved around 6% of the total taxi-out time over all the departures, as shown in **Figure 31**. A more in depth description of this result can be found in Section 6.2.

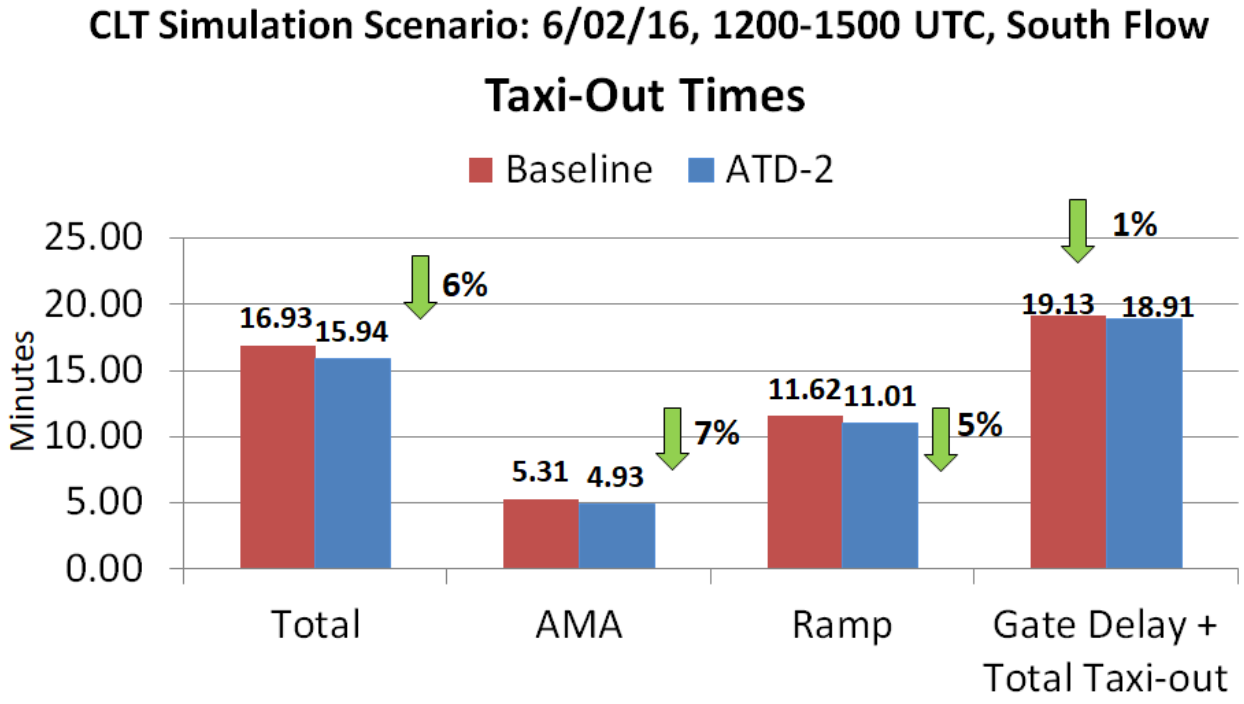

Figure 118. Taxi-Out Time Savings Benefits Estimated by Baseline VS ATD-2 Simulations for the 06/02/2016 1200-1500 UTC simulation scenario

Figure 45 shows the impact that the ATD-2 had on Taxi-In times.

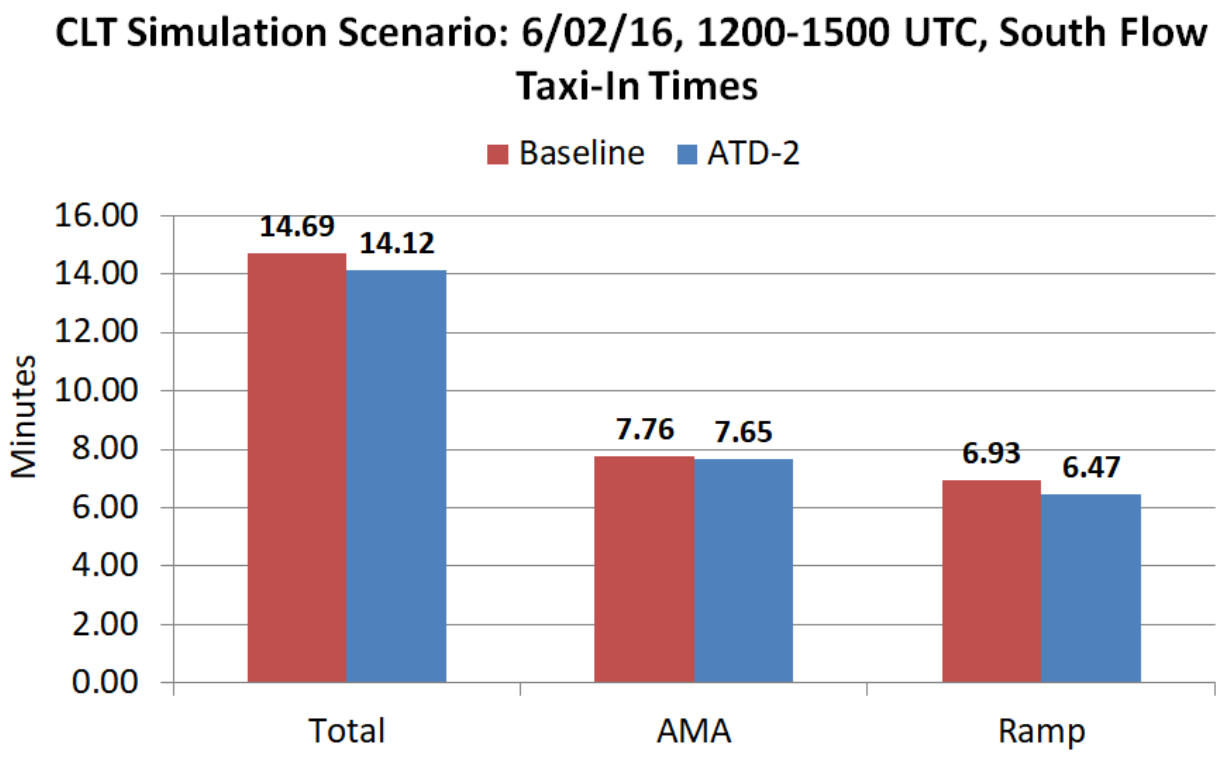

Figure 119. Taxi-In Time Savings Benefits Estimated by Baseline VS ATD-2 Simulations for the 06/02/2016 1200-1500 UTC simulation scenario

12.1.1.2. Analysis of On-Time Performance for Departure Flights

Figure 46 shows the results of the on-time analysis.

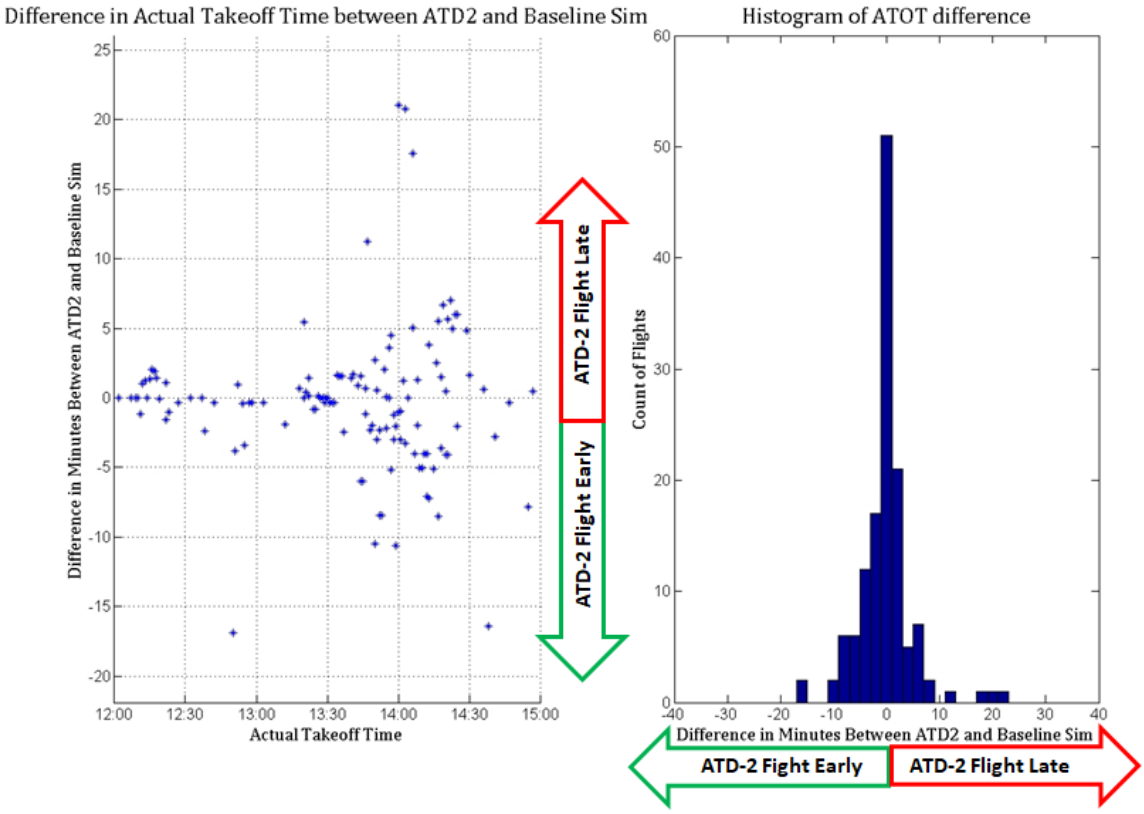

Figure 120. Analysis of On-Time Runway Takeoff Performance – Baseline VS ATD-2

12.1.1.3. Simulation Validation

This section presents results from comparing simulation outputs with operational metrics from real operational data on the same historical day, as well as with a distribution of the same operational metrics computed over a set of similar days over a period of three months. The left-hand side of **Figure 50** shows the comparison of takeoff counts per 15-minute bin over the duration of the simulation, with the simulated counts shown by the red line, the actual counts on the day of operations shown by the blue line, and a region covering the 10-th to 90-th percentile takeoff counts per 15-minute bin over similar historical time-bins shown by the green region.

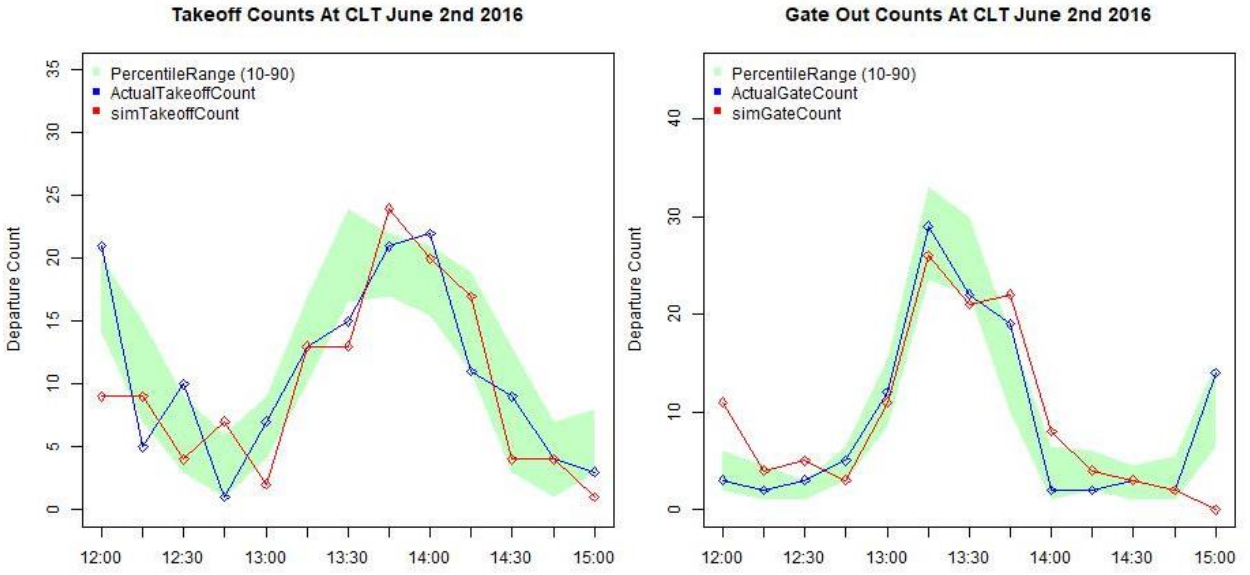

Figure 121. Runway Off and Gate Out Counts Validation – Simulation Versus Real Operations

Further, we also validated the taxi-out times by comparing simulated times against real historical operational taxi-out times from the same day as well as with a distribution of taxi-out times over similar days. **Figure 51** shows the comparison of simulated and actual taxi-out times, with AMA taxi-out time comparison showed in the left half of the figure and the total (AMA + Ramp) taxi-out time comparison shown in the right half of the figure.

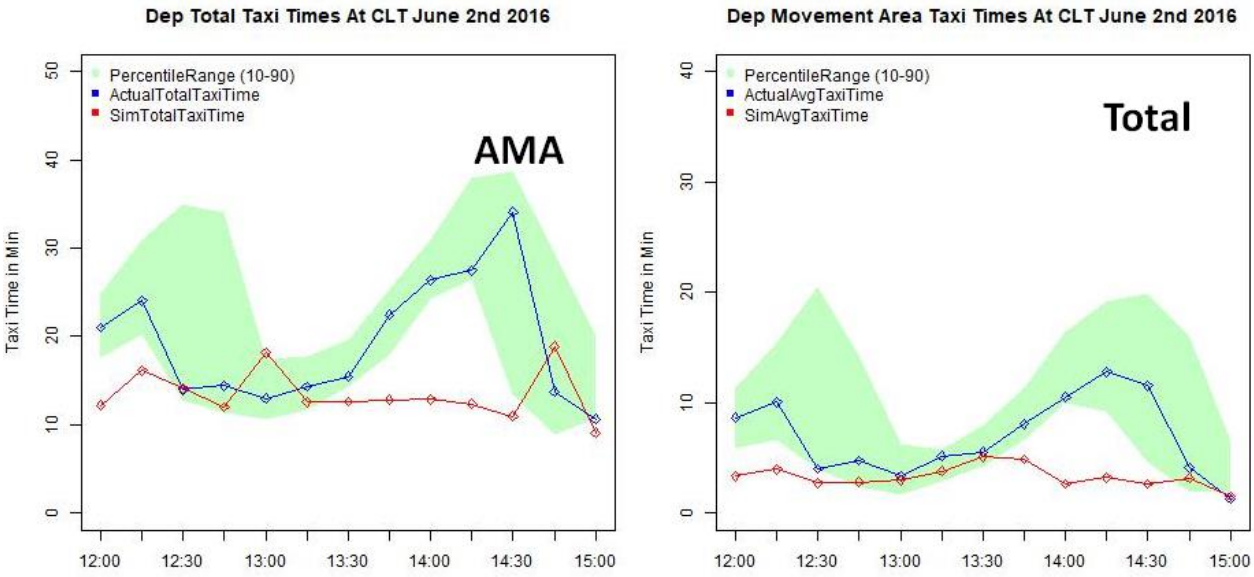

Figure 122. Taxi-Out Time Validation – Simulation Versus Real Operations

12.1.2. CLT Simulation Day 4 Results (5/17/2016, South Flow)

The first scenario we describe involved the simulation of CLT airport arrival and departure traffic on 05/17/2016 during the 0900-1700 UTC timeframe. During this day the airport was operating in the South flow configuration.

12.1.2.1. Benefits Results: Taxi-time Savings Charts

Our simulation results for this scenario showed that the ATD-2 system saved around 3% of the total taxi-out time over all the departures, as shown in **Figure 31**.

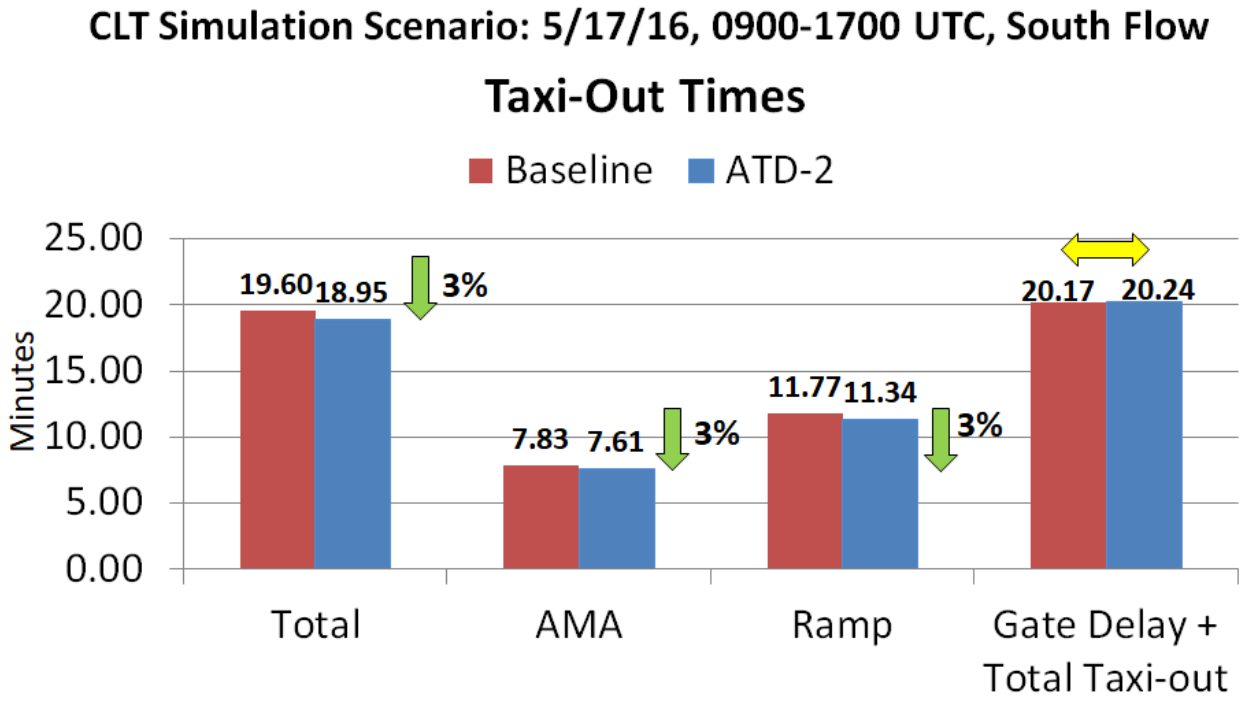

Figure 123. Taxi-Out Time Savings Benefits Estimated by Baseline VS ATD-2 Simulations for the 05/17/2016 0900-1700 UTC simulation scenario

Figure 45 shows the impact that the ATD-2 had on Taxi-In times.

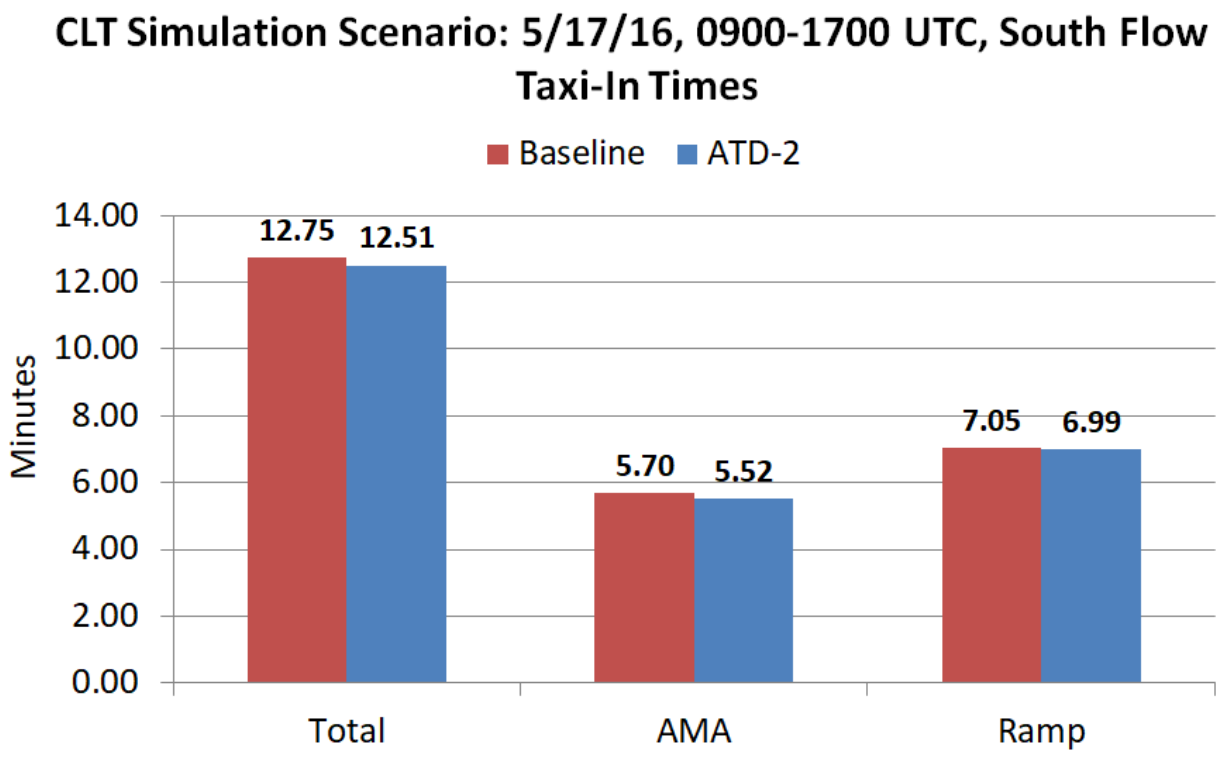

Figure 124. Taxi-In Time Savings Benefits Estimated by Baseline VS ATD-2 Simulations for the 05/17/2016 0900-1700 UTC simulation scenario

12.1.2.2. Analysis of On-Time Performance for Departure Flights

Figure 46 shows the results of the on-time analysis.

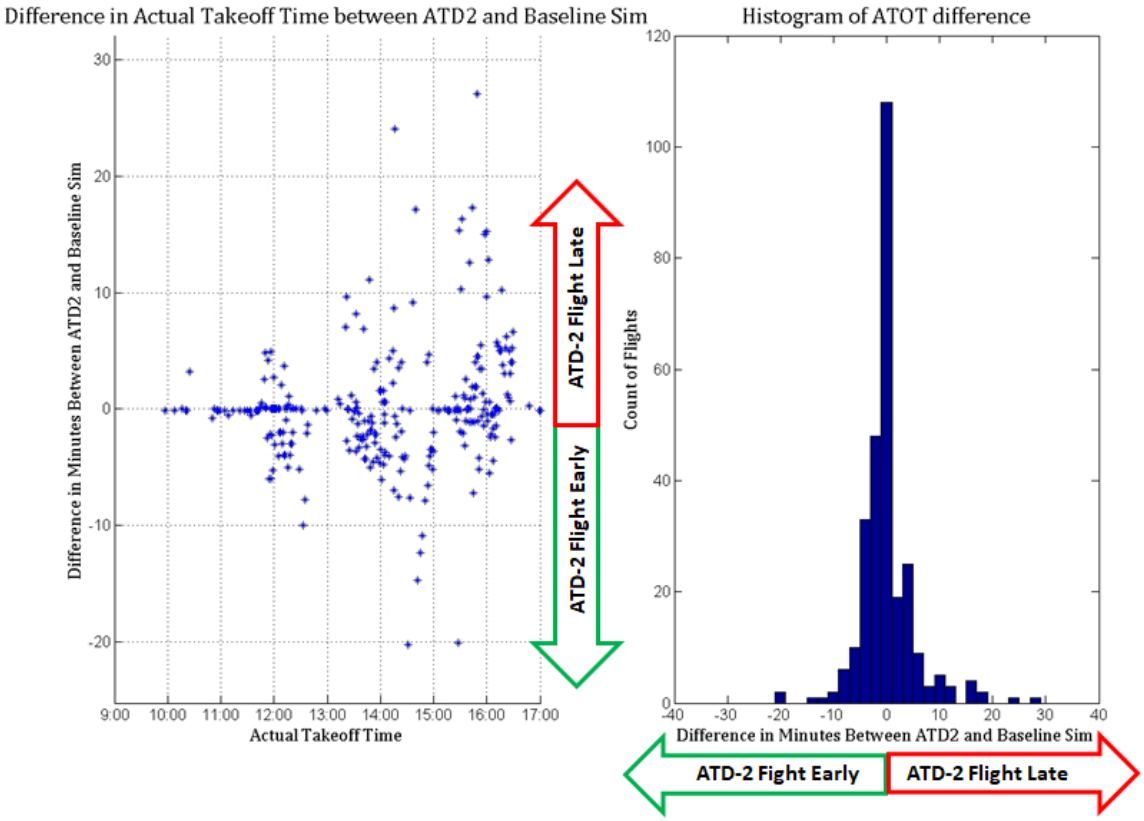

Figure 125. Analysis of On-Time Runway Takeoff Performance – Baseline VS ATD-2

12.1.2.3. Simulation Validation

This section presents results from comparing simulation outputs with operational metrics from real operational data on the same historical day, as well as with a distribution of the same operational metrics computed over a set of similar days over a period of three months. The left-hand side of **Figure 50** shows the comparison of takeoff counts per 15-minute bin over the duration of the simulation, with the simulated counts shown by the red line, the actual counts on the day of operations shown by the blue line, and a region covering the 10-th to 90-th percentile takeoff counts per 15-minute bin over similar historical time-bins shown by the green region.

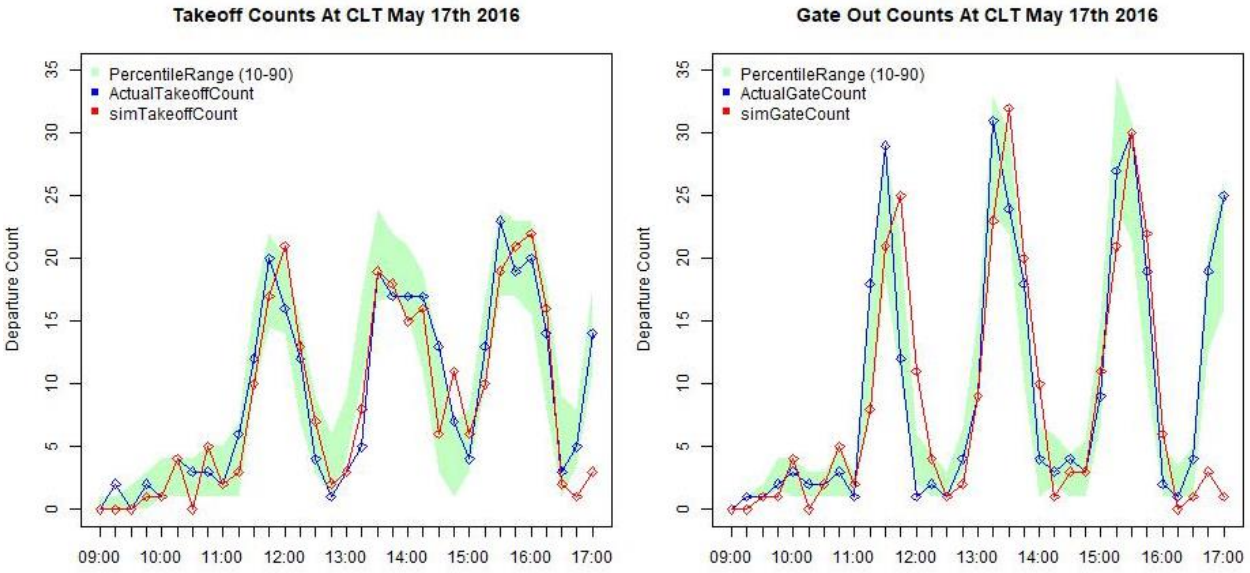

Figure 126. Runway Off and Gate Out Counts Validation – Simulation Versus Real Operations

Further, we also validated the taxi-out times by comparing simulated times against real historical operational taxi-out times from the same day as well as with a distribution of taxi-out times over similar days. **Figure 51** shows the comparison of simulated and actual taxi-out times, with AMA taxi-out time comparison showed in the left half of the figure and the total (AMA + Ramp) taxi-out time comparison shown in the right half of the figure.

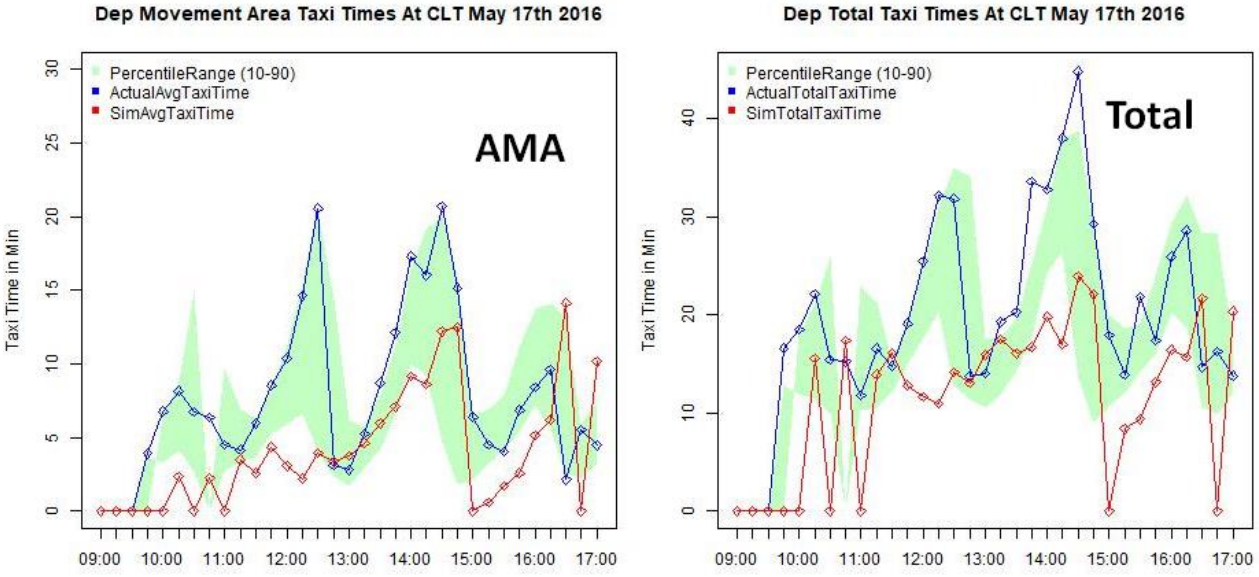

Figure 127. Taxi-Out Time Validation – Simulation Versus Real Operations

12.1.3. CLT Simulation Day 5 Results (5/06/2016, North Flow)

The first scenario we describe involved the simulation of CLT airport arrival and departure traffic on 05/06/2016 during the 1600-2100 UTC timeframe. During this day the airport was operating in the North flow configuration.

12.1.3.1. Benefits Results: Taxi-time Savings Charts

Our simulation results for this scenario showed that the ATD-2 system saved around 15% of the total taxi-out time over all the departures, as shown in **Figure 31**.

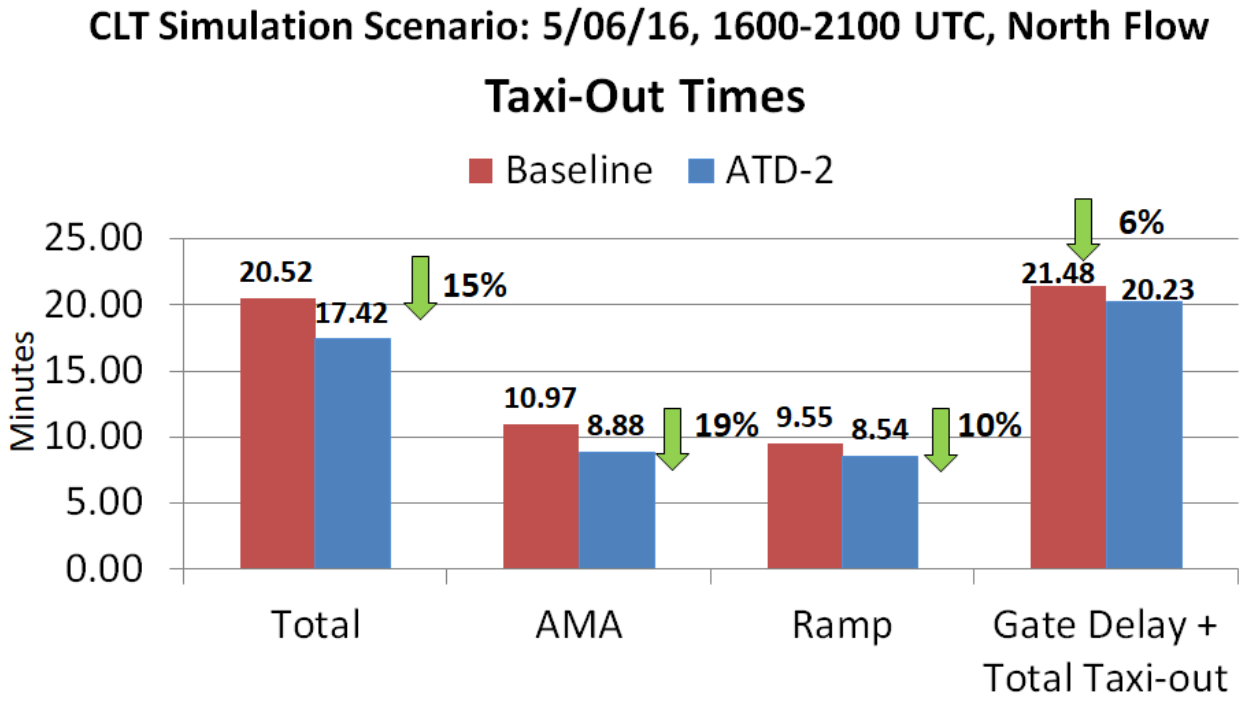

Figure 128. Taxi-Out Time Savings Benefits Estimated by Baseline VS ATD-2 Simulations for the 05/06/2016 1600-2100 UTC simulation scenario

Figure 45 shows the impact that the ATD-2 had on Taxi-In times.

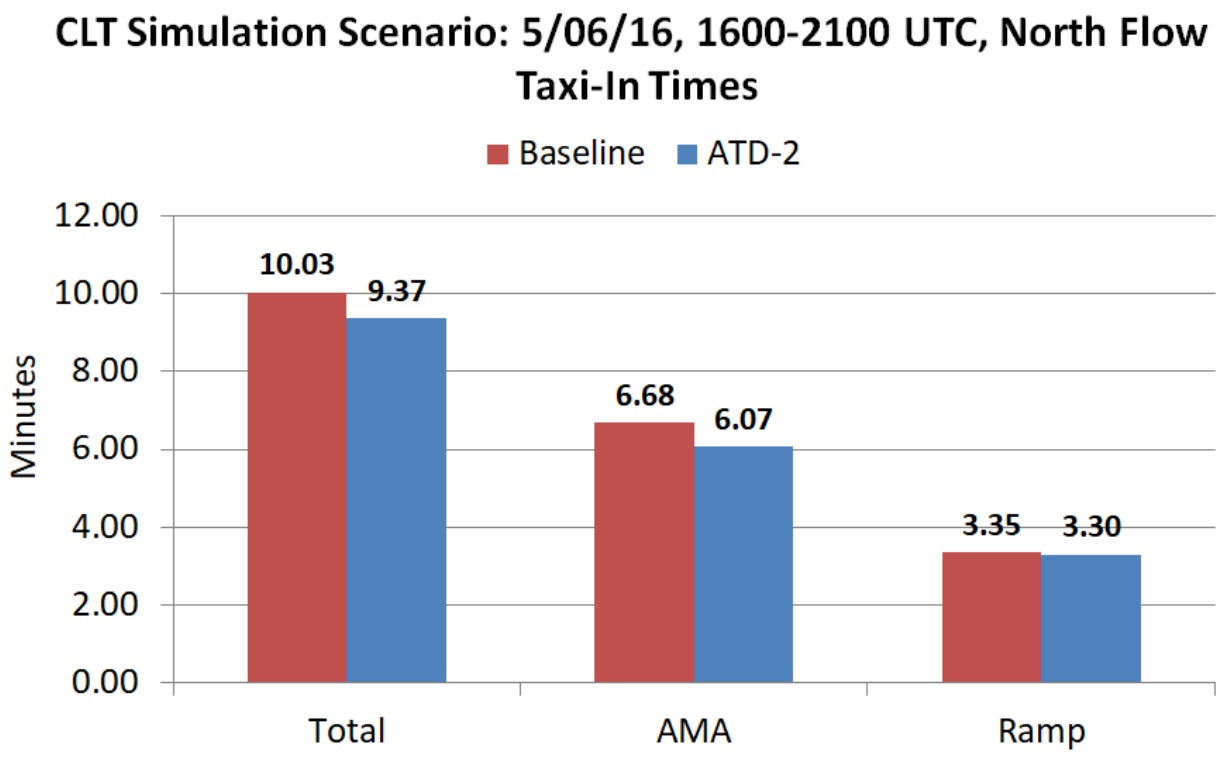

Figure 129. Taxi-In Time Savings Benefits Estimated by Baseline VS ATD-2 Simulations for the 05/06/2016 1600-2100 UTC simulation scenario

12.1.3.2. Analysis of On-Time Performance for Departure Flights

Figure 46 shows the results of the on-time analysis.

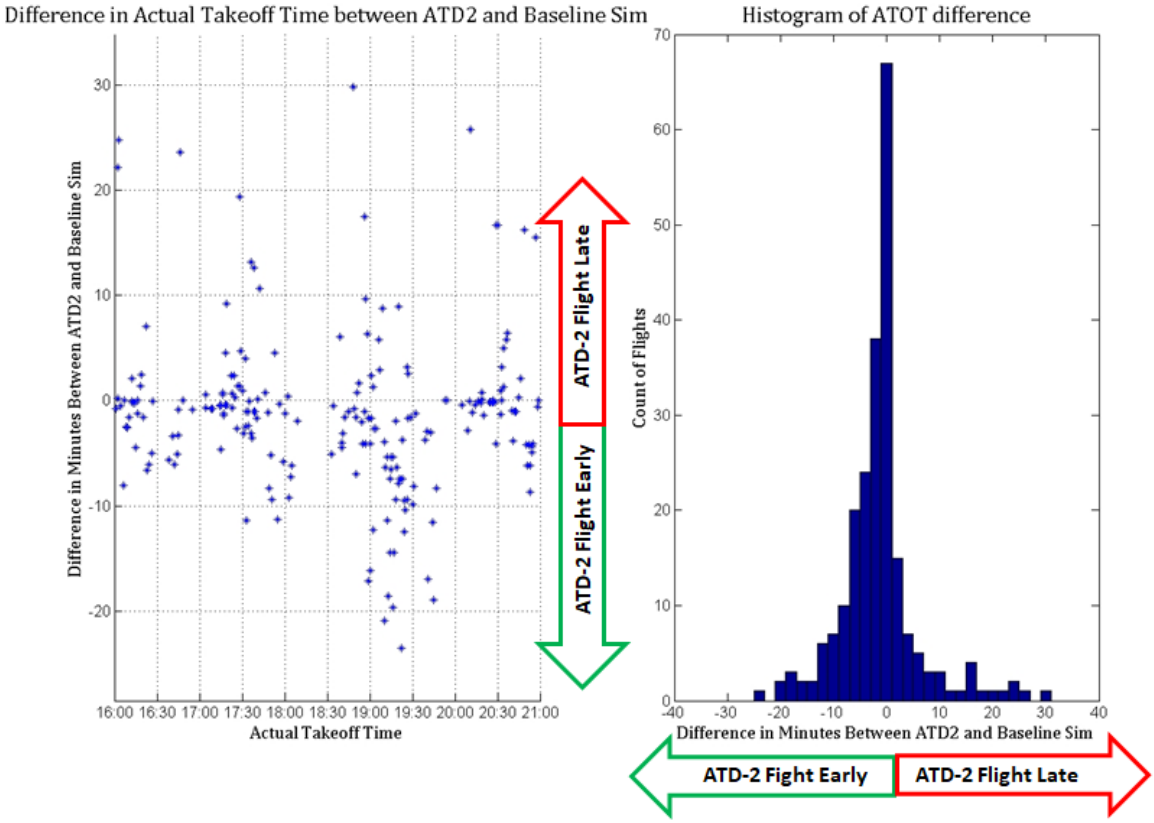

Figure 130. Analysis of On-Time Runway Takeoff Performance – Baseline VS ATD-2

12.1.3.3. Simulation Validation

This section presents results from comparing simulation outputs with operational metrics from real operational data on the same historical day, as well as with a distribution of the same operational metrics computed over a set of similar days over a period of three months. The left-hand side of **Figure 50** shows the comparison of takeoff counts per 15-minute bin over the duration of the simulation, with the simulated counts shown by the red line, the actual counts on the day of operations shown by the blue line, and a region covering the 10-th to 90-th percentile takeoff counts per 15-minute bin over similar historical time-bins shown by the green region.

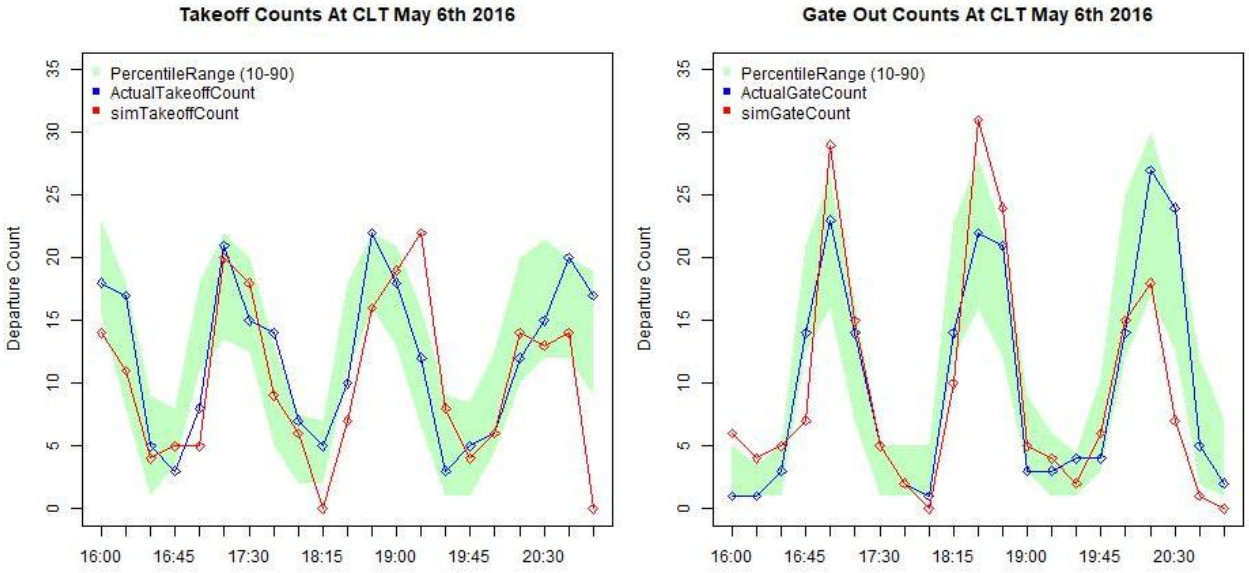

Figure 131. Runway Off and Gate Out Counts Validation – Simulation Versus Real Operations

Further, we also validated the taxi-out times by comparing simulated times against real historical operational taxi-out times from the same day as well as with a distribution of taxi-out times over similar days. **Figure 51** shows the comparison of simulated and actual taxi-out times, with AMA taxi-out time comparison showed in the left half of the figure and the total (AMA + Ramp) taxi-out time comparison shown in the right half of the figure.

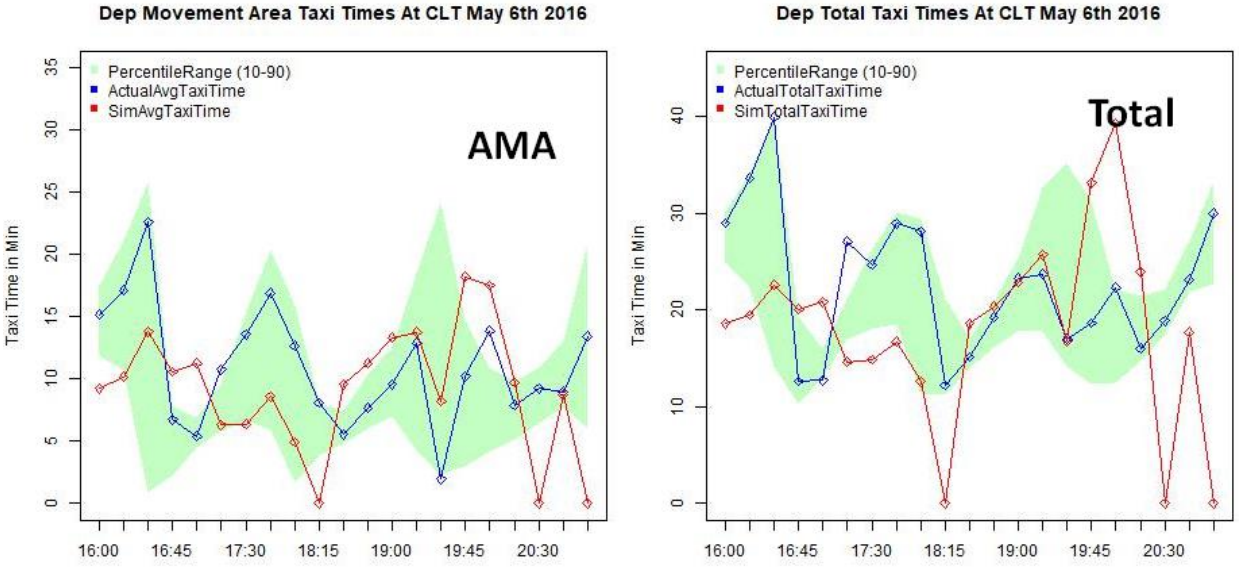

Figure 132. Taxi-Out Time Validation – Simulation Versus Real Operations

12.1.4. CLT Simulation Day 6 Results (5/31/2016, North Flow)

The first scenario we describe involved the simulation of CLT airport arrival and departure traffic on 05/31/2016 during the 1600-2100 UTC timeframe. During this day the airport was operating in the North flow configuration.

12.1.4.1. Benefits Results: Taxi-time Savings Charts

Our simulation results for this scenario showed that the ATD-2 system saved around 4% of the total taxi-out time over all the departures, as shown in **Figure 31**.

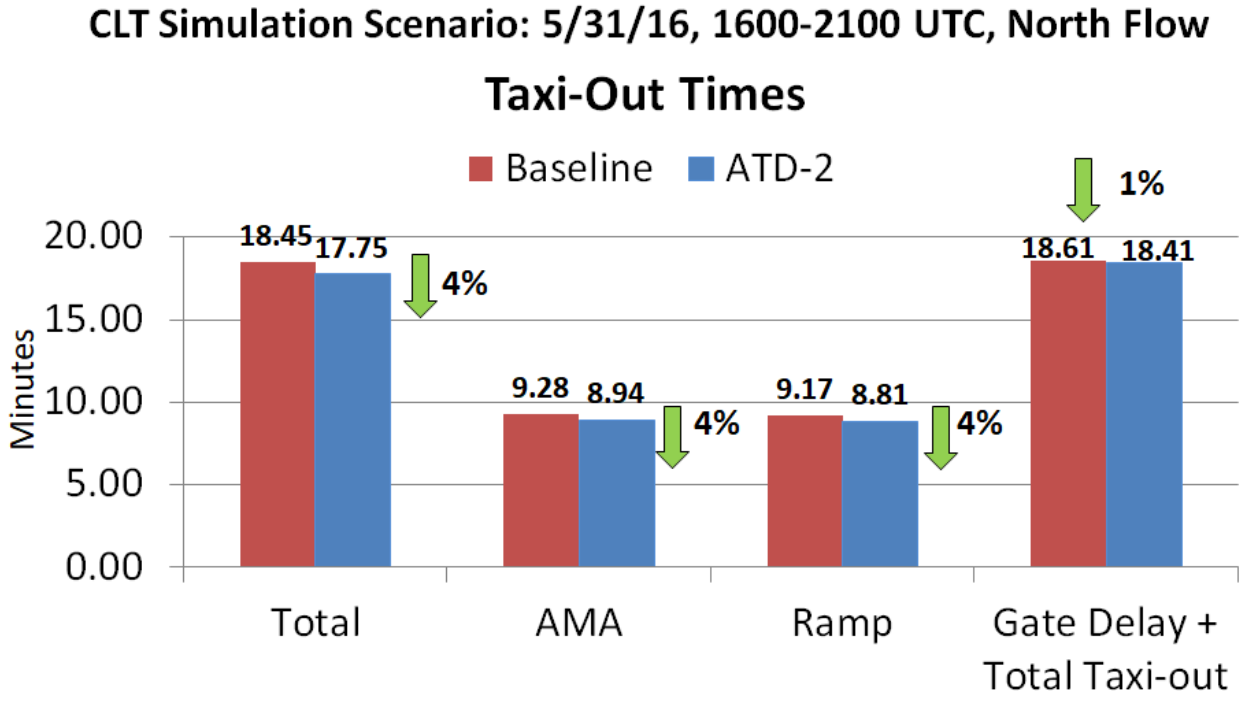

Figure 133. Taxi-Out Time Savings Benefits Estimated by Baseline VS ATD-2 Simulations for the 05/31/2016 1600-2100 UTC simulation scenario

Figure 45 shows the impact that the ATD-2 had on Taxi-In times.

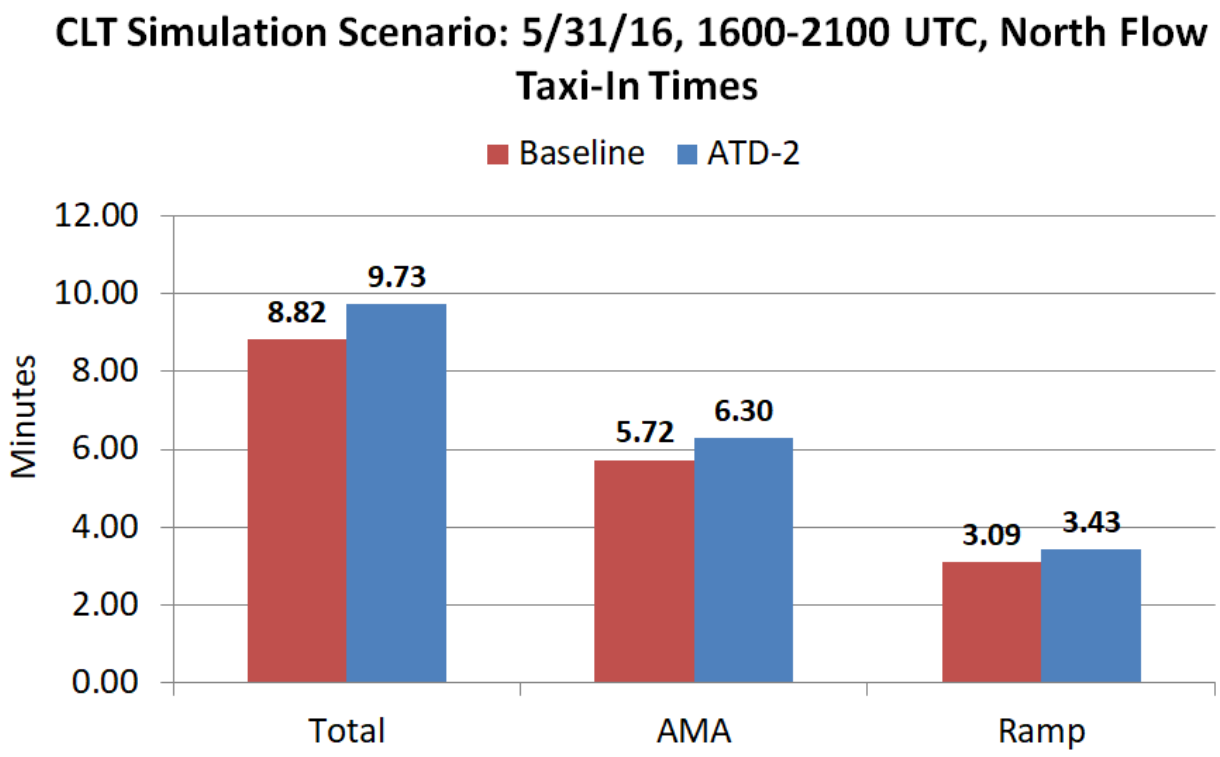

Figure 134. Taxi-In Time Savings Benefits Estimated by Baseline VS ATD-2 Simulations for the 05/31/2016 1600-2100 UTC simulation scenario

12.1.4.2. Analysis of On-Time Performance for Departure Flights

Figure 46 shows the results of the on-time analysis.

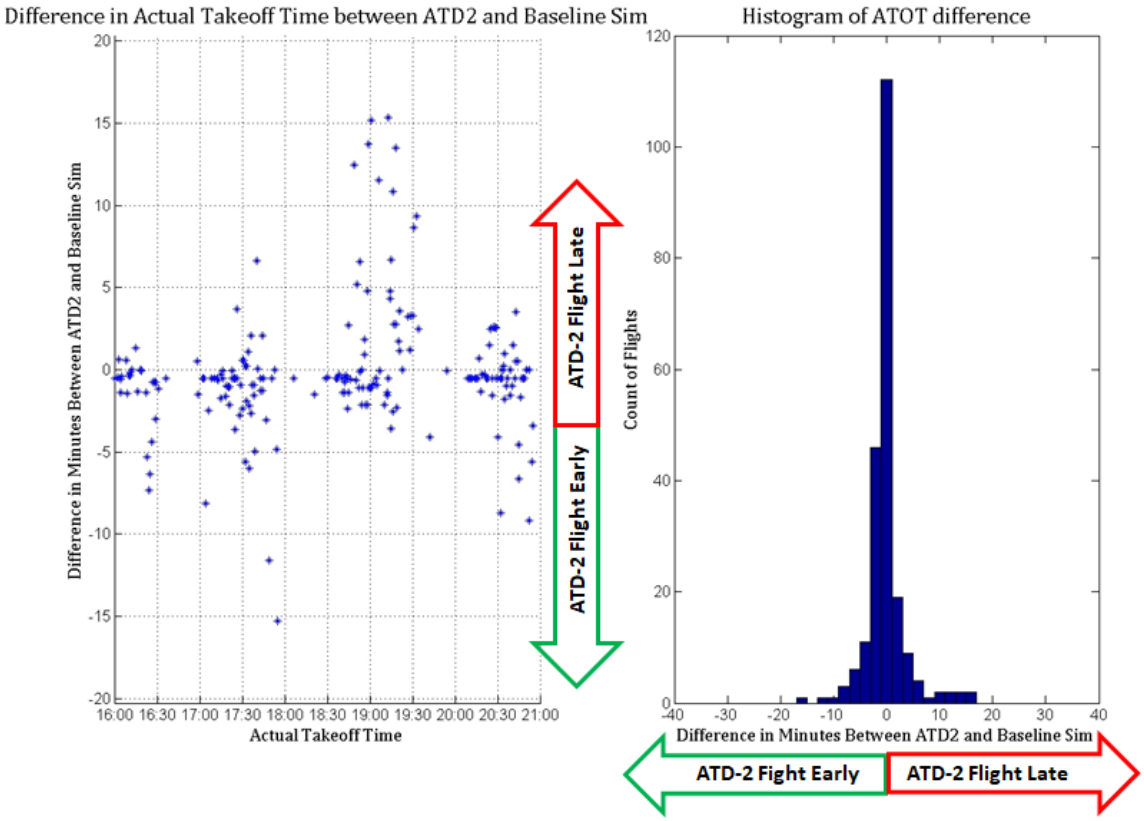

Figure 135. Analysis of On-Time Runway Takeoff Performance – Baseline VS ATD-2

12.1.4.3. Simulation Validation

This section presents results from comparing simulation outputs with operational metrics from real operational data on the same historical day, as well as with a distribution of the same operational metrics computed over a set of similar days over a period of three months. The left-hand side of **Figure 50** shows the comparison of takeoff counts per 15-minute bin over the duration of the simulation, with the simulated counts shown by the red line, the actual counts on the day of operations shown by the blue line, and a region covering the 10-th to 90-th percentile takeoff counts per 15-minute bin over similar historical time-bins shown by the green region.

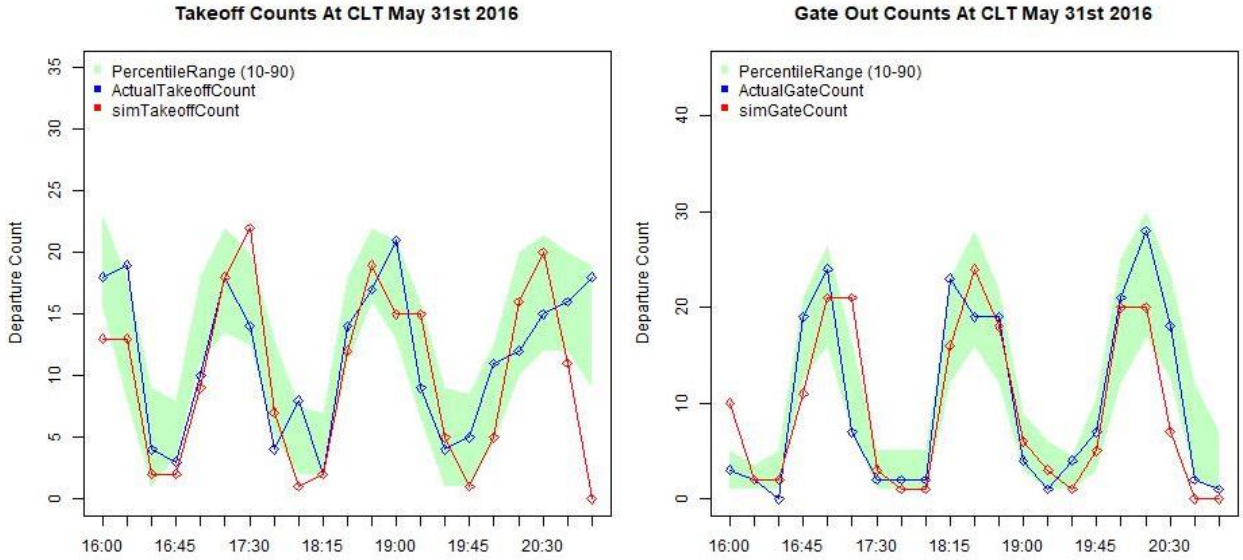

Figure 136. Runway Off and Gate Out Counts Validation – Simulation Versus Real Operations

Further, we also validated the taxi-out times by comparing simulated times against real historical operational taxi-out times from the same day as well as with a distribution of taxi-out times over similar days. **Figure 51** shows the comparison of simulated and actual taxi-out times, with AMA taxi-out time comparison showed in the left half of the figure and the total (AMA + Ramp) taxi-out time comparison shown in the right half of the figure.

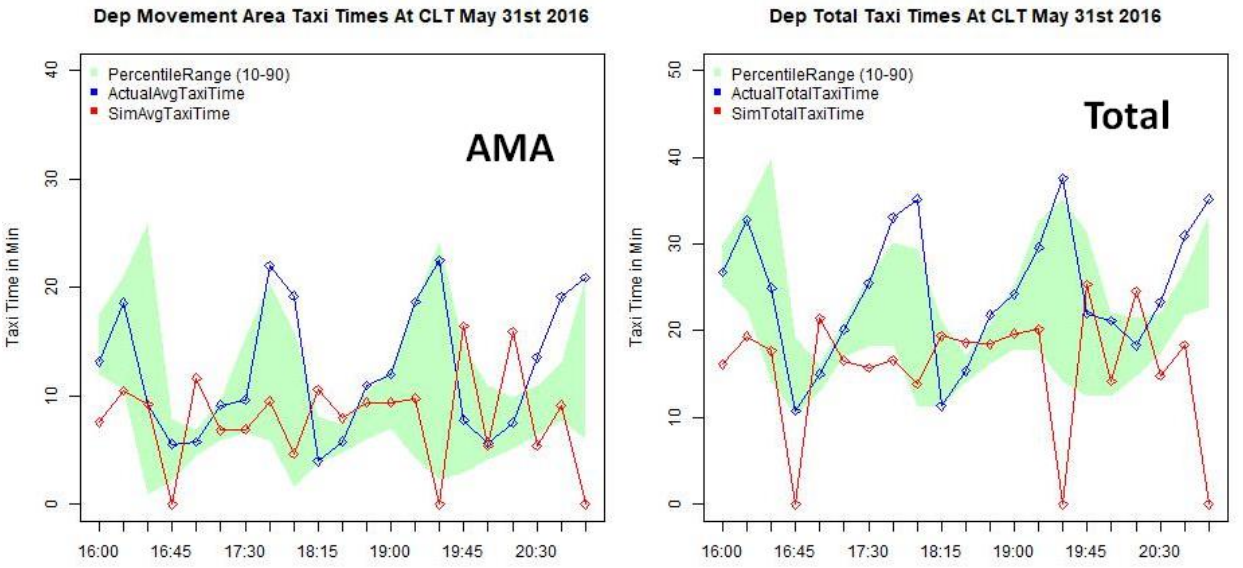

Figure 137. Taxi-Out Time Validation – Simulation Versus Real Operations

12.2. DFW Simulation Days

12.2.1. DFW Simulation Day 3 Results (6/04/2016, East Flow)

The first scenario we describe involved the simulation of DFW airport arrival and departure traffic on 06/04/2016 during the 1700-2300 UTC timeframe. During this day the airport was operating in the East flow configuration.

12.2.1.1. Benefits Results: Taxi-time Savings Charts

Our simulation results for this scenario showed that the ATD-2 system saved around 14% of the total taxi-out time over all the departures, as shown in **Figure 31**.

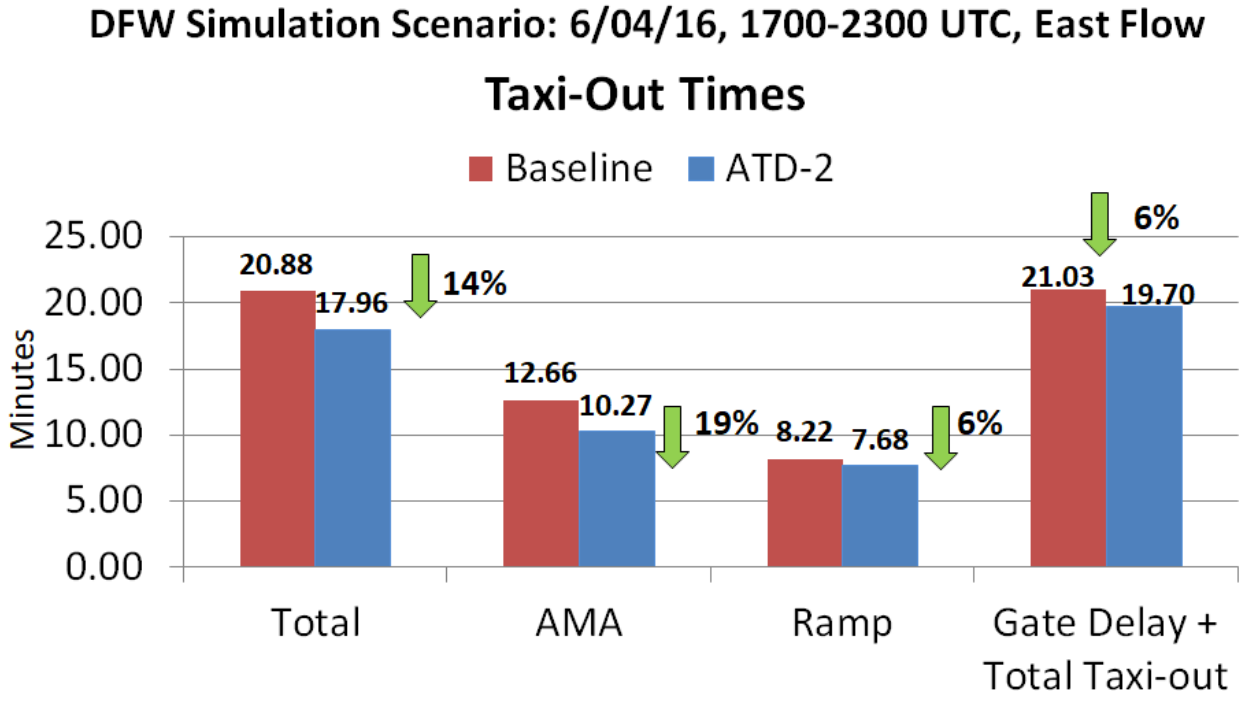

Figure 138. Taxi-Out Time Savings Benefits Estimated by Baseline VS ATD-2 Simulations for the 06/04/2016 1700-2300 UTC simulation scenario

Figure 45 shows the impact that the ATD-2 had on Taxi-In times.

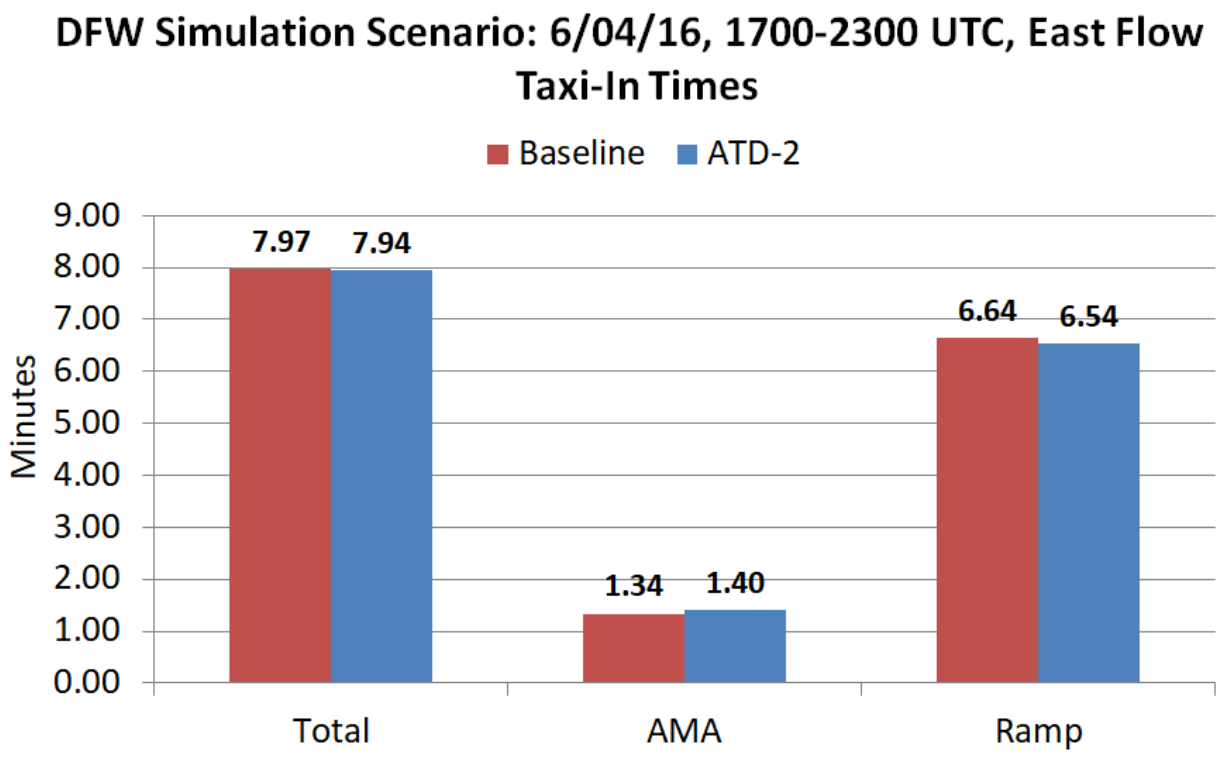

Figure 139. Taxi-In Time Savings Benefits Estimated by Baseline VS ATD-2 Simulations for the 06/04/2016 1700-2300 UTC simulation scenario

12.2.1.2. Analysis of On-Time Performance for Departure Flights

Figure 46 shows the results of the on-time analysis.

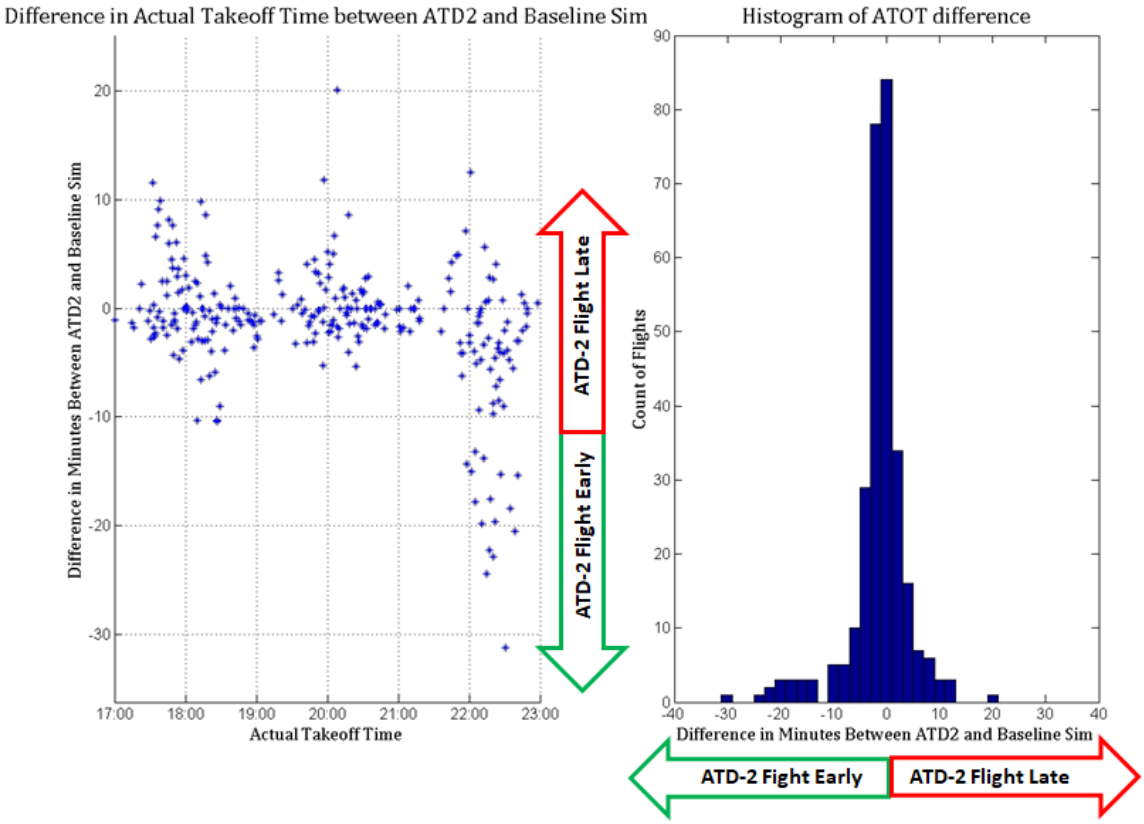

Figure 140. Analysis of On-Time Runway Takeoff Performance – Baseline VS ATD-2

12.2.1.3. Simulation Validation

This section presents results from comparing simulation outputs with operational metrics from real operational data on the same historical day, as well as with a distribution of the same operational metrics computed over a set of similar days over a period of three months. The left-hand side of **Figure 50** shows the comparison of takeoff counts per 15-minute bin over the duration of the simulation, with the simulated counts shown by the red line, the actual counts on the day of operations shown by the blue line, and a region covering the 10-th to 90-th percentile takeoff counts per 15-minute bin over similar historical time-bins shown by the green region.

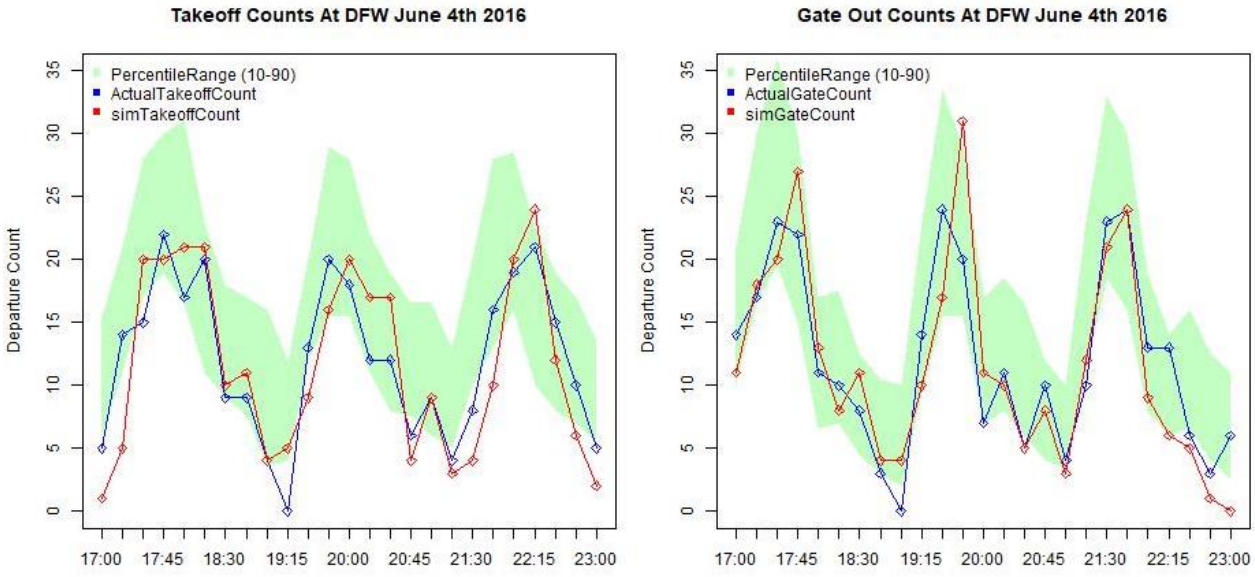

Figure 141. Runway Off and Gate Out Counts Validation – Simulation Versus Real Operations

Further, we also validated the taxi-out times by comparing simulated times against real historical operational taxi-out times from the same day as well as with a distribution of taxi-out times over similar days. **Figure 51** shows the comparison of simulated and actual taxi-out times, with AMA taxi-out time comparison showed in the left half of the figure and the total (AMA + Ramp) taxi-out time comparison shown in the right half of the figure.

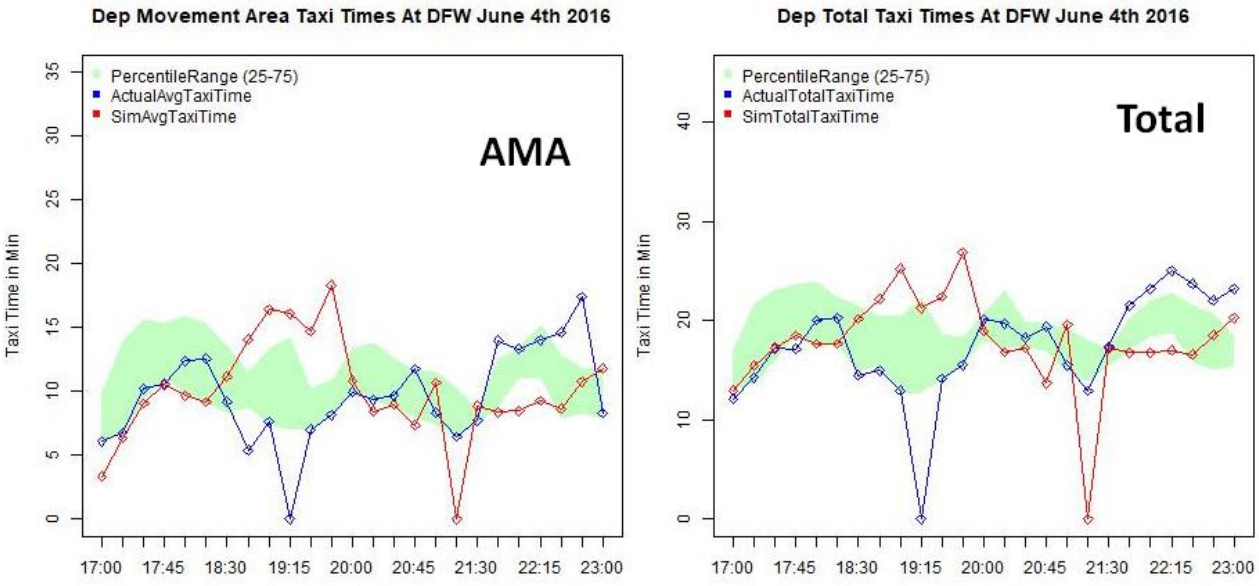

Figure 142. Taxi-Out Time Validation – Simulation Versus Real Operations

12.2.2. DFW Simulation Day 4 Results (7/05/2016, West Flow)

The first scenario we describe involved the simulation of DFW airport arrival and departure traffic on 07/05/2016 during the 1500-2100 UTC timeframe. During this day the airport was operating in the West flow configuration.

12.2.2.1. Benefits Results: Taxi-time Savings Charts

Our simulation results for this scenario showed that the ATD-2 system saved around 10% of the total taxi-out time over all the departures, as shown in **Figure 31**.

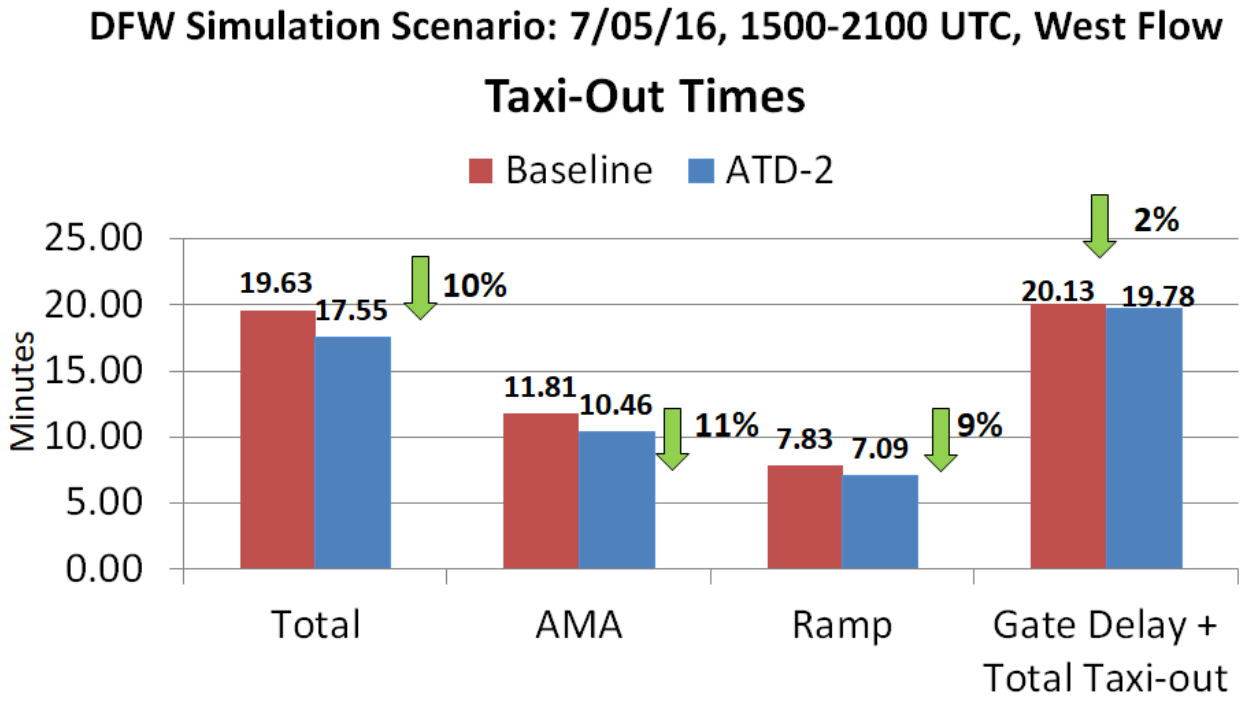

Figure 143. Taxi-Out Time Savings Benefits Estimated by Baseline VS ATD-2 Simulations for the 07/05/2016 1500-2100 UTC simulation scenario

Figure 45 shows the impact that the ATD-2 had on Taxi-In times.

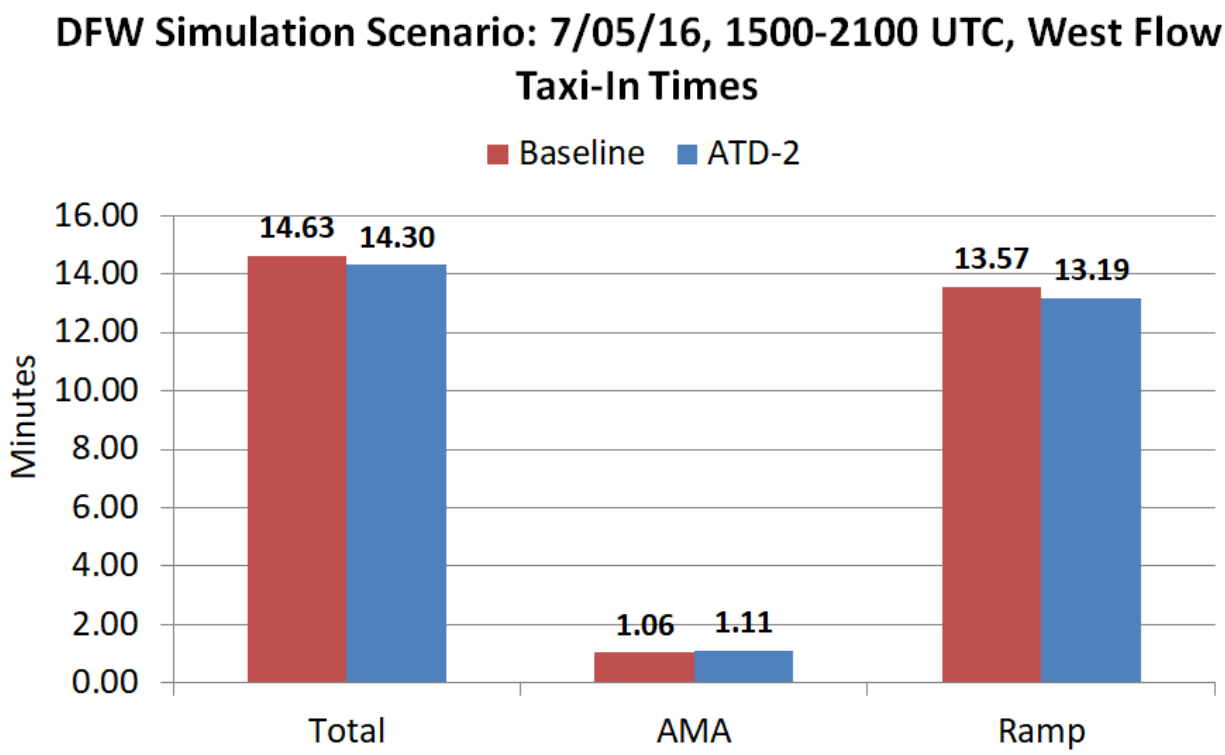

Figure 144. Taxi-In Time Savings Benefits Estimated by Baseline VS ATD-2 Simulations for the 07/05/2016 1500-2100 UTC simulation scenario

12.2.2.2. Analysis of On-Time Performance for Departure Flights

Figure 46 shows the results of the on-time analysis.

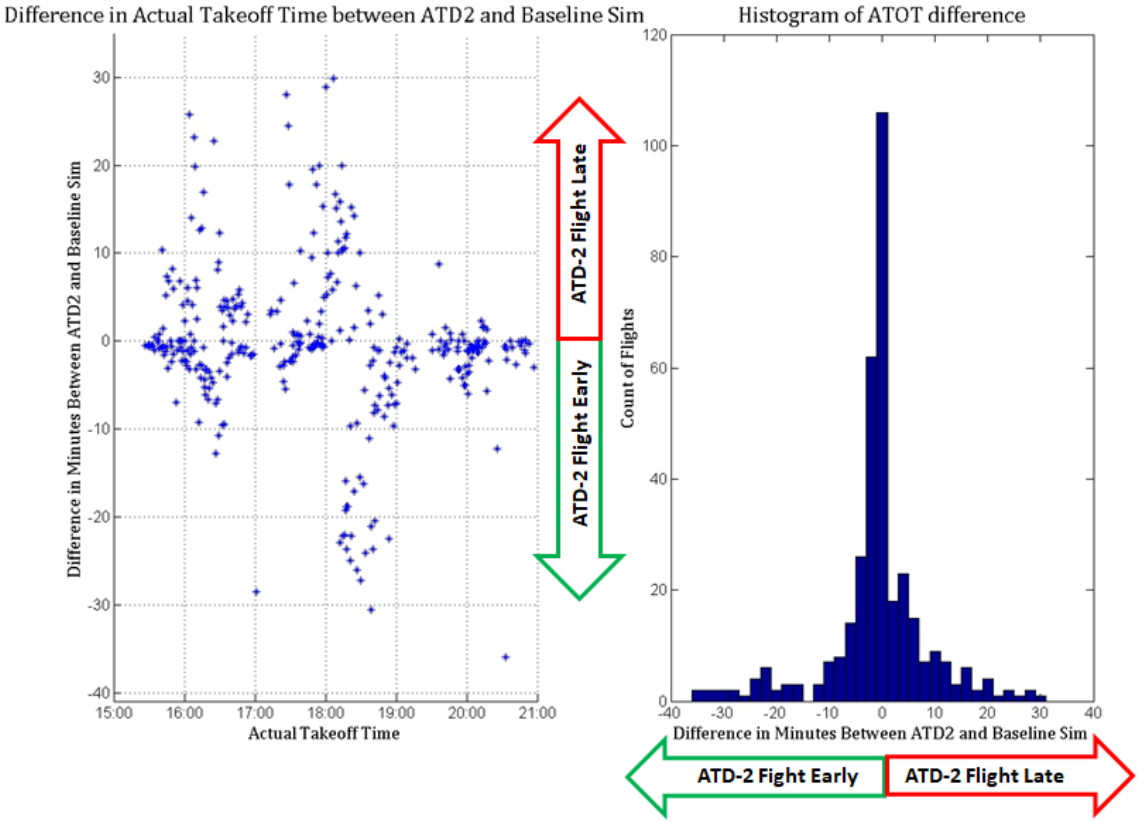

Figure 145. Analysis of On-Time Runway Takeoff Performance – Baseline VS ATD-2

12.2.2.3. Simulation Validation

This section presents results from comparing simulation outputs with operational metrics from real operational data on the same historical day, as well as with a distribution of the same operational metrics computed over a set of similar days over a period of three months. The left-hand side of **Figure 50** shows the comparison of takeoff counts per 15-minute bin over the duration of the simulation, with the simulated counts shown by the red line, the actual counts on the day of operations shown by the blue line, and a region covering the 10-th to 90-th percentile takeoff counts per 15-minute bin over similar historical time-bins shown by the green region.

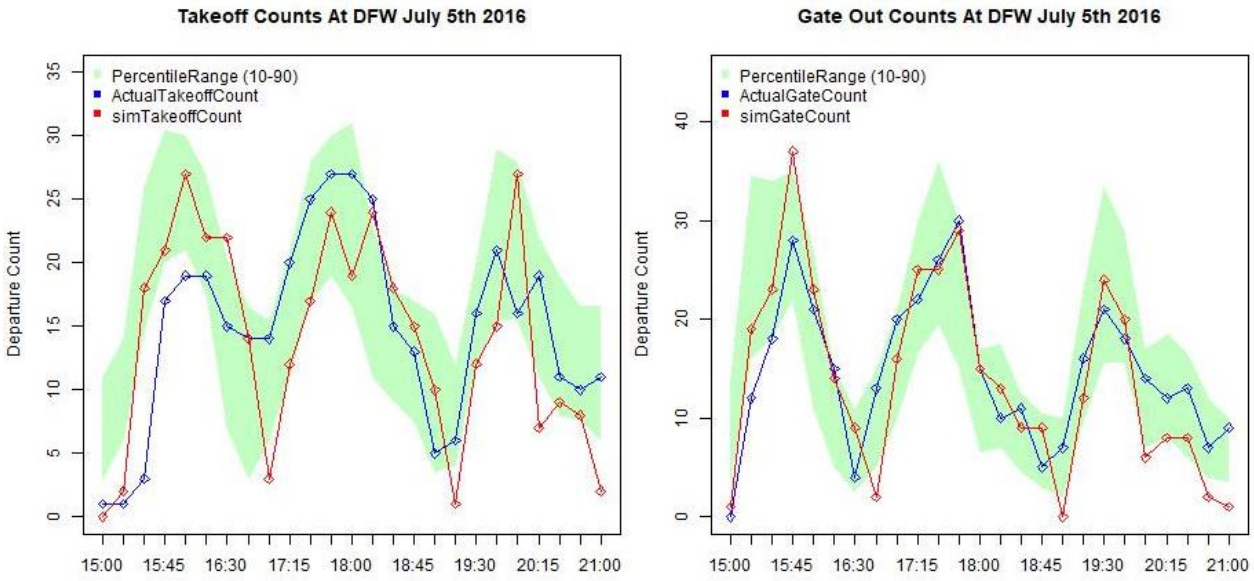

Figure 146. Runway Off and Gate Out Counts Validation – Simulation Versus Real Operations

Further, we also validated the taxi-out times by comparing simulated times against real historical operational taxi-out times from the same day as well as with a distribution of taxi-out times over similar days. **Figure 51** shows the comparison of simulated and actual taxi-out times, with AMA taxi-out time comparison showed in the left half of the figure and the total (AMA + Ramp) taxi-out time comparison shown in the right half of the figure.

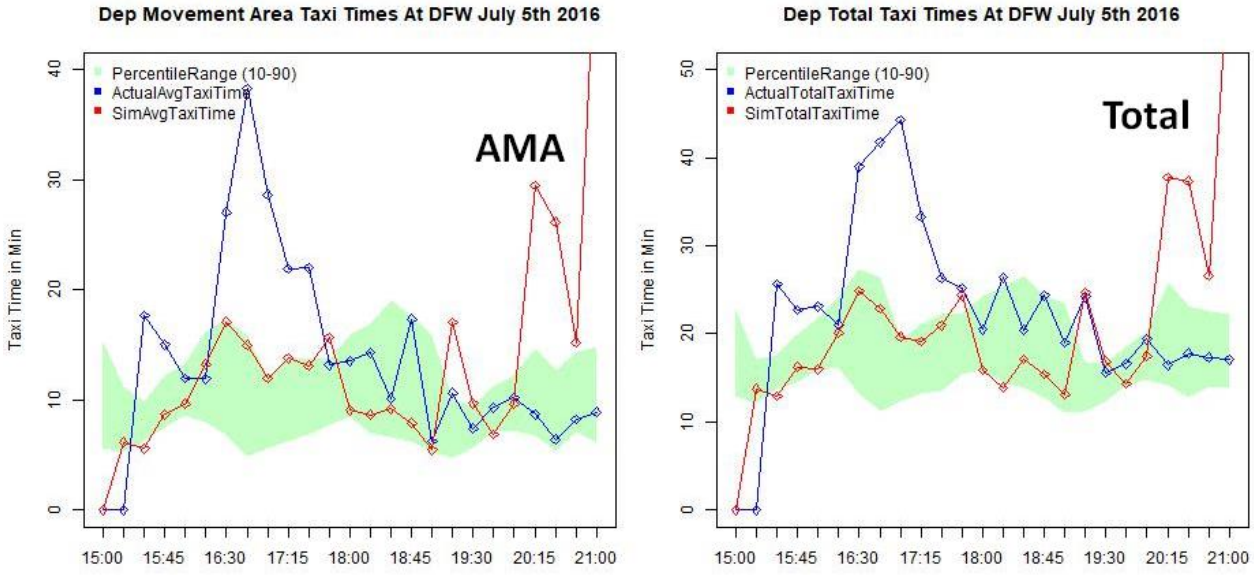

Figure 147. Taxi-Out Time Validation – Simulation Versus Real Operations

12.2.3. DFW Simulation Day 5 Results (7/17/2016, West Flow)

The first scenario we describe involved the simulation of DFW airport arrival and departure traffic on 07/17/2016 during the 1000-1600 UTC timeframe. During this day the airport was operating in the West flow configuration.

12.2.3.1. Benefits Results: Taxi-time Savings Charts

Our simulation results for this scenario showed that the ATD-2 system saved around 11% of the total taxi-out time over all the departures, as shown in **Figure 31**.

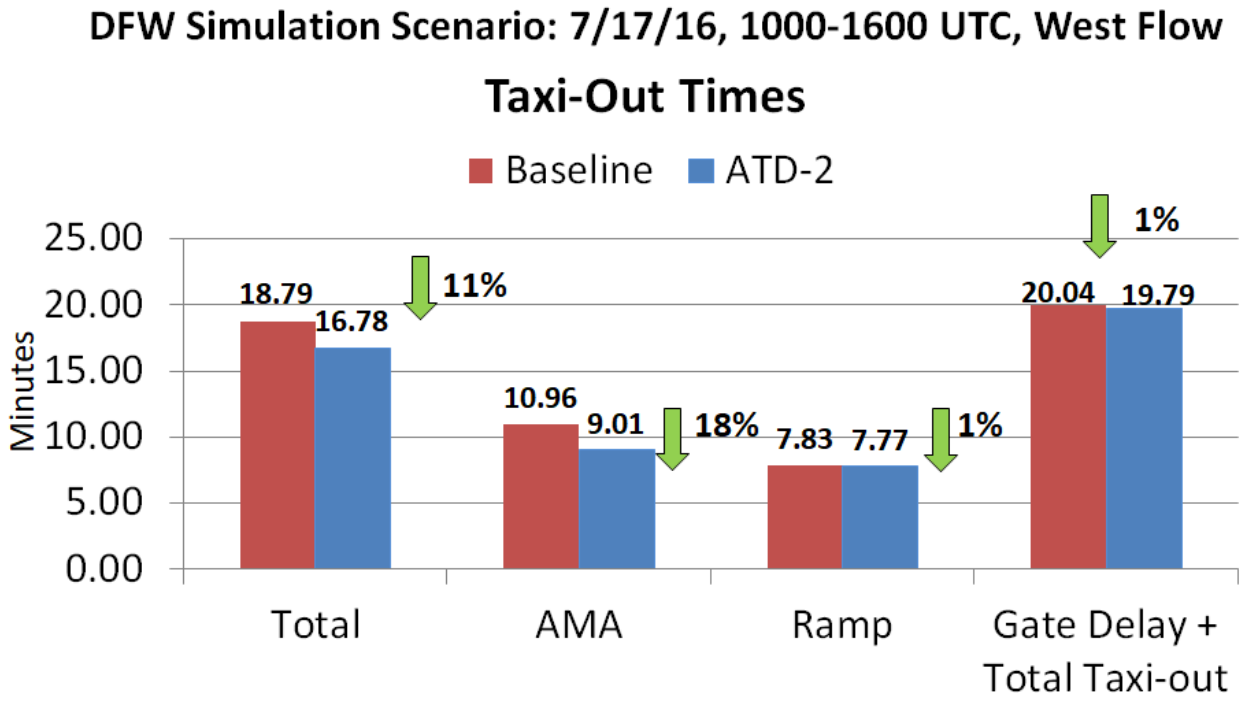

Figure 148. Taxi-Out Time Savings Benefits Estimated by Baseline VS ATD-2 Simulations for the 07/17/2016 1000-1600 UTC simulation scenario

Figure 45 shows the impact that the ATD-2 had on Taxi-In times.

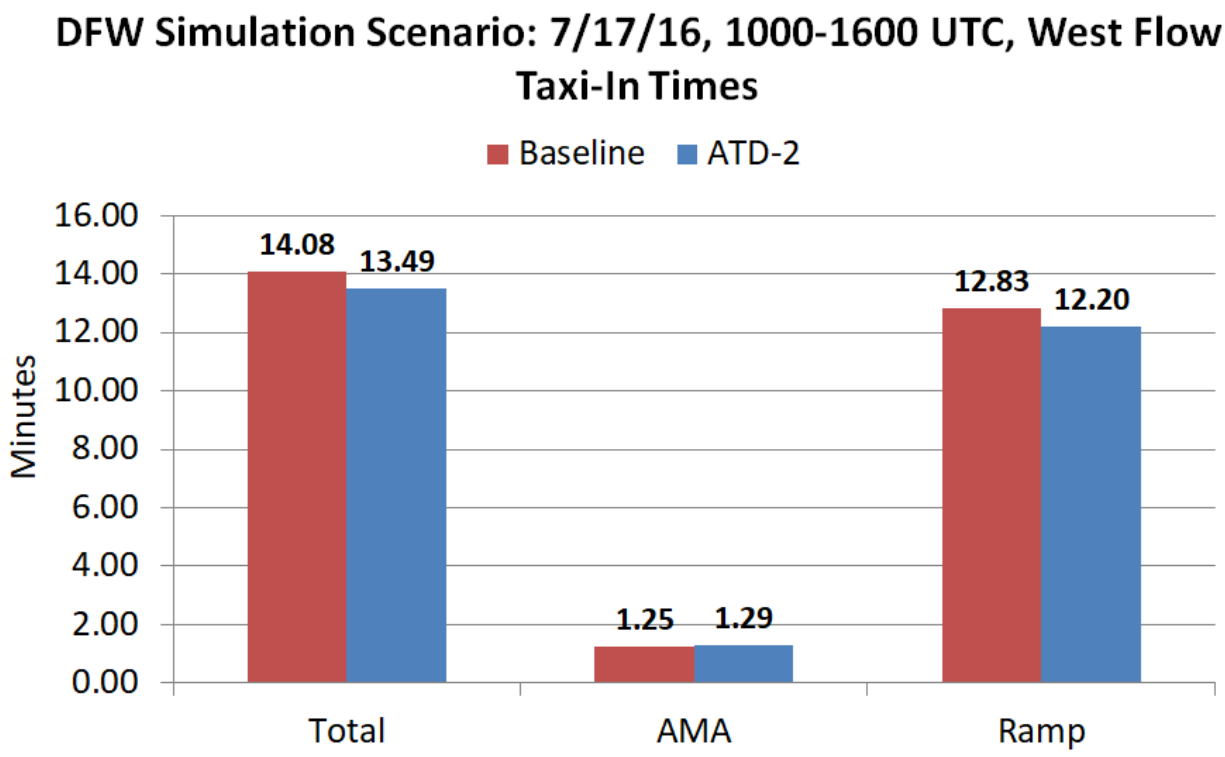

Figure 149. Taxi-In Time Savings Benefits Estimated by Baseline VS ATD-2 Simulations for the 07/17/2016 1000-1600 UTC simulation scenario

12.2.3.2. Analysis of On-Time Performance for Departure Flights

Figure 46 shows the results of the on-time analysis.

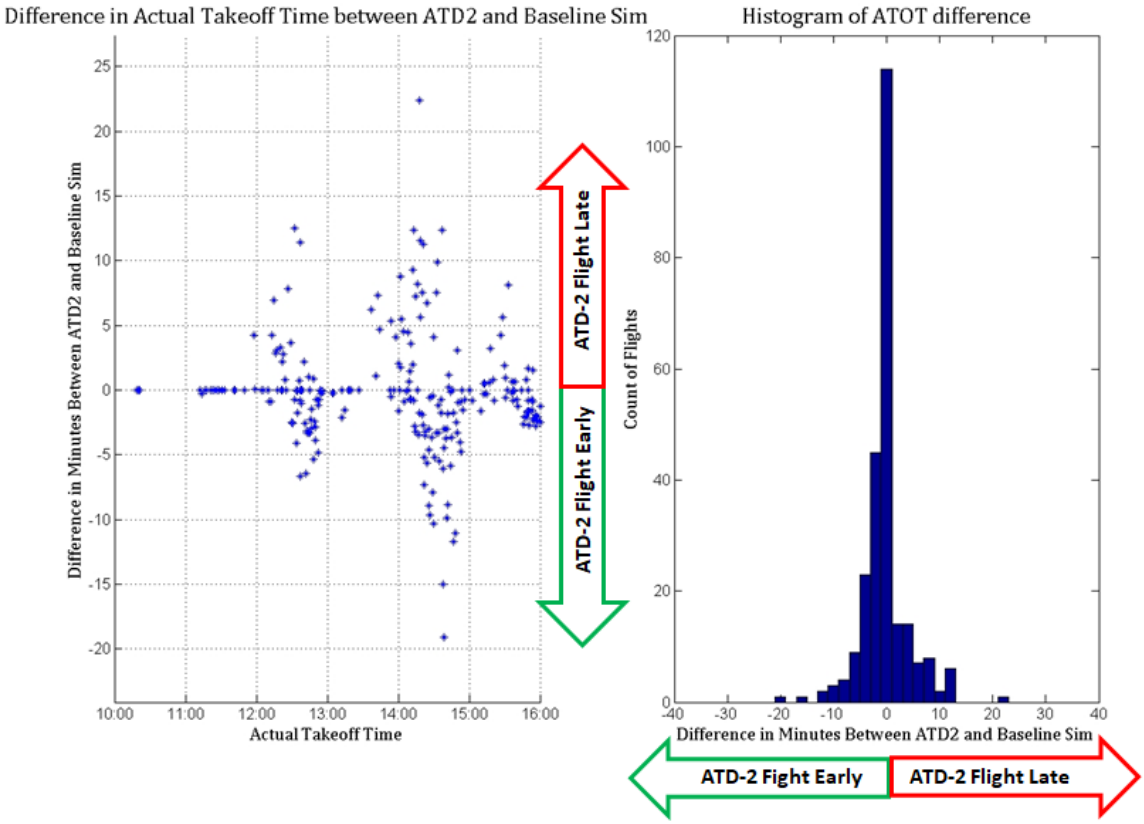

Figure 150. Analysis of On-Time Runway Takeoff Performance – Baseline VS ATD-2

12.2.3.3. Simulation Validation

This section presents results from comparing simulation outputs with operational metrics from real operational data on the same historical day, as well as with a distribution of the same operational metrics computed over a set of similar days over a period of three months. The left-hand side of **Figure 50** shows the comparison of takeoff counts per 15-minute bin over the duration of the simulation, with the simulated counts shown by the red line, the actual counts on the day of operations shown by the blue line, and a region covering the 10-th to 90-th percentile takeoff counts per 15-minute bin over similar historical time-bins shown by the green region.

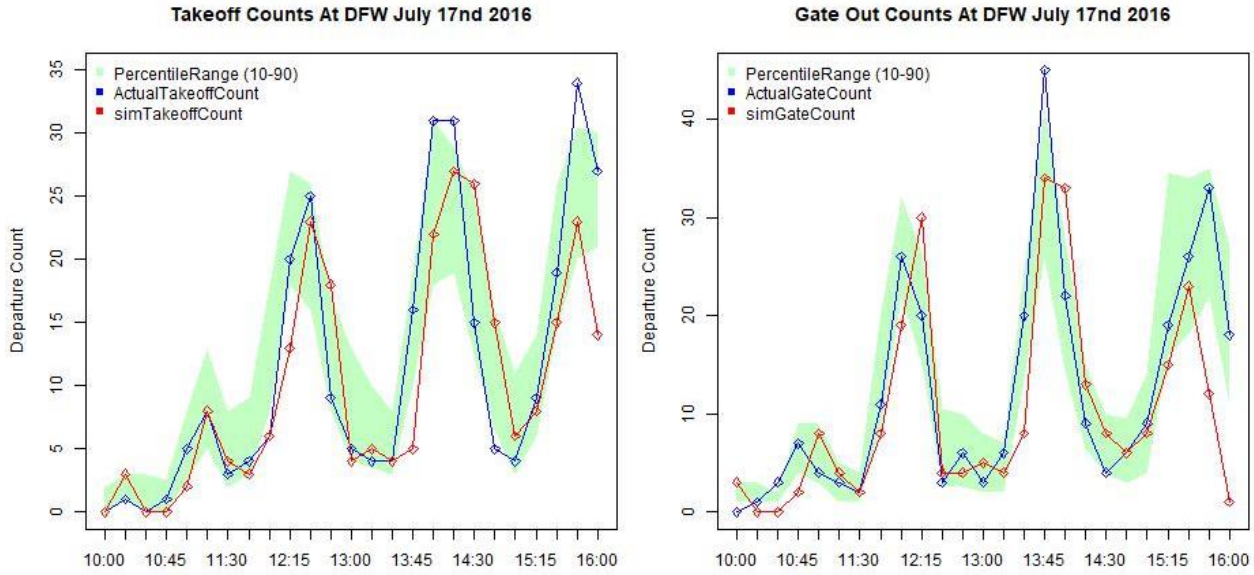

Figure 151. Runway Off and Gate Out Counts Validation – Simulation Versus Real Operations

Further, we also validated the taxi-out times by comparing simulated times against real historical operational taxi-out times from the same day as well as with a distribution of taxi-out times over similar days. **Figure 51** shows the comparison of simulated and actual taxi-out times, with AMA taxi-out time comparison showed in the left half of the figure and the total (AMA + Ramp) taxi-out time comparison shown in the right half of the figure.

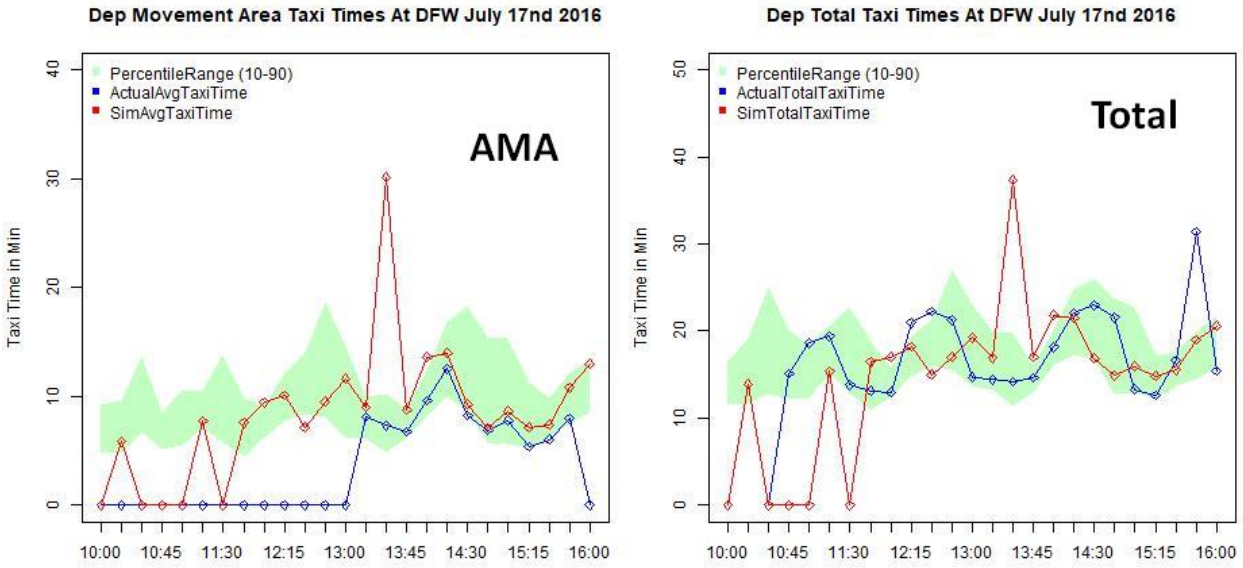

Figure 152. Taxi-Out Time Validation – Simulation Versus Real Operations

12.2.4. DFW Simulation Day 6 Results (7/28/2016, West Flow)

The first scenario we describe involved the simulation of DFW airport arrival and departure traffic on 07/28/2016 during the 1000-1600 UTC timeframe. During this day the airport was operating in the West flow configuration.

12.2.4.1. Benefits Results: Taxi-time Savings Charts

Our simulation results for this scenario showed that the ATD-2 system saved around 6% of the total taxi-out time over all the departures, as shown in **Figure 31**.

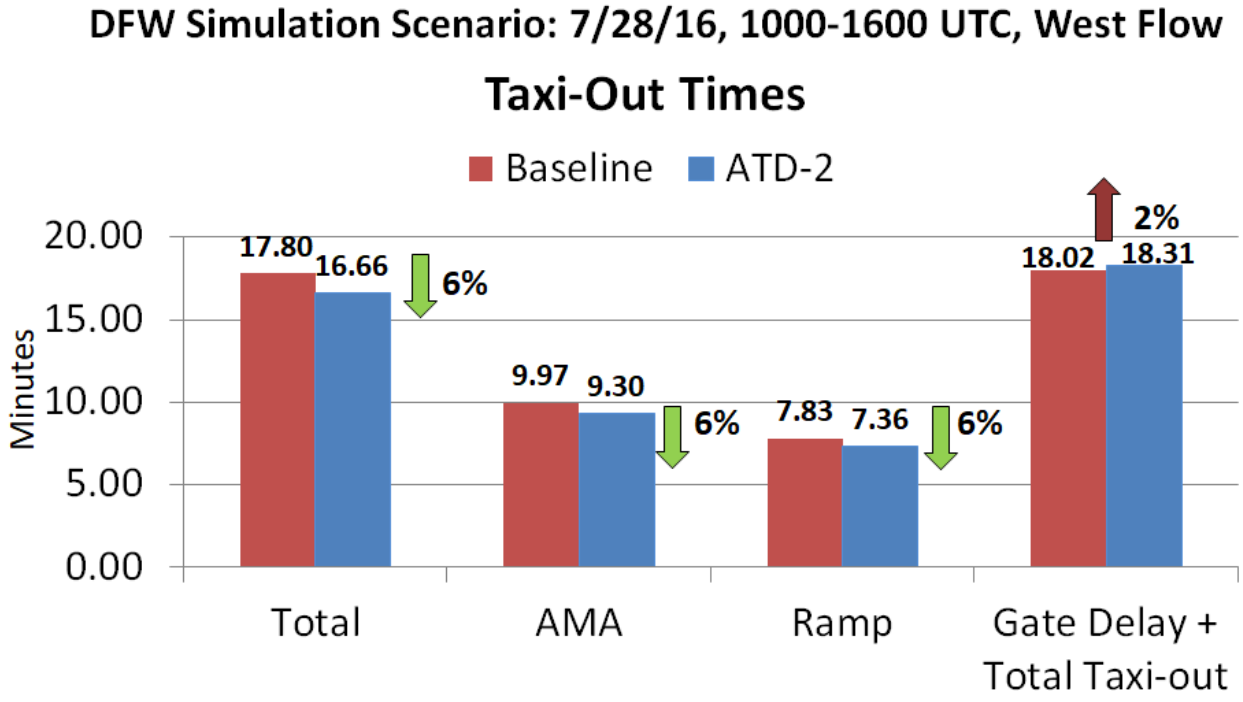

Figure 153. Taxi-Out Time Savings Benefits Estimated by Baseline VS ATD-2 Simulations for the 07/28/2016 1000-1600 UTC simulation scenario

Figure 45 shows the impact that the ATD-2 had on Taxi-In times.

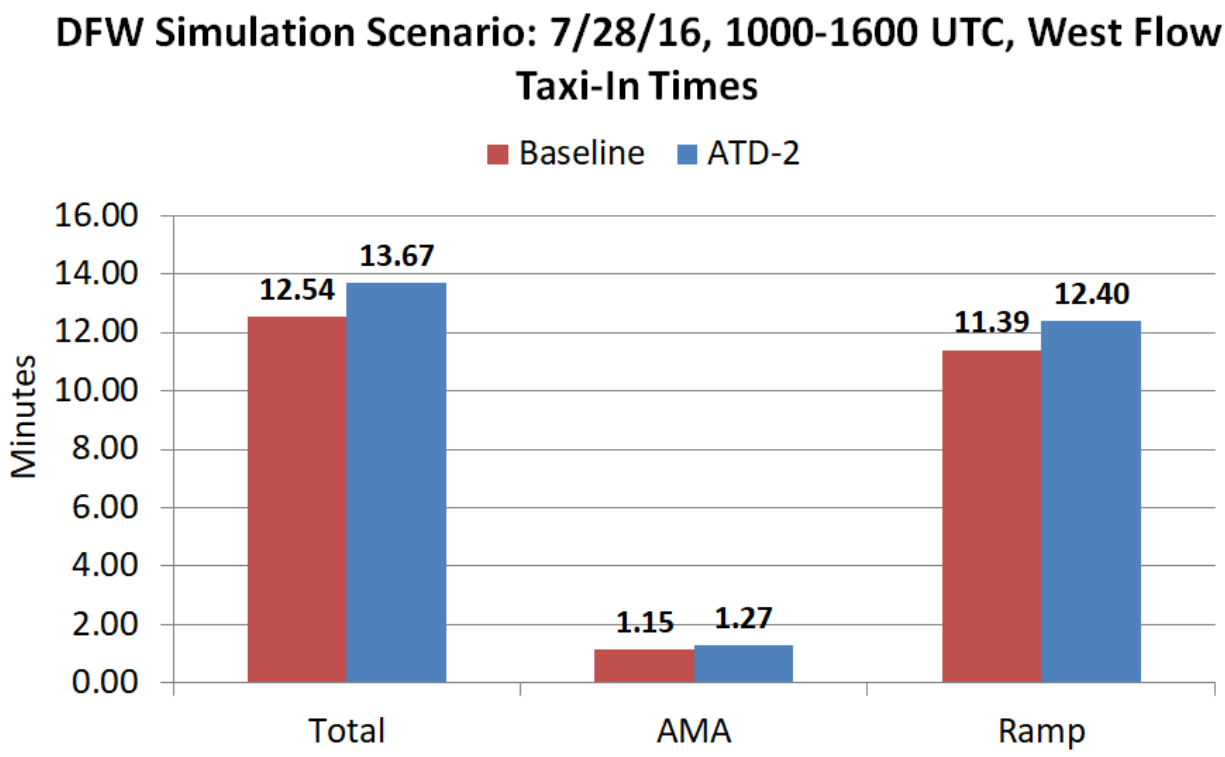

Figure 154. Taxi-In Time Savings Benefits Estimated by Baseline VS ATD-2 Simulations for the 07/17/2016 1000-1600 UTC simulation scenario

12.2.4.2. Analysis of On-Time Performance for Departure Flights

Figure 46 shows the results of the on-time analysis.

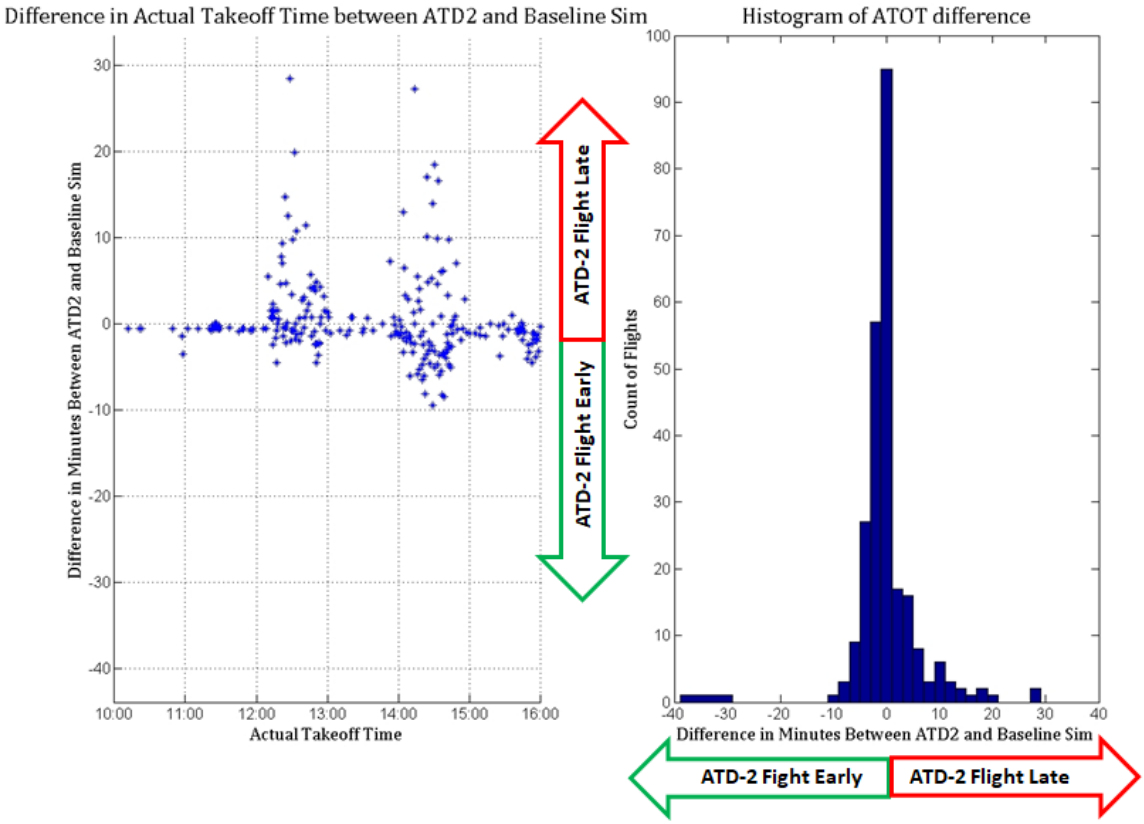

Figure 155. Analysis of On-Time Runway Takeoff Performance – Baseline VS ATD-2

12.2.4.3. Simulation Validation

This section presents results from comparing simulation outputs with operational metrics from real operational data on the same historical day, as well as with a distribution of the same operational metrics computed over a set of similar days over a period of three months. The left-hand side of **Figure 50** shows the comparison of takeoff counts per 15-minute bin over the duration of the simulation, with the simulated counts shown by the red line, the actual counts on the day of operations shown by the blue line, and a region covering the 10-th to 90-th percentile takeoff counts per 15-minute bin over similar historical time-bins shown by the green region.

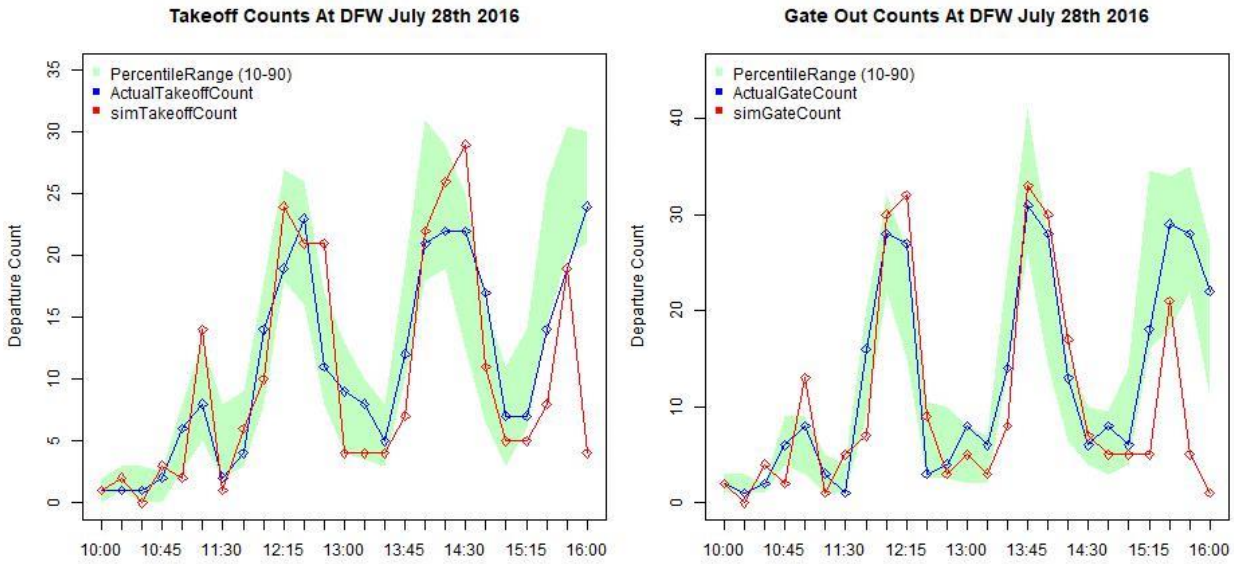

Figure 156. Runway Off and Gate Out Counts Validation – Simulation Versus Real Operations

Further, we also validated the taxi-out times by comparing simulated times against real historical operational taxi-out times from the same day as well as with a distribution of taxi-out times over similar days. **Figure 51** shows the comparison of simulated and actual taxi-out times, with AMA taxi-out time comparison showed in the left half of the figure and the total (AMA + Ramp) taxi-out time comparison shown in the right half of the figure.

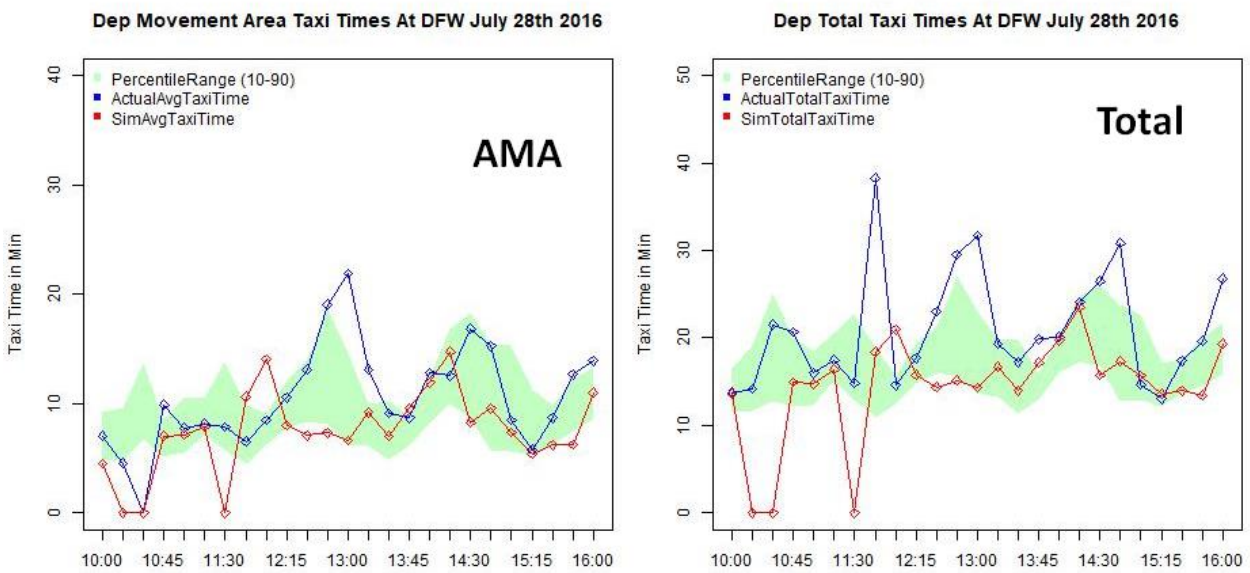

Figure 157. Taxi-Out Time Validation – Simulation Versus Real Operations

12.3. EWR Simulation Days

12.3.1. EWR Simulation Day 3 Results (7/03/2016, South Flow)

The first scenario we describe involved the simulation of EWR airport arrival and departure traffic on 07/03/2016 during the 0900-1600 UTC timeframe. During this day the airport was operating in the South flow configuration.

12.3.1.1. Benefits Results: Taxi-time Savings Charts

Our simulation results for this scenario showed that the ATD-2 system saved around 12% of the total taxi-out time over all the departures, as shown in **Figure 31**.

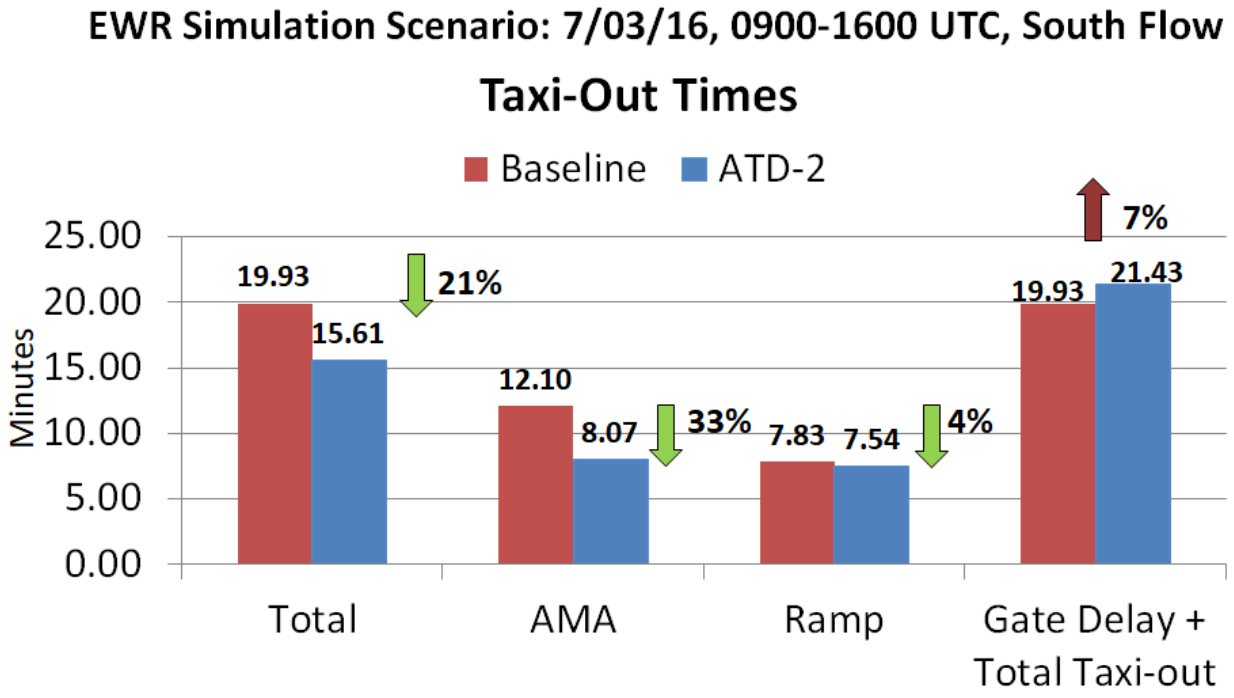

Figure 158. Taxi-Out Time Savings Benefits Estimated by Baseline VS ATD-2 Simulations for the 07/03/2016 0900-1600 UTC simulation scenario

Figure 45 shows the impact that the ATD-2 had on Taxi-In times.

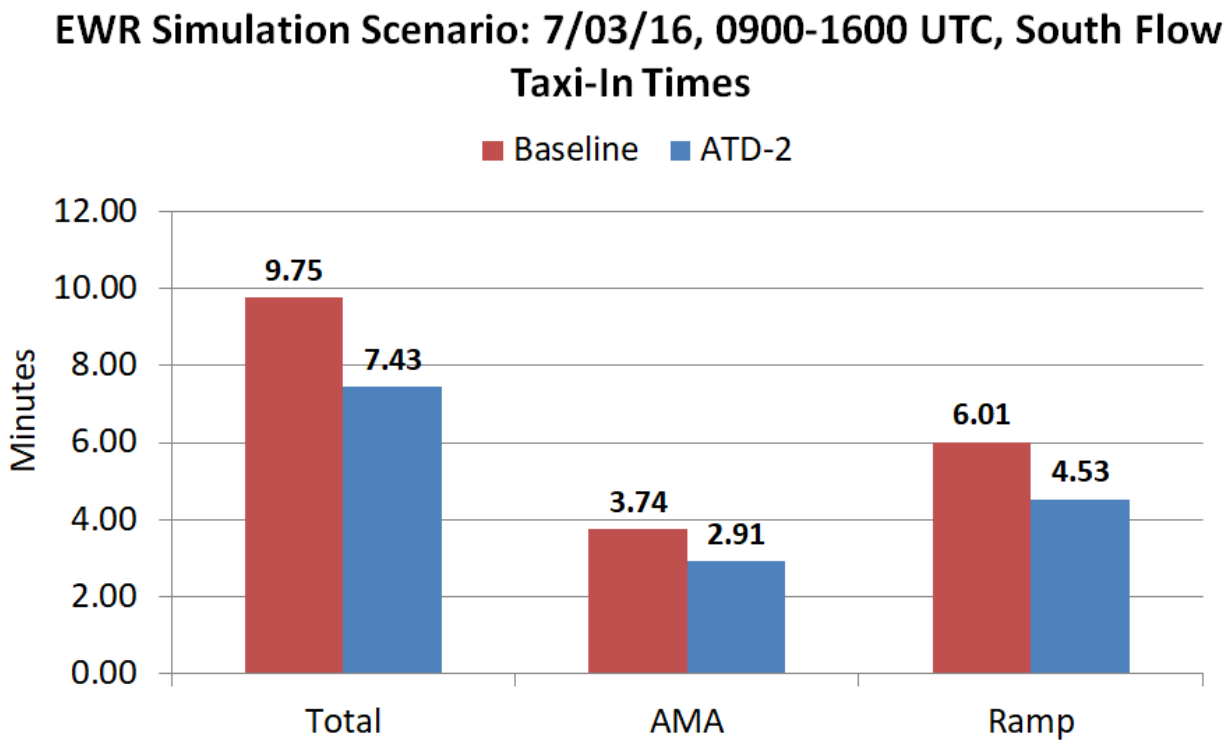

Figure 159. Taxi-In Time Savings Benefits Estimated by Baseline VS ATD-2 Simulations for the 07/03/2016 0900-1600 UTC simulation scenario

12.3.1.2. Analysis of On-Time Performance for Departure Flights

Figure 46 shows the results of the on-time analysis.

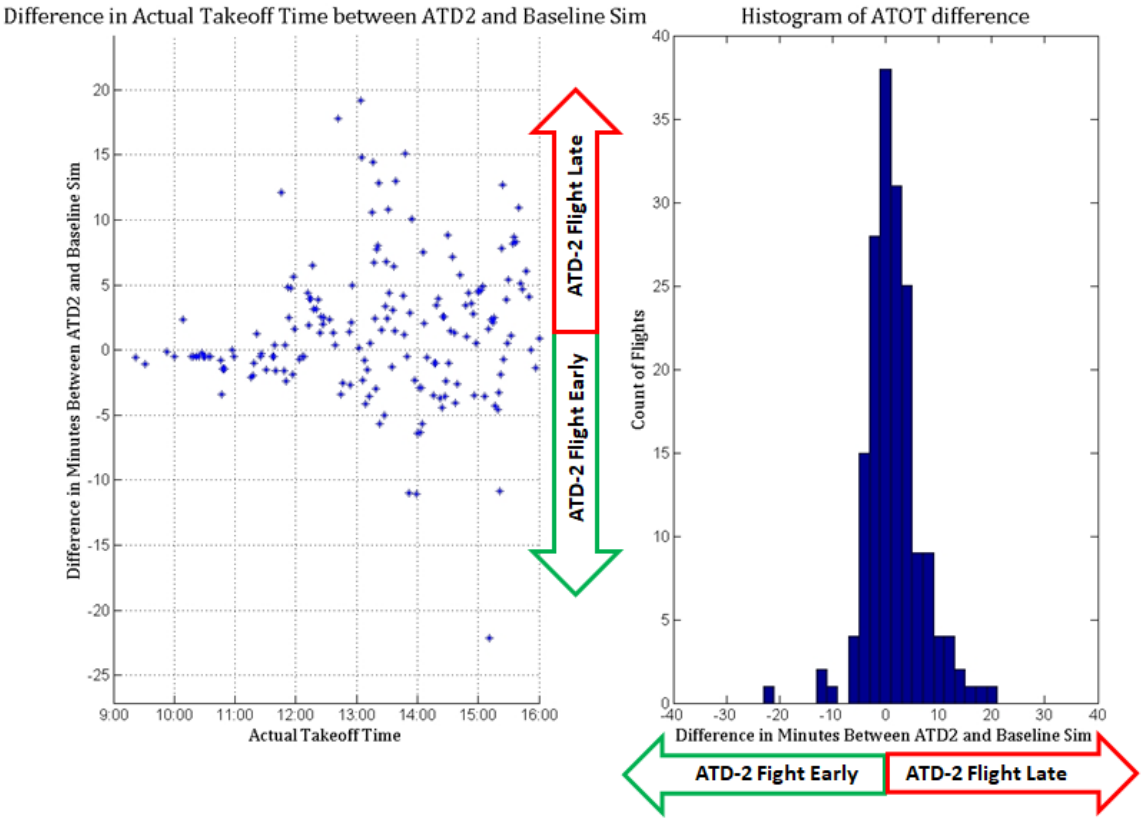

Figure 160. Analysis of On-Time Runway Takeoff Performance – Baseline VS ATD-2

12.3.1.3. Simulation Validation

This section presents results from comparing simulation outputs with operational metrics from real operational data on the same historical day, as well as with a distribution of the same operational metrics computed over a set of similar days over a period of three months. The left-hand side of **Figure 50** shows the comparison of takeoff counts per 15-minute bin over the duration of the simulation, with the simulated counts shown by the red line, the actual counts on the day of operations shown by the blue line, and a region covering the 10-th to 90-th percentile takeoff counts per 15-minute bin over similar historical time-bins shown by the green region.

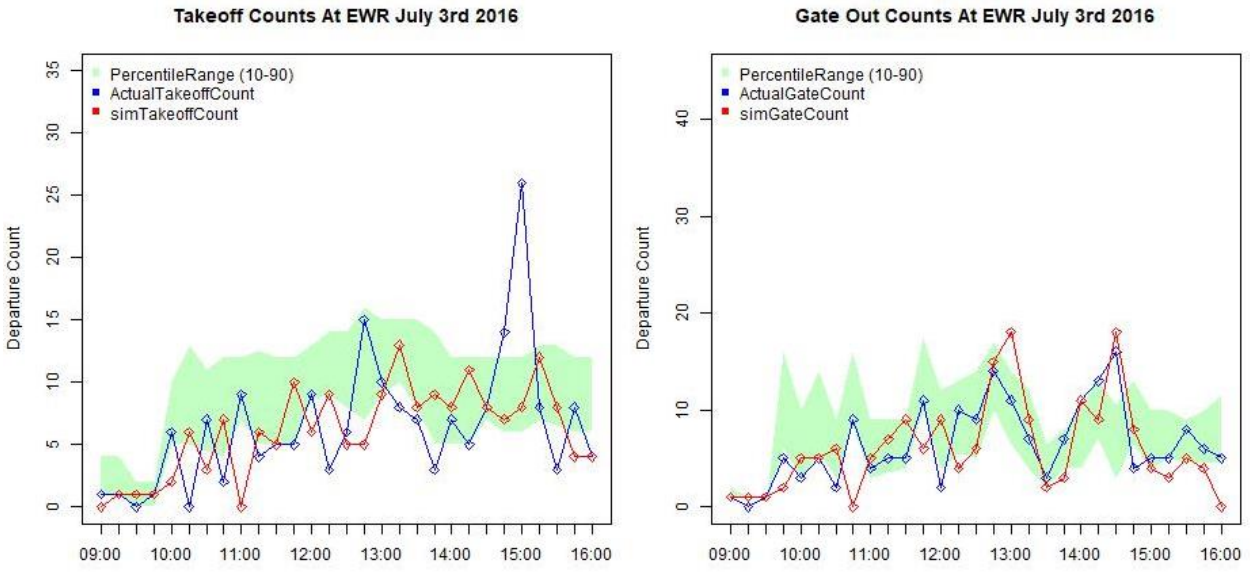

Figure 161. Runway Off and Gate Out Counts Validation – Simulation Versus Real Operations

Further, we also validated the taxi-out times by comparing simulated times against real historical operational taxi-out times from the same day as well as with a distribution of taxi-out times over similar days. **Figure 51** shows the comparison of simulated and actual taxi-out times, with AMA taxi-out time comparison showed in the left half of the figure and the total (AMA + Ramp) taxi-out time comparison shown in the right half of the figure.

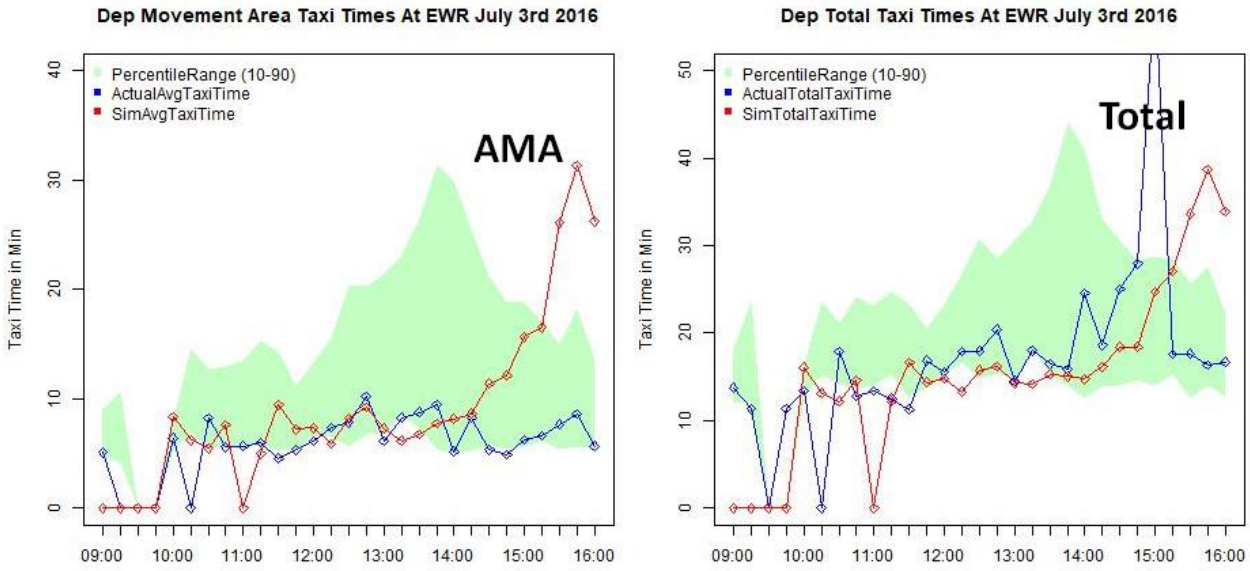

Figure 162. Taxi-Out Time Validation – Simulation Versus Real Operations

12.3.2. EWR Simulation Day 4 Results (5/06/2016, North Flow)

The first scenario we describe involved the simulation of EWR airport arrival and departure traffic on 05/06/2016 during the 1400-2000 UTC timeframe. During this day the airport was operating in the North flow configuration.

12.3.2.1. Benefits Results: Taxi-time Savings Charts

Our simulation results for this scenario showed that the ATD-2 system saved around 9% of the total taxi-out time over all the departures, as shown in **Figure 31**.

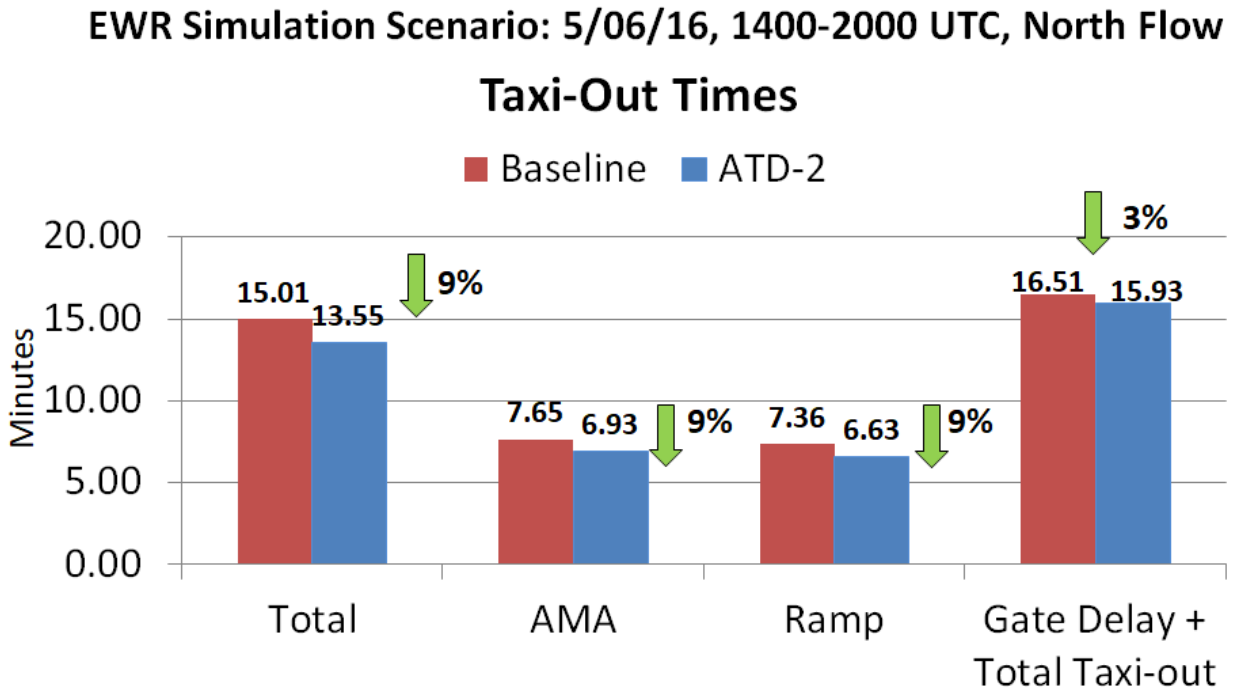

Figure 163. Taxi-Out Time Savings Benefits Estimated by Baseline VS ATD-2 Simulations for the 05/06/2016 1400-2000 UTC simulation scenario

Figure 45 shows the impact that the ATD-2 had on Taxi-In times.

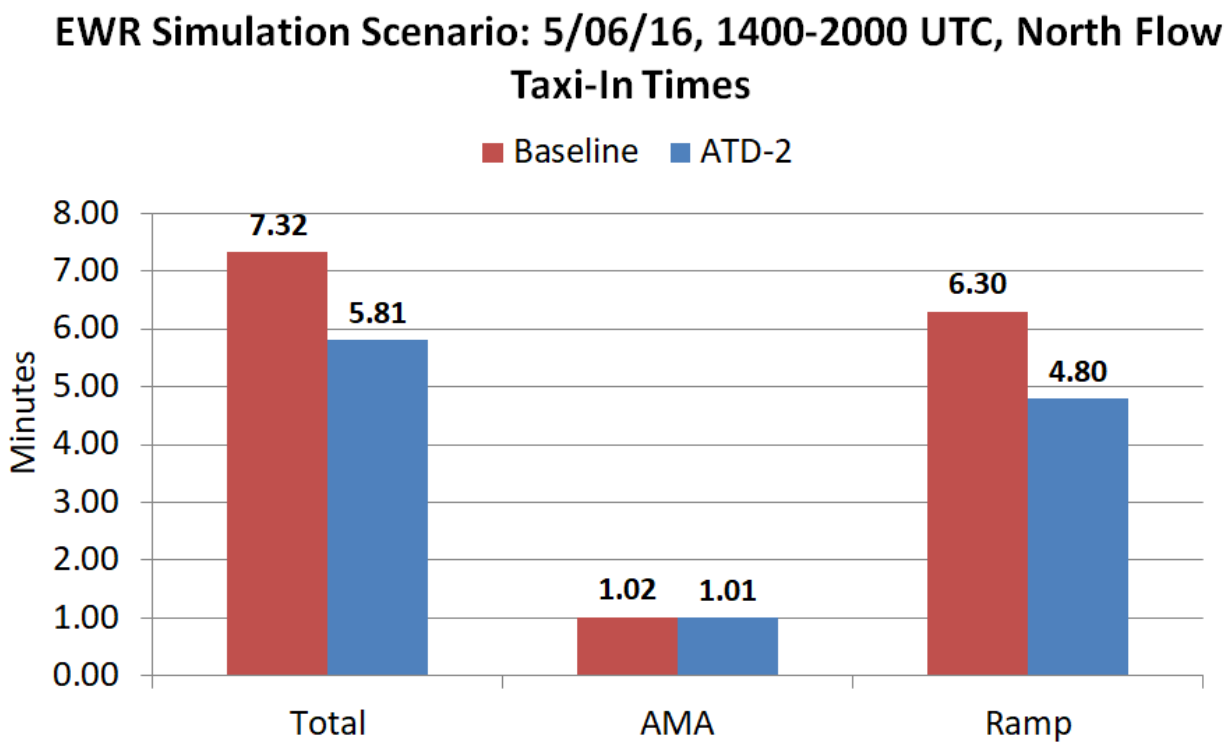

Figure 164. Taxi-In Time Savings Benefits Estimated by Baseline VS ATD-2 Simulations for the 05/06/2016 1400-2000 UTC simulation scenario

12.3.2.2. Analysis of On-Time Performance for Departure Flights

Figure 46 shows the results of the on-time analysis.

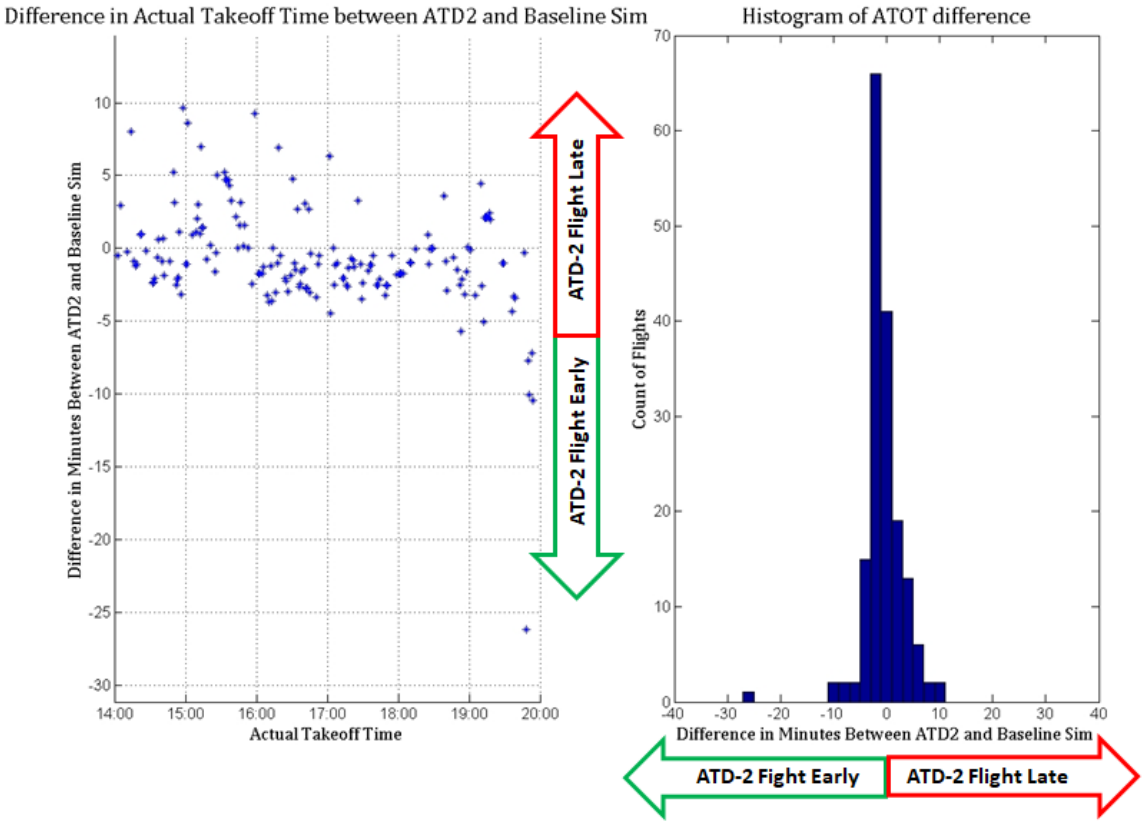

Figure 165. Analysis of On-Time Runway Takeoff Performance – Baseline VS ATD-2

12.3.2.3. Simulation Validation

This section presents results from comparing simulation outputs with operational metrics from real operational data on the same historical day, as well as with a distribution of the same operational metrics computed over a set of similar days over a period of three months. The left-hand side of **Figure 50** shows the comparison of takeoff counts per 15-minute bin over the duration of the simulation, with the simulated counts shown by the red line, the actual counts on the day of operations shown by the blue line, and a region covering the 10-th to 90-th percentile takeoff counts per 15-minute bin over similar historical time-bins shown by the green region.

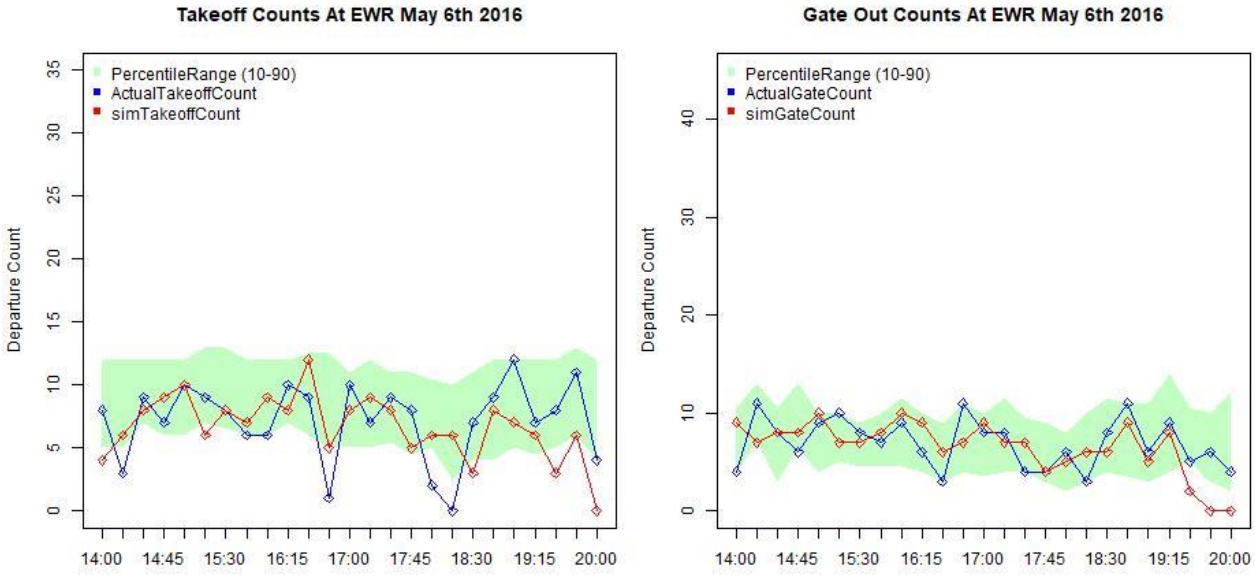

Figure 166. Runway Off and Gate Out Counts Validation – Simulation Versus Real Operations

Further, we also validated the taxi-out times by comparing simulated times against real historical operational taxi-out times from the same day as well as with a distribution of taxi-out times over similar days. **Figure 51** shows the comparison of simulated and actual taxi-out times, with AMA taxi-out time comparison showed in the left half of the figure and the total (AMA + Ramp) taxi-out time comparison shown in the right half of the figure.

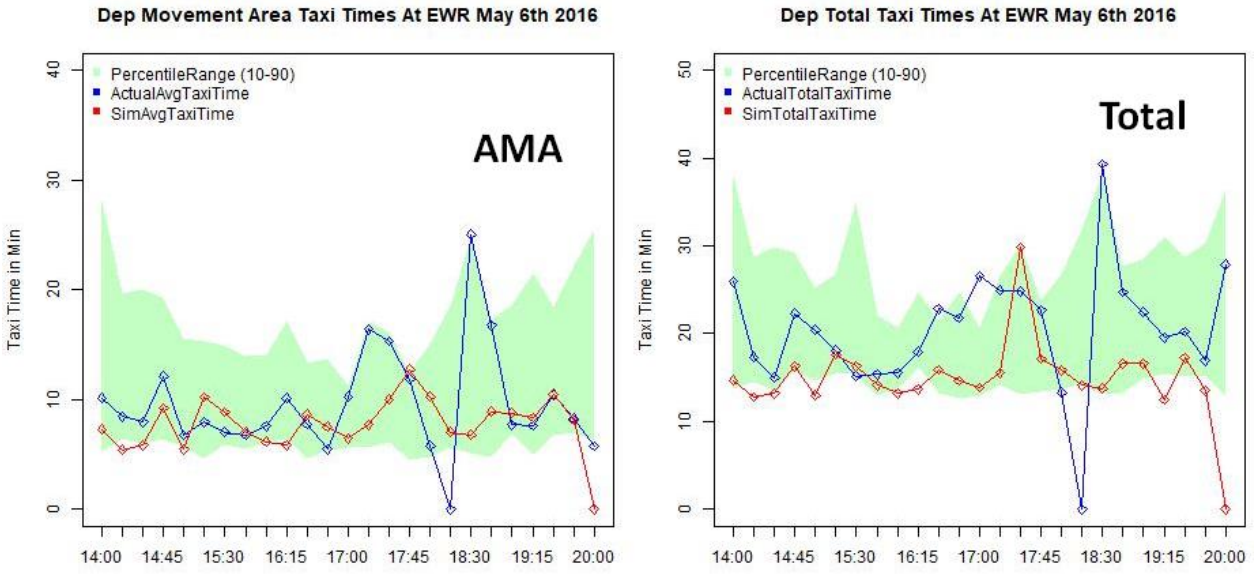

Figure 167. Taxi-Out Time Validation – Simulation Versus Real Operations